PORIN-MEDIATED TRANSPORT OF FLUOROQUINOLONES IN *MYCOBACTERIUM TUBERCULOSIS*

JANSY PASSIFLORA SARATHY

B. Sc (Hons.), NUS

A THESIS SUBMITTED FOR THE DEGREE OF DOCTOR OF PHILOSOPHY TO THE DEPARTMENT OF PHARMACOLOGY, NATIONAL UNIVERSITY OF SINGAPORE

2013

DECLARATION

I hereby declare that this thesis is my original work and it has been written by me in its entirety. I have duly acknowledged all the sources of information which have been used in the thesis.

This thesis has also not been submitted for any degree in any university previously.

_____

Jansy Passiflora Sarathy

ACKNOWLEDGEMENTS

The past four years have been like one long and crazy roller coaster ride. I look back in fondness at the memories that I have created both in and out of the lab. I must first and foremost thank my supervisors Dr. Veronique Dartois and Professor Edmund Lee. I have come to depend on Veronique's encouragement and unwavering faith in me and I look forward to working with her in the future. I will always remember Prof. Lee's kindness and compassion. I am grateful that I crossed paths with him over five years ago as an honors student. I would also like to express my appreciation to Martin Gengenbacher for mentoring me in my first year as a graduate student.

I would like to thank fellow students and staff of the Novartis Institute for Tropical Diseases for their guidance and support. I have grown very fond of many of them and will miss them all dearly as I move on to my next research position. I appreciate every word of advice and every moment spared to teach and mentor. I would also like to thank all the past and present staff of the Pharmacogenetics Laboratory at the NUS Yong Loo Lin School of Medicine.

I thank my parents for always encouraging me to pursue my education. Having my family and RJ to go home to everyday has made the challenges so much more bearable. I am always grateful for their love and support. I also appreciate my dearest friends for standing by me and helping me keep my sanity. And last but not least, I owe my deepest gratitude to Matt Zimmerman for his love and patience.

List of Tables

List of Figures

List of Abbreviations

(Listed in alphabetical order)

ABC	ATP-binding cassette
ACN	Acetonitrile
ADS	Albumin-dextrose-saline
ATP	Adenosine triphosphate
BCG	Bacillus Calmette-Guérin
BSL3	Biosafety Level 3
CAD	Cadaverine
CCCP	Carbonyl cyanide m-chlorophenyl hydrazine
cDNA	Complementary DNA
CFX	Clinafloxacin
CFU	Colony-forming Unit
CPX	Ciprofloxacin
DNA	Deoxyribonucleic acid
EDTA	Ethylenediaminetetraacetic acid
EMB	Ethambutol
GFX	Gatifloxacin
HPLC	High-performance liquid chromatography
IBC	Institutional Biosafety Committee

IC/EC	Intracellular concentration – Extracellular concentration ratio
INH	Isoniazid
LCC	Loebel cidal concentration
LC/MS	Liquid chromatography coupled to Mass spectrometry
LLOQ	Lower limit of quantification
LNZ	Linezolid
LVX	Levofloxacin
MATE	Multi antimicrobial extrusion protein
MeOH	Methanol
MDR	Multi-drug resistant
MBC	Minimum bactericidal concentration
ME	Matrix Effects
MEF	Mefloquine
MFS	Major facilitator superfamily
MIC	Minimum inhibitory concentration
MRM	Multiple reaction monitoring
MTB	*Mycobacterium tuberculosis*
MXF	Moxifloxacin
NADH	Nicotinamide adenine dinucleotide
NRP	Non-replicating persistence
OADC	Oleic acid albumin dextrose complex

OD	Optical density
OFX	Ofloxacin
OMP	Outer membrane protein
PAS	*para*-aminosalicylic acid
PBS	Phosphate-buffered saline
PMF	Proton motive force
PSA	Polar surface area
RES	Reserpine
RIB	Rifabutin
RIF	Rifampicin
RIP	Rifapentine
RNA	Ribonucleic acid
RND	Resistance nodulation division
RT-PCR	Reverse transcription polymerase chain reaction
SMR	Small multidrug resistance
SPM	Spermidine
SPX	Sparfloxacin
SSC	Steady-state concentration
TB	Tuberculosis
TMC	TMC207
TMS	Transmembrane segment

TMHMM Transmembrane prediction using Hidden Markov Model

TNBS Trinitrobenzensulfonic acid

TRZ Thioridazine

VER Verapamil

XDR Extremely drug resistance

List of Publications

1. **Sarathy JP, Dartois V, Lee EJD.** The Role of Transport Mechanisms in Mycobacterium Tuberculosis Drug Resistance and Tolerance. *Pharmaceuticals.* 2012; 5(11):1210-1235.
2. **Sarathy JP, Lee EJD, Dartois V.** Polyamines inhibit fluoroquinolone uptake in mycobacteria. *PLoS One.* 2013; 8(6): e65806.
3. **Sarathy JP, Dartois V, Dick T, Gengenbacher M.** Impaired drug uptake contributes to phenotypic resistance in nutrient-starved non-replicating *Mycobacterium tuberculosis*. *Antimicrobial Agents and Chemotherapy*. 2013; 57(4): 1648-53.

Disambiguation of Terminology

In order to avoid confusion regarding the use of certain terminology in this thesis, some definitions have been provided.

1. Drug uptake and Drug accumulation

   Drug uptake refers to the specific process of movement of drugs from the extracellular environment into the intracellular matrix, be it by passive or active mechanisms.

   Drug accumulation refers to the built-up intracellular content of a drug. This accumulation is the net effect of drug uptake, efflux and enzymatic conversion processes.

   Steady –state drug accumulation refers specifically to the achievement of equilibrium between drug uptake and efflux process such that an extension of the incubation period does not result in a further increase in intracellular accumulation.

2. Diffusion and Facilitated diffusion

   Diffusion is defined as the passive process of movement of molecules down a concentration gradient, from a region of high concentration to a region of low concentration of the compound.

   Facilitated diffusion refers to the specific transport process where special transport proteins (ie. carrier proteins and ion channels) assist molecules to transverse a biological membrane. This is similar to passive diffusion in the way it does not require the spending of metabolic energy.

3. Drug resistance and Phenotypic drug resistance

   Drug resistance generally refers to decreased drug susceptibility that is brought about by either genotypic or phenotypic changes.

   Phenotypic drug resistance refers to the reversible phenomenon where decreased drug susceptibility is not the result of genetic mutations. Such drug tolerance is mediated by the physiological state of dormancy and full susceptibility is usually restored upon the resumption of bacterial growth.

CHAPTER 1

LITERATURE REVIEW AND STUDY OJECTIVES

Parts of this project have been included in the following manuscript:

Sarathy JP, Dartois V, Lee EJD. The Role of Transport Mechanisms in *Mycobacterium Tuberculosis* Drug Resistance and Tolerance. *Pharmaceuticals.* 2012; 5(11):1210-1235.

1.1 Tuberculosis: The Global Phenomenon

In 2009, it was estimated that there were 9.4 million incident cases of tuberculosis (TB) infections and 1.7 million tuberculosis-related deaths worldwide (240). Despite the availability of effective treatment options since the 1950s, and the implementation of well-structured treatment programs, the TB epidemic is not being controlled. Frontline anti-tuberculous drugs have gradually become ineffective because of the increasing incidence of resistance. Multidrug-resistant TB (MDR-TB) is a difficult-to-treat form of *M. tuberculosis* that fails to respond to the two most effective first-line anti-tuberculous drugs, rifampicin and isoniazid. The World Health Organization (WHO) estimated that in 2009, around 5% of all new tuberculosis cases of infections involved MDR-TB (241). Strains that combine MDR with additional resistance to fluoroquinolones and at least one injectable drug have been appropriately named extensively drug-resistant tuberculosis (XDR-TB). The burden of tuberculosis on global health has pushed the research community into focusing efforts on the development of new vaccines, diagnostics and chemotherapy against *Mycobacterium tuberculosis*, the causative agent.

The TB pathology is diverse, generating different types of lesions, containing several micro-environments each harboring metabolically distinct bacterial sub-populations, some of which are not effectively killed by most existing drugs (148). This drug tolerance phenomenon typical of tuberculosis has been coined 'phenotypic drug resistance' (198), and is partly attributed to the pathogen's ability to remain sequestered in macrophages and other stress-inducing micro-environments in a non-replicating state of persistence **(Figure 1)** (42). These dormant bacilli are primarily responsible for the persistent and latent forms of the disease, but retain the potential to resume growth and produce an active infection, making them a critical target population of antimycobacterial agents (42, 238, 239).

The development of new antimycobacterials active against dormant cells and resistant strains is in need of novel drug targets. The failure of existing chemotherapeutic options to control the TB epidemic can be attributed in part to sub-therapeutic concentrations at the site of action (113). The longer a pool of bacteria is exposed to sub-inhibitory levels of an antimicrobial agent, the more likely the emergence and selection of resistant clones becomes (49). This has prompted researchers and drug discovery experts to turn to strategies which would potentiate existing therapeutics by increasing their intracellular levels through the use of small molecule inhibitors against efflux pumps (129).

The cell envelope of mycobacteria is notorious for being several-fold less permeable to chemotherapeutic agents when compared to functionally similar cell walls of other bacteria (105). The knowledge of drug transport pathways could assist in the successful design of novel chemotherapeutic combinations against *M. tuberculosis*. **Figure 2** illustrates the various transport processes that take place across the mycobacterial outer membrane. In this introduction section, we review the current understanding of the various influx and efflux pathways in mycobacteria while focusing our attention on details specific to *M. tuberculosis*. The function and expression of transport proteins such as porins, drug importers and efflux pumps are summarized and their respective influence on the drug-resistant and non-replicating persistent states is highlighted. Collectively, the literature data compiled here show that *M. tuberculosis* and other mycobacteria have evolved several intrinsic and adaptive mechanisms to increase their level of tolerance towards xenobiotic substances, by preventing or minimizing their entry: (i) natural or intrinsic resistance mediated by the thickened highly hydrophobic and waxy envelope; (ii) reduced permeability resulting from physiological adaptations under unfavorable environmental conditions; (iii) drug-induced resistance acquired via increased expression of various classes of

efflux pumps; and (iv) genetically encoded resistance conferred by mutations in efflux complexes.

Figure 1 Illustration of a classic tuberculous granuloma with a caseous centre that can be found in both actively- and latently-infected patients. *M. tuberculosis* in such granuloma can be found intra-cellularly within macrophages or extra-cellularly. Graphic representations are not drawn to scale.

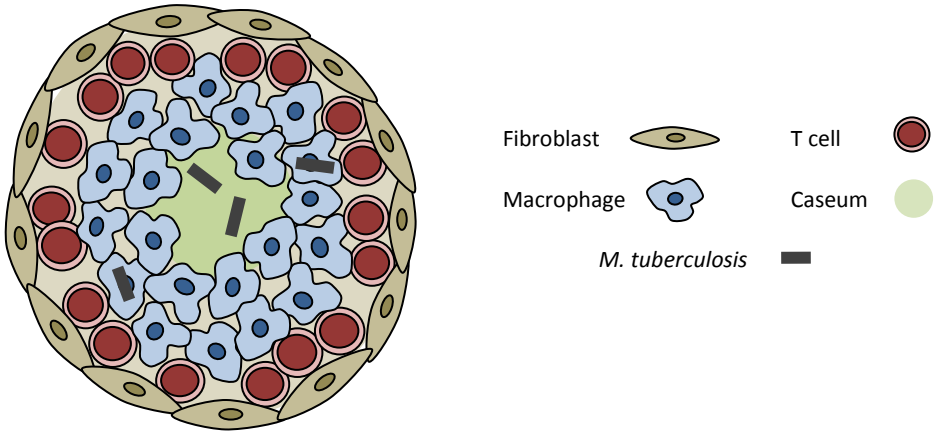

Figure 2 Mechanisms of drug influx and efflux across the mycobacterial outer membrane. Arrows (↑ and ↓) indicate directions of drug transport. Solid lines represent influx pathways, whereas dashed ones represent efflux pathways.

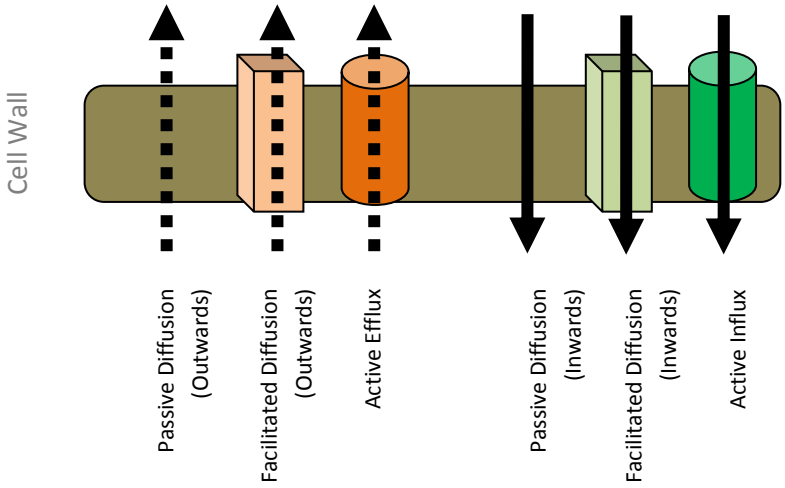

1.2 Antituberculosis Chemotherapy

Despite the availability of antituberculosis for over 50 years, this infectious disease remains one of the deadliest known to mankind. Treatment is difficult, and requires the co-administration of multiple antibiotics over long periods of time. Since the 1980s, short-course 6-month treatment regiments that involve the use of isoniazid, rifampicin, ethambutol and pyrazinamide have been widely effective at treating tuberculosis infections. Second-line agents such as fluoroquinolones, thioamides and aminoglycosides have been made available for the treatment of MDR-TB. Non-compliance and mismanagement of chemotherapy has led to the development of drug resistant infections in patients. DOTS, or Directly Observed Therapy-Short Course, is the recommended treatment strategy for TB control. It encompasses several components which include a regular, uninterrupted supply of high quality drugs and direct observations during treatment.

1.2.1 Fluoroquinolones

Fluoroquinolones are fluorine-containing nalidixic acid-derivatives put into clinical practice in the 1980s as second-line agents for the treatment of tuberculosis infections. Fluoroquinolones are now considered a mainstay of treatment for patients with MDR- and XDR-TB, delivering better clinical outcomes than other drug classes (39, 41). The pharmacophore that is characteristic of quinolones with antibacterial activity is 4-pridone-3-carboxylic acid with a ring at the 5 or 6 position **(Figure 3)** (210). Since discovery, several generations of fluoroquinolones have been developed for treatment of not only tuberculosis, but also other forms of bacterial infections of the respiratory, gastrointestinal and urinary tracts **(Figure 4)**. *In vitro* efficacy of fluoroquinolones against *M. tuberculosis* generally ranges between 0.2 – 2 µg/ml. In humans, fluoroquinolones are absorbed readily following once-daily dosing by oral administration, and

display effective distribution into lungs and alveolar macrophages. When first-line anti-tuberculosis agents are administered in combination with fluoroquinolones against intra-macrophage *M. tuberculosis*, greater bactericidal activity is recorded than with the individual drugs alone (83). Reported adverse effects of fluoroquinolones in humans include tendonitis, photosensitivity, seizures, QT interval prolongation, hepatitis and renal dysfunction (9).

DNA topoisomerases make up a set of ubiquitous enzymes that maintain chromosomes in their appropriate topological state. These enzymes are responsible for regulating DNA supercoiling during DNA replication and transcription. In majority of the species, fluoroquinolones target DNA gyrase (topoisomerase II) and topoisomerase IV, bringing about cell death. In *M. tuberculosis*, the A and B subunits of DNA gyrase are encoded for by *gyrA* and *gyrB* respectively. A conserved region of *gyrA* and gyrB, called the quinolone-resistance-determining region (QRDR) has been found to be most critical for the development of fluoroquinolone resistance in *M. tuberculosis* (224). Clinical- and laboratory-selected isolates on *M. tuberculosis* habour mutations of *gyrA* that are largely clustered at codons 74, 83, 87, 90, 91 and 94 (249). *gyrB* mutations in isolates are relatively infrequent. High levels of resistance are associated with at least 2 mutations in *gyrA* or concomitant mutations on *gyrA* and *gyrB* (224). It has been noted that the frequency of mutations conferring fluoroquinolone resistance varies with the selection pressure (incubation concentration). Increasing fluoroquinolone concentrations reduce the variety of occurring mutations to a few high-level mutations (251). Decreased cell wall permeability is suspected to influence fluoroquinolone resistance in *M. tuberculosis*. The *rv2686c-rv2687c-rv2688c* operon encodes an ATP-binding cassette transporter whose efflux activity confers resistance to ciprofloxacin, amongst other fluoroquinolones, to *M. smegmatis*

(174). It has not yet been established how this operon is elaborated in the development of clinical resistance to fluoroquinolones.

Evidence is recently being presented for the use of fluoroquinolones as a first-line agent to reduce the total course of anti-tuberculosis therapy. Briefly, moxifloxacin has shown to be superior to ethambutol at early bactericidal killing and achieves significantly more sputum conversions to negative at the critical 8-week mark (54, 223). Concern that the wide-spread use of fluoroquinolones as a first-line agent will result in the high prevalence of fluoroquinolone-resistant tuberculosis still remains. However, several studies have shown that the prevalence of fluoroquinolone-resistant tuberculosis stays low despite wide-spread fluoroquinolone use (223). Current anti-tuberculosis chemotherapy is a 6-month long process. Phase III trials testing the effectiveness of 4-month first-line regiments containing moxifloxacin are in progress.

Figure 3 The required pharmacophore of quinolones (210).

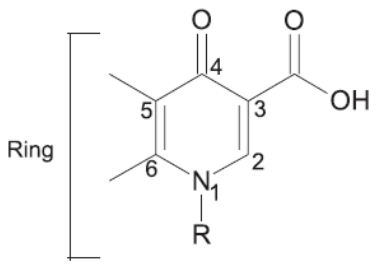

Figure 4 The chemical structures, as provided by Hayashi *et al*., of some of the more common first, second, third and fourth-line fluoroquinolones that have entered clinical practice. Some have since been removed because of toxicity issues or have been discontinued by their manufacturers. The drugs most frequently prescribed fluoroquinolones today consist of Avelox (moxifloxacin), Cipro (ciprofloxacin), Levaquin (levofloxacin) (92).

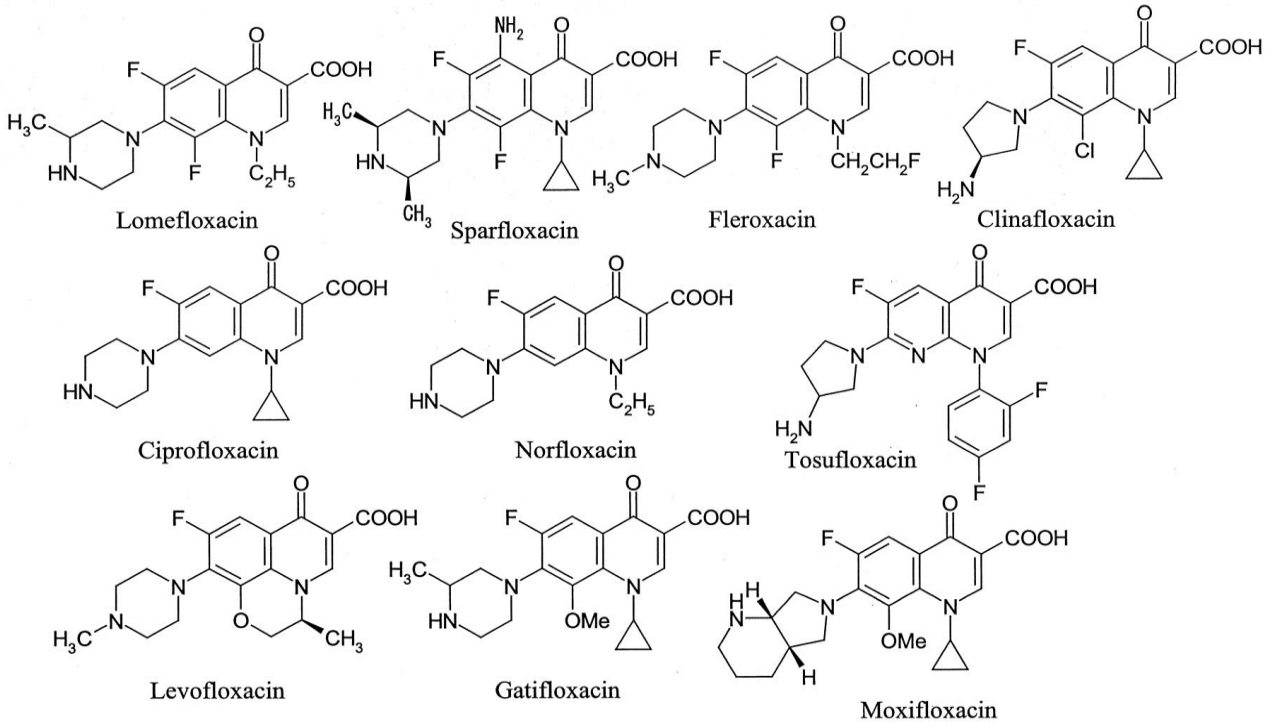

1.3 The Mycobacterial Outer Membrane

The cell envelope of mycobacteria is structurally distinct from that of both Gram-positive and Gram-negative bacteria. The entire mycobacterial cell envelope can be broken down into two main structural components: cell membrane and cell wall. The outer leaflet of the cell wall is composed of mycolic acids which are covalently linked to the arabinogalactan-peptidoglycan complex of the inner leaflet. Mycobacteria are capable of producing a multitude of mycolic acids with varying lengths and modifications depending on species, strain and growth conditions (15, 32, 59). It is widely believed that the unusually high mycolic acid content, combined with a variety of other intercalated lipids, contributes to the wall's limited permeability (14). The mycobacterial cell wall is also composed of phosphotidyl-*myo*-inositol derived glycolipids such as lipomannan and lipoarabinomannan which have potent immunomodulatory activities (147).

The mycolyl-arabinogalactan-peptidogalactan complex is acknowledged as being a more efficient permeability barrier than cell walls of any other class of bacteria (105). Jarlier and Nikaido attempted to clearly define the mycobacterial permeability barrier to hydrophilic molecules by studying the uptake kinetics of small nutrient molecules (glucose, glycine, leucine and glycerol) in *M. chelonae* (106). The permeability coefficients (P) for these nutrients were found ranging from 1.4 to 62 nm/s; specifically 2.8 nm/s for glucose. K_m values of the overall transport of glucose and glycerol were 1,000µM and 200µM respectively as measured in the same study. In comparison, a different study had measured a permeability coefficient of glucose for *E.coli* (1.4×10^5 nm/s) that was about five orders of magnitude higher (55). It should be noted that the precise values of permeability differ among different species of mycobacteria. *M. chelonae*, being one of the most drug-resistant species, has a cell wall that is about one to two orders of magnitude less permeable than *M. tuberculosis*, *M. smegmatis* and *M. phlei* (55, 105).

This intra-species difference in cell wall permeability may be attributed to variability in its content and organization. Detailed structural and quantitative analysis has revealed a higher mycolate-to-peptidoglycan ratio in *M. leprae* than *M. tuberculosis*; peptidoglycan coverage by mycolate was estimated at 80% and 63% for *M. leprae* and *M. tuberculosis* respectively (25).

This unique cell wall composition and organization is believed to render mycobacteria less susceptible than other bacterial pathogens to various antibiotic classes (33, 105). Several pathways exist for compounds to cross this permeability barrier. It is assumed that hydrophobic compounds should be able to penetrate cell walls by simply dissolving into and through the lipophilic cell wall unassisted, whereas the influx of hydrophilic compounds is largely facilitated by porins, which are water-filled open channels that span the cell wall (166). It appears that the mycobacterial plasma membrane plays a limited role in pathogenicity and maintenance of the influx-efflux equilibrium (59, 60).

1.3.1 Passive Diffusion of Hydrophobic Molecules

In principle, antimicrobial agents of the more lipophilic classes such as the rifamycins, macrolides and fluoroquinolones are more likely to diffuse into and through the lipid-rich environment of the mycobacterial cell wall in order to transverse its depth (33). This passive transport has been coined "hydrophobic (or lipid) pathway", characterized by the nature of the interactions between structural lipids and small molecules (136). However, lipophilic agents are presumably slowed down by the low fluidity and unusual thickness of the cell wall (124). It has been demonstrated that lipophilic derivatives within single drug classes are more active against mycobacteria when compared to their hydrophilic counterparts (33). This was more recently supported by evidence from a comparison of Minimum Inhibitory Concentrations (MIC) between hydrophilic and hydrophobic fluoroquinolone analogs. Moxifloxacin (cLogP 0.6) was 32-fold more effective than norfloxacin (cLogP -0.1) at inhibiting the growth of *M. smegmatis* (61). Brennan *et al* postulated that an increase in the rate of drug penetration resulting from an increase in incubation temperature is also evidence of the predominant role of the hydrophobic pathway or passive diffusion in drug penetration (33).

1.3.2 Active Efflux Processes

1.3.2.1 Influx transporters

Based on *M tuberculosis* genome sequence analysis, Braibant *et al.* have concluded that there is an under-representation of importers in *M. tuberculosis*, with the exception of phosphate importers, when compared to other bacterial species such as *E. coli* and *B. subtilis* (31). In addition, the ratio of exporter-to-importer proteins, based on sequence homology, is markedly higher in *M. tuberculosis* than in *E. coli.* This observation may again contribute to the reduced uptake of small molecules by *M. tuberculosis* bacilli. Though bacterial ABC transporters can mediate both influx and efflux, only their efflux activity has been observed and characterized in mycobacterial species (131). Identified substrates for ABC influx activity thus far include sugars, amino acids, metals and anions (64).

1.3.2.2. Efflux Pumps

1.3.2.2.1 Resistance Phenotype I – Natural Abundance

The presence of active multi-drug efflux pumps is also thought to play a significant role in the development of natural and induced drug resistance in mycobacteria. In 1998, the complete genome sequencing of *M. tuberculosis* revealed at least 14 members of the Major Facilitator Family (MFS) and the ATP-binding Cassette (ABC) transporter family (52). In 2000, analysis of transcriptional clusters and homology searches of transporters from other organisms allowed for the reconstitution of 26 complete and 11 incomplete ABC transporters from the various subunits encoded for by the complete *M. tuberculosis* genome (31). In the same study, it was concluded

that ABC transporters account for 2.5% of the genome of *M. tuberculosis*. This compares with 5% of the entire *E. coli* genome that encodes for 69 ABC transporters (122). ATP-binding cassettes (ABC), the major facilitator superfamily (MFS), the multidrug and toxic compound extrusion (MATE) family, the small multidrug resistance (SMR) family and the resistance-nodulation-division (RND) superfamily are the five families of bacterial drug efflux pumps that have been categorized thus far (95, 119, 120). The mechanisms of efflux-mediated drug resistance in bacteria have been well-studied and reviewed over the past decade, and are only briefly summarized here.

ABC transporter proteins are known for coupling ATP-hydrolysis with the alternation between outward- and inward-facing conformations to bring about substrate transport (99). MFS and RND transporters, on the other hand, are classified as secondary active transporters because they are driven by the proton-motive force (PMF) (142). SMR transporters are the smallest multidrug resistant proteins, with lengths of about a 110 amino acids only. Despite the general correlation between genome size and the number of ABC transport systems, the *M. tuberculosis* genome encodes fewer ABC systems per megabase than any other organism surveyed in a comprehensive analysis of the solute transport systems within the genomes of 18 prokaryotes. It was suggested that the relative abundances of ABC and MFS transporters reflects the overall use of energy coupling mechanism in each organism. *M. tuberculosis*, being a strict aerobe, is more dependent on PMF-type secondary transporters as compared to fermentative organisms that depend on substrate level phosphorylation to generate ATP. Also worth noting is the largest RND-family representation in *M. tuberculosis* compared to the other prokaryotes surveyed. These are believed to play a significant role in the extrusion of lipids and other cell envelope components (176).

Several ABC, MFS, RND and SMR efflux pumps of *M. tuberculosis* and other mycobacteria have been characterized as antibiotic transporters **(Table 1).** TetV and LfrA, which have been identified in *M. smegmatis* as drug transporters but not in *M. tuberculosis* have also been included in the table. Some of these putative pumps have been associated with reduced mycobacterial susceptibility to agents such as isoniazid, tetracycline, fluoroquinolones and aminoglycosides (67). Differences in efflux pump expression between mycobacterial species are important because they offer insights into the acquisition of drug resistance. One study which investigated flux and efflux rates of pyrazinamide and pyrazinoic acid, respectively, revealed that the efflux rate for *M. smegmatis* is 900 fold higher than for *M. tuberculosis* when no significant variability was noticed in flux rates. It is not known whether this difference is due to variability in the type or expression level of pumps present in both species but it potentially explains the innate resistance of *M. smegmatis* to pyrazinamide as compared to the relative susceptibility of *M. tuberculosis* (252).

Table 1 Summary of several known mycobacterial efflux pumps, their drug substrates and their energy sources.

Pump	Gene	Transporter Family	Known Substrates	Known Inhibitors	Energy Source	Mycobacteria	References
-	*rv2686c-rv2687c-rv2688c*	ABC	Fluoroquinolones	Verapamil Reserpine CCCP	ATP	*M. tuberculosis*	(174)
-	*rv1218c*	ABC	Novobiocins Pyrazolones Pyrroles	Verapamil Reserpine CCCP	ATP	*M. tuberculosis*	(8)
-	*rv0194*	ABC	Ampicillin Chloramphenicol Streptomycin Novobiocin	Reserpine	ATP	*M. tuberculosis*	(61)
DrrAB	*drrA-drrB*	ABC	Doxorubicin	Verapamil Reserpine	ATP	*M. tuberculosis*	(46)
MmpL7	*mmpL7*	RND	Isoniazid	Reserpine CCCP	PMF	*M. tuberculosis*	(175)
Tap	*rv1258c*	MFS	Tetracycline Rifampicin	Piperine	PMF	*M. tuberculosis* *M. fortuitum*	(4, 188, 211)
P55[b]	*rv1410c*	MFS	Rifampicin Clofazimine Aminoglycosides Tetracycline	CCCP Valinomycin	PMF	*M. tuberculosis* *M. bovis*	(189, 212)

JefA	*rv2459*	MFS	Isoniazid Ethambutol Streptomycin	Verapamil CCCP	Not speculated	*M. tuberculosis*	(88)
EfpA	*rv2846c*	MFS	Not determined	-	PMF	*M. tuberculosis* *M. smegmatis* *M. leprae* *M. avium*	(67, 75)
IniA[a]	*iniA*	-	Isoniazid Ethambutol	Reserpine	Not speculated	*M. tuberculosis*	(51)
Mmr	*rv3065*	SMR	Not determined	CCCP	PMF	*M. tuberculosis*	(68,77)
Tet(V)	*tet(V)*	MFS	Tetracycline	CCCP	PMF	*M. smegmatis* *M.fortuitum*	(68)
LfrA	*lfrA*	MFS	Fluoroquinolones Doxorubicin	CCCP	PMF	*M. smegmatis*	(125)

[a] IniA is itself a pump component that hypothetically participates in the formation of a multimeric structure with a central pore.

[b]The function of P55 is connected to P27, a proposed glycolipid transporter (76). Both proteins are encoded in the IprG-Rv1410c operon of *M. tuberculosis* (26).

Abbreviations: ABC: ATP-Binding Cassette transporters; MFS: Major Facilitator Superfamily transporters; RND: Resistance-Nodulation-Cell Division transporters; ATP: Adenosine triphosphate; CCCP: Carbonyl cyanide m-chlorophenyl hydrazone, PMF: Proton Motive Force

1.3.2.2.2. Resistance Phenotype II – Induction of expression

Studies have shown that the exposure to various anti-tuberculous drugs can trigger increased expression of selected efflux pumps leading to drug-mediated phenotypic resistance. Two possible mechanisms are thought to contribute to higher expression of pump-encoding genes: transitory induction by the substrate of these pumps and mutations in the promoter and regulatory region leading to increased or constitutive expression (67, 159). The latter is discussed in the next section. The study of kill kinetics of isoniazid against wild-type *M. tuberculosis* revealed that while rapid concentration-dependent killing was seen upon initial drug exposure, subsequent re-growth was observed over a wide range of isoniazid concentrations which was caused by the development of isoniazid-resistant sub-populations. Susceptibility of this subpopulation to isoniazid was restored in the presence of an efflux pump inhibitor for 98% of the resistant clones (69), suggesting that the majority of the isoniazid-resistant population represents efflux pump-mediated phenotypic drug tolerance, though genetic mutations in efflux pump-encoding genes were not formally excluded in this study. More recently, it was established that susceptible and rifampicin mono-resistant *M. tuberculosis* strains develop a resistance to isoniazid after 3 weeks that is could be reduced by means of efflux pump inhibitors (132). Such induction of resistance to isoniazid has been associated with the overexpression of efflux pump genes such as *mmpl7*, *p55*, *efpA*, *mmr*, *Rv1258* and *Rv2459* (132, 195, 244). In the presence of isoniazid, wild-type *M. bovis* BCG and *M. tuberculosis* increased the expression of *iniA* by up to 10-fold (51). Though it does not appear to directly transport isoniazid out of the cell, this predicted transmembrane protein has been postulated to serve as a pump component that participates in the formation of a multimeric structure containing a central pore.

Gupta *et al.* demonstrated the overexpression of 10 efflux pump genes in MDR strains following exposure to a range of anti-tuberculous drugs. The simultaneous expression of *Rv2459*, *Rv3728* and *Rv3065*, for example, has been associated with resistance to the specific combination of isoniazid and ethambutol, while *Rv2477* and *Rv2209* overexpression has been associated with ofloxacin stress (88). One MDR clinical isolate bearing defined mutations in *katG* and *rpoB* displayed *rv1258c* and *Rv1410c* overexpression upon rifampicin or isoniazid exposure, and *Rv1819c* overexpression upon isoniazid exposure alone (107).

Interestingly, evidence exists for the reduction in susceptibility of *M. tuberculosis* to one drug upon exposure to another. The exposure of rifampicin-resistant strains to rifampicin resulted in a reduction in susceptibility to ofloxacin which could be restored by the introduction of efflux pump inhibitors (130). One could hypothesize that the up-regulated efflux pumps are promiscuous in their activity and that the cyclic nature of both drugs facilitates recognition by similar pumps.

1.3.2.2.3 Resistance Phenotype III – Efflux pump mutations

Drug efflux is typically described as an intrinsic or natural resistance mechanism in bacteria. However, mutations in efflux pump genes and their regulator sequences can lead to increased efflux activity and, hence, enhanced drug resistance. Such mutational events either cause an inducible increase in pump expression upon antibiotic exposure, or the constitutive expression of otherwise tightly controlled pump genes above basal levels (144). Several such mutations have been documented in various bacterial systems, particularly in Gram-negative species (108, 140, 237). Often, the mutations are stable point mutations that reduce the DNA binding affinity of particular repressors for their target regulatory region within promoters and lead to constitutive expression of efflux components (144).

In *M. tuberculosis*, mutations in the bioactivating enzymes or in the target of rifampicin, isoniazid, pyrazinamide and the fluoroquinolones cannot explain all clinically observed resistance. For example, approximately 20 to 30% of INH-resistant *M. tuberculosis* isolates do not have mutations in any of the known genes associated with INH resistance (187). Similarly, approximately 5% of clinical RIF-resistant *M. tuberculosis* isolates do not harbor mutations in the RIF resistance-determining region of the *rpoB* gene (226). A number of studies based on gene expression profiling and efflux pump inhibition point towards the role of active extrusion in genotypic drug resistance (131). However, due to incomplete understanding of efflux substrate specificities and regulatory mechanisms, the distinction between expression induction by the substrate resulting in transient tolerance versus DNA mutations leading to inherited up-regulation at the transcriptional level has not been clearly made in most cases. The growing pool of whole genome sequences from clinically resistant isolates provides a unique opportunity to elucidate some of the mechanisms underlying efflux-mediated drug resistance in *M. tuberculosis*.

Recently, La Rosa *et al* identified mutations in *M. tuberculosis* MmpL3, a putative transporter with sequence homology to the RND super-family of efflux pumps, which confer resistance to a range of anti-tuberculous small molecules of different chemical scaffolds (115). Similar results have been obtained recently by our and other groups (85, 222). Surprisingly, increased efflux does not appear to be the mechanism by which resistance to the respective small molecules is conferred, calling for caution when assuming protein function from sequence homology.

1.3.3 Mycobacterial Porins

Porins are large water-filled channels in both Gram –positive and –negative bacteria that allow for the penetration of small hydrophilic molecules without requiring energy consumption. The specificity of these diffusion channels can vary. OmpF of *E. coli*, for instance, has no substrate specificity except for being weakly cation –selective. OprB, OprP and OprO of *P. aeruginosa*, on the other hand, specifically transport glucose, phosphate and pyrophosphate respectively (22). Often believed to be static and permanently –open pores, these channels can switch between open and closed conformations, and even occupy a prolonged inactivated state (no conductance). Such gating activity and inactivation is regulated by a number of physical and chemical parameters. In doing so, porins are believed to play a major role in modulating outer membrane permeability and, hence, antibiotic susceptibility of bacteria in response to various environmental stimuli (72). Substrates that transverse the outer membrane via porins then diffuse across the periplasm to be taken up across the inner membrane by hypothetical transporter proteins into the cytosol (162). The mechanisms of inner membrane transport are still being elucidated. **Figure 5** provides illustration of this uptake pathway. Porin channels caters to a limited range of compounds since channel diameters at the narrowest point define the exclusion limit, and parameters such as channel length and the number of open pores determine the velocity of transport (230). As demonstrated by studies in *E.coli*, diffusion rates through porins are further affected by the charge, hydrophobicity, and size of the solute (166, 167, 169). Several types of porins have been identified and studied in Gram-negative and some Gram-positive bacteria. To date, two putative classes of porins have been identified and characterized in mycobacteria; they are MspA-like and OmpA-like porins in *M. smegmatis* and *M. tuberculosis* respectively (61).

Figure 5 Model for porin –mediated uptake through the mycobacterial cell envelope. Porins (in blue) in the open state allow substrates to transverse the outer membrane. Hypothetical transporter proteins (in green) take substrate molecules from the periplasm across the inner membrane into the cytosol. The figure is not drawn to scale.

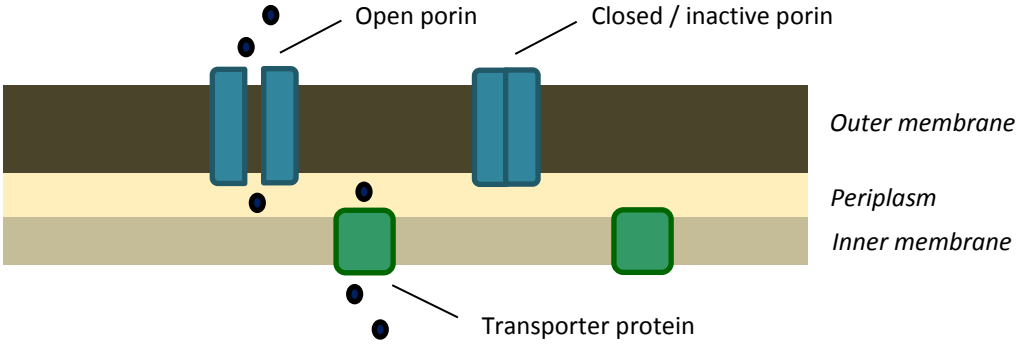

1.3.3.1 MspA of *M. smegmatis*

MspA was the first porin of its class identified in a mycobacterial species, with proven oligomerization and channel-forming activity *in vitro* and when cloned in *E. coli* (164). Subsequent sequencing of the *M. smegmatis* genome revealed three more porin genes with homology to *mspA*, namely *mspB, mspC* and *mspD* (219). Numerous studies have documented MspA-enabled transport of hydrophilic solutes and drug molecules across the cell wall of *M. smegmatis*. **Table 2** summarizes drug transport specificities of various *M. smegmatis* porins and their impact on drug uptake and MIC. The studies show that porin deletion is clearly linked to increases in MICs of various antibiotics. In several instances, this increase in MIC has been associated with reduction in drug uptake. Furthermore, heterologous expression of *M smegmatis mspA* accelerated the growth and increased the susceptibility of *M. tuberculosis* and *M. bovis* BCG to various classes of antibiotics (136). This establishes the relationship between porin function, small molecule and nutrient uptake, and drug susceptibility in *M. smegmatis.*

Porins are only minor proteins in the mycobacterial cell wall unlike enterobacterial porins which are the most abundant proteins in the cell (136, 230). Direct counting of stained pores by electron microscopic analysis revealed a 45-fold lower number of MspA pores on the outer membranes of *M. smegmatis* when compared to pore counts of the outer membranes of Gram-negative bacteria (161). The octameric MspA porin consists of two consecutive hydrophobic β-barrels, a more hydrophilic globular rim domain, and a single central channel of 9.6nm in length. This porin is largely embedded into the cell membrane of *M. smegmatis* with the embedded region including a portion of the hydrophilic rim domain (135). Crystal structures revealed that the constriction zone of MspA is rich in aspartate residues. Together with the high number of negative charges in the vestibule and channel interior, this could explain the cation preference of MspA (160).

1.3.3.2 OmpATb of *M. tuberculosis*

OmpATb was the first porin protein suggested for *M. tuberculosis.* Encoded by the *rv0899* gene, the name OmpATb was coined because of its homology to the *E.coli* porin OmpA (207). A study by Teriete *et al* showed that Rv0899 does not form a transmembrane β-barrel, but a mixed α/β globular structure encompassing two independently folded modules which correspond to the B and C domains of the protein. The core of this B domain appears hydrophobic while its exterior is both polar and acidic (228). Altogether, this proposed structure for OmpATb makes it unlikely for it to function as a porin. More recent structural elucidation by Yang *et al.* suggests that OmpATb forms a heptameric ring complex, driven by interactions between the α/β structured monomers, and is hypothetically capable of inserting itself into a biological membrane and form channels (246), allowing ion diffusion as observed in vitro. This model is based on NMR data of minor oligomeric populations of OmpATb in solution, and lies in contrast with available data suggesting the lack of functional porin assembly *in vitro* (217).

OmpATb plays a key role in conferring *M. tuberculosis* the ability to survive under acidic conditions. Deletion mutants in *ompATb* exhibit a significant reduction in permeability to several hydrophilic molecules and impaired ability to grow at reduced pH. The role of OmpA in acid resistance was reinforced by the observation of increased *ompATb* transcription levels in *M. tuberculosis* growing within macrophages, given that vacuole acidification is known to occur in infected phagocytes (196). More recent functional studies revealed no obvious porin activity of OmpATb. Rather, chemical analysis of low-pH *M. tuberculosis* culture filtrates showed that OmpATb is involved in rapid ammonia secretion capable of neutralizing medium pH and restoring exponential bacterial growth. This is further substantiated by the discovery that Rv0899-like proteins are present predominantly in bacteria with functions in nitrogen fixation and metabolism (139). OmpATb-mediated ammonia extrusion may be one of the multiple adaptations of *M. tuberculosis* to acidic environments and, on its own, is not critical for virulence in mice (217). The porin function of OmpATb in *M. tuberculosis* clearly remains a controversial issue.

1.3.3.3 Other porins of *M. tuberculosis*

MspA is understood to share its amphiphilic beta-barrel structure and potential to be secreted with outer membrane proteins (OMPs) of gram-negative bacteria. Based on these properties, bioinformatics approaches have led to the prediction of several OMPs of *M. tuberculosis* (133, 218). One such attempt has led to the identification of Rv1698 and Rv1973. Both proteins have been proven to localize to the outer membrane (218). Since then, the channel-forming activity of Rv1698 has been successfully characterized; *Rv1698* expression has proven to restore sensitivity of MspA-deletion mutants of *M. smegmatis* to ampicillin and chloramphenicol, and complement the permeability defect of the mutant for glucose. Single homologues of Rv1698 are found only

in mycolic-acid containing bacteria belonging to the suborder Corynebacterineae of the Actinomycetales, which includes mycobacteria. It therefore represents the first protein identified as specific for this suborder (214). Orthologous porins PorM1 and PorM2 have since been characterized in *M. fortuitum* (209).

Interestingly, *M. tuberculosis* does not express the Msp-like porins that are found in faster-growing *M. smegmatis* (161). This and other significant differences between the pathogenic and saprophytic mycobacterial species call into question the appropriateness of *M. smegmatis* as a model organism for anti-tuberculosis drug discovery and virulence studies of *M. tuberculosis* (14).

1.3.3.4 Porin-mediated Drug Uptake

Table 3 summarizes several biophysical characteristics of mycobacterial and other bacterial porins. Single-channel conductance often provides an estimation of channel diameters of porins, and gives an indication of the relative mobilities of solutes through them. It can be observed from Table 3 that some proportionality exists between channel width, channel conductance and size exclusion limits. If OmpATb of *M. tuberculosis* does indeed form functional porin units, this trend would place its limit in the approximate range of 600 – 800Da. This implies that the rifamycin and macrolide classes are too large to utilize OmpATb to transverse the cell wall. Danilchanka *et al* attempted to illustrate the fit of a drug when oriented along their longest axes within the MspA porin constriction zone by using 3D structure visualization and surface representations of structural models of antibiotics. They predicted that ampicillin, chloramphenicol and norfloxacin are able to utilize this porin molecule, as opposed to antibiotics such as erythromycin, kanamycin and vancomycin (61).

The specific role played by porins in intracellular drug accumulation within other bacterial species has been well studied. The outer membrane porin protein OprD of *Pseudomonas aeruginosa* has been directly implicated in the influx of imipenem; a staggering 98% of imipenem- and meropenem-resistant *P. aeruginosa* clinical isolates have been identified as being negative for OprD porin production (155). Similarly, studies on expression levels of the porin protein OmpF in clinical isolates of *E. coli* have linked the decreased expression levels of this porin with resistance to quinolones (109, 225). In such enterobacterial pathogens, the reduction in the number of functional porins per cell is due to a decrease or complete shutdown of synthesis, or the expression of an altered porin, and that these changes bring about decreased susceptibility to antimicrobials and favor the acquisition of additional mechanisms of bacterial resistance (65). Changes in the expression levels of functional porins should therefore be viewed as potential contributing factors in the development of resistance in mycobacteria.

In conclusion, porins appear to be less varied and less abundant in mycobacteria than in other bacterial families such as the enterobacteriaceae, though the possibility remains that we have only detected a small fraction of the total mycobacterial porin panel. The wide range of metabolic and physiologic adaptations seen in *M. tuberculosis*, combined with the generally complex regulation of porin expression in other species, suggest that *M. tuberculosis* may have likewise exploited porin modulation as a strategy to fence itself off from harmful small molecules.

Table 2 Summary of specific drug transport activities of mycobacterial porins. Information is limited to Msp porins of *M. smegmatis*. In all instances, porin-deletion mutants were used to determine drug transport specificity; the extent of dependence of individual drugs on porin transport is exemplified by fold-reduction in drug uptake and fold-increase in MIC.

Species	Deleted Porin	Drug	Fold-reduction in Drug Uptake	Fold-increase in MIC	Ref.
M. smegmatis	MspA & C double deletion	Ampicillin	-	16	(59)
		Cephaloridine	-	8	
		Chloramphenicol	1-2	4	
		Norfloxacin	4	2	
	MspA	Ampicillin	-	16	(220)
		Cephaloridine	9	8	
		Vancomycin	-	10	
	MspA	Cephaloridine	9	-	(219)

Table 3 Biophysical characteristics of OmpATb from *M. tuberculosis* and porins from other selected bacterial species. Exclusion limits were determined based on the uptake of saccharides of varied weight.

Species	Porin	Channel Width (nm)	Single-Channel Conductance (nS)	Exclusion Limit (Da)	Ref.
M. tuberculosis	OmpATb	1.4 - 1.8	0.7	Undetermined	(207)
M. smegmatis	MspA	2.2 – 2.4	4.6	Undetermined	(79,)
E. coli	OmpA	0.6 - 0.7	0.14 (at 37°C)	550*	(22, 156, 200)
	OmpF	1.2	0.82		
P. aeruginosa	OprF	2.2	5	6000	(20, 90)
S. typhimurium	Not specified	1.4	2.3	700	(21, 156)

1.3.3.5 Polyamines

Polyamines are ubiquitous polycationic molecules found in all living organisms. The four most common polyamines are putrescine, cadaverine, spermidine and spermine **(Figure 6).** Larger linear and branched-chain polyamines have been detected in a variety of cell types. Apart from being water-soluble, all polyamines are positively charged at physiological pH.

1.3.3.5.1 Biosynthesis and Excretion

All cell types have the ability to synthesize putrescine, cadaverine and spermine. Spermidine production, however, appears to be limited to animals, plants and some species of fungi, archaea and bacteria (178). Polyamine biosynthesis begins with the conversion of arginine to ornithine. In mammals and fungi, ornithine decarboxylase converts ornithine to putrescine. An alternative pathway exists in micro-organisms and some plants where putrescine is formed via the production of agmatine. The cytoplasmically-located spermidine synthase transfers an aminopropylic group to putrescine, producing spermidine. Spermidine is then converted to spermine by spermine synthase by the addition of a second aminopropylic group (151). Cadaverine, on the other hand, is synthesized from lysine in a one-step reaction with lysine decarboxylase. These biosynthetic pathways have been illustrated in **Figure 7.** Polyamines can also be taken up from the medium. Polyamine uptake in *E. coli* has been found to take place both by energy-dependent and -independent absorption (221).

In *E. coli*, the intracellular concentration of spermidine is believed to reach approximately 6mM, with 90% bound to RNA. Intracellular concentrations of putrescine, on the other hand, have been known to reach 20mM under normal conditions, with the potential to be further increased under

acidic conditions (16). Since only 40% of all intracellular putrescine is bound to nucleic acids, increased biosynthesis due to stimulation is believed to lead to excretion of the polyamine. Putrescine transporter PotE is also inducible and has been shown to facilitate both uptake and excretion processes. Putrescine excretion is suggested to facilitate survival under conditions of low pH and osmotic up-shock. Cadaverine is similarly excreted under acidic conditions via the membrane-bound lysine-cadaverine antiporter CadB (203).

Figure 6 Molecular structures of the four key polyamines in animals, plants and micro-organisms: spermidine, spermine, cadaverine and putrescine.

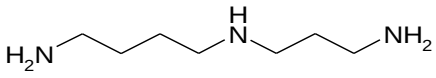

Spermidine

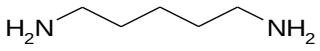

Cadaverine

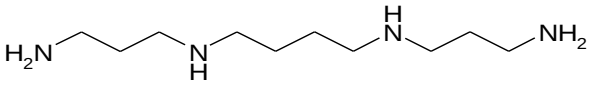

Spermine

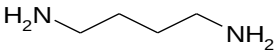

Putrescine

Figure 7 (A) The biosynthetic pathway of putrescine, spermidine and spermine as illustrated by Morgan *et al* (151). (B) The biosynthetic pathway of cadaverine. The enzymes indicated are as follows: (1) arginase; (2) ornithine decarboxylase; (3) arginine decarboxylase; (4) agmatinase; (5) agmatine deiminase; (6) *N*-carbamoylputrescine amidase; (7) *S*-adenosylmethionine decarboxylase; (8) spermidine synthase; (9) spermine synthase; (10) spermidine/spermine N^1-acetyltransferase; (11) polyamine oxidase; (12) lysine decarboxylase.

A

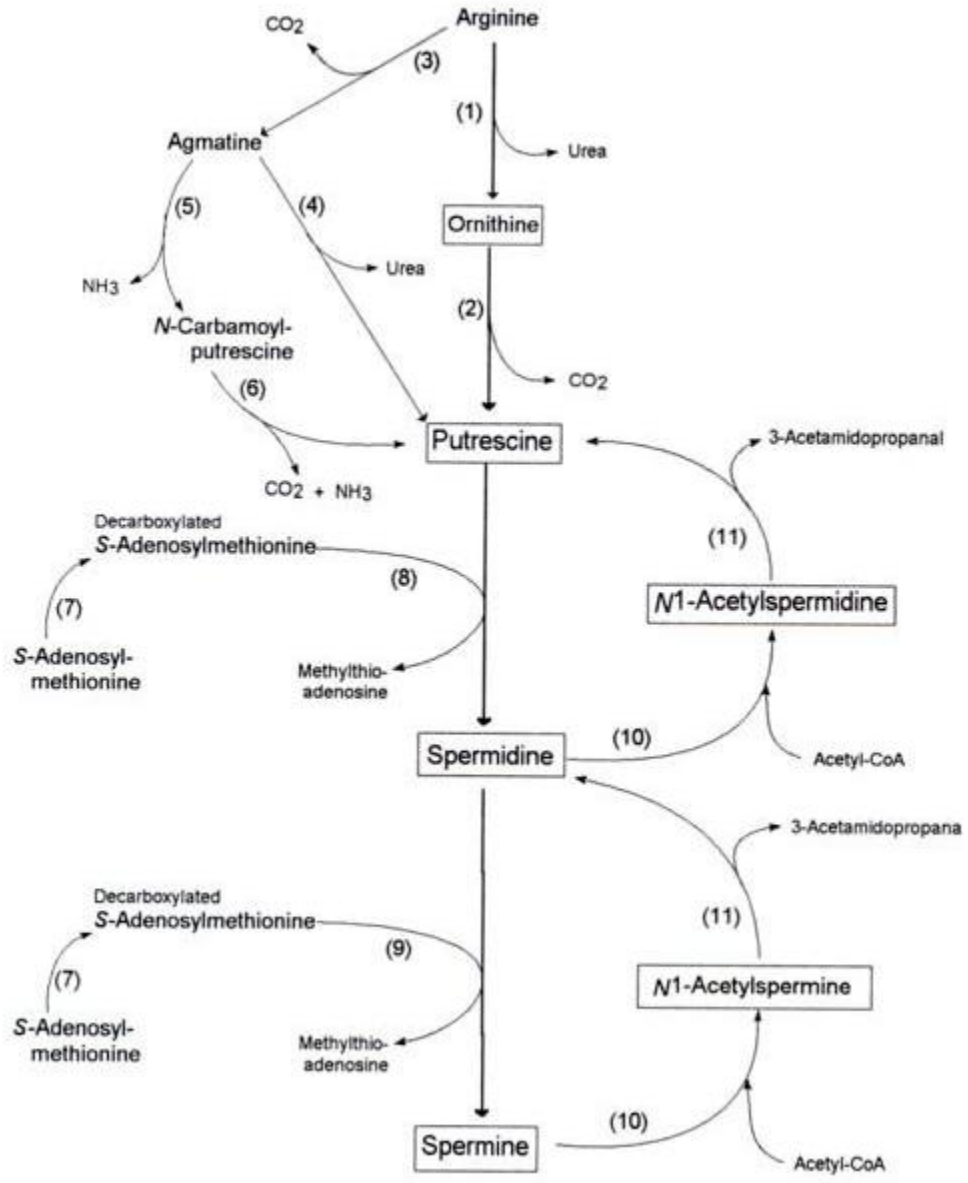

B

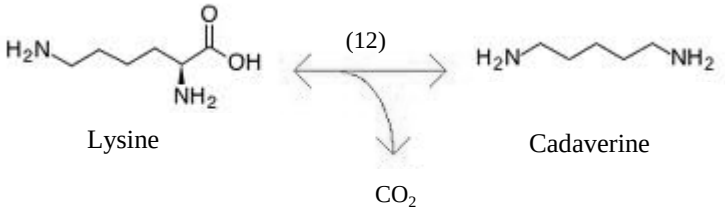

1.3.3.5.2 Functions

Although it remains unclear what the specific roles of polyamines are, we know that they are necessary for optimal growth and replication of almost all cell types. In mammalian cells, polyamines influence transcription and translation, and perform as intracellular messengers. In plants and insects, polyamines are precursors and constituents for many compounds such as alkaloids and toxins respectively (151).

The effects of four polyamines (spermine, spermidine, cadaverine and putrescine) on the activity of OmpC and OmpF have been documented. Electrophysiological techniques such as patch-clamping have been used to study the modulation of these *E. coli* porins. These polyamines were shown to suppress channel opening, enhance channel closure as well as promote the inactive state (103). delaVega and Delcour explain that although the possibility of steric blocking of the open porin channel cannot be excluded, it is more likely that the binding of polyamines to sites within the transmembrane field brings about conformational changes in the protein that promote the prolonged occupancy of the closed state (71). The positive charge of polyamines is crucial for its mode of action given that their inhibitory effects are relieved at higher pH. Also, these small molecules exert their effects on pore proteins allosterically, by increasing the frequency of cooperative closures in trimeric OmpC and OmpF (71).

Thus far, little data is available regarding the *in vitro* effects of polyamines on the uptake of antibiotics in *E. coli*. Spermidine has been shown to reduce norfloxacin and β-lactam diffusion through OmpF and cadaverine has been shown to reduce ampicillin susceptibility in *E. coli* (45, 70, 202). Norfloxain uptake in *E. clocae* specifically is drastically altered in the presence of spermine and almost completely inhibited by high concentrations of the polyamine (45). We hypothesize that polyamines may therefore act as pore-modulators in the presence of porin-utilizing antibiotics, and may reduce the overall penetration rate of these agents in mycobacteria as well.

1.3.3.5.3 Induction

Studies show that a decrease in pH stimulates *cadA* transcription and, hence, cadaverine production and excretion (16). It is now understood that the environmental sensor CadC binds to the promoter region, inducing the *cadBA* operon in *E. coli*. Researchers found that the addition of exogenous cadaverine allows wild-type *E. coli* cells to better survive a 30min exposure to pH3.6 when compared to mutant cells expressing cadaverine-insensitive OmpC. Although long-term secretion of the polyamine leads to some neutralization of the acidic environment, cadaverine brings about a more rapid decrease in outer membrane permeability via enhanced porin closures. It has therefore been suggested that the excretion of cadaverine to inhibit porin-mediated chemoflux represents a novel mechanism that provides bacteria with the ability to survive acidic pH (203).

1.4 Phenotypic drug tolerance

1.4.1 The NRP state

Non-replicating persistence (NRP) is defined as the physiological state of bacteriostasis in addition to metabolic, chromosomal and structural changes in the bacilli that enable the conservation of energy (239). Sufficient evidence has emerged for long-term NRP of *M. tuberculosis* in the human host within tuberculous granulomas and necrotic lesions in pulmonary tissue. Nutrient limitation and hypoxic conditions within granulomas trigger the shut-down in central metabolism that shifts subpopulations of bacilli to dormancy (81). Several *in vitro* models have been developed thus far to mimic these conditions of hypoxia and nutrient starvation (24, 82, 238). Studies have shown that the NRP state brings about phenotypic resistance to anti-tuberculous agents, contributing to the challenge of effective disease control (247). Ofloxacin and the sulbactam-ampicillin combination, for example, have shown reduced activity on stationary-phase cultures of *M. tuberculosis* (94). While rifampicin, streptomycin, moxifloxacin and isoniazid are highly bactericidal for actively-replicating *M. tuberculosis*, they have little or no effect on the viability of nutrient-starved cultures (24, 69). The MBC_{90} of rifampicin increased 50 and 2500 times under conditions of oxygen- and nutrient-starvation respectively, and isoniazid's cidal activity was completely lost on *M. tuberculosis* cultured under both conditions for concentrations up to 100μM (82). In another study where 17 agents were tested against nutrient-starved *M. tuberculosis* at concentrations up to 160μM, only 4 were able to achieve 99% killing (MBC_{99}), and only when considerably higher test concentrations were used than against growing bacteria (245).

It has been suggested that, because anti-tuberculous agents typically target functions essential for growth and replication, they are less effective at eradicating NRP tuberculosis (81). However, it is also believed that NRP bacilli develop alterations in their cell wall that affect permeability to antibiotics. Ziehl-Neelsen staining of *M. tuberculosis* in lung sections gradually fades with the persistence of an infection (206). The progression to the Ziehl-Neelsen-negative state is the result of cell wall composition alterations upon the onset of dormancy. Further studies are underway to understand the mechanisms driving the loss of acid-fastness.

NRP conditions lead to induction of the 'dormancy regulon', a collection of at least 48 genes that are controlled by the dormancy survival regulator DosR (28, 29, 172). Under conditions of oxygen starvation, *M. tuberculosis* displays activation of several transport mechanisms including the up-regulated expression of predicted transporters for metal cations (*ctpA* and *ctpV*), sulphate (*Rv1739c*, *cysW*), molybdate (*modA*) and peptides (*dppA*) (154). In a separate study, nutrient starvation caused phosphate uptake proteins (PstA1, PstB, PhoS1 and PstA2) to be down-regulated, and sulphate transport system proteins (CysA, CysW, CysT and SubI) to be up-regulated (24). The regulation of expression of efflux pumps with antibiotic substrates under NRP conditions is still unclear. However, it is understood that the inactivation of Tap (Rv1258c), a known tetracycline efflux pump (188), in *M. bovis* BCG during stationary phase triggers a stress response that leads to a downshift in cell wall biosynthesis because of the accumulation of an unknown toxic substrate. This emphasizes that Tap is essential for the maintenance of balanced physiological function in the late stationary phase and indicates the potential role for the efflux pump during latency (190).

In bacterial species where it has been extensively studied, the regulation of porin expression has proven to be a fine-tuned and complex phenomenon modulated by multiple factors (66). It is

tempting to hypothesize that reduced porin density may contribute to the development of phenotypic drug tolerance in *M. tuberculosis*. Ongoing studies by our group aim to understand how starvation conditions affect the intracellular concentrations of standard anti-tuberculosis drugs in quiescent *M. tuberculosis* bacilli.

1.4.2 Cell wall thickening

Recent ground breaking studies using cryo-electron tomography (CET) have revealed that the mycobacterial outer membrane is a symmetrical bilayer and might be less thick than generally believed in actively growing *M. smegmatis* and *M. bovis* BCG (98, 253). Cell wall thickening of the bacilli upon the onset of dormancy has been suggested based on transmission electron microscopy (TEM) studies and would have important implications on the persistence of *M. tuberculosis*. Caution should be exercised when interpreting TEM images, since electron microscopy analyses of ultrathin sections are performed with specimens from which water had been removed, a prerequisite for electron microscopy observation at room temperature. Consequently, water-soluble molecules may aggregate and lipid molecules may be prone to extraction or rearrangement by organic solvents during dehydration. This said, comparative analysis by TEM of *M. bovis* BCG and *M. tuberculosis* cultured under aerobic, micro-aerobic and anaerobic conditions revealed significant homogenous thickening of the cell wall in non-replicating quiescent bacilli (58). More recently, thickening of the cell wall was observed in anaerobically grown quiescent *M. tuberculosis*, this time using atomic force microscopy (234). Though these observations await confirmation in vitro and in vivo, as well as in-depth biochemical and structural analysis, a reinforced cell wall may constitute an additional

permeability barrier, at least for some drug classes. Because porin dimensions and channel lengths presumably remain static despite these external changes, porin channels may not be able to span the depth of the thickened cell wall, thereby causing reduced access to the channel entrance by small molecules.

1.4.3 Intracellular *M. tuberculosis*

As is the case for many bacterial pathogens, *M. tuberculosis* is phagocytosed by macrophages via the process of endocytosis. Some strategies for surviving the hostile intracellular environment of macrophages include the inhibition of phagosome-lysosome fusion and the inhibition of phagosome acidification (145, 236). In a recent elegant study, induction of drug tolerance in intracellular mycobacteria was attributed to macrophage-induced bacterial efflux mechanisms (1). By using *M. tuberculosis*-infected cultured macrophages and *M. marinum*-infected zebrafish, the authors have shown that drug-tolerant bacteria arose within individual macrophages soon after infection and prior to granuloma formation. In contrast with the prevalent dogma, this drug tolerance was associated with a replicating intracellular bacterial population rather than macrophage-induced stasis. The study further showed that bacterial efflux pumps such as rifampicin-specific Rv1258c were induced upon macrophage infection, mediating drug tolerance. Interestingly, this drug tolerance was found to be retained for a period of time after bacteria resumed extracellular growth. Efflux pump P55 plays a significant role in *M. bovis* replication and persistence in the macrophages. It is functionally connected to P27 of the same operon (IprG-Rv1410c). The *p27-p55* knock-out mutation in *M. bovis* severely compromises virulence and intracellular replication (26).

M. tuberculosis also seems to have evolved a strategy to protect itself from mildly acidic conditions encountered within the macrophage phagosome, through the closing of OmpATb at low pH (149). *M. tuberculosis* porins are thought to be the key proteins for the uptake of small hydrophilic drugs, such as isoniazid, pyrazinamide and ethambutol, three out of the four current first line anti-tuberculosis drugs. Though porin function remains to be demonstrated for OpmATb, one interesting implication of its pH-mediated closure is the likely negative effect on the penetration of small hydrophilic drugs into lysosome-engulfed bacilli, leading to enhanced drug tolerance in these quiescent populations.

1.5 Specific Drug Accumulation in *M. tuberculosis*

In the hunt for novel anti-tuberculosis drugs, the physico-chemical properties driving cell wall permeation by chemotherapeutic agents remain a critical but largely unsolved question. **Table 4** lists biological and molecular properties of selected anti-TB agents, compiled in an attempt to detect correlation trends between intracellular accumulation and physico-chemical properties. The level of drug accumulation within *M. tuberculosis* cells varies significantly between drug classes but drawing comparisons between them is difficult due to differences in experimental methods used to measure accumulation. Intracellular concentrations of the fluoroquinolones listed were determined by measuring their fluorescence in cell lysates (182). Pyrazinamide, isoniazid and rifampicin intracellular concentrations were calculated from scintillation counts of radio-labeled compounds in whole-cell preparations (12, 183, 191), which includes cell wall-associated drug content. This results in a possible overestimation of intracellular drug concentration. In the study of efficacy of drugs targeting cytosol-localized proteins, only the drug content of the cytosol compartment is of concern. This provides a possible explanation as to why *M. tuberculosis* intracellular rifampicin concentrations determined by mass-spectrometric analysis of cell lysates in our lab are much lower than those listed here.

Molecular weight is often speculated to be an important determinant of the rate of diffusion and cell wall permeation; the smaller the compound the higher the rate of passive diffusion (123), while ClogP, a measure of the hydrophobicity / lipophilicity of a compound, reflects partitioning into the hydrophobic phase of the cell wall (80). Attempts to plot these parameters as a function of intra-bacillary accumulation failed to reveal any significant correlation **(Figure 8),** consistent with the growing realization that many anti-TB agents lie outside the drug-like chemical space (113). Weak correlations hinted that smaller and more hydrophilic drugs accumulated

intracellularly more efficiently. These observations may support the hypothesis that diffusion through porins serves as a route of transport across the mycobacterial cell wall for this class of compounds. Altogether, weak correlations are very likely due to the fact that many of these anti-tuberculous agents are transported via a combination of pathways. This analysis is also limited by the small number of drugs included and the fact that we attempted to compare physico-chemical properties across different compound classes. The intracellular concentrations of pro-drugs that require enzymatic activation are not always reflective of their potency; the intracellular concentration of active metabolites may be more relevant in the cases of isoniazid and pyrazinamide.

Pyrazinamide appears to accumulate 6-fold within the bacilli. Its transport has been determined as being ATP-dependent and reliant on the nicotinamide transport pathway (191). However, the other drugs listed that accumulate intracellularly above the extracellular concentration have been speculated as being passively taken up by mycobacteria. In the case of isoniazid which accumulates 4-5 times within *M. tuberculosis*, the calculated accumulation factor should be more accurately described as the cellular content of radioactive derivatives of isoniazid. Constant conversion by KatG ensures a consistent pro-drug concentration gradient between the intracellular and extracellular compartments, driving intracellular accumulation of isoniazid (12). Fluoroquinolones appear to concentrate within the intracellular compartment despite being un-metabolized. The ability to concentrate a drug within the intracellular environment of *M. tuberculosis* should reflect the presence of active drug importers which have yet to be identified.

In conclusion, there is no simple formula linking physico-chemical parameters to intracellular accumulation of small molecules in *M. tuberculosis*. As mentioned above, the contribution of a variety of passive and active mechanisms of uptake and efflux precludes the use of a simple

equation to solve this question. Further studies focusing on relatively large numbers of molecules within the same chemical scaffold should help identify the major determinants of uptake for a given class of small molecules or therapeutic agents.

Table 4 Physico-chemical properties and intracellular accumulation factors of several antibiotics in *M. tuberculosis* as previously reported. Intracellular accumulation factors were defined as the ratio between intracellular and extracellular drug concentrations.

Antibiotic	Molecular Weight	CLogP*	PSA ($Å^2$)*	Target	IC_{50} (mg/L)	MIC_{90} (mg/L)	Accumulation Factor[a]	Hypothesized Transport Mechanism	Ref.
Pyrazinamide	123.12	-0.676	68.87	Fatty acid sysnthase I[b]	N.A.	16 – 50 (pH5.5)	5.4 – 6.2	ATP-dependent	(191, 249)
Isoniazid	137.14	-0.668	68.01	Enoyl-acyl carrier protein reductase	N.A.	0.02 – 0.2	4 – 5	Passive Diffusion	(191,249)
Ciprofloxacin	331.35	-0.725	77.04	DNA Gyrase	3.2 (*M. smeg*)	1.0	3.3 – 4.1	Passive Diffusion	(86, 182)
Levofloxacin	361.38	-0.508	77.48	DNA Gyrase	3.0 (*M. smeg*)	0.5	1.1 – 1.3	Passive Diffusion	(182) (86)
Ofloxacin	361.38	-0.508	77.48	DNA Gyrase	7.9 (*M. smeg*)	0.5	2.2 – 2.7	Passive Diffusion	(86, 182)
Norfloxacin	319.34	-0.780	77.04	DNA Gyrase	Information unavailable	2	1.8 – 2.2	Passive Diffusion	(182)
Moxifloxacin	401.44	-0.082	86.27	DNA Gyrase	Information unavailable	0.5	1 – 1.3	Passive Diffusion	(182)
Ethambutol	204.32	0.119	64.52	Arabinosyl-transferase	Information unavailable	1 - 5	<1	Passive Diffusion	(18,249)
Rifampicin	822.96	3.710	220.15	RNA polymerase	0.07 (*M. avium*)	0.05 - 1	22.3 – 27.1	Passive Diffusion	(182)

[a] Assuming cellular volume of 2.4 – 3.0µl per mg dry weight(12, 191); [b] See also work by Zhang *et al* where an alternative mode of action for pyrazinamide is proposed (248); *CLogP and PSA were calculated by the cheminformatics profiling program InSilico Profile (v4.1)

Figure 8 Correlations between intracellular drug accumulation factors and (A) molecular weight, (B) ClogP or (C) PSA for the anti-tuberculous drugs listed in Table 3 (excluding data from Rifampicin). Pearson's correlation coefficients (r) indicate the strength of correlations.

A

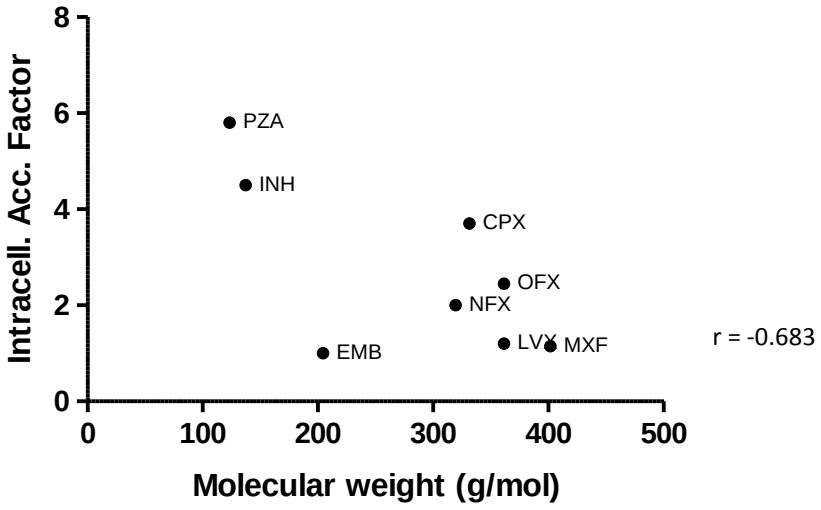

B

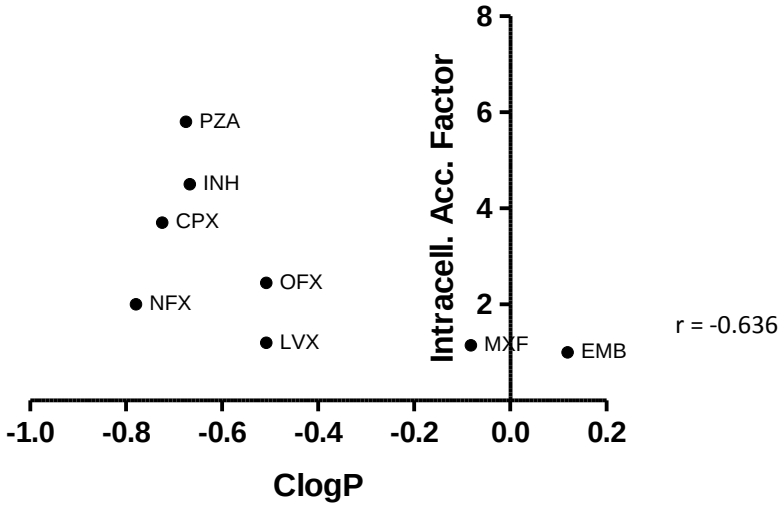

C

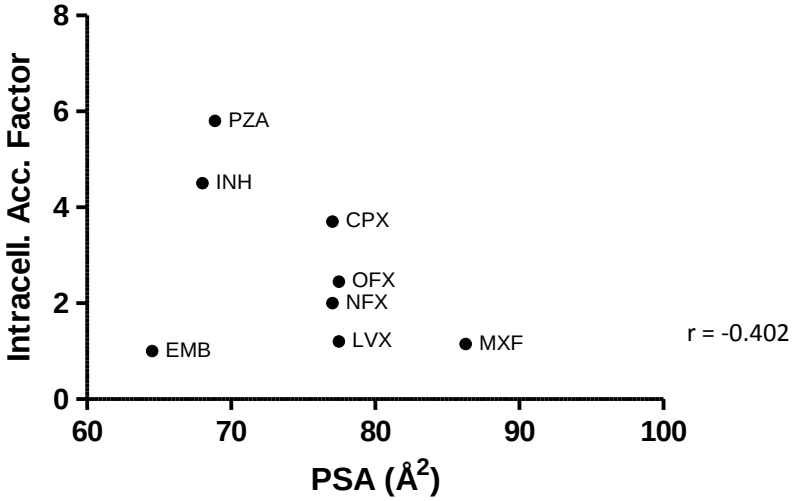
Intracell. Acc. Factor
8
6
4
2
0
60
70
80
90
100
PSA (Å2)
PZA
INH
CPX
OFX
NFX
LVX
MXF
EMB
r = -0.402

1.6 Measuring Drug Uptake in Mycobacteria

Because a significant proportion of drug targets are located in intracellular compartments, the measure of intracellular accumulation of a drug is often regarded as an estimation of the efficacy of a drug. It is believed that the lack of permeability of the mycobacterial cell wall is significant limiting factor to the efficacy of anti-tuberculous agents. Several experimental methods to quantify intracellular drug accumulation in both prokaryotic and eukaryotic cells have been developed. The resilience of the mycobacterial cell wall, however, compounds the difficulty of cell lysis and cytosol extraction.

1.6.1 *M. bovis* BCG as a model for the study of *M. tuberculosis*

Being highly pathogenic, the study of *M. tuberculosis* is often hindered by policy and infrastructure. The BSL3 containment that is required for working on this pathogen imposes logistical constraints. Added to the facts that is has a generation time of 24 hours and it takes 3-4 weeks to yield colonies on agar plates, it seems pertinent to use a faster-growing non-pathogenic mycobacterial species as surrogate models. Reyrat and Kahn argued for the use of *M. smegmatis* as an appropriate model on the basis that it shares homologues of numerous virulence genes in *M. tuberculosis* (192). It offers the technical benefits of being fast-growing (2-3 hour generation time) and bearing negligible risk to laboratory workers. It offers the additional advantage of being similarly able to successfully adapt to oxygen limitation in *in vitro* models of dormancy (232). This opinion is, however, not shared universally because *M. smegmatis'* complete lack of virulence and its inability to survive within macrophages indicate that any use of comparative biology should be interpreted cautiously (13).

Being an attenuated strain of the live bovine tuberculous bacillus (*M. bovis*), BCG is a biosafety level 2 surrogate that bears over 99.9% genetic similarity to *M. tuberculosis*. Both are members of a group of highly-related mycobacterial species called the *M. tuberculosis* complex (34). Molecular analysis of the genetic differences between the two species revealed that the loss of virulence by BCG is due to the deletion of several regulatory sequences that repress protein expression. Controlled expression of these genes may be necessary to prevent the display of immunogenic proteins to the immune system so as to disrupt clearance of the infection in the host (134).

Both *M. smegmatis* and BCG were evaluated as drug discovery models by conducting chemical library screens to identify anti-mycobacterial compounds. BCG proved to be more sensitive model in these library screens; 50% of the compounds detected as having inhibitory activity against *M. tuberculosis* were not identified in the screen with *M. smegmatis*. This is compared to 21% with BCG. One reason for this difference is that 30% of *M. tuberculosis* proteins do not have conserved orthologues in *M. smegmatis*. Only 3% of such proteins are absent in BCG (5). BCG bears the additional advantage of being able to persist and multiply within host macrophages by way of survival mechanisms mentioned earlier in this review. This makes it ideal for use in macrophage infection models which help us understand this adaption. It is also shifts down to a persistent state during oxygen depletion in a manner similar to what has been observed with *M. tuberculosis* (121). BCG is, therefore, widely accepted as the most effective surrogate for tuberculosis.

1.6.2 Experimental Methods for Quantification of Intracellular Drug Accumulation

The most established method thus far involves the use of radio-labeled compounds. Cultures are incubated with [H^3]- or [C^{14}]-labeled compounds and scintillation counting is performed on whole-cells without any attempt at cell lysis. This method has been used to calculate cellular uptake of isoniazid, pyrazinamide, rifampicin and ethambutol (12, 18, 183, 191). While radiolabelled probes allow for accurate estimation of cellular uptake, they are expensive to produce and dangerous to handle. Also, scintillation counts do not distinguish between pro-drugs and their metabolized forms.

With compounds that are natural fluorophores, the measurement of fluorescence using excitation and emission wavelengths specific to each compounds provides an alternative to radio-labeling them. This is an especially common method of quantifying fluoroquinolone uptake in bacterial cells (43, 61, 243). These assays include the lysis of cells to release their intracellular contents before quantification of drug content. Fluorometric methods, however, have to take into account the presence of background-fluorescence that most likely results from the presence of porphyrins in mycobacteria (57). The use of this method is unfortunately limited due to the lack of fluorescent moieties in many antibacterial compounds.

A more seldom-used method of drug uptake quantification involves a microbiological assay where dilutions of cell lysates are applied to filter paper discs which are subsequently transferred onto agar plates containing *E. coli* cultures. The drug content on the discs causes inhibition of bacterial growth; the diameters of these zones of growth inhibition are a measure of cell lysate drug concentrations. Standard curves can be generated using discs with known concentrations of

the drug. The microbiological assay has been used to quantify fosmidomycin uptake in *P. aeruginosa* (36). This method is tedious and results in low-throughput analysis.

More advanced assays for the quantification of intracellular drug accumulation include the use of liquid chromatography- mass spectrometric methods (LC/MS). LC/MS-based methodologies are more sensitive and specific than their counterparts. The use of specific MRM (multiple reaction monitoring) transitions for each analyte means that such assays are not limited to specific compound- classes. Rapid turnaround of LC/MS analysis also allows for the drug penetration assays to be conducted in a medium-throughput manner.

1.6.3 Experimental Methods for Lysis of Mycobacterial Cells

For the purposes of accurate measurement of intracellular drug quantification, bacterial cells should be lysed and lysates drug content should be distinguished from the level of drug absorption onto the surface of the outer membrane. The highly resilient mycobacterial outer membrane often requires the use of harsh methods of disruption in order to achieve cell lysis. These disruption methods can be classified as being of mechanical, enzymatic, or chemical natures. Mechanical disruption techniques include the use of high pressure (French press), bead-beating (with glass / zirconium beads) or probe-sonication. Lysozyme is a commonly used enzyme in mycobacterial cell lysis buffers. For the purposes of fractionation of mycobacterial cellular compartments (cell wall, cell membrane and cytosol), Rezwan *et al* found that probe-sonication combined with lysozyme treatment produced the best results with outer membrane disruption (193).

In a comprehensive study of disruption methods for the purpose of mycobacterial proteome extraction, Lanigan *et al* compared the effectiveness of bead-beating and sonication. Protein concentrations and two-dimensional gel electrophoresis of mycobacterial lysates were used to evaluate the effectiveness of disruption techniques. Although both methods provided similar representations of mycobacterial proteomes, bead-beating was picked as the preferable method for rapid and effective proteome extraction. Open-tube sonication of pathogenic mycobacterial species with microprobe tips brings with it the associated risk of aerosol formation (116). Homogenization by bead-beating is often advised as the best method for isolation of genomic DNA, though this high-velocity mechanical process results in some shearing of DNA (19, 250). Several protocols detail the use of detergents such as Triton X-100 and SDS (sodium dodecyl sulphate) to further increase the effectiveness of permeabilization of the outer membrane (47). The use of detergents is, however, incompatible with LC-MS analytical methods as they suppress the ionization process (6). Several studies suggest the use of glycine hydrochloride (pH3) to lyse mycobacteria and the efficiency of this procedure has been assessed by transmission electron microscopy. Cell lysis by this method requires an overnight incubation period with agitation (on a shaker) at 37°C (57, 61, 243).

1.7 Study Rationale

The standard treatment of tuberculosis infections requires the use of multiple drugs simultaneously for a minimum of 6 months. The success of the treatment regimen is variable and is partly dependent on the permeability of the drugs at three different levels: penetration in pulmonary tissue and lesions (63, 110), penetration in macrophages (73, 150, 215), and penetration in *M. tuberculosis* bacilli. Anti-tuberculous agents remain distinct from other anti-bacterials because they generally do not follow Lipinski's 'rule of 5' which defines the properties of a compound that makes it a likely drug candidate (113). The large disconnect between drug potency *in vitro* (target-based screens) and potency *in vivo* has led to much frustration with numerous recent anti-tuberculosis drug discovery projects (177). Whole-cell screens, however, have had relatively more success in churning out new drug candidates (ie. TMC207, PA-824) (74). Taken together with our knowledge of the mycobacterial outer membrane (see Chapter 1), we understand that permeation is a significant limiting factor for drug efficacy in *M. tuberculosis*.

The development of a standard assay for assessing drug permeation of *M. tuberculosis* is well-overdue. A drug permeation assay would facilitate the study of transport processes of the mycobacterial outer membrane, and the understanding of mode-of-action of existing anti-tuberculous compounds. If included as part of standardized testing for drug discovery molecules, permeation data could also help optimize for drug efficacy in the way elucidating structure-activity relationships (SAR) helps improve *in vitro* potency. Previous studies on drug permeation focused on the evaluation of assays for specific drug classes rather than for across-the-board testing in a medium-throughput manner. With this arises the need to use analytical methods that are not only sensitive, but also applicable to all compound-classes. Detection methods involving high-performance liquid chromatography (HPLC), coupled with mass spectrometric (MS)

techniques (LC/MS), have proved in recent years to be a valuable tool to bioanalysts developing highly sensitive assays for biological fluids. LC/MS techniques are now considered the method of choice for supporting pharmacokinetic studies (141). Therefore, a major objective of this study is the development and validation of an LC/MS -based drug penetration assay for *M. tuberculosis*.

In recent years, increasing attention has been paid to fluoroquinolones for being effective anti-tuberculous agents. Chemotherapeutic regiments containing fluoroquinolones are being tested in Phase II and III trials to shorten the duration of therapy from 6 – 9 months to just 4 months. Also, fluoroquinolones are now considered cornerstone drugs for the treatment of MDR- and XDR-TB (3). Unfortunately, resistance to fluoroquinolones is fast-emerging (2), especially due to its frequent prescription for simpler lower respiratory tract infections (3, 83). It has therefore become important for us to understand the mechanism of fluoroquinolone uptake and resistance-development in mycobacteria to mitigate against the inevitable demise of this class of drugs. Mutations on *gyrA* and *gyrB* do not account for all occurrences of resistance. Instead, additional causes such as decreased cell wall permeability and enhanced drug efflux pump mechanisms are being explored (83, 131).

The current understanding of fluoroquinolone uptake in mycobacteria is limited to observations of rapid, unsaturable uptake. Most studies imply that fluoroquinolones accumulation takes place via passive diffusion, while fewer studies have suggested that this diffusion is facilitated by porins (61, 243). Using our own validated drug penetration assay, we intended to characterize fluoroquinolone uptake in *M. bovis* BCG and *M. tuberculosis*. Unfortunately, the study of porin-mediated transport is restricted to the generation of porin knock-out mutants. This appears to be the limiting factor with species such as *M. tuberculosis*, which has yet to have unambiguously

identified and characterized porin proteins. Unlike active efflux pumps, there are no conventional inhibitors of porins which are used in uptake assays. The review of existing literature has brought to light the modulation of porin channel activity by endogenous polyamines in *E. coli* (203). We hypothesized that these polyamines could be applied exogenously to *M. tuberculosis* to effect inhibition of porin-mediated uptake, therefore bypassing the need to first identify the porin in question. Specifically, we aimed to examine the effects of polyamines on fluoroquinolone uptake. We also attempted to explore the possibility that *M. tuberculosis* self-modulates its porin channel activity via the production and secretion of endogenous polyamines. Such a study could potentially shed a whole new light on the study of mycobacterial transport processes.

The ability for *M. tuberculosis* to reversibly enter a non-replicating state when in the presence of unfavourable environmental conditions such as hypoxia and nutrient –starvation within lesions presents a daunting problem to the treatment process. The predictive values of current cell culture- and animal- models are insufficient as they do not reflect the difficulty of eradicating persistent tuberculosis infections in the human host. These 'persister' cells exhibit phenotypic drug resistance that is characterized by drastic down-shifts in antibiotic susceptibility (69, 82, 245). These shifts are believed to be the result of altered cell wall permeability. Cell wall–thickening and changes in the expression of cell wall components have been shown to occur in non-replicating *M. tuberculosis*. With a robust drug penetration assay at hand, we planned to definitively quantify differences in intracellular accumulation of fluoroquinolones and other agents between replicating and non-replicating cultures.

Taking our study a step further, we hoped to help identify if changes in expression or availability of specific porins may be responsible for the decrease in fluoroquinolone susceptibility of non-replicating *M. tuberculosis*. Several studies have already explored the role that porins play in

bacterial antibiotic resistance via mechanisms that include altered gene expression and modified protein products (89, 171). Clinical resistance to quinolones is already linked to decreased porin (OmpF) expression in *E. coli* (109, 225). Although scientists have not yet confidently identified a true porin of *M. tuberculosis*, bioinformatics approaches have churned out lists of putative porin proteins. We suggested that expression analysis of selected putative porins could help us better understand the drug permeability problems that non-replicating *M. tuberculosis* presents.

1.8 Study Objectives

1. **Develop and validate an a drug penetration assay for *M. tuberculosis* using *M. bovis* BCG as a surrogate model**
    - Compare fluoroquinolone recovery and loss between various cell lysis methods
    - Compare signal strength and matrix effects between lysates from different procedures
    - Exclude errors incurred by cell-surface drug adsorption
    - Validate the appropriateness of a fixed time-point for the assay based on the equilibration of accumulation and maintenance of cell viability
    - Assess accuracy and precision of our LC/MS analysis methods

2. **Characterize the process of fluoroquinolone uptake in *M. bovis* BCG**
    - Study the kinetics (time-course and saturability) of fluoroquinolone accumulation in BCG
    - Understand intra-class variation in intracellular accumulation by assessing the influence of various physicochemical properties
    - Attempt to competitively inhibit fluoroquinolone uptake with β-lactams and another fluoroquinolone
    - Understand the role played by active efflux mechanisms in fluoroquinolone accumulation
    - Explore the influence of external pH on fluoroquinolone accumulation and activity

3. **Study the inhibition of porin-mediated fluoroquinolone uptake in *M. bovis* BCG by polyamines**
    - Compare the efficacy of various polyamines as inhibitors of fluoroquinolone accumulation
    - Understand intra-class variation of fluoroquinolones in response to polyamines
    - Explore the effects of polyamines on non-fluoroquinolones
    - Understand specific characteristics of polyamine activity such as dose-, pH-dependence and reversibility
    - Investigate the hypothesis that exposure to exogenous polyamines can effect resistance to fluoroquinolones
    - Investigate the possibility that mycobacteria produce and secrete polyamines endogenously

4. **Understand the effect nutrient-starvation has on fluoroquinolone susceptibility and uptake in *M. tuberculosis***
    - Compare drug susceptibility between replicating and non-replicating cultures
    - Investigate whether shifts in susceptibility are due to changes in drug permeability by quantifying drug accumulation in non-replicating bacteria
    - Investigate the role of active efflux mechanisms in the acquisition of phenotypic drug resistance
    - Investigate the role of porin-mediated uptake in the acquisition of phenotypic drug resistance

5. **Study porin expression in non-replicating *M .tuberculosis***

    - Understand the effect on nutrient-starvation on the expression on various OMPs
    - Identify porins that are down-regulated during latency

CHAPTER 2

DEVELOPMENT OF A DRUG PENETRATION ASSAY FOR USE ON *M. BOVIS* BCG

2.1 Overview

The main purpose of this section of the project was to develop a safe and efficient way to measure intracellular drug accumulation in *M. tuberculosis*. As was discussed in the Literature Review, *M. bovis* BCG is the most appropriate surrogate for *M. tuberculosis*, and was hence used during assay development. The process of developing a drug penetration assay required the optimization of several assay conditions. For the purposes our objectives, the drug penetration assay was primarily validated for the study of fluoroquinolone uptake processes. Hence, moxifloxacin was chosen as the compound with which method development was performed. These results are presented in the following Results section. However, the assay was also validated using rifabutin and mefloquine (non-fluoroquinolones) to ensure a more universal applicability. These drugs were chosen because preliminary testing indicated that they accumulate better within *M. bovis* BCG than other drugs. Additional validation experiments involving rifabutin and mefloquine have been included in the Appendix section III and have been made reference to.

Since one of the objectives of the assay is to avoid the use of expensive and dangerous techniques, radiometric assays using labeled compounds were completely excluded from consideration. An alternative approach involving a LC/MS-based assay was pursued. LC/MS analytical methods were developed for a range of anti-tuberculous agents and presented in the Materials and Methods section. Mycobacterial outer membranes are very tough and require the use of more extreme methods of disruption to achieve cell lysis. Several lysis procedures were compared for their effectiveness in releasing moxifloxacin out of cells for before quantitation using LC/MS analytical methods. The use of LC/MS analytical methods precluded the use of detergents as lysis agents in our method development process. Chemical (glycine HCl),

mechanical (bead-beating) and enzymatic (lysozyme) cell lysis methods were considered. Differences in drug recovery were observed with the various cell lysis procedures. Further efforts were made to understand effects of non-specific binding to silica beads and signal suppression due to the lysozyme content of the matrix. We found that using glycine HCl as a cell lysis agent, combined with water-bath sonication to achieve more extensive cell disruption, is superior to the bead-beating method with respect to releasing the intracellular moxifloxacin content.

The extent of non-specific drug adsorption onto the bacterial outer membrane during the assay was also determined to ensure that it does not result in the over-estimation of intracellular drug content. The appropriateness of a fixed time point for the assessment of steady-state drug accumulation was assessed based on the examination of the kinetics of moxifloxacin accumulation while checking that there is maintenance of cell viability during the course of the assay. The precision and accuracy of LC/MS analytical methods were also investigated by assessing intra- and inter- day variabilities in analysis. The validated assay ultimately allowed for the quantification of accumulation of a range of anti-tuberculous agents in *M. bovis* BCG and *M. tuberculosis*.

2.2 Materials and Methods

2.2.1 Chemicals

Moxifloxacin, gatifloxacin, rifabutin and linezolid were purchased from Sequoia Research Products (UK), while ciprofloxacin, levofloxacin and rifampicin were purchased from Fluka (Missouri, U.S.A.). Ofloxacin, sparfloxacin, rifapentine, mefloquine, ethambutol, thioridazine and *para*-aminosalicylic acid were obtained from Sigma (Missouri, U.S.A.). Clinafloxacin was obtained from Alexis Biochemicals (California, U.S.A.). TMC207 was a gift from Srinivasa Rao from the Novartis Institute for Tropical Diseases (Singapore). Stock solutions of 10mM were prepared for these compounds and stored at 4°C. Phosphate-buffered saline (PBS) was provided by Invitrogen (Carlsbad, California). HPLC-grade methanol and acetonitrile, and laboratory-grade toluene, were purchased from Fisher Scientific (New Hampshire, U.S.A.). Glycine from Biorad (California, U.S.A.) was dissolved in water to 0.1M and adjusted to pH3 with hydrochloric acid (HCl). Lyophilized lysozyme from chicken egg white was also purchased from Sigma; a 10mg/ml aqueous solution was prepared and stored at 4°C.

2.2.2 Strains and Culture Conditions

M. bovis BCG and *M. tuberculosis* H37Rv were cultured in Middlebrook 7H9 broth (Difco, UK) supplemented with 0.4% ADS, 0.2% glycerol and 0.05%Tween80 or grown on Middlebrook 7H11 agar (Difco) supplemented with 10% OADC and 0.5% glycerol. Broth cultures were incubated at 37°C till an OD_{600} of 0.3-0.4 was reached. Agar plates were incubated at 37°C and bacterial colonies were counted after 2-3 weeks.

2.2.3 Drug Penetration Assay Development

2.2.3.1 Growth Kinetics

A total of 100ml of supplemented 7H9 broth was inoculated with a single stock vial (1ml) of *M. bovis* BCG stored at -80°C. This culture was incubated at 37°C with constant rolling and triplicate 1ml samples were removed each day. Growth was evaluated by measuring the optical density (OD) of the culture at 600nm in a spectrophotometer (Ultrospec 3300 Pro, Amersham Biosciences). Fresh 7H9 medium was used as blanks for OD measurements.

2.2.3.2 Evaluation of cell lysis procedures

Several lysis procedures were tested on *M. bovis* BCG and the extent of drug recovery from cell lysate was compared. Specifically, the bead-beating method was compared against overnight incubation with glycine HCl, while evaluating the additional effects of lysozyme treatment and water-bath sonication respectively. BCG was incubated with moxifloxacin at 10µM for 30min, washed once with PBS and pelleted. For the bead-beating method, drug-treated BCG was resuspended in PBS and transferred to screw-capped tubes containing half the sample-volume of silica/zirconia beads (Biospec). Tubes were shaken in a bead-beater (Precellys 24, Bertin Technologies) for 3 x 60s cycles at 6,000rpm with at least 1min rest periods on ice between cycles. Beads and cell debris were pelleted at 13,000rpm and cell lysates were filter-sterilized. To test the additional effect of lysozyme treatment on the bead-beating procedure, drug-treated BCG was pre-treated with lysozyme at 2mg/ml (in PBS) for 1hr at 37°C before being subjected to the bead-beating procedure as described. Alternatively, BCG was lysed by incubating it in 0.1M glycine HCl (pH3) overnight at 37°C with constant shaking at 400rpm. The next day, cell

debris was pelleted at 13,000rpm and cell lysates were filter-sterilized. The additional effect of sonication was evaluated by subjecting the samples to an ultrasonic water-bath (Fisher Scientific) for 5min after overnight incubation but before filter-sterilization. All lysate samples were then crashed with methanol and acetonitrile and analysed for moxifloxacin content.

2.2.3.3 LC/MS/MS quantitative analysis

Quantification of drug concentration was achieved by liquid chromatography tandem mass spectrometry (LC/MS/MS). Mass analysis and detection were performed on an API 4000 Q-trap triple-quadrupole mass spectrometer (Applied Biosystems, USA) equipped with a turbo ion-spray ionization source. The HPLC system is of the Agilent (USA) 1200 series with a degasser, binary pump, autosampler and thermosatted column compartment. The mass spectrometer operated in the positive mode with an ion-spray voltage of +5KV and at the probe temperature of 500°C. The mass transitions for each precursor/ product ion pair, and their elution times, are recorded in **Table 5**. Mobile phases, water and acetonitrile, were acidified with 0.1% acetic acid. The mobile phase gradients, flow rates, analytical columns and temperatures used to achieve elution of fluoroquinolones and non-fluoroquinolones used in this study are presented in **Tables 6 - 11**. Injection volumes were fixed at 10µl. Calibration standards for all drugs were prepared from stock solutions to give final concentrations of 5nM to 500nM. Calibration curves and quality control checks were conducted with each batch of analysis. Drug concentrations of each injection were inferred from the integrated areas of the specific peak on the chromatogram. The goodness of fit (r^2) for all linear calibration curves were >0.98. Integration of peak area and calibration curve fitting were performed by the Analyst® sofware (AB Sciex, Massachusetts,

USA). The lower limits of quantitation (LLOQs) for all drugs range from 0.5 to 15nM (Table 5). Quality control (QC) samples (of known concentrations) were placed at intervals within the run to ensure accuracy of the assay. Snapshots of chromatograms, standard curves, and specific compound-dependent parameters that were optimized for MRM (multiple reaction monitoring) transitions of each drug tested have been presented in **Appendix II (Figures 1 – 16, Tables 1 – 16).**

Table 5 Mass transitions monitored for each drug, elution times and lower limits of quantitation (LLOQs).

Drug	Parent ion mass	Daughter ion mass	Elution time (min)	LLOQ (nM)
Ciprofloxacin	332.3	288.4	4.6	0.5
Moxifloxacin	402.4	384.3	4.6	1.0
Ofloxacin (& Levofloxacin)	361.9	318.4	4.6	0.1
Gatifloxacin	376.0	289.7	4.6	15.0
Clinafloxacin	365.9	322.1	4.6	0.5
Sparfloxacin	392.7	349.3	4.9	0.75
Rifampicin	823.6	791.9	5.2	0.1
Rifabutin	847.2	815.8	4.7	0.1
Rifapentine	877.6	845.7	4.7	0.1
Ethambutol	205.1	116.0	1.3	0.1
Mefloquine	379.0	361.1	4.7	2.5
Linezolid	338.2	296.2	5.1	0.5
Thioridazine	371.3	126.1	5.2	0.1
TMC207	555.2	328.1	5.2	0.5
para-aminosalicylic acid	152.0	107.8	6.1	10

Table 6 Gradient method for all fluoroquinolones tested in this study.

Time	% Aqueous Phase	% Organic Phase	Flow Rate	Column	Column Temp. (°C)
0.0	97	3	0.8ml/min	Gemini C18; 150 x 4.6mm, 5µm (Phenomenex)	40
0.5	97	3			
1.2	60	40			
3.2	60	40			
3.3	97	3			
7.0	97	3			

Table 7 Gradient method for rifampicin, rifabutin, mefloquine, thioridazine and linezolid.

Time	% Aqueous Phase	% Aqueous Phase	Flow Rate	Column	Column Temp. (°C)
0.0	97	3	0.8ml/min	Gemini C6-Phenyl; 150 x 4.6mm, 5µm (Phenomenex)	40
0.5	97	3			
1.2	50	50			
3.2	50	50			
3.3	97	3			
7.0	97	3			

Table 8 Gradient method for rifapentine.

Time	% Aqueous Phase	% Organic Phase	Flow Rate	Column	Column Temp. (°C)
0.0	97	3	0.8ml/min	Gemini C6-Phenyl; 150 x 4.6mm, 5µm (Phenomenex)	40
0.5	97	3			
1.2	30	70			
3.2	30	70			
3.3	97	3			
7.0	97	3			

Table 9 Gradient method for ethambutol.

Time	% Aqueous Phase	% Organic Phase	Flow Rate	Column	Column Temp. (°C)
0.0	97	3	0.8ml/min	Gemini C6-Phenyl; 150 x 4.6mm, 5µm (Phenomenex)	40
0.5	97	3			
1.0	50	50			
2.8	50	50			
3.0	97	3			
5.5	97	3			

Table 10 Gradient method for TMC207.

Time	% Aqueous Phase	% Organic Phase	Flow Rate	Column	Column Temp. (°C)
0.0	97	3	0.8ml/min	Gemini C6-Phenyl; 150 x 4.6mm, 5µm (Phenomenex)	40
0.5	97	3			
1.2	50	50			
3.2	50	50			
3.5	97	3			
7.0	97	3			

Table 11 Gradient method for *para*-aminosalicylic acid (PAS).

Time	% Aqueous Phase	% Organic Phase	Flow Rate	Column	Column Temp. (°C)
0.0	97	3	0.8ml/min	Gemini C18; 150 x 4.6mm, 5µm (Phenomenex)	40
0.5	97	3			
0.7	0	100			
3.0	0	100			
3.2	97	3			
7.0	97	3			

2.2.4 Assay Validation Methods

2.2.4.1 Estimation of Matrix Effects

The specific matrix effects (ME) of lysozyme on compound detection by LC/MS analysis was estimated based on the method described by Trufelli *et al* (231). Briefly, ion suppression was calculated using the following formula:

$$ME\ (\%) = 100 - (\ B/A \times 100\ )\ ,$$

where A represents the average analyte peak area of a standard PBS-based solution, and B represents the peak area of a solution also containing 2mg/ml lysozyme (both solutions are spiked with equal concentrations of the compound).

2.2.4.2 Spectrophotometric detection of cell -surface adsorption

In order to determine the extent of cell-surface adsorption of moxifloxacin on *M. bovis* BCG, concentrated cultures (OD_{600} 4.0) were treated with 10µM moxifloxacin and incubated for 30min. Samples of unwashed, washed and lysed (bead-beaten) cells were measured for moxifloxacin content. All samples were resuspended in PBS. 200µl of each sample was loaded onto a flat-bottomed, non-treated, 96-well black plate (Costar®). Fluorescence detection of moxifloxacin was achieved using a spectrophotometer (SpectraMax Plus, Molecular Devices) at the excitation and emission wavelengths of 294nm and 504nm respectively (181). Appropriate blanks (ie. untreated whole cells, untreated lysate) were also measured.

2.2.4.3 Assessment of Accuracy and Precision of LC/MS Analysis

The accuracy and precision of the assay was determined using intra- and inter- day runs as described in the current validation requirements detailed by Bansal *et al* (10). Standard solutions of low, medium and high concentrations representing the entire range of the calibration curve were analysed using the LC/MS analytical methods we developed. The concentration of the low QC is chosen near the LLOQ. At least 5 replicate-injections of each standard solution was made per day for 3 consecutive days. The accuracy of the method is reflected by the relative error (RE%) of the measured analyte concentrations. RE was calculated using the following formula.

$$\text{RE (\%)} = \frac{\text{Measured Conc.} - \text{Standard Conc.}}{\text{Standard Conc.}} \times 100\%$$

For the low concentration standard solution, RE should be within ±20%. The coefficient of variation (CV), which indicates precision, should be < 20%. For the medium and high concentration standard solutions, RE should fall within ±15% and CV should be <15%. CV was measured by the following equation.

$$\text{CV (\%)} = \frac{\text{Standard Deviation}}{\text{Mean Measured Conc.}} \times 100\%$$

2.2.5 Statistical Tests

For the determination of statistical significance of differences in drug uptake under different conditions we used unpaired *t*-tests with Welch's correction (assuming unequal variances) (GraphPad Prism v5.0).

2.3 Results

2.3.1 Selection of Growth Phase of *M. bovis* BCG

The growth curve obtained for *M. bovis* BCG is shown in **Figure 9**. An initial lag phase was observed, spanning days 0 - 3 during which bacterial growth was slow. Bacterial growth then became more rapid in the exponential (logarithmic) phase, which lasted for 5 days. Subsequently, growth of the dense culture slowed as it entered the stationary phase, and plateaued off by day 8. A culture with an OD_{600} of 0.3 - 0.6 was hence identified as containing replicating bacteria in the mid-exponential phase.

Figure 9 (A) Growth curve for *M. bovis* BCG. Growth was evaluated by OD_{600} measurements. (B) Plot of BCG growth on a log scale. The experiment was conducted with biological triplicates. Standard deviations are shown as error bars and are hidden by data points in most instances.

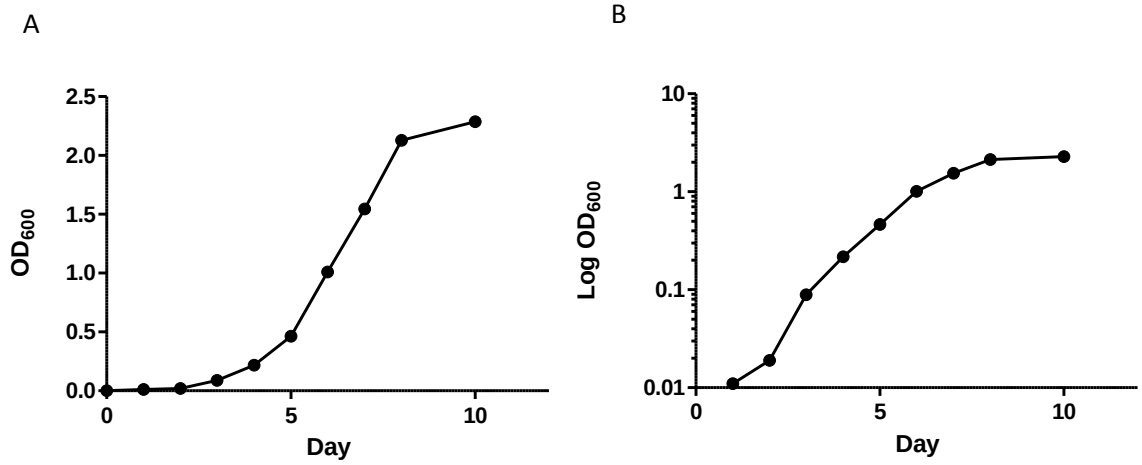

2.3.2 Assessment of the efficiency of various lysis procedures at releasing intracellular drug content

2.3.2.1 Absolute fluoroquinolone recovery from different lysis procedures

To eventually set up a drug penetration assay for *M. tuberculosis*, several lysis procedures were compared for their effectiveness in maximizing moxifloxacin recovery. Four different lysis procedures (or combination of procedures) were compared: bead-beating, bead-beating with lysozyme pre-treatment, incubation with glycine HCl (pH3) alone, and in combination with sonication. The cell lysates prepared were analyzed for moxifloxacin content using LC/MS methods and the results are presented in **Figure 10A**. A brief period of water-bath sonication after overnight lysis with glycine HCl improved the recovery of moxifloxacin from *M. bovis* BCG by about 10%. Similarly, pre-treatment of BCG with lysozyme for an hour before the bead-beating process improved the recovery of moxifloxacin by 13.5%. Overall, the combined procedure of glycine HCl and sonication increased the moxifloxacin content of lysate by 1.3-fold when compared to the bead-beating – lysozyme combined procedure.

Rifabutin and mefloquine recoveries were also compared for the purposes of more thoroughly validating our assay. The results of these experiments are presented in **Figures 17A & 18A** of **Appendix III**. With both rifabutin and mefloquine, the addition of the sonication step did not affect the final drug content of the cell lysates. The glycine HCl – sonication combined procedure was 1.3 and 1.5 –times more effective at releasing rifabutin and mefloquine, respectively, into the cell lysate. The addition of lysozyme treatment to the bead-beating procedure drastically reduced rifabutin and mefloquine recovery by 34% and 76% respectively.

2.3.2.2 Extent of compound-loss during the bead-beating procedure

It was observed that with the bead-beating procedure there is a loss in sample volume due to the residual amount that remains adhered to the zirconia / silica beads. It was also hypothesized that a proportion of the drug in cell lysate may adsorb onto the surface if these beads. In order to prove that moxifloxacin recovery is compromised with the bead-beating procedure (as compared to chemical lysis without beads), PBS was spiked with known concentrations of moxifloxacin and then subjected to the bead-beating process without the addition of any bacterial cells. The standard solutions were then filtered and crashed with organic solvents in the way regular cell lysates were treated. The moxifloxacin content of these solutions were then analysed by LC/MS and compared against control samples that were not bead-beaten. The results showed that the process of bead-beating standard samples reduced moxifloxacin recovery by up to 60% **(Figure 10B).** This helps account for the difference in compound recovery between lysis procedures.

Figure 10 (A) The relative levels of moxifloxacin (MXF) recovery from different cell lysis procedures. (B) Determination of loss in recovery of MXF from samples due to the bead-beating procedure. Results are expressed as the concentrations of MXF in cell lysates. The experiment was conducted with biological triplicates and standard deviations are shown as error bars.

A

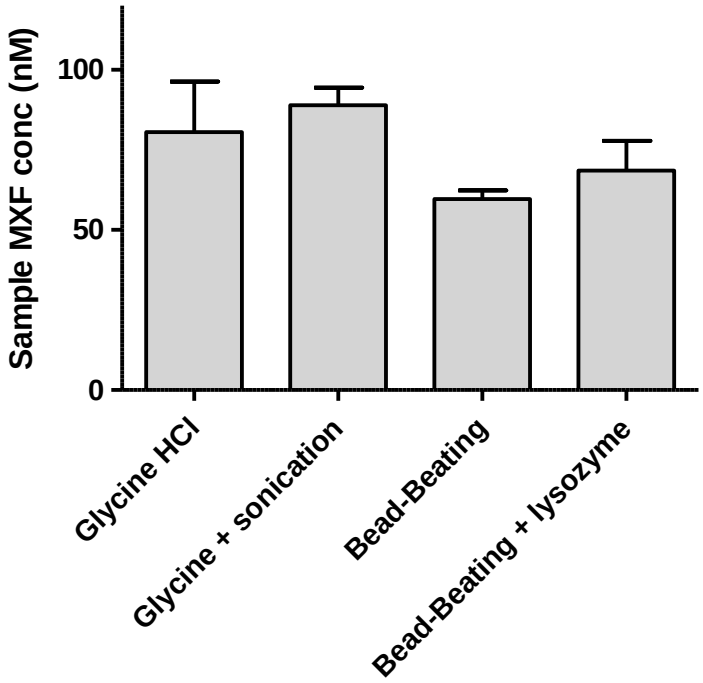

B

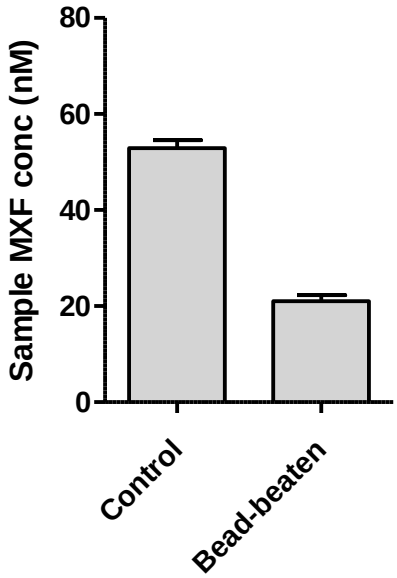

2.3.3 Assessment of assay sensitivity

2.3.3.1 Suppressive effects of lysozyme on compound detection

Matrix effects have been known to be detrimental to important LC/MS method parameters (ie. limit of detection, linearity, accuracy) (141, 231). The different matrices, such as PBS and glycine HCl, used for lysate preparations in this study may compromise the quantitation of drug accumulation although the absolute drug content of the lysates remains the same. The effects of various matrices on moxifloxacin signal-detection by our LC/MS method were assessed. PBS (with and without 2mg/ml lysozyme) and glycine HCl were spiked with equal concentrations of moxifloxacin, crashed with equal volumes of organic solvents, and analysed by LC/MS. The absolute analyte signal peak areas were compared between standard solutions **(Figure 11)**. The addition of lysozyme to PBS drastically reduced the signal of moxifloxacin in standard PBS solutions by 3.5 -fold. This difference in response indicates ion suppression by lysozyme. Based on the formula described in Trufelli *et al* (231), we calculated the suppressive matrix effect (ME) of 2mg/ml lysozyme on moxifloxacin detection as 70%. The analyte signal from glycine HCl is also significantly lower than from PBS, but still greater than in the lysozyme-PBS combined matrix.

Similar observations were made with rifabutin **(Appendix III, Figure 17B)**. The presence of lysozyme resulted in a 1.5-fold decrease in rifabutin detection in standard PBS solutions (ME = 32%). The absolute signal strength of rifabutin in glycine HCl was lower than in PBS alone but this difference was insignificant. The signal strength of mefloquine was significantly higher (by 3.2-fold) in glycine HCl than both PBS-based standard solutions **(Appendix III, Figure 18B)**. The addition of lysozyme to PBS also reduced the signal strength of mefloquine (ME = 20%).

Figure 11 Comparison of signal strengths of MXF from standard solutions (100nM) prepared in different matrices. Data is presented as absolute signal peak areas from LC/MS chromatograms. The experiment was conducted with biological triplicates and standard deviations are shown as error bars.

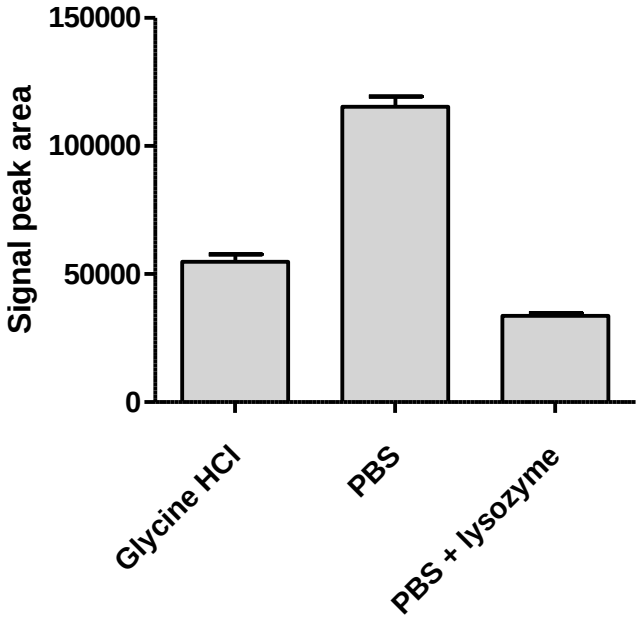

2.3.3.2 Quantitation limits of various assays

The lower limits of quantitation (LLOQs) of moxifloxacin, rifabutin and mefloquine in standard solutions of different matrices were compared **(Table 12)**. These standard solutions were prepared in PBS (with and without lysozyme) and glycine HCl as described previously. Little variation of the quantitation limits was observed for all three drugs and the methods. Overall, these analytical methods displayed more than sufficient sensitivity for the purposes of quantifying drug accumulation with our assay.

Table 12 LLOQs of moxifloxacin (MXF), rifabutin (RIB) and mefloquine (MEF) in different matrices for their respective analytical methods.

	Detection Limit (nM)		
Matrix	MXF	RIB	MEF
Glycine HCl	0.6	0.05	0.5
PBS	0.2	0.05	1.5
PBS + Lysozyme	0.3	0.05	1.0

2.3.4 Fluorescence-detection of cell-surface adsorbance of fluoroquinolones

Significant adsorption onto the cell surface is often feared to cause the misestimation of intracellular drug accumulation. In our drug penetration assay, sample filtration is performed following cell lysis in order to remove debris containing insoluble cellular components (ie. cell wall) and unbroken cells. We investigated the hypothesis that this insoluble fraction contains bound-moxifloxacin. The fluorometric method of fluoroquinolone detection was used here because of the lack of optimized protocols for the maximal extraction of drug from cell debris which is necessary prior to accurate quantitation by LC/MS methods.

M. bovis BCG was treated with moxifloxacin and the relative fluorescence signals were compared between whole cells, lysate and cell debris. Moxifloxacin was detected in all three preparations of treated BCG cells, including the cell debris fraction. It was observed that the net fluorescent signal from the combined lysate and debris preparation is approximately equal to the sum of signals from individual lysate and debris fractions **(Figure 12A)**.

The effect of a single PBS wash on the level of moxifloxacin absorbance onto the outer membrane was also studied. The relative fluorescence detected from control (untreated) cell debris and the cell debris fraction obtained from moxifloxacin-treated BCG that was washed once did not differ significantly ($p > 0.05$). However, the cell debris fraction from treated but unwashed BCG fluoresced twice as much **(Figure 12B)**. This shows that the single wash step of the drug penetration assay is crucial for the removal of the majority of moxifloxacin absorbed onto the cell.

Figure 12 (A) Fluorescence-detection of moxifloxacin in lysed fractions of *M. bovis* BCG. (B) Study of the effect of a wash step on the detection of moxifloxacin in cell debris fractions. Light and dark bars distinguish between moxifloxacin-treated and -untreated samples respectively. The amount of moxifloxacin present is expressed as relative fluorescence units (RFU). The experiment was conducted with biological triplicates and standard deviations are shown as error bars.

A

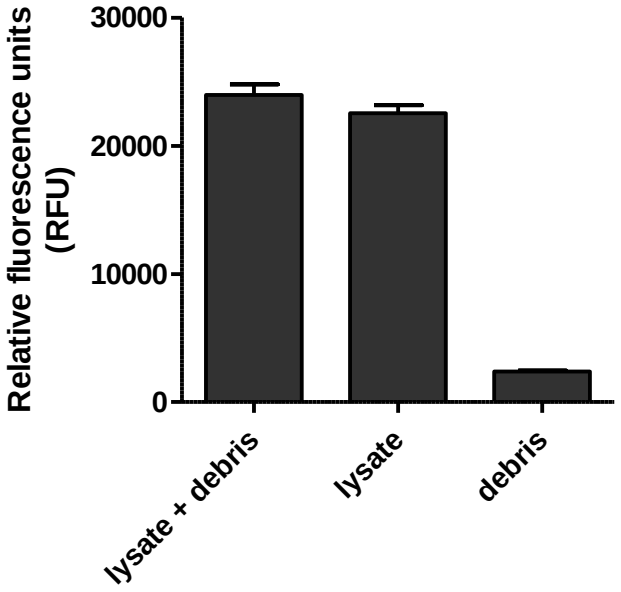

B

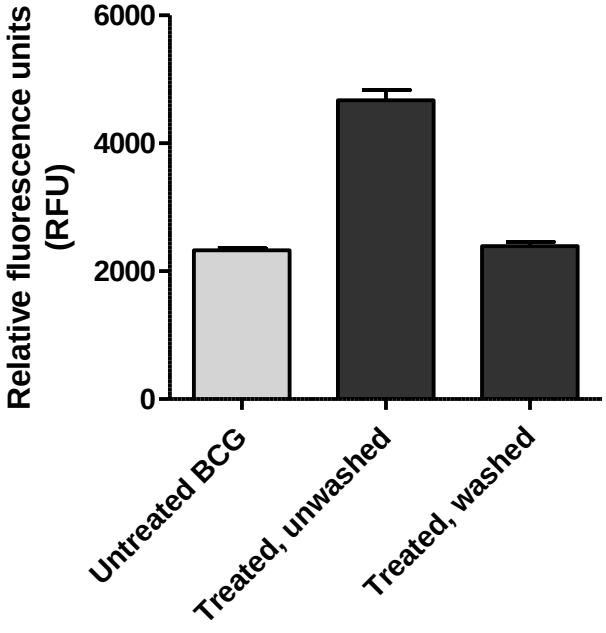

2.3.5 Selection of a fixed time-point for the measure of steady-state accumulation

2.3.5.1 Time-course of moxifloxacin accumulation

For the purposes of development of a standard assay, a common length of incubation period had to be decided upon based on the achievement of steady-state accumulation of drugs within the bacillus. The accumulation of moxifloxacin (and other fluoroquinolones) within *M. bovis* BCG was observed. The results for moxifloxacin are presented **Figure 13**. Because it was observed that this accumulation is rapid within the first few minutes and equilibrates within 20-30min of incubation, a 30min incubation period was deemed satisfactory for the evaluation of steady-state intracellular drug concentrations in the rest of this study. The time-course of intracellular accumulation for other fluoroquinolones is further elaborated on in Chapter 3.

2.3.5.2 Maintenance of cell viability

A standard incubation concentration (10µM) was chosen for the comparison of steady-state accumulation between different drugs. Incubation concentrations higher than the MICs are often used during drug accumulation studies (182, 183). An attempt was made to ensure that cell viability of *M. bovis* BCG was not compromised by the high fluoroquinolone concentrations during the course of the incubation period. Cell viability was assessed by CFU enumeration. BCG was incubated with 10µM of moxifloxacin and CFU counts were obtained at regular time intervals over 60min. The slight decrease observed in the number of viable bacilli within the total 60min of drug incubation was found to be insignificant ($p > 0.05$) **(Figure 14)**.

Figure 13 Kinetics of moxifloxacin (MXF) accumulation in *M. bovis* BCG over a 30 min period at an incubation concentration of 10µM. The results are expressed as MXF concentration in cell lysate (nM).

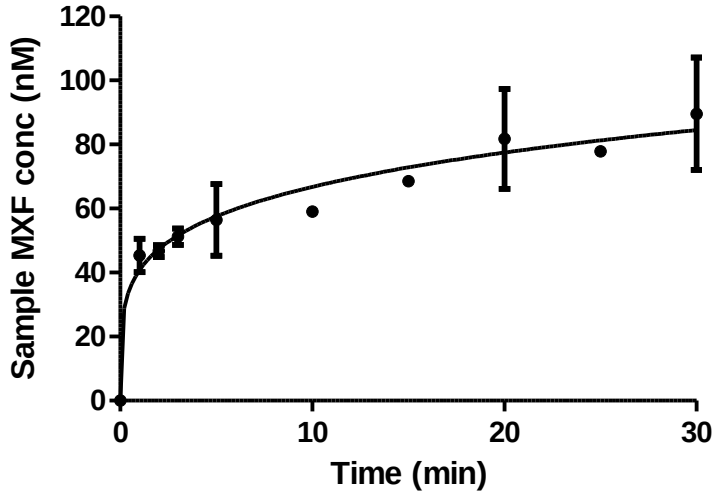

Figure 14 Kill-kinetics of 10µM of moxifloxacin against BCG for the first 60min of incubation. Standard deviations are shown as error bars.

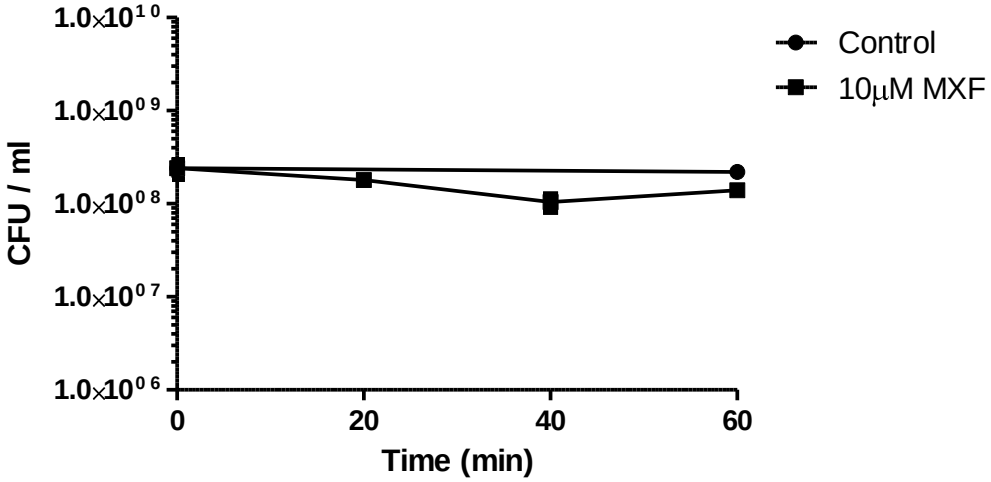

2.3.6 Intra- and inter-day variability

The intra-day and inter-day variability of LC/MS analysis of moxifloxacin in cell lysate is shown in **Table 13**. Results were obtained by analyzing 6 standard samples at low, medium and high concentrations on 3 consecutive days. The concentrations 5nM, 50nM and 500nM were chosen to represent the full scale of the calibration curve for moxifloxacin. The relative errors (RE) of intra- and inter- day measurements for the 50nM and 500nM solutions were within the acceptable range of ±15%. The coefficients of variance (CV) for these solutions fell below 15% for both categories. For the 5nM solutions, the RE and CV fell between the acceptable range of ±20% and 20% respectively. Similar results were obtained with the tests of variability in rifabutin and mefloquine analysis **(Appendix III, Table 17)**.This shows that the analytical methods are of acceptable precision and accuracy.

Table 13 Intra- and inter-day variabilities of moxifloxacin analysis. RE, relative error; CV, coefficient of variation.

	Standard conc. (nM)	Mean measured conc. (nM)	RE range (%)	CV (%)
Intra-day variability (n = 6)	5	5.43	-0.4 – 12	4.6
	50	49.2	-4.6 – 1.2	2.0
	500	502.2	-3.6 – 3.4	3.3
Inter-day variability (n = 18)	5	5.12	-14 – 12	8.0
	50	47.7	-13 – 1.2	4.1
	500	503.8	-4.4 – 9.8	3.5

2.4 Discussion

M. bovis BCG was used as a surrogate for *M. tuberculosis* for the purposes of development of a drug penetration assay given its comparable sensitivity to compounds with anti-tuberculous activities (5). In our study of drug accumulation, incubation concentrations were standardized at 10μM. This is above the MICs of all drugs tested for *M. tuberculosis* and *M. bovis* BCG. However, studies of intracellular drug accumulation often report that the use of incubation concentrations above MICs is optimal as long as cell viability is not compromised. Exact concentrations in those studies were dependent on the sensitivity of the analytical method used (182, 183). The duration of drug incubation was also standardized. It was previously reported that steady-state accumulation of a variety of drugs (including fluoroquinolones, rifampicin, pyrazinamide) in *M. tuberculosis* occurs within minutes of drug exposure (182, 183, 191). Our study of the intracellular accumulation of 6 fluoroquinolones also showed that this accumulation is rapid within the first few minutes and equilibrates within 30min of exposure. Importantly, during the time-course of the experiment, no significant decrease in the viable cell count was detected. The check on the effect of moxifloxacin on BCG cell viability was sufficient because MIC tests revealed that moxifloxacin is the most potent of the 6 fluoroquinolones (MXF = GFX, CNX, SPX > CPX > OFX) **(Appendix III, Figure 20)**. Therefore, the common sampling time-point of 30min was selected for all fluoroquinolones for the general purposes of comparing steady-state accumulation. We kept the density of the culture constant by adjusting the optical density (OD_{600}) before the start of each assay. We found that CFU counts were relatively consistent ($5 \times 10^8 < CFU < 1 \times 10^9$ cells/ml) between assays. Several culture densities were initially tested on the assay but an OD_{600} of 4.0 produced the highest assay sensitivity without resulting in clumping of the bacterial cells.

In this assay, the centrifugation separation method with a single PBS-wash step is used to pellet and separate the bacterial cells from the incubation medium. No attempts were made to validate the suitability of this method over the silicon oil separation method, where the aliquots of the culture are places over the oil and centrifuged to pellet the bacterial cells. The aqueous layer containing the incubation medium is then removed and the tube is snap-frozen so that the oil can be removed by careful pipetting. No wash step was included with this silicon oil separation method (118). This method has the advantage of quick separation of cells from the drug, but studies have shown that drug adsorption onto the cell causes an overestimation of drug accumulation because of the lack of a wash step (243). The centrifugation separation method was therefore decided as preferable without testing. We did, however, show that the single PBS wash step is effective at removing the amount of moxifloxacin adsorbed onto the outer membrane. While it still may be argued that the adsorption of drugs onto the outer membrane results in an over-estimation of intracellular concentrations, we observed that the procedure of filtration of the lysate, which was actually initially intended for the assurance of sample sterility, also has the additional benefit of removing aggregated fragments of lipid membrane layers. No evidence of this has been provided as this was merely a visual observation. However, we suggest that this ensures that drug molecules still left adsorbed onto fragments of the outer membrane can be removed from the cell lysate fraction.

With regards to the cell lysis procedures, several important factors had to be considered. Chemical lysis methods involving detergents such as SDS and Triton-X could not be tested due to their incompatibility with LC/MS analytical methods (6). In this study, overnight chemical lysis with glycine HCl (pH 3) proved to effectively release the intracellular content of moxifloxacin from *M. bovis* BCG. Sonication in a water-bath was considered as an additional

procedure because it was hypothesized that, while glycine HCl is well-understood to weaken the outer membrane and causes lysis is come bacteria (197), it might require additional mechanical agitation to disrupt the whole-cells. It was observed that sonication did indeed increase the moxifloxacin content of cell lysates, although only slightly. Nevertheless, the sonication step was included in the protocol.

It was observed with moxifloxacin, rifabutin and mefloquine that the bead-beating lysis procedure consistently resulted in lesser drug recovery from *M. bovis* BCG cultures than the lysis procedure using glycine HCl. We were able to show with cell-free experiments that the bead-beating alone results in loss of moxifloxacin content. These results may be easily explained by the consistent observation that the volume of lysate recovered from this procedure is often reduced due to the unavoidable residual volume that is left adhering to the zirconia / silica beads within the tube. The additional problem of drug-binding to the high combined surface area of the beads possibly further reduces drug recovery. To test this hypothesis, standard solutions spiked with known concentrations of moxifloxacin, rifampicin and mefloquine were subjected to the bead-beating process. We observed that bead-beating consistently resulted in the loss of analyte. Although bead-beating is often considered the ideal method of achieving mycobacterial cell disruption in genomic DNA and protein extraction protocols (116, 250), analyte -loses contribute to the underestimation of intracellular drug accumulation and, therefore, makes it less suitable for use in a drug penetration assay.

Matrix effects (ME), which refer to matrix -dependent signal suppression or enhancement represent a major drawback in LC/MS analysis. ME can significantly affect the reproducibility, linearity and accuracy of analytical methods, leading to inaccurate quantitation results (231). It was observed during method validation that lysozyme treatment had varying effects on the drug

recovery depending on the drug. While it resulted in a slight increase in moxifloxacin recovery from the bead-beating cell lysis procedure, it caused significant decreases in rifabutin and moxifloxacin recovery. The testing of standard solutions in the absence of cell lysate confirmed that lysozyme consistently reduces analyte signal intensities. One possible explanation for this is that the co-elution of lysozyme during analysis causes competition for available charges during ionization and access to the droplet surface for gas-phase emission. The inconsistent suppressive effects of lysozyme (different impacts on different analytes) observed here are consistent with the concept that ME is unpredictable and that variation is response can be observed even with the same sample and methods (231). This problem of signal loss could potentially be resolved by the design of more efficient chromatographic separation (LC) methods, or more extensive sample clean-up procedures (protein-crashing). However, the process of evaluating ME and optimizing the assay for each drug defeats the intention to have a drug permeability assay with universal applicability. Therefore, even though lysozyme is widely regarded as a useful lysis agent for *M. tuberculosis* in numerous protocols, its use in LC/MS-based drug penetration assay is undesirable.

Finally, while the extent of drug recovery is an important factor in the evaluation of cell lysis procedures, the ease and speed of the performance of the procedure should also be considered. Though lysis with glycine HCl is on the whole a slower procedure (due to the overnight incubation period) it is actually faster when comparing total time spent at the bench. The repeated cycles of bead-beating and cooling on ice makes for a cumbersome procedure. Added to the fact that aerosols generated during the bead-beating process are a biosafety concern when working with the pathogenic *M. tuberculosis*, the glycine HCl procedure appears much preferable.

Ultimately, the glycine HCl method of lysis paired with a brief period of sonication in a water-bath proved effective at the release of intracellular fluoroquinolone content for the purposes of quantification of accumulation. Our LC/MS analytical methods have demonstrated accuracy and precision; Inter- and intra-day variabilities were within the recommended range for all three test compounds. Variability was in any case controlled for by the establishment of individual calibration curves for each batch of samples despite same day analysis. This drug penetration assay was used to characterize fluoroquinolone transport in *M. bovis* BCG and *M. tuberculosis*, as will be presented in the later sections of this thesis. The IBC-approved protocol that includes instructions for the safe-handing of the BSL3 pathogen has been included in **Appendix I**. The assay is also applicable for the study of non-fluoroquinolones. The accumulation of 8 other drugs with anti-tuberculous activity (including first, second and third line drugs, compounds in clinical development, and drugs with other clinical applications) in *M. bovis* BCG was studied and presented in **Figure 19 (Appendix III)**. The assay is not without its limitations. This includes the difficulty of quantifying the accumulation of compounds that are metabolized within the bacilli, unless the specific metabolites are known and can be tracked individually. This is the case with isoniazid which is converted to a number of free-radicals. In such instances, the radiometric method of drug quantification is preferable because the labeled moiety can be tracked despite structural changes (12). Compounds that degrade in acidic medium are also not compatible with this assay given the low pH of the glycine HCl solution (pH3). The accumulation of *p*-aminosalicylic acid (PAS), the second-line anti-tuberculous agent, could not be quantified by our assay because of its degradation to *m*-aminophenol (MAP) in acidic medium (233). Despite these limitations, this drug penetration assay is superior given its robustness, wide applicability and ease of performance.

CHAPTER 3

CHARACTERIZATION OF FLUOROQUINOLONE UPTAKE IN *M. BOVIS* BCG

3.1 Overview

Little is known about the way fluoroquinolones are transported across the mycobacterial outer membrane. In general, the uptake of most fluoroquinolones in Gram-positive and -negative bacteria is believed to take place via simple diffusion through porin channels (37). The study of fluoroquinolone accumulation in mycobacteria has traditionally involved the use of fluorometric methods of detection (61, 182, 243). These studies concluded that the uptake of fluoroquinolones in mycobacteria is also a passive process (57, 182). Moxifloxacin, a hydrophobic fluoroquinolone, is believed to be particularly efficient at diffusing across the lipid membrane (61). Others have also suggested the possibility of porin-mediated fluoroquinolone transport, as has been shown with *E. coli* (17, 152). The hydrophilic norfloxacin, for example, is believed to utilize the porin transport pathway in mycobacteria (61, 243). Using over-expression models, efflux pumps such as Rv2686c-Rv2687c-Rv2688c and LfrA have been associated with resistance to fluoroquinolones in mycobacteria (125, 174). However, it remains unsure to what extent efflux pump activity affects fluoroquinolone accumulation in wild-type strains.

The main objective of this section of this study is to characterize fluoroquinolone transport in *M. bovis* BCG so as to provide further insight into the mechanism of uptake. We used the drug penetration assay presented in Section 1 to measure accumulation of various fluoroquinolones in *M. bovis* BCG. The panel of 6 fluoroquinolones studied included ciprofloxacin, moxifloxacin, ofloxacin, gatifloxacin, clinafloxacin and sparfloxacin. The kinetics of fluoroquinolone uptake was studied, and intra-class variability in steady-state accumulation examined. The correlation between fluoroquinolone accumulation and their anti-mycobacterial activity was analysed. The effects of various physicochemical properties were also considered. We found that fluoroquinolone uptake is rapid and steady-state accumulation correlates well with their

hydrophilicity. Following that, the effects of external drug concentration on intracellular accumulation were studied. We found with all 6 fluoroquinolones that accumulation was non-saturable and also proportional to the external concentration. Co-incubation with a second fluoroquinolone or β-lactams (known substrates of porin-mediated transport) failed to inhibit fluoroquinolone accumulation. We also found that efflux pump inhibitors had no significant effect on fluoroquinolone accumulation.

The effects of acidic external pH on fluoroquinolone uptake in mycobacteria had not been previously reported. Nikaido and Thanassi had summarized that an increase in the acidity of the external medium causes a reduction in intracellular accumulation and activity of fluoroquinolones in *E. coli* and *S. aureus* (168). We investigated to see if fluoroquinolone accumulation in *M. bovis* BCG is similarly dependent on medium pH. We noted significant decreases in intracellular accumulation of three fluoroquinolones. We also observed corresponding decreases in anti-mycobacterial activity with an increase in acidity. We summarized that the characteristics of fluoroquinolone transport in *M. bovis* BCG are consistent with facilitated transport by porin-like structures.

3.2 Materials and Methods

3.2.1 Chemicals

The efflux pump inhibitors verapamil and reserpine were obtained from Sigma (Missouri, U.S.A.). Stock solutions of 10mM were prepared for these compounds and stored at 4°C. The sources of all antibiotics have been stated in the previous chapter.

3.2.2 Drug Penetration Assay and Quantitative Analysis

Cultures were harvested by centrifugation at 3,200g for 10min. The pellets were re-suspended in fresh 7H9 broth medium or PBS-Tween80 to an OD_{600} of 4.0. Unless otherwise mentioned, all standard drug penetration assays were conducted at an incubation concentration of 10µM, for an incubation period of 30min at 37°C. Three 300µl aliquots were pelleted at 13,200g for 3.5min at 4°C. The pellets were washed in an equal volume of PBS. The cells were then lysed overnight in an equal volume of glycine-HCl (pH3) at 37°C with constant agitation (61, 182). The following day, samples were subjected to sonification in a water bath for 5min before cell debris was pelleted by centrifugation. Lysates (supernatants) filtered with 0.22µm filter units (Millipore MILLEX-GV filter units, PVDF, 13mm) to ensure sample sterility. Compound extraction was achieved by the addition of 80µl of methanol and 40µl of acetonitrile. Lysate samples were subsequently stored at -20°C. A schematic diagram of this assay is provided in **Figure 15**. Following each assay, serial dilutions of the concentrated cultures were prepared and spread onto 7H11 agar plates. CFU counts were performed 2-3 weeks later. This enabled the normalization of drug penetration results to the density of the culture, and the determination of amount of drug per bacillus when necessary.

When the kinetics of fluoroquinolone accumulation was being examined, samples were taken over the following time intervals: 0, 1, 2, 3, 5, 10, 15, 20, 25, and 30min (constant incubation concentration of 10μM). The effects of external fluoroquinolone concentration were investigated by incubating BCG in the following drug concentrations: 5, 10, 25, 50, 75, 100, 125, 150 and 200μM; samples were taken after just 30s in order to reflect the initial rate of uptake. In efflux pump inhibition experiments, verapamil and reserpine were added (75μM and 20μM respectively) 3min after the addition of the anti-tuberculous agent (10μM). The pH of supplemented 7H9 medium was adjusted from 6.5 to 5.0 by the addition of hydrochloric acid when specified. Quantitative analysis of drug concentration was achieved by LC/MS as described previously.

Figure 15 Schematic diagram of the validated drug penetration assay used in this study. Specific parameters cater to a standard protocol for the measurement of steady-state intracellular drug accumulation. Parameters such as incubation concentration and duration of incubation and the addition of inhibitors can vary with the objective of the experiment.

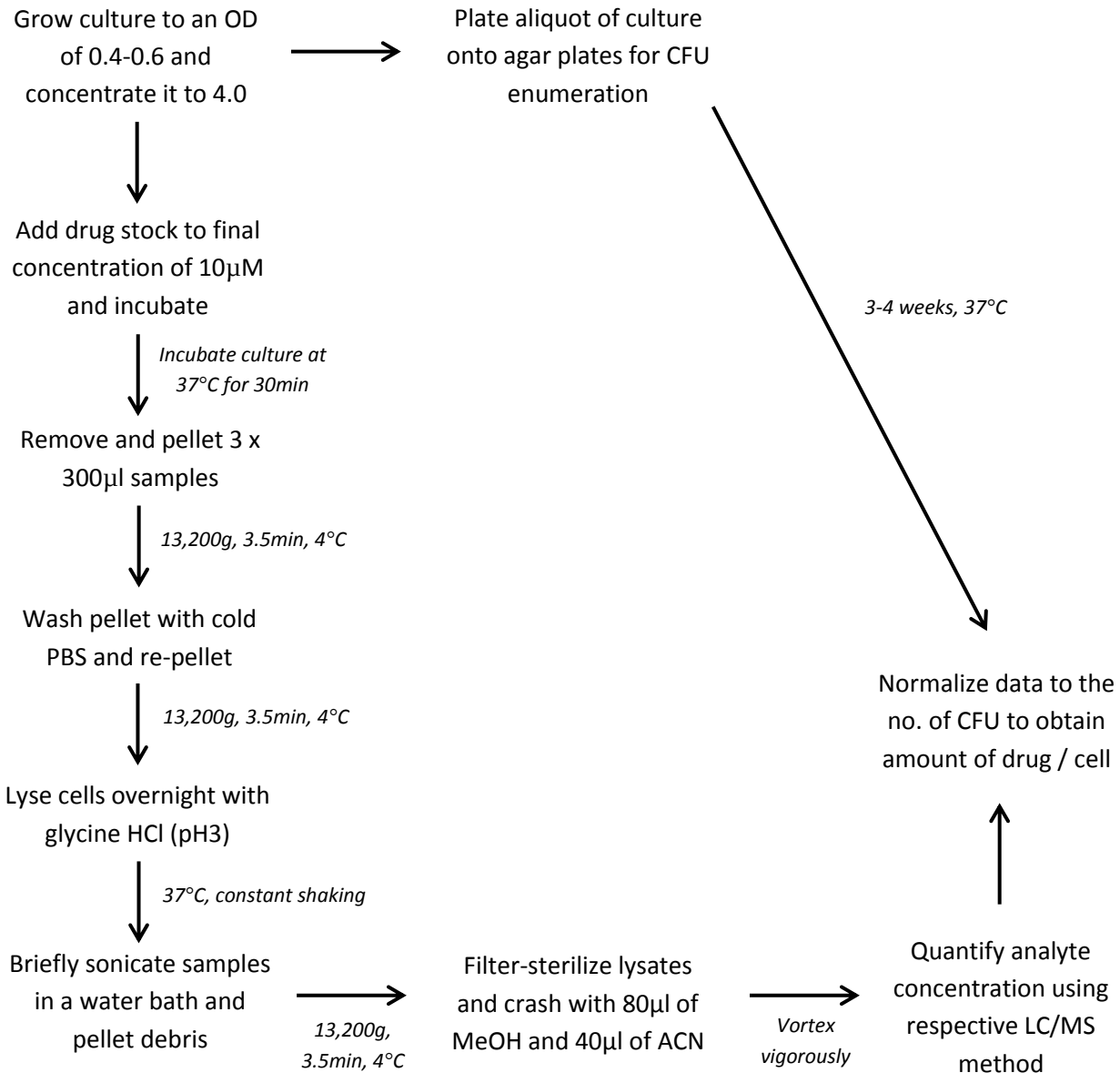

3.2.3 Susceptibility Testing

In this study, MIC_{90} (minimum inhibitory concentration 90) was defined as the concentration of drug required to inhibit bacterial growth by 90%. BCG broth cultures were diluted to an OD_{600} of 0.02 and 200µl aliquots were transferred to 96-well plates. Testing of fluoroquinolone activity was conducted within the concentration range of 0.01 to 10µM. All 96-well plates were incubated at 37°C and their optical densities were read after 5 days. IC_{50} values were determined by GraphPad Prism v5.0 using non-linear regression of dose-response curves (ie. Log(agonist) vs Response, Variable slope, Four parameters).

3.2.4 *In silico* Profiling and Statistical Testing

The calculated partition coefficient (CLogP) and polar surface area (PSA) of various drug molecules were provided by the Novartis-owned cheminformatics profiling program InSilico Profile (v4.1) (153). To assess the correlation between fluoroquinolone uptake and these physicochemical properties, correlation regression analyses (GraphPad Prism v5.0) were conducted. All r values are Pearson's correlation coefficients from the analysis and indicate the strength of the correlations. For the determination of statistical significance of differences in drug uptake under different conditions, unpaired *t*-tests with Welch's correction (assuming unequal variances) (GraphPad Prism v5.0) were used. Significant, very significant and extremely significant differences were benchmarked at *p*-values of 0.05 (*), 0.01 (**) and 0.005 (***) respectively.

3.3 Results

3.3.1 Kinetics of fluoroquinolone accumulation

In an effort to understand the kinetics of fluoroquinolone accumulation by *M. bovis* BCG, a time-based assay was conducted where 10µM of fluoroquinolones were added to cultures and sample aliquots were removed at regular time intervals over a 30min incubation period. Fluoroquinolone content was normalized to the number of viable cells and presented as the amount of drug per CFU over that length of time **(Figure 16)**. Results indicate that accumulation of fluoroquinolones is rapid, with 50% of steady-state intracellular accumulation being achieved within the first 3min of incubation with the drug. Accumulation began to level off at the 20min mark and equilibrium conditions were achieved within 30min of drug incubation.

Figure 16 The kinetics of (A) ciprofloxacin, (B) moxifloxacin, (C) ofloxacin, (D) gatifloxacin, (E) clinafloxacin and (F) sparfloxacin accumulation at 10µM by *M. bovis* BCG. Drug uptake is expressed as the absolute quantity of each fluoroquinolone (nmol) per CFU. Best-fit curves were fit using non-linear regression (GraphPad v5.0). The experiments were conducted with biological triplicates and standard deviations are shown as error bars.

A

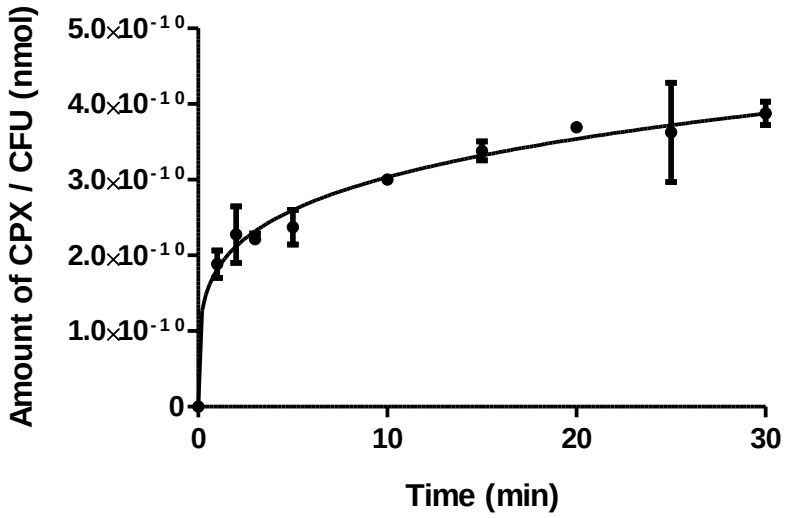

B

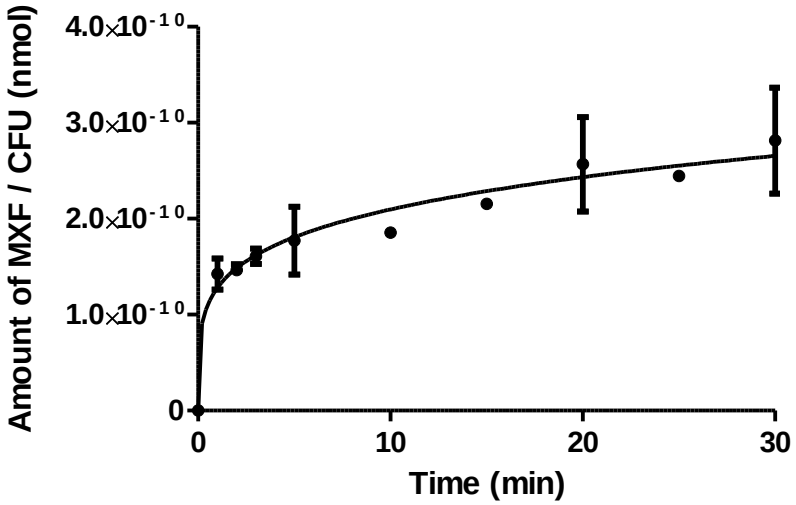

C

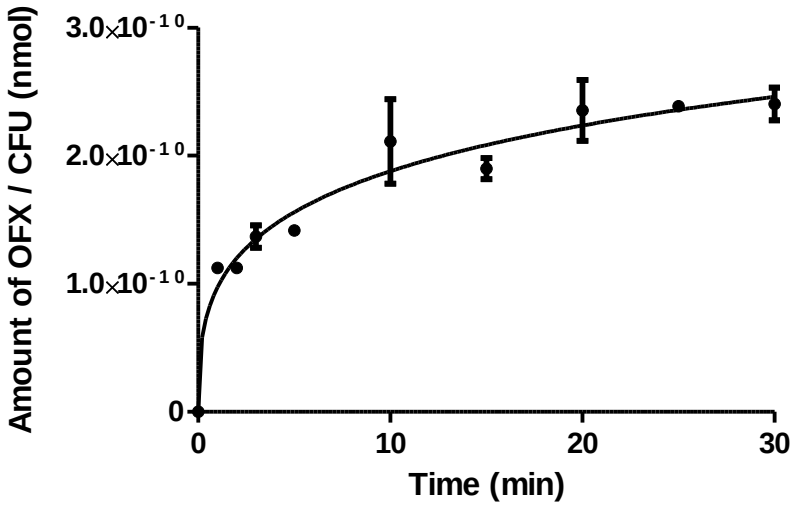
Amount of OFX / CFU (nmol)
3.0×10-10
2.0×10-10
1.0×10-10
0
0
10
20
30
Time (min)

D

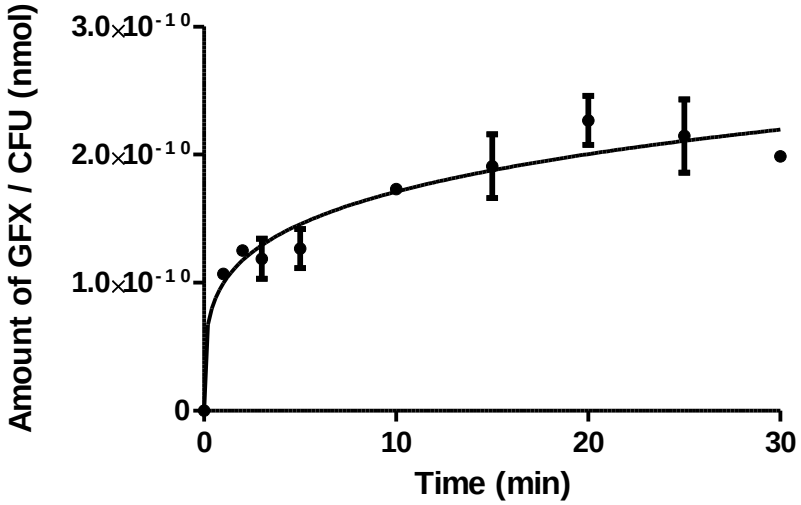
Amount of GFX / CFU (nmol)
3.0×10-10
2.0×10-10
1.0×10-10
0
0
10
20
30
Time (min)

E

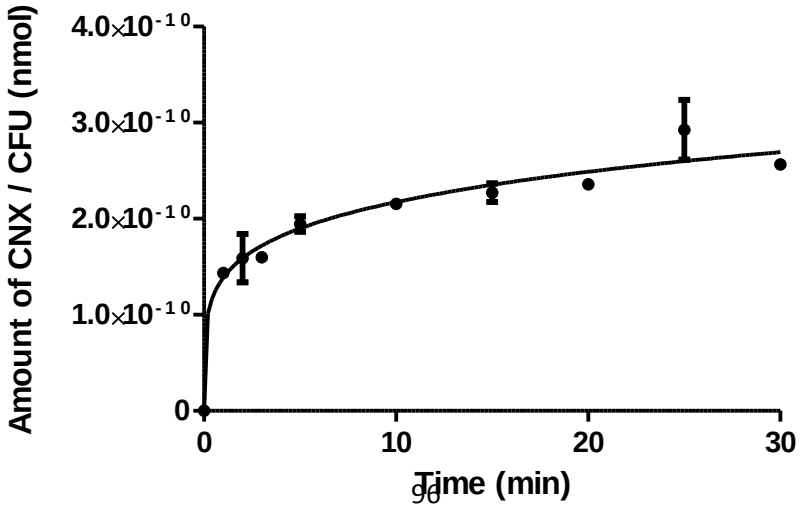
Amount of CNX / CFU (nmol)
4.0×10-10
3.0×10-10
2.0×10-10
1.0×10-10
0
0
10
20
30
Time (min)

F

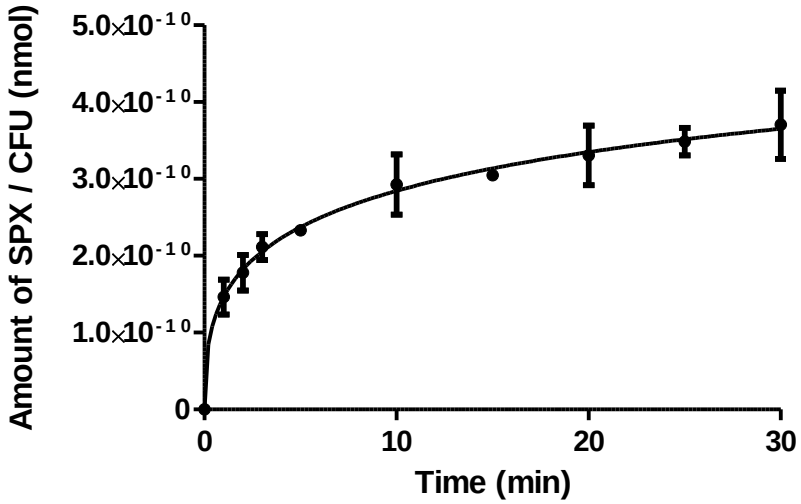
Amount of SPX / CFU (nmol)
5.0×10-10
4.0×10-10
3.0×10-10
2.0×10-10
1.0×10-10
0
0
10
20
30
Time (min)

3.3.2 Intra-class variability in steady-state concentrations

To assess intra-class variability in intracellular accumulation, steady-state concentrations (SSC) of fluoroquinolones were compared. For the purposes of this study, SSC was defined as intracellular drug content at the 30^{th} minute of incubation. SSCs of the 6 fluoroquinolones presented in **Figure 16** were determined from the fitted non-linear regression curves and listed in **Table 14**. At an incubation concentration of 10µM, ciprofloxacin accumulated within the intracellular compartment most extensively (3.9×10^{-10} nmol/CFU) **(Figure 17)**. This was followed by sparfloxacin, clinafloxacin, moxifloxacin and ofloxacin. Gatifloxacin accumulated least effectively in BCG (2.2×10^{-10} nmol/CFU). Overall, the intracellular accumulation of fluoroquinolones did not vary significantly, with less than a one-fold difference between ciprofloxacin and gatifloxacin.

The activities of all 6 fluoroquinolones were determined (MIC_{90}) and listed in **Table 14** (MIC curves are presented in the **Appendix III, Figure 20**). Moxifloxacin, gatifloxacin, clinafloxacin and sparfloxacin displayed comparable activities against *M. bovis* BCG, while ciprofloxacin and ofloxacin were the least active. There was no identifiable correlation between SSC and MIC_{90} ($r = 0.08$) **(Figure 18A)**. **Table 14** also lists several physicochemical properties of the fluoroquinolones in this study. A weak correlation was obtained between intracellular accumulation and molecular weight ($r = -0.33$) **(Figure 18B)**. The correlation implies that the uptake of smaller fluoroquinolones in BCG more efficient than that of larger fluoroquinolones. This corresponds with the similar correlation ($r = -0.38$) between accumulation and volume of the fluoroquinolone molecules (not shown). No correlation was obtained between intracellular fluoroquinolone accumulation and polar surface area (PSA) ($r = 0.20$) **(Figure18D)**. However, the accumulation of all 6 drugs displayed a strong correlation with their calculated partition

coefficients (ClogP) (r = -0.74) **(Figure 18C)**. The strong negative correlation indicates that fluoroquinolones with greater hydrophilicity accumulate intracellularly more effectively. All r values are Pearson's correlation coefficients from correlation regression analysis (GraphPad Prism v5.0).

Table 14 The steady-state concentrations (SSC) in *M. bovis* BCG, activities and physicochemical properties of six fluoroquinolones. MIC, minimum inhibitory concentration; ClogP, calculated partition coefficient; PSA, polar surface area.

Fluoroquinolone	SSC (nmol / CFU)	MIC_{90} (µM)	Molecular weight (g / mol)	ClogP	PSA
Ciprofloxacin	3.86×10^{-10}	0.64	331.4	-0.73	77.0
Moxifloxacin	3.77×10^{-10}	0.10	401.4	-0.082	86.3
Ofloxacin	2.45×10^{-10}	0.95	361.4	-0.51	77.5
Gatifloxacin	2.18×10^{-10}	0.13	375.4	-0.27	86.3
Clinafloxacin	2.71×10^{-10}	0.12	365.8	-0.42	91.0
Sparfloxacin	3.64×10^{-10}	0.12	392.4	-0.61	103.1

Figure 17 The steady-state concentration of 6 fluoroquinolones in *M. bovis* BCG. Results reflect accumulation at 10µM at the 30min mark as determined from fitted non-linear regression curves (see Figures 14). Average accumulation is expressed as the amount of drug (nmol) per colony forming unit (CFU).

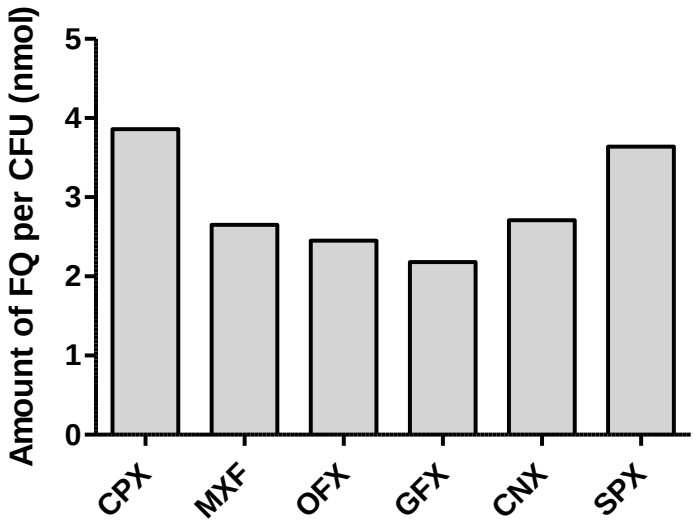

Figure 18 Correlations between the steady-state concentrations of six fluoroquinolones and (A) MIC_{90} and the following physicochemical properties: (B) molecular weight, (C) calculated partition coefficient (ClogP), and (D) polar surface area (PSA). Pearson's correlation coefficients (r) indicate the strength of correlations.

A

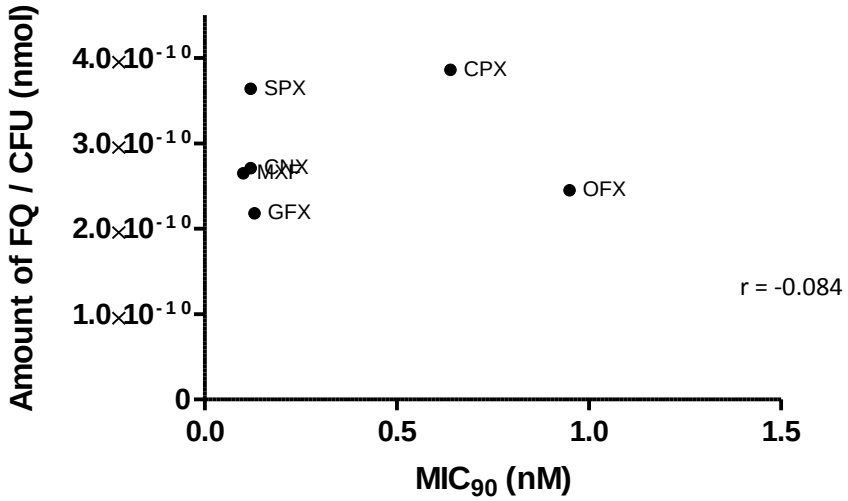

B

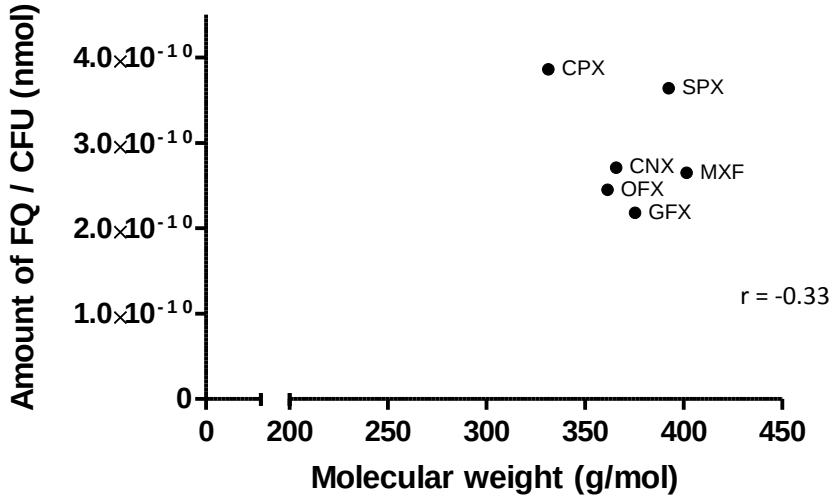

C

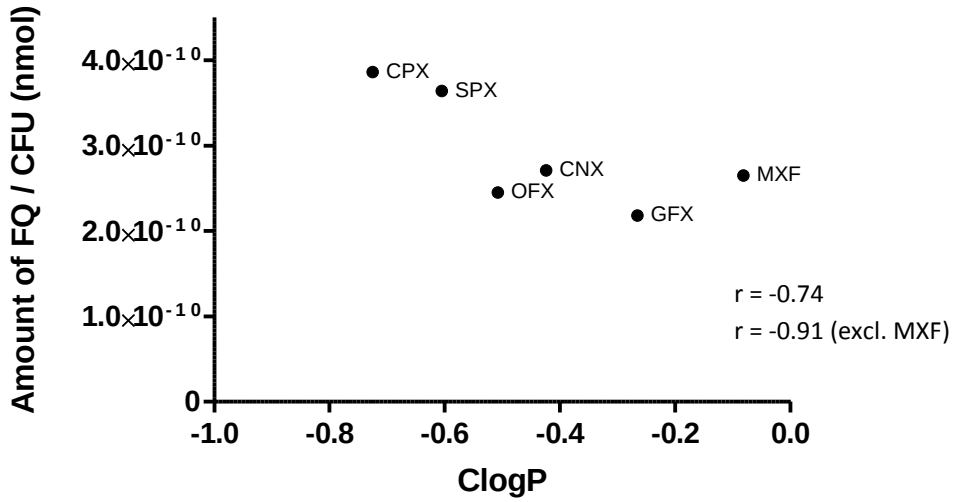
Amount of FQ / CFU (nmol)
4.0×10-10
3.0×10-10
2.0×10-10
1.0×10-10
0
CPX
SPX
CNX
OFX
MXF
GFX
r = -0.74
r = -0.91 (excl. MXF)
-1.0
-0.8
-0.6
-0.4
-0.2
0.0
ClogP

D

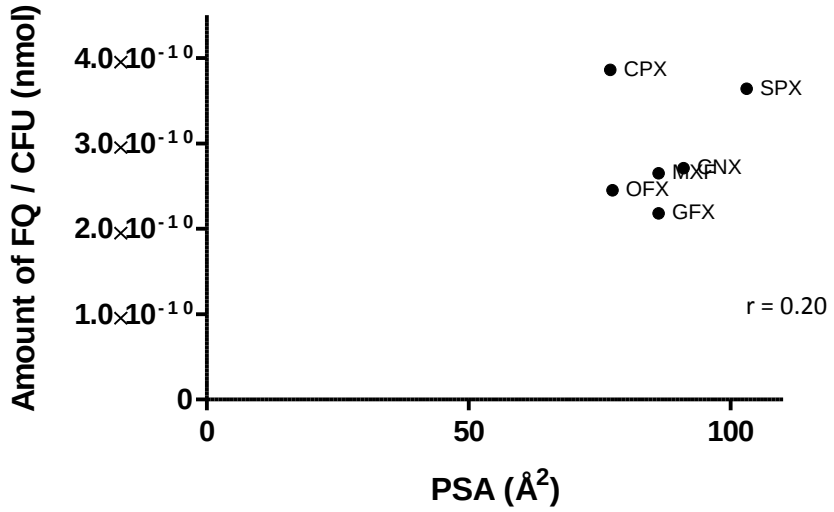
Amount of FQ / CFU (nmol)
4.0×10-10
3.0×10-10
2.0×10-10
1.0×10-10
0
CPX
SPX
CNX
MXF
OFX
GFX
r = 0.20
0
50
100
PSA (Å2)

3.3.3 Effects of external concentration on fluoroquinolone accumulation

The saturability of fluoroquinolone uptake was explored by incubating *M. bovis* BCG with increasing concentrations of fluoroquinolone (5, 10, 25, 50, 75, 100, 125, 150 and 200µM). Sampling of the drug-treated cultures was performed 30s after fluoroquinolone addition in order to reflect the initial rate of uptake (published and unpublished data suggest that the majority of ciprofloxacin penetration in *M. bovis* BCG occurs within the first minute) (182). The concentrations of fluoroquinolones accumulated intracellularly increased proportionately with increases in exogenous fluoroquinolone concentrations. **Figure 19 (A – F)** shows that the accumulation of all 6 fluoroquinolones in *M. bovis* BCG is non-saturable up to 200µM.

Figure 19 The effect of exogenous drug concentration on the initial rate of (A) ciprofloxacin, (B) moxifloxacin, (C) ofloxacin, (D) gatifloxacin, (E) clinafloxacin and (F) sparfloxacin accumulation by *M. bovis* BCG. Sampling was performed after 30s. The rate of drug accumulation is expressed as the absolute quantity of each fluoroquinolone per CFU (nmol / CFU/ min). Best-fit lines were fit using linear regression (GraphPad v5.0). The experiment was conducted with biological triplicates and standard deviations are shown as error bars.

A

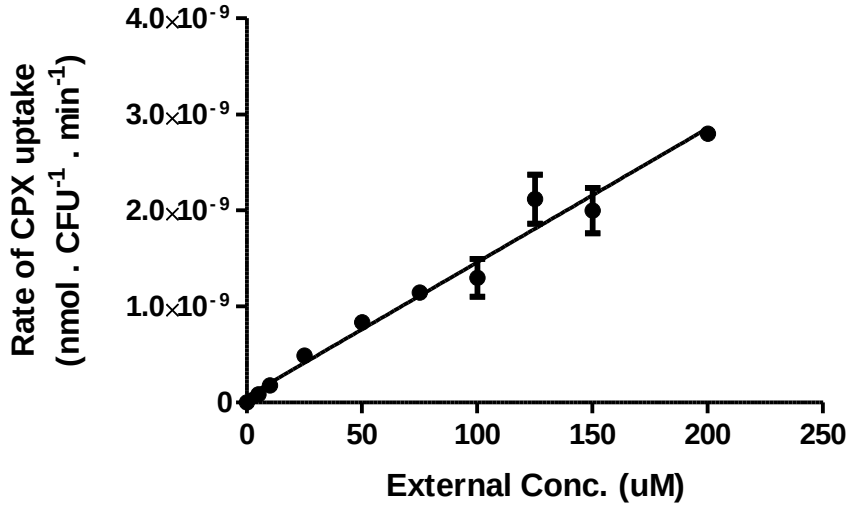

B

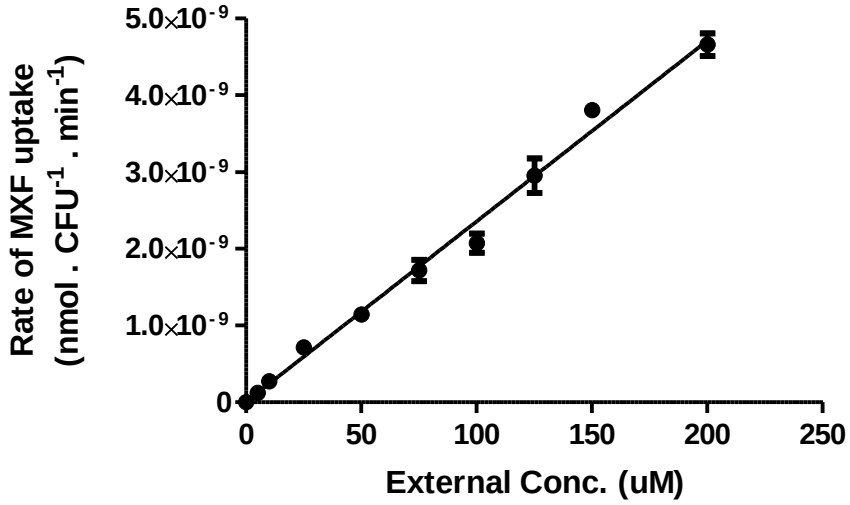

C

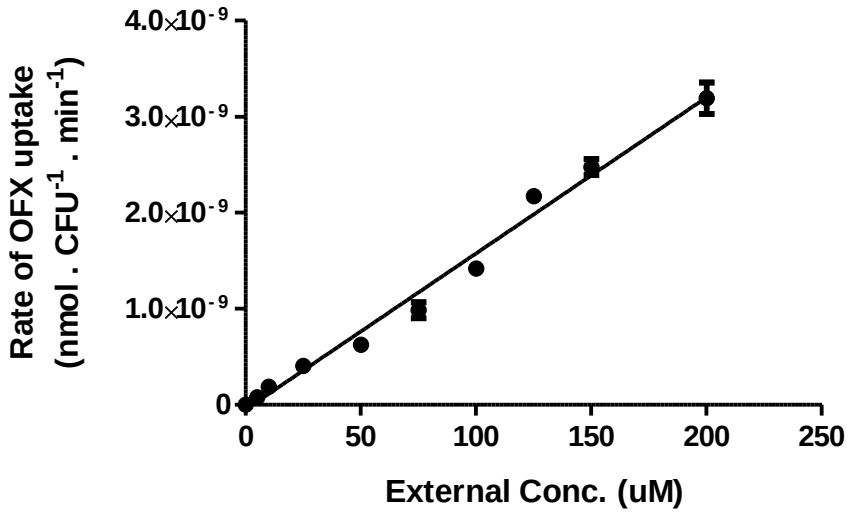
Rate of OFX uptake
(nmol . CFU-1 . min-1)
4.0×10-9
3.0×10-9
2.0×10-9
1.0×10-9
0
0
50
100
150
200
250
External Conc. (uM)

D

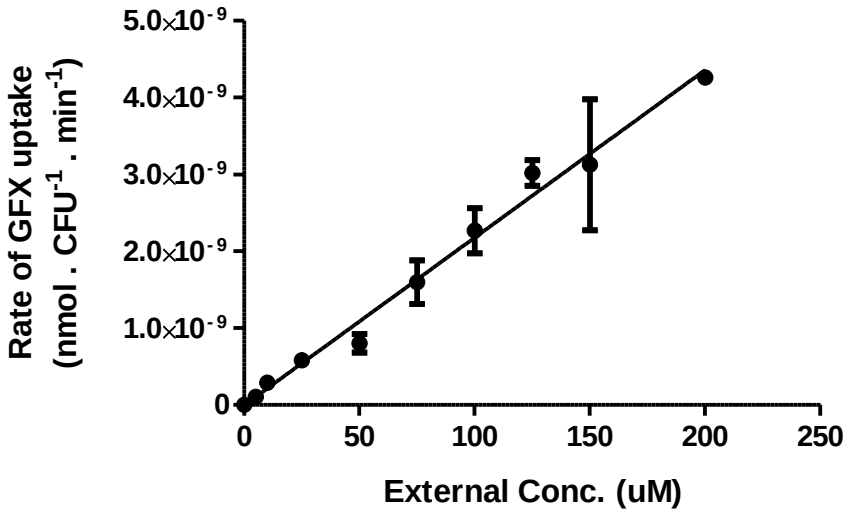
Rate of GFX uptake
(nmol . CFU-1 . min-1)
5.0×10-9
4.0×10-9
3.0×10-9
2.0×10-9
1.0×10-9
0
0
50
100
150
200
250
External Conc. (uM)

E

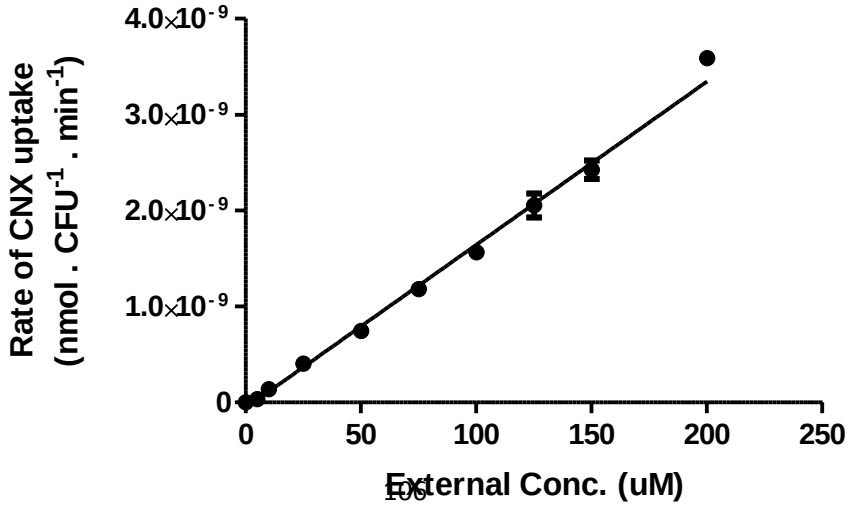
Rate of CNX uptake
(nmol . CFU-1 . min-1)
4.0×10-9
3.0×10-9
2.0×10-9
1.0×10-9
0
0
50
100
150
200
250
External Conc. (uM)

F

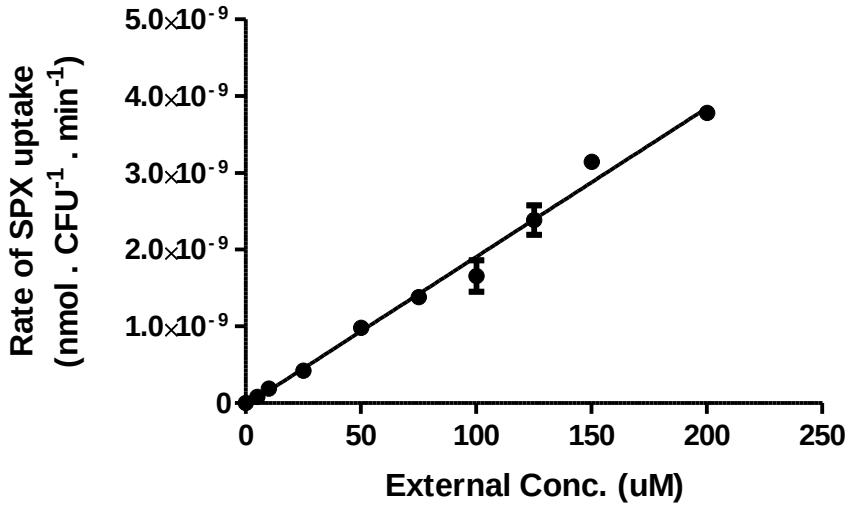
Rate of SPX uptake
(nmol . CFU-1 . min-1)
5.0x10-9
4.0x10-9
3.0x10-9
2.0x10-9
1.0x10-9
0
0
50
100
150
200
250
External Conc. (uM)

3.3.4 Investigating competitive inhibition of fluoroquinolone uptake

We set out to investigate if ciprofloxacin uptake would be inhibited in *M. bovis* BCG when co-incubated with another fluoroquinolone or with a known substrate of porin-mediated transport. BCG was incubated with 10μM of both ciprofloxacin and moxifloxacin and the extent of intracellular ciprofloxacin accumulation was compared against bacteria that incubated with the single drug. The addition of a second fluoroquinolone did not have a significant effect on ciprofloxacin accumulation ($p > 0.05$) **(Figure 20A)**. Next, we attempted a similar experiment with the β-lactam meropenem. It is understood that β-lactams utilize the porin transport pathway in both mycobacteria and non-mycobacterial species (112, 136). Co-incubation of ciprofloxacin and meropenem did not effect a significant change in ciprofloxacin accumulation in BCG ($p > 0.05$) **(Figure 20B)**. A range of meropenem concentrations was tested because it was unsure if the affinity of the porin in BCG responsible for fluoroquinolone uptake would be similar to its affinity for β-lactams. Ultimately, the competitive inhibition of fluoroquinolone uptake in mycobacteria was not achieved experimentally.

Figure 20 Competitive inhibition of ciprofloxacin accumulation. *M. bovis* BCG was co-incubated with ciprofloxacin (CPX) and (A) moxifloxacin (MXF) or (B) meropenem (MPN). MPN was tested at concentrations ranging between 10 and 100µM. The experiment was conducted with biological triplicates and standard deviations are shown as error bars.

A

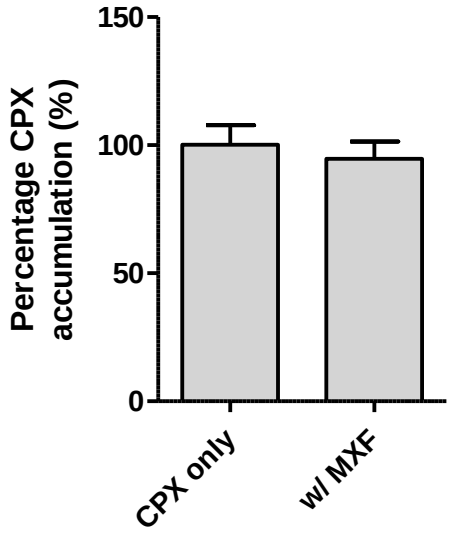

B

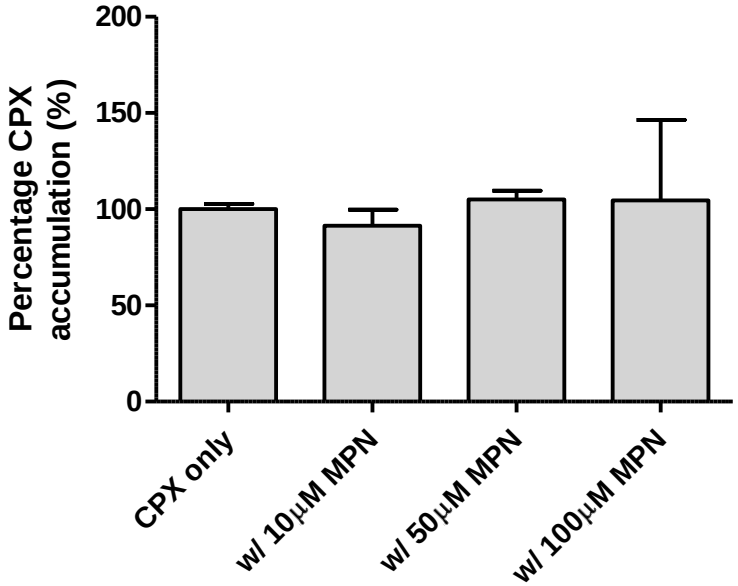

3.3.5 Effect of efflux pump inhibitors on fluoroquinolone accumulation

To determine whether active efflux influences intracellular accumulation of fluoroquinolones in mycobacteria, the penetration of ciprofloxacin, moxifloxacin or gatifloxacin in *M. bovis* BCG was examined in the presence of known efflux pump inhibitors. Verapamil and reserpine are both potent inhibitors of a wide range of efflux pumps in mycobacteria (174, 175, 212). Neither verapamil nor reserpine, at concentrations of 75µM and 20µM respectively, was able to produce significant change in the uptake of ciprofloxacin, moxifloxacin or gatifloxacin ($p > 0.05$) **(Figure 21)**.

Figure 21 The effects of efflux pump inhibitors, verapamil and reserpine, on ciprofloxacin (CPX), moxifloxacin (MXF) and gatifloxacin (GFX) accumulation in *M. bovis* BCG. The relative accumulation of each drug is expressed as percentage of uninhibited drug accumulation respectively. The experiment was conducted with biological triplicates and standard deviations are shown as error bars.

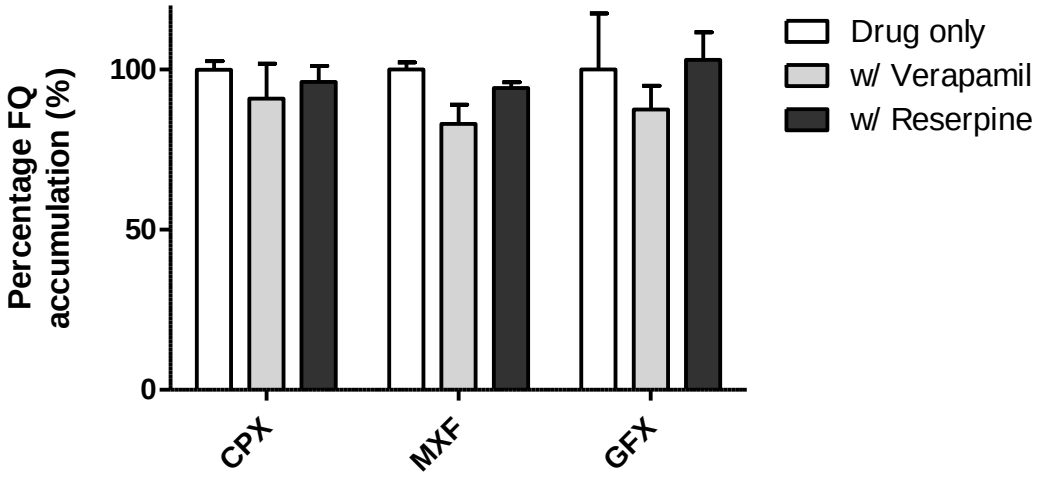

3.3.6 Investigating the dependence of fluoroquinolone accumulation and activity on carboxyl-group deprotonation

3.3.6.1 Effect of medium pH on fluoroquinolone accumulation

The effects of acidic external pH on fluoroquinolone penetration in mycobacteria were also investigated. The accumulation of ciprofloxacin, moxifloxacin and gatifloxacin in *M. bovis* BCG was measured at pH 6.5 (unadjusted 7H9 medium) and at pH 5. An increase in acidity of the medium resulted in significant decreases in intracellular accumulation of all three fluoroquinolones **(Figure 22)**. The reduction in intracellular accumulation ranged between 58% - 81%, with ciprofloxacin displaying the most drastic reduction.

3.3.6.2 Effect of medium pH on fluoroquinolone activity

Given that acidic conditions decrease the permeation of fluoroquinolones in *M. bovis* BCG, we proceeded to test whether their activities would similarly decrease. BCG was grown in pH-adjusted medium (pH 5.0) in the presence of ciprofloxacin, moxifloxacin and gatifloxacin over a range of concentrations for 5 days. The resulting observations of growth inhibition at pH 5.0 were normalized to data from bacteria grown in unadjusted medium. For all 3 fluoroquinolones, a decrease in external pH from 6.5 to 5.0 resulted in a loss in anti-mycobacterial activity **(Figures 23)**. The MIC_{90} of ciprofloxacin increased most drastically (8-fold) **(Table 15)**. The MIC_{90}s of moxifloxacin and gatifloxacin increased 4 and 5-fold respectively.

Figure 22 The effects of acidic external pH on the accumulation of ciprofloxacin (CPX), moxifloxacin (MXF) and gatifloxacin (GFX) in *M. bovis* BCG. Accumulation at pH 5.0 is expressed as the percentage of accumulation at pH 6.5 (unadjusted medium). The experiment was conducted with biological triplicates and standard deviations are shown as error bars.

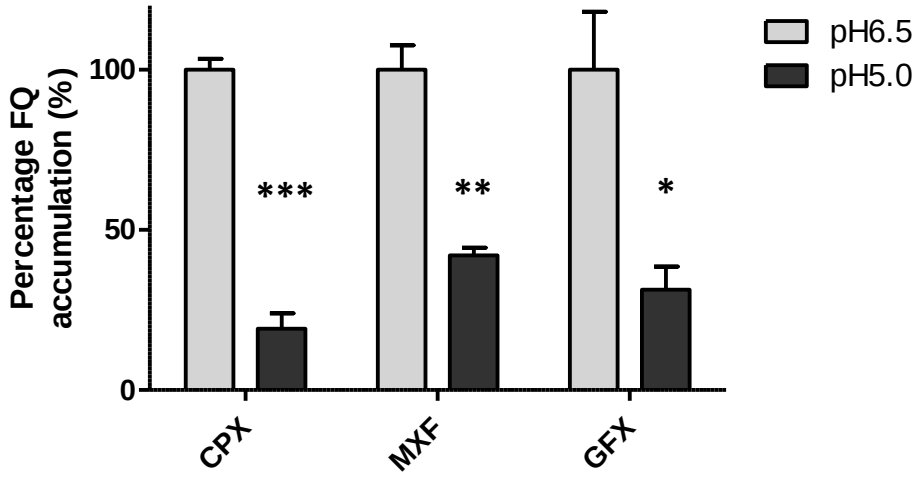

Figure 23 MIC curve-shifts for (A) ciprofloxacin, (B) moxifloxacin and (C) gatifloxacin as a result of increased medium acidity. Growth at pH 5.0 was assayed as OD_{600} readings and normalized against growth at pH6.5 and represented in percentages.

A

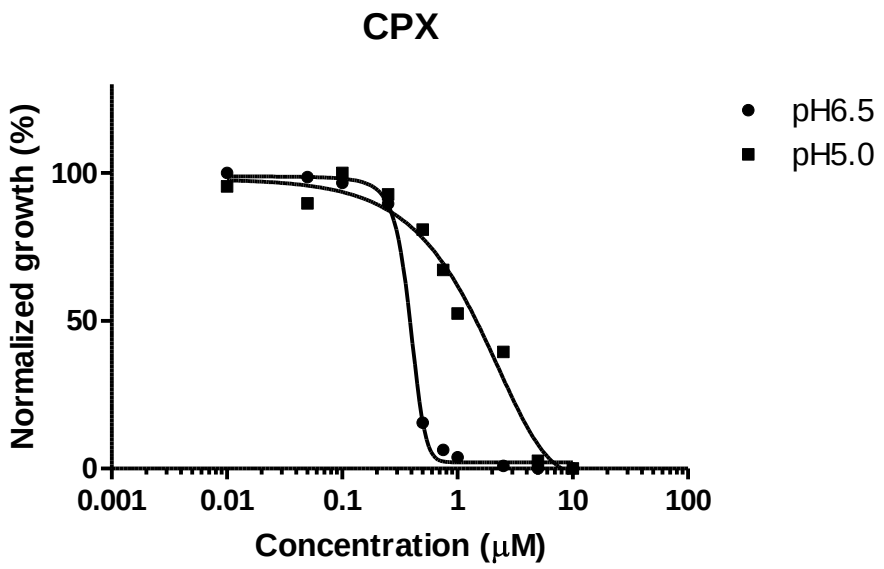

B

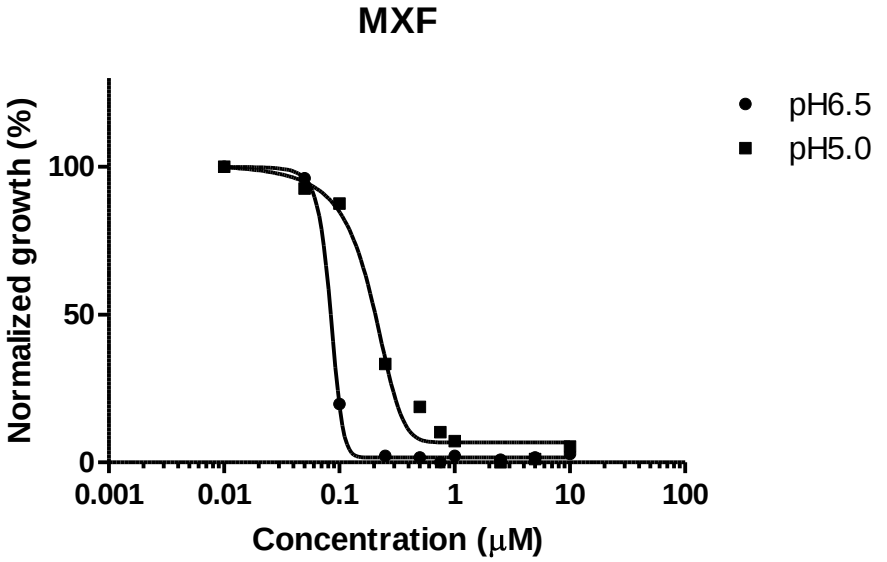

C

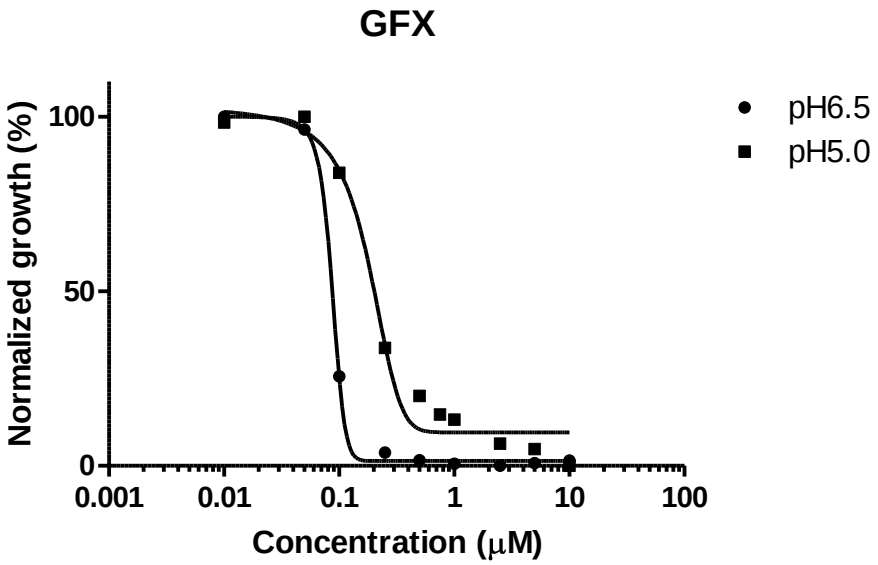

Table 15 MIC_{90} of ciprofloxacin, moxifloxacin and gatifloxacin against *M. bovis* BCG at pH6.5 and pH5.

MICs (μM)	CPX	MXF	GFX
pH6.5	0.55	0.1	0.1
pH5.0	4.6	0.4	0.5

3.4 Discussion

Fluoroquinolone uptake has been studied using various assays in a variety of bacterial species that include *E. coli*, *P. aeruginosa*, and *S. aureus* (143). The specific study of fluoroquinolone transport in mycobacteria thus far appears split between two hypotheses; fluoroquinolones uptake is believed to take place via either (1) passive diffusion through the lipid-rich outer membrane or (2) facilitated diffusion though porins located in the outer membrane. We attempted to study this uptake process using our newly-developed penetration assay and to further characterize it. Results showed that fluoroquinolone accumulation in *M. bovis* BCG is rapid, with steady-state intracellular concentrations being achieved within the first few minutes of exposure to the drugs. Our data also demonstrated that an increase in fluoroquinolone concentration between 5 and 200µM resulted in proportional increases in concentrations accumulated intracellularly. Also, this uptake was non-saturable within that concentration range. These results agree with published data on norfloxacin accumulation in *Mycobacteria aurum*; intracellular accumulation of norfloxacin was non-saturable over the concentration range of 0 - 100µg/ml (0 - 313µM) (243). Fluoroquinolone uptake in other bacterial species has also been reported as rapid and non-saturable (44, 143).

Physicochemical properties such as hydrophilicity, polarity and molecular weight frequently used to help understand the penetration properties of small molecules. ClogP is a general measure of the hydrophobicity / lipophilicity of a compound. The fluoroquinolones tested in this study were primarily hydrophilic (ClogP < 1). Interestingly, a strong correlation exists between the hydrophobicity the 6 fluoroquinolones and intracellular accumulation. Hydrophobic compounds are better equipped to directly diffuse through lipid membranes. Our observation that more hydrophilic fluoroquinolones are able to better permeate into mycobacteria indicates the

likelihood that channel proteins such as porins are responsible for their transport across the outer membrane. Molecular weight of fluoroquinolones only weakly correlated with intracellular accumulation. There was little variation in weight between the 6 fluoroquinolones in this panel, possibly explaining why only a weak correlation could be established. A previous study using a fluorometric assay also noted that there was no correlation between the anti-mycobacterial activity of fluoroquinolones and accumulation (182). Ultimately, rapid fluoroquinolone permeation in replicating wild-type *M. bovis* BCG or *M. tuberculosis,* combined with good affinity for the target enzyme, contributes towards their overall potency as anti-tuberculous agents.

Our data also shows that the accumulation of fluoroquinolones in *M. bovis* BCG is unaffected by efflux pump inhibitors reserpine and verapamil, similar to what has been demonstrated with *M. aurum*, *M. smegmatis* and *M. tuberculosis* with metabolic inhibitors such as reserpine, 2,4-dinitrophenol (DNP) and carbonyl cyanide m-chlorophenyl hydrazone (CCCP) (57, 182, 243). Verapamil is a calcium channel antagonist and reserpine is a P-glycoprotein inhibitor. Both compounds are commonly used to identify active efflux processes in microbial systems. The concentrations of reserpine and verapamil used here were based on similar experiments in previous studies (36, 174). These results apparently contradict the findings from a previous study of an efflux pump in *M. tuberculosis* with fluoroquinolones as substrates that responds to various chemical inhibitors (See Chapter 1, **Table 1**). However, those results were obtained by over-expressing a specific efflux pump which is not reflective of wide-type strains (174).

The effects of pH on fluoroquinolone susceptibility and penetration in *M. tuberculosis*, and mycobacteria in general, have not been elucidated prior to this study. It is known that a decrease in the pH of the medium results in an increase in MIC of norfloxacin against *E. coli* by up to 50 –

fold. Several-fold change in MIC of norfloxacin against *S. aureus* was also observed upon the increase in acidity of the medium (227). Based on these previous observations, we set out to determine the effects of acidic external pH on fluoroquinolone accumulation in *M. bovis* BCG. Interestingly, we were able to demonstrate that a decrease in the medium pH from 6.5 to 5 produced significant reductions in intracellular fluoroquinolone accumulation by up to 80%. Increases in fluoroquinolone MICs by several-fold as a result of the same decrease in external pH were also observed. Amongst the three fluoroquinolones tested at acidic pH, the magnitudes of reduction in fluoroquinolone activity correlated with magnitudes of reduction in intracellular accumulation (CPX > GFX > MXF). This phenomenon is believed to be due to decreased chelation of fluoroquinolones with Mg^{2+} in acidic pH due to a reduction in the deprotonation of their carboxyl groups (from COOH to COO^-) (168). From the pKa of ciprofloxacin (6.09 and 8.62) (11), we calculated that the ratio between protonated and deprotonated molecules is 30-times higher at pH5.0 than at pH6.5. It was previously suggested that quinolones chelate Mg^{2+} available on the surface of the outer membrane and acquire net positive charges that allow them to preferentially diffuse through porin channels, which usually have preferences for cations (168). The increasing acidity of incubation medium is therefore expected to compromise intracellular fluoroquinolone accumulation. Our study is the first to show that this phenomenon is evident in mycobacteria as well.

The decrease in fluoroquinolone penetration at acidic pH has wider *in vivo* applications. It is well understood that intracellular *M. tuberculosis* persists within the acidic environment of phagocytic vesicles. Although it is known to inhibit phagosome acidification as a survival mechanism, vacuole pH has been measured as being maintained at moderately acidic pH (180). Our findings make the case for the use of finafloxacin, a new investigational fluoroquinolone, for the

treatment of TB infections. Finafloxacin is known for its enhanced activity against *E. coli*, *S. aureus*, and *L. monocytogenes* at moderately acidic pH, compared to reduced potency of ciprofloxacin under those conditions (78, 117). Furthermore, an increase in potency of finafloxacin against *S. aureus* under acidic conditions was specifically shown to directly correspond with an increase in intracellular accumulation (117). As of yet, there is no published material on the study of finafloxacin activity against *M. tuberculosis* which is well worth pursuing in light of the results of this study.

Overall, the observations that fluoroquinolone accumulation in *M. bovis* BCG is dependent on its hydrophilicity and its potential to chelate metal ions indicate the preference for this class of compounds to utilize the porin transport pathway. The non-saturability, and inability to competitively inhibit this fluoroquinolone uptake with another fluoroquinolone or a β-lactam, appear to disprove the hypothesis that a specific transport protein is involved. However, this phenomenon could be explained by Nikaido's description of non-specific porin channel activity as being linearly dependent on substrate concentrations. This is compared to specific porins or porin-like channels that have true substrate specificities and are saturable (165). Further investigation in subsequent chapters was necessary in order to isolate and study this fluoroquinolone transport pathway.

CHAPTER 4

INHIBITION OF PORIN-MEDIATED FLUOROQUINOLONE TRANSPORT BY POLYAMINES

Parts of this project have been included in the following manuscript:

Sarathy JP, Lee EJD, Dartois V. Polyamines inhibit porin-mediated fluoroquinolone uptake in mycobacteria. *PLoS One.* 2013; 8(6): e65806.

4.1 Overview

As was explained in the previous chapter, porin-mediated transport seems a likely mechanism for the uptake of fluoroquinolones in *M. tuberculosis*. A previous study had demonstrated reduced fluoroquinolone susceptibility and / or accumulation in porin knock-out mutants of *M. smegmatis* (61). The identification of porins of *M. tuberculosis*, however, has been slow, and limiting to the performance of similar studies on this species. OmpATb, once believed to be the first porin to be successfully identified in *M. tuberculosis*, has been rejected on the basis of functional and structural analyses (217, 228). Only Rv1698 has so far demonstrated potential to be a true porin on *M. tuberculosis* although further investigation is necessary (214). Unfortunately, the difficulty of studying of porin-mediated drug uptake is compounded by the fact that chemical inhibitors are not traditionally used to isolate this pathway. The activities of efflux pumps, for instance, are often characterized by using inhibitors such as verapamil and reserpine (235). Even active uptake processes are isolated using uncouplers such as CCCP (191). Without chemical inhibitors of porins, the study of their transport capabilities remains limited to knock-out mutants.

Interestingly, the review of published literature revealed the existence of a class of compounds that inhibit the channel activity of porins in *E. coli*. Polyamines, which are ubiquitous to both prokaryotic and eukaryotic cells, have demonstrated the ability to suppress channel opening, enhance channel closure as well as promote the inactive state. It has been suggested that the main mechanism of porin channel modulation involves changes in the intrinsic rate constants for gating, which leads to the stabilization of the closed states (103). Drug accumulation studies have proven that the application of exogenous spermidine specifically reduces norfloxaxin influx through OmpF, a well-characterized porin of *E. coli* (45). Such evidence led us to the hypothesis that these small molecules could be used in a similar capacity to effect inhibition of porins-

mediated drug transport in mycobacteria as well without the need for prior identification of the specific porin /s involved.

In this chapter of the study, we explored the effects of polyamines on the intracellular accumulation of fluoroquinolones in *M. bovis* BCG. The potencies of spermidine, spermine, cadaverine and putrescine were compared, and it was shown that efficacy requires the application of polyamines in the millimolar range. The inhibitory activity of spermidine, the most potent inhibitor of the group, was characterized for its dose- and pH-dependencies. It was proven in this study that the positive charge on the polyamine is important for inhibition. These results correspond with those of studies on OmpF and OmpC of *E. coli* (71). Furthermore, we tested to see if a reduction in fluoroquinolone permeation would translate to decreased susceptibility of *M. bovis* BCG. Spermidine clearly increased the survival of *M. bovis* BCG to a 5-day exposure to ciprofloxacin by up to 25 times.

Our study went further by attempting to quantify the extent of polyamine production and quantification in *M. bovis* BCG which has not been previously accomplished. This was based on published evidence that *E. coli* secretes endogenous cadaverine to modulate its outer membrane permeability during exposure to harsh conditions such as acidic external medium (203). Our measurement of high intracellular cadaverine concentration indicates that *M. tuberculosis* may similarly alter its outer membrane permeability in response to harsh external stimuli.

4.2 Materials and Methods

4.2.1 Chemicals

Spermidine, spermine, cadaverine and putrescine were obtained from Sigma-Aldrich (Missouri, U.S.A.). Stock solutions of 1M were prepared for all polyamines and stored at 4°C. 2,4,6-trinitrobenzenesulfonic acid (TNBS) and sodium carbonate were obtained from Sigma and aqueous solutions of 10.2mM and 1M, respectively, were prepared.

4.2.2 Drug Penetration Assay and Quantitative Analysis

The standard drug penetration was assay was conducted as described in Chapter 3 for the measurement of steady-state intracellular drug accumulation. When the kinetics of fluoroquinolone uptake over a 30min period was being examined, samples were taken over the following time intervals: 0, 1, 2, 3, 5, 10, 15, 20, 25, and 30min. In polyamine-inhibition experiments, cultures were pre-incubated with the specified polyamine for a period of 10min at a concentration of 10mM unless otherwise mentioned. The pH of supplemented 7H9 medium was adjusted from 6.5 to 8.0 and 9.0 by the addition of sodium hydroxide when specified. Quantitative analysis of drug concentration was achieved by LC/MS as described previously. The LC-gradient methods used for each compound have been listed in Chapter 2.

4.2.3 Susceptibility Testing

The MIC_{90}s of polyamines were assessed in a manner similar to what was described in the Chapter 2. Spermidine and cadaverine activities were assessed within the range of 0.001 to 50mM. In fluoroquinolone MIC-shift experiments, dilutions of ciprofloxacin were prepared to achieve the final range of 0.05-2.0µM; spermidine and cadaverine were co-spotted with ciprofloxacin when needed to achieve the final concentrations of 0.01, 0.1 and 1mM. In kill-kinetics assays, broth cultures with an OD_{600} of 0.2 were incubated with specific concentrations of ciprofloxacin and polyamine; 20µl aliquots were removed after specific time intervals and spread onto agar plates following ten-fold serial dilutions.

4.2.4 Generation of spontaneous mutants

Middlebrook 7H11 plates were prepared as described earlier with the addition of a range of concentrations of spermidine. These concentrations were several -fold higher than the MIC_{90} of spermidine against *M. bovis* BCG (3.5mM). The final concentrations of spermidine were 4mM, 5mM, 7.5mM, 10mM, and 15mM. Mycobacterial cultures were grown to an OD_{600} of 0.3-0.4. 100ml of culture was harvested by centrifugation at 3,200rpm for 10min. The pellet was re-suspended in 1ml of fresh 7H9 medium to give the approximate cell density of 1×10^{11} cells/ml. A series of 10X dilutions of this culture were prepared in fresh 7H9 medium. 100µl of bacterial culture containing 10^9, $10^7$and 10^5 cells/ ml were spread onto compound-containing 7H11 agar plates. To estimate the exact original viable cell count of the culture, culture dilutions were also spread on drug-free 7H11 agar plates. All culture dilutions were plated in triplicates. Plates were incubated at 37°C under aerobic conditions for 4-6 weeks.

4.2.5 Statistical tests

For the determination of statistical significance of differences in drug uptake between polyamine –treated and –untreated *M. bovis* BCG, unpaired *t*-tests with Welch's correction (assuming unequal variances) (GraphPad Prism v5.0) were used. Significant, very significant and extremely significant differences were benchmarked at *p*-values of 0.05 (*), 0.01 (**) and 0.005 (***) respectively.

4.2.6 Quantification of cadaverine production and secretion

The assay used is adapted from procedures described elsewhere, with several modifications (179, 202). The procedure is based on the principle that cadaverine, a product of lysine decarboxylase, forms a coloured reaction-product with 2,4,6-trinitrobenzene sulfonate (TNBS) that is soluble in toluene. The product formed with reaction precursor, lysine, is not soluble in toluene **(Figure 24)**. Briefly, *M. bovis* BCG cultures were grown to an OD_{600} of 0.3 - 0.4 and concentrated to an approximated OD_{600} of 4.0 in PBS. The bacilli were then subjected to bead-beating in screw-capped micro-centrifuge tubes containing 0.1mm zirconia / silica beads. Tubes were shaken in a bead-beater (Precellys 24, Bertin Technologies) for 3 x 60s cycles at 6,000rpm with at least 1min rest periods on ice between cycles. Beads and cell debris were pelleted at 13,000rpm and cell lysates were filter-sterilized. Each 500µl of cell lysate was mixed with 500µl of 1.0M sodium carbonate and 500µl of 10.2mM TNBS. This mixture was incubated for 5min at 42°C. The cadaverine-TNBS adduct was extracted by vigorous vortexing of the mixture with 1ml of toluene for 20s and centrifugation at 2,500rpm for 5min. 200µl of the organic layer was transferred to 96-well plates and the absorbance at 340nm detected by a spectrophotometer (SpectraMax Plus,

Molecular Devices) with the use of appropriate blanks. Standard curves were similarly established for cadaverine in the concentration range of 5 – 250µM.

4.2.7 Sequence alignment

Multiple sequence alignment of CadB orthologues from various mycobacterial species was performed by ClustalW (Kyoto University Bioinformatics Centre; Japan) which was made available at www.genome.jp/tools/clustalw/ (27).

Figure 24 A schematic diagram showing adduct-formations between TNBS and lysine / cadaverine. The coloured products have different solubilities in toluene. This diagram was obtained from Phan *et al* (179).

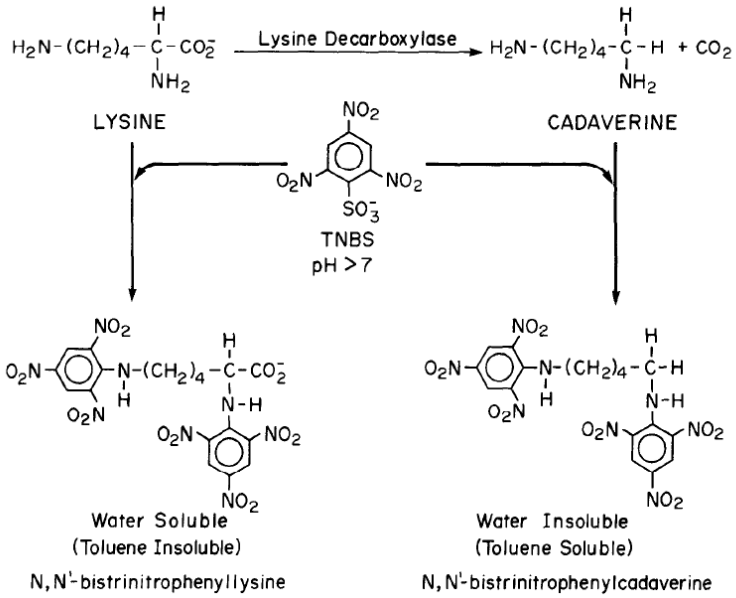

4.3.2 Results

4.3.1 Inhibitory effects of polyamines on fluoroquinolone accumulation

4.3.1.1 Potencies of various polyamines

We set out to investigate the effect of polyamines on fluoroquinolone accumulation in mycobacterium. In this study, drug accumulation was assessed at the steady-state (unless otherwise mentioned), 30min after exposure to the drug. Pre-incubation with 10mM of spermidine, spermine, cadaverine and putrescine reduced intracellular accumulation of ciprofloxacin in *M. bovis* BCG **(Figure 25)**. At 10mM, spermidine proved most potent at decreasing ciprofloxacin accumulation, reducing the final ciprofloxacin intracellular accumulation by 69% relative to the control assay (p <0.001). Putrescine was least effective, causing a reduction in steady-state intracellular concentrations of only 19% (insignificant). The inhibitory effects of spermidine, spermine and cadaverine on ciprofloxacin accumulation were assessed over the concentration range of 0.01 – 30mM **(Figures 26)**, and the IC_{50}s were determined **(Table 16)**. The inhibitory activities of all three polyamines were evident in the millimolar range. Spermidine was most potent (IC_{50} = 3.9mM), followed by spermine and cadaverine. Spermidine was hence selected for subsequent experiments unless otherwise mentioned. Interestingly, 100% inhibition of ciprofloxacin accumulation was not achieved by any polyamine even though it was evident that their effects had maximized by the highest tested concentration of 30mM.

Figure 25 Inhibition of ciprofloxacin (CPX) accumulation in *M. bovis* BCG by treatment with 4 different polyamines. Relative uptake of CPX is expressed as percentage of average uninhibited uptake. The experiment was conducted with biological triplicates and standard deviations are shown as error bars. Asterisks denote data points that differed significantly between spermidine-treated and -untreated BCG.

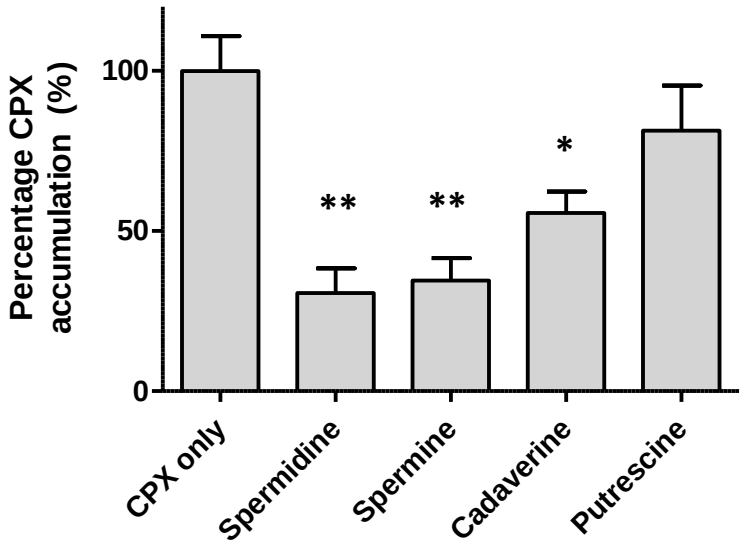

Figure 26 Ciprofloxacin accumulation in *M. bovis* BCG in response to increasing concentrations of (A) spermidine, (B) spermine, (C) cadaverine. Ciprofloxacin uptake in each figure is expressed as the percentage of uninhibited uptake (100%) respectively. Polyamine concentrations are plotted on a log scale. The experiments were conducted with biological triplicates and standard deviations are shown as error bars.

A

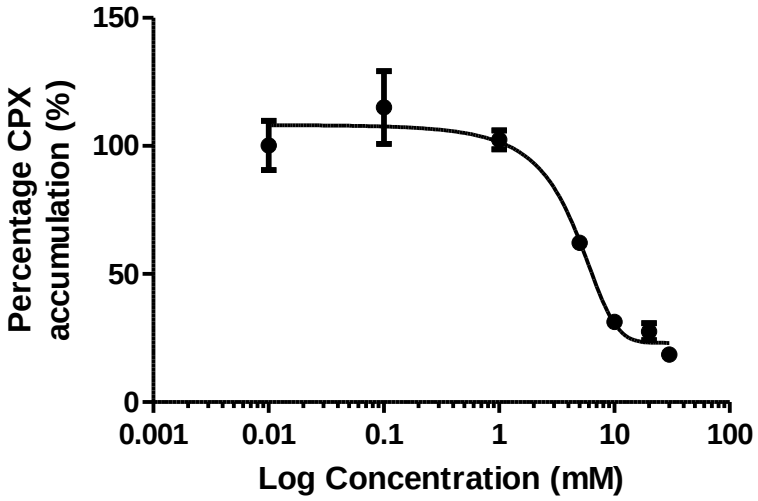

B

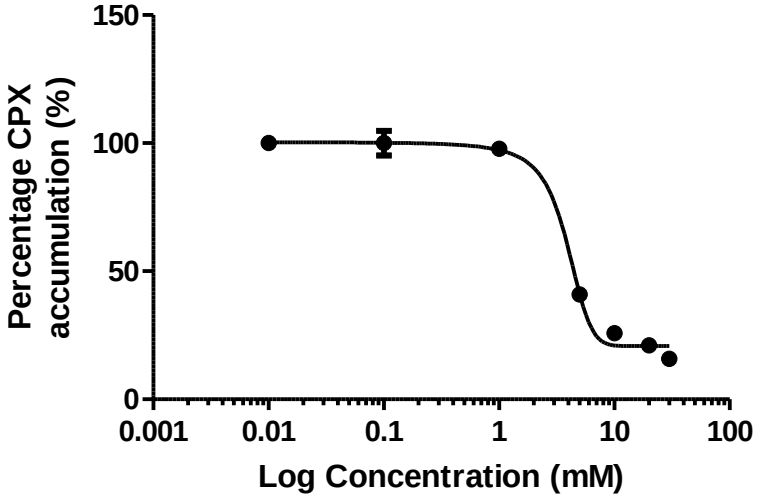

C

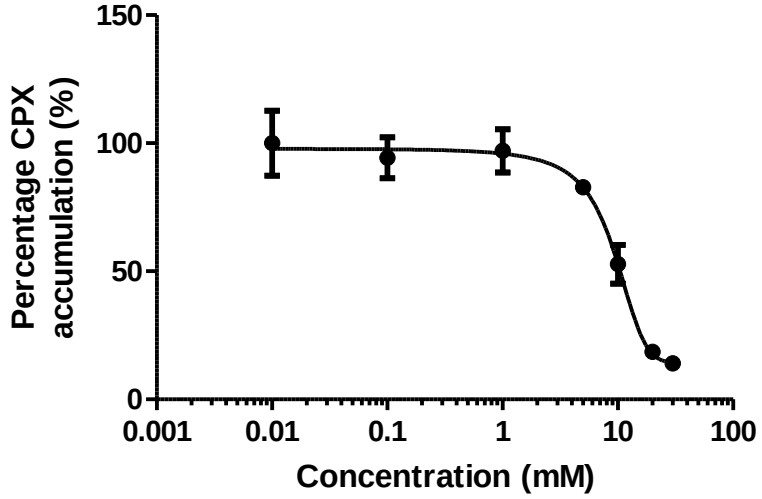

Table 16 The IC_{50}s of polyamines on the uptake of ciprofloxacin by *M. bovis* BCG. IC_{50} was defined as the concentration required to achieve 50% inhibition of ciprofloxacin accumulation.

Polyamine	IC50 (mM)
Spermidine	3.9
Spermine	3.8
Cadaverine	9.1

4.3.1.2 Effects of spermidine on the kinetics of fluoroquinolone accumulation

The effects of spermidine on the kinetics of ciprofloxacin accumulation during a 30 min incubation period were determined. Spermidine clearly reduced steady-state accumulation of the drug rather than just delaying it, resulting in a downward shift of the time-based curve **(Figure 27)**. Spermidine-treated BCG only took 3 min to achieve equilibrium conditions while non-treated bacteria took 20 – 30min to equilibrate uptake. In order to ensure that any reduction in drug uptake by *M. bovis* BCG brought about by spermidine was the result of inhibition of porin-mediated uptake rather than cell death, a time-kill experiment was conducted. A 60min incubation period with 10mM of spermidine did not significantly reduce the number of colony-forming units **(Figure 28)**.

4.3.1.3 Intra -class variation in response to polyamine treatment

Reductions in moxifloxacin, ofloxacin and gatifloxacin steady-state intracellular accumulation were also observed in the presence of spermidine, proving that this phenomenon is reproducible across the fluoroquinolone class **(Figure 29A)**. The extent of reduction in accumulation varied between 69% and 31% across the four fluoroquinolones, with ciprofloxacin accumulation displaying the greatest reduction. In order to investigate if the effect of polyamine pre-treatment on drug uptake is fluoroquinolone-specific, further experiments were conducted with ethambutol, rifampicin and linezolid. The presence of 10mM of spermidine resulted in a 33% and 25% reduction in steady-state intracellular accumulation of linezolid and ethambutol respectively **(Figure 29B)**. Rifampicin, however, displayed an increase in accumulation by 58%, further supporting the notion that spermidine does not affect cell viability at concentrations up to 10mM.

Figure 27 The effects of 10mM of spermidine on the kinetics of CPX accumulation (at 10µM) during a 30min period. Standard deviations are shown as error bars.

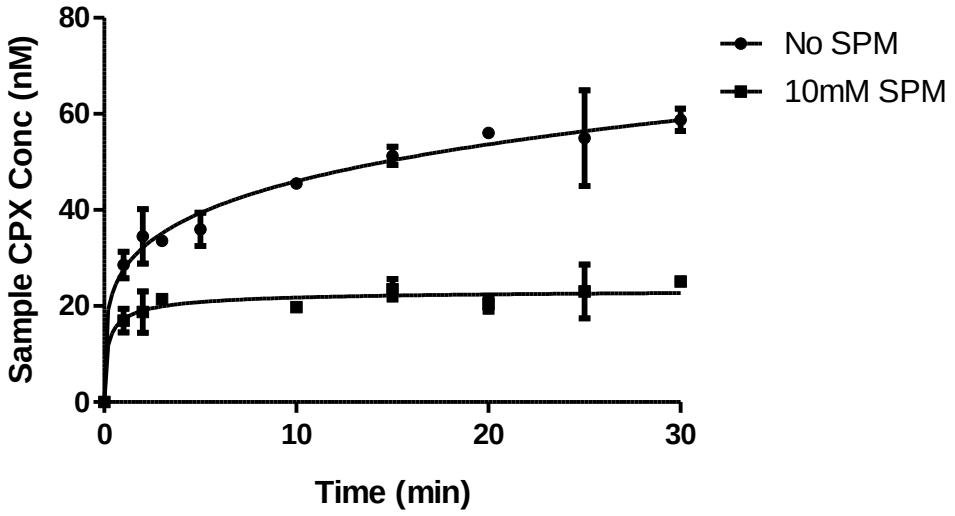

Figure 28 Kill -kinetics of 10mM of spermidine against *M. bovis* BCG for the first 60min of incubation. Standard deviations are shown as error bars.

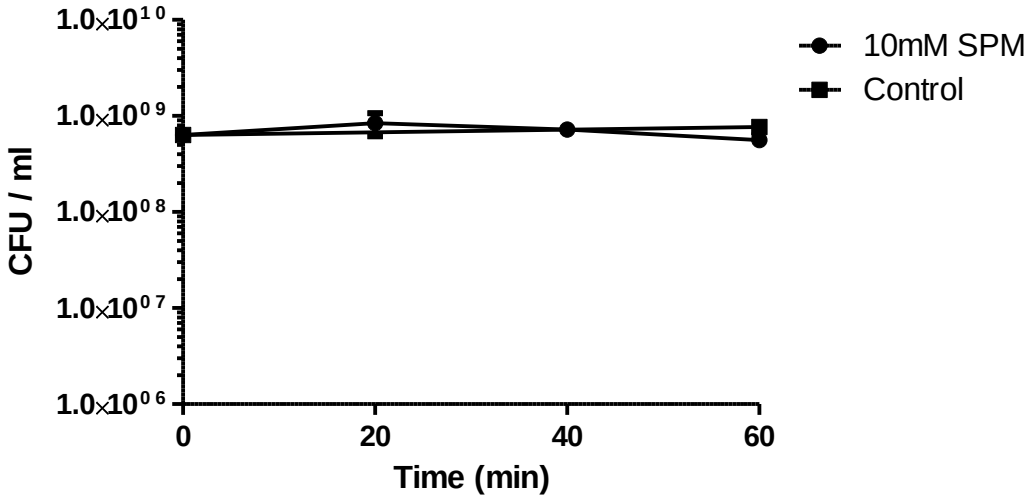

Figure 29 (A) The inhibitory effect spermidine has on the accumulation of moxifloxacin (MXF), ofloxacin (OFX) and gatifloxacin (GFX), as compared to CPX, in *M. bovis* BCG. (B) The effect spermidine has on the uptake of linezolid (LNZ), rifampicin (RIF) and ethambutol (EMB) in *M. bovis* BCG. Relative uptake of each drug is expressed as percentages of uninhibited drug uptake respectively. The experiment was conducted with biological triplicates and standard deviations are shown as error bars. Asterisks denote data points that differed significantly between spermidine treated and untreated BCG.

A

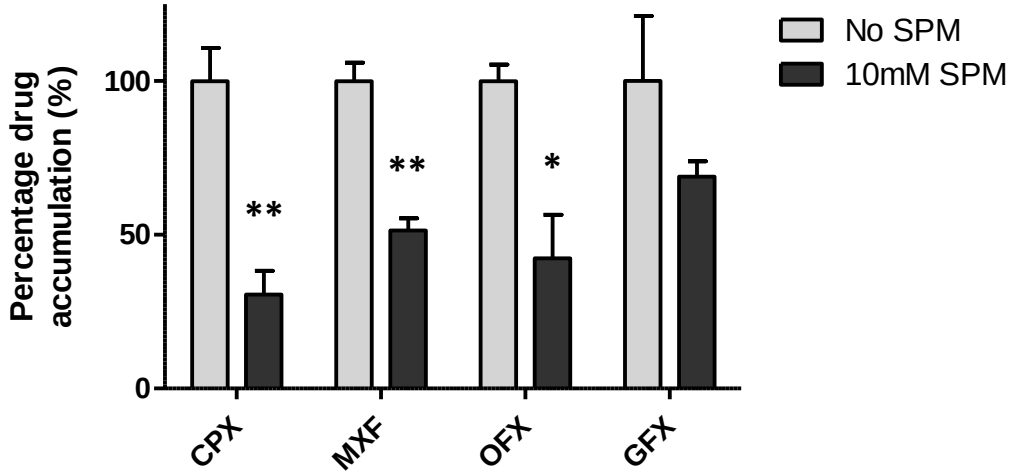

B

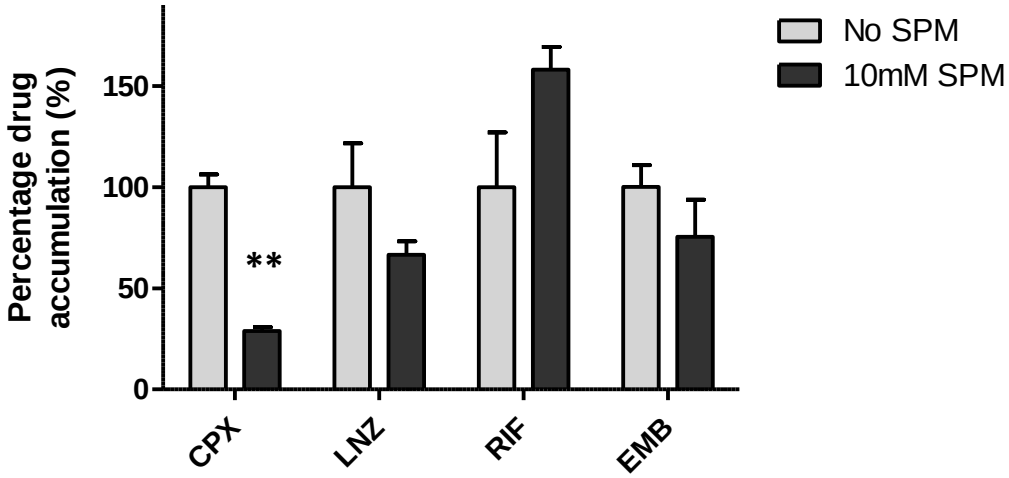

4.3.2 Reversibility of effects of polyamines

The reversibility of the effects of polyamine treatment was investigated in order to further characterize the porin-inhibitory mechanism. When *M. bovis* BCG cultures that were pre-incubating with spermidine were washed with PBS prior to incubation with ciprofloxacin, a partial recovery in steady-state ciprofloxacin accumulation was observed **(Figure 30)**. Saline washes brought about an increase in ciprofloxacin uptake to approximately 80% of uninhibited uptake. No significant difference resulted from washing the bacilli twice rather than once. These results indicate that inhibition of porin-mediated fluoroquinolone uptake is mostly reversible. It is possible that a fraction of spermidine remains tightly adhered to the outer membrane or binding sites on porins despite two PBS washes. Alternatively, recovery in ciprofloxacin uptake may be underestimated at each additional wash step due to the partial loss of bacilli.

4.3.3 Effect of pH changes on polyamine activity

Ciprofloxacin penetration assays were performed on *M. bovis* BCG in pH-adjusted media in order to demonstrate the effect of increasing pH on the polyamine inhibitory activity. Steady-state intracellular ciprofloxacin concentrations in BCG pre-incubated with spermidine were normalized against uninhibited ciprofloxacin accumulation under the respective pH conditions. **Figure 31** shows that when supplemented 7H9 medium was adjusted to pH 8, spermidine reduced ciprofloxacin accumulation by 68% which is comparable to results obtained with unadjusted medium (pH6.5). At pH9, spermidine only produced a 36% reduction in ciprofloxacin accumulation. Cell viability remained unaffected for the incubation duration of 30min at pH9.

Figure 30 The effects of PBS washes on the inhibition of ciprofloxacin (CPX) accumulation in *M. bovis* BCG that has been pre-incubating with spermidine. Relative ciprofloxacin accumulation is expressed as percentages of maximum (uninhibited) uptake. The experiment was conducted with biological triplicates and standard deviations are shown as error bars.

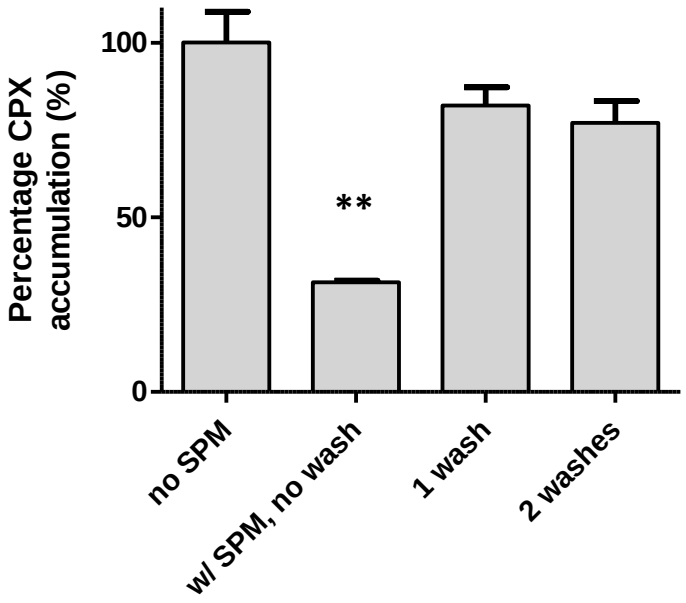

Figure 31 The effects of increasing pH on the inhibitory effects of spermidine. Ciprofloxacin accumulation in the presence of spermidine was normalized against uninhibited accumulation for the respective pH conditions. Standard deviations are shown as error bars.

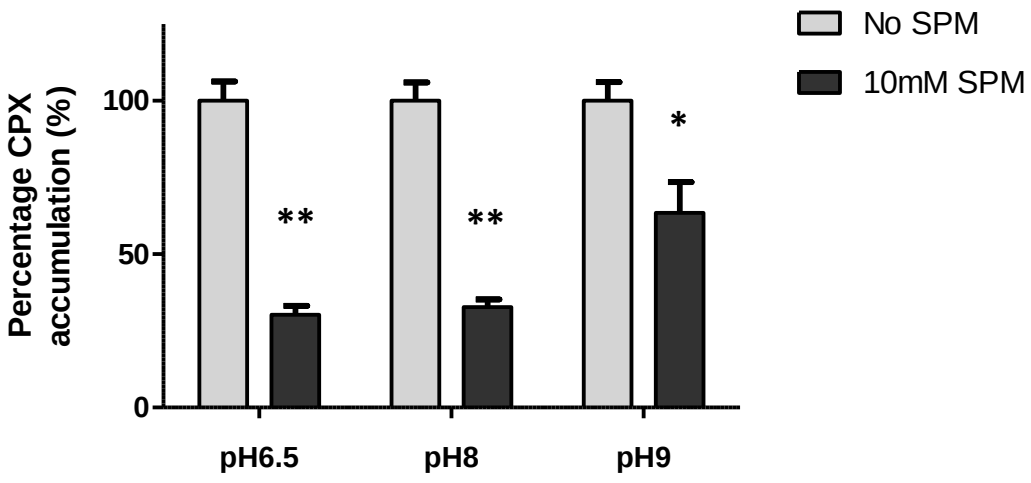

4.3.4 Effect of spermidine on mycobacteria susceptibility to ciprofloxacin

Given the reduced uptake of ciprofloxacin in the presence of polyamines, we hypothesized that the anti-mycobacterial activity of ciprofloxacin could be weakened in the presence of spermidine. We first tested the growth inhibitory properties of spermidine and cadaverine on their own. OD_{600} measurements made after a 5 day incubation period revealed that both spermidine and cadaverine begin to inhibit *M. bovis* BCG growth at concentrations above 1mM **(Figure 32).** Concentrations below 1mM for both polyamines were hence chosen in experiments aimed at evaluating polyamine-induced changes in ciprofloxacin susceptibility. At 0.01, 0.1 and 1.0mM, neither polyamine brought about a shift in ciprofloxacin-mediated growth inhibition **(Figure 33)**, with the MIC_{90} of ciprofloxacin against *M. bovis* BCG remaining constant at 0.7µM. However, enumeration of colony-forming units revealed that ciprofloxacin-mediated killing of *M. bovis* BCG was reduced by 10 and 25-fold in the presence of 1.0mM and 2.5mM of spermidine respectively over a 5 day period **(Figure 34)**. The differences in the number of viable bacilli between spermidine-treated and -untreated cultures are statistically significant at the 5-day mark ($p < 0.001$).

Figure 32 MIC curves of spermidine and cadaverine against *M. bovis* BCG. Growth of BCG was evaluated as OD readings at 600nm.

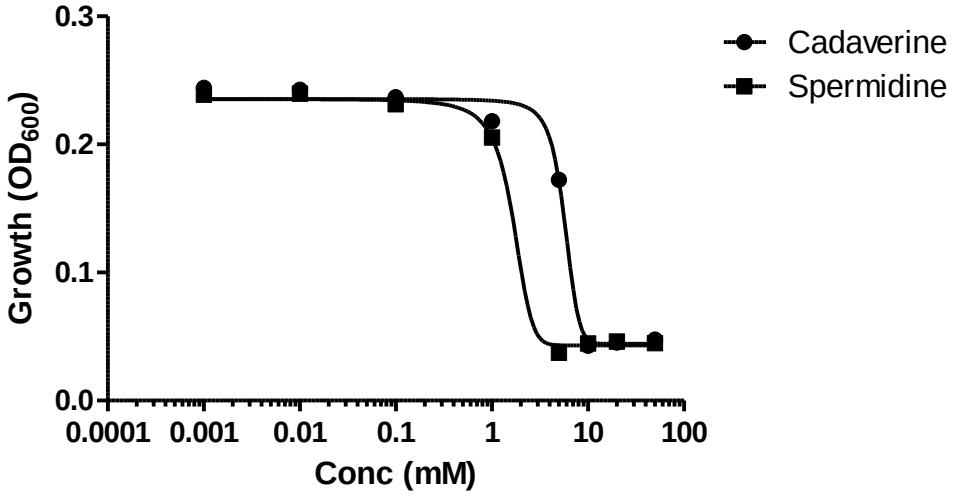

Figure 33 MIC curves of ciprofloxacin against *M. bovis* BCG in the presence of varying concentrations (0.01, 0.1 & 1.0mM) of spermidine and cadaverine.

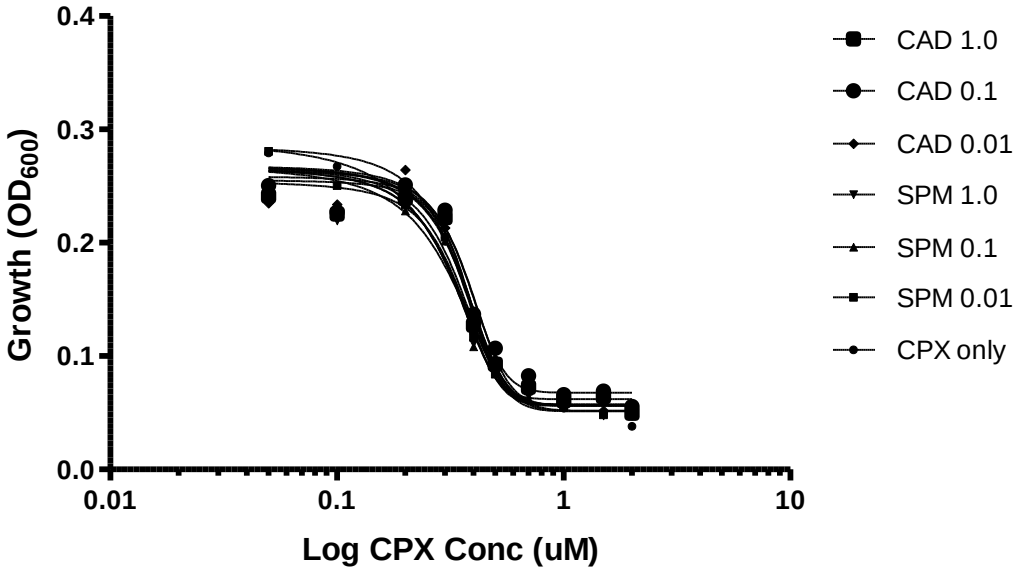

Figure 34 Kill-kinetics of *M. bovis* BCG during a 5-days incubation period with ciprofloxacin and spermidine. The effects of pre-incubation with 100µM and 1mM of spermidine (SPM) were compared against incubation with 10µM ciprofloxacin (CPX) alone. The experiment was conducted with biological triplicates and standard deviations are shown as error bars.

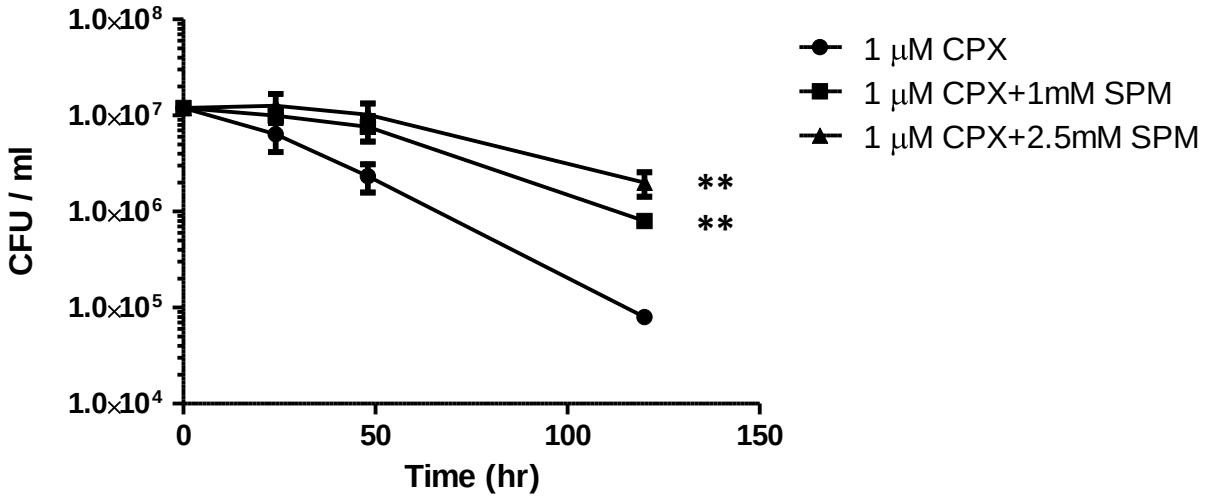

4.3.5 Spontaneous Mutant Generation

Attempts were made to generate *M. bovis* BCG mutants against spermidine by plating cultures onto 7H11 agar plates containing a range of concentrations of the polyamine. Multiple generations of bacteria from several inoculums were tested. No spontaneous mutants were generated at any of the spermidine concentrations above 3.5mM (up to 15mM) despite the plating of bacterial densities as high as 1×10^9 (approximate). At 3.5mM itself and below, a lawn of colonies was obtained.

4.3.6 Cadaverine Production and Secretion

The cadaverine content of *M. bovis* BCG growing in 7H9 medium was measured without stimulation by addition of lysine or exogenous cadaverine. Similar to what was demonstrated by Samartzidou *et al* (202), cadaverine standard curves showed that the assay was linear between absorbance values of 0.1 and 1.0, with the latter corresponding to 250µM cadaverine **(Appendix III, Figure 21)**. Cadaverine concentrations of cell lysates were normalized to the number of CFU. The calculated amount of cadaverine per viable bacillus averaged at $(2.54 \pm 0.31) \times 10^{-8}$ nmol (n = 3). Assuming a cellular volume of $0.5\mu m^3$ based on the dimensions of the tubercle bacillus (56, 91), the estimated intracellular concentration of cadaverine in BCG was 50mM.

4.4 Discussion

In *E. coli*, the inhibitory effect of polyamines on the outer membrane permeability is due to their specific interactions with the OmpF and OmpC porins (70). Porins are trans-membrane proteins that act as channels for a wide variety of molecules. In facilitating chemotaxis and the flux of antibiotics, porins contribute significantly to the overall permeability of the outer membrane. There is general consensus that polyamine binding in *E. coli* causes a conformational change in the porin, which promotes the prolonged occupancy of the closed state, though it cannot be excluded that some steric blocking of the open channel may occur (71). It is plausible that polyamines may inhibit mycobacterial porins in a similar manner. In this study, we have explored the possibility of chemically inhibiting fluoroquinolone transport in mycobacteria by use of polyamines. Similar to published work in *E. coli* (45, 71, 103), we have demonstrated that significant reduction of mycobacterial outer membrane permeability requires polyamines in the millimolar range. It is known that the intracellular concentration of spermidine approximates 6mM in *E. coli*. Under normal conditions, the intracellular concentration of putrescine in *E. coli* is estimated at about 20mM, with the potential to be further increased by high pH (16). We hypothesized that millimolar concentrations of polyamines are also present in mycobacteria and that they are involved in the modulation of outer membrane permeability. Since the effects of cadaverine production and excretion in *E. coli* have been particularly emphasized in literature (202, 203, 216), we proceeded with the study of mycobacterial cadaverine production.

A spectrophotometric assay based on the formation of toluene-soluble cadaverine adducts of TNBS allowed for the measurement of cadaverine content of *M. bovis* BCG lysate. We estimated the intracellular concentration of cadaverine in un-stimulated BCG to be 50mM. Though this is significantly higher than the reported polyamine content of other bacteria, it could help explain

why the mycobacterial outer membrane is so much less permeable than its counterparts. The *cadA* gene, which encodes for lysine decarboxylase, is responsible for cadaverine production in *E. coli*. A BLAST search for an orthologue of CadA in *M. tuberculosis* revealed amino acid sequence homology with Rv2531 (24% identity, 41% positives). Rv2531 is believed to be an ornithine / arginine / lysine decarboxylase although its exact function has not been characterized (102). We suggest that this gene may be responsible for cadaverine production in *M. tuberculosis*.

Attempts were also made to study cadaverine excretion by *M. bovis* BCG by analyzing filtered media from growing cultures. Unfortunately, supplemented 7H9 medium is rich in compounds that absorb at 340nm (the wavelength used in the assay for cadaverine quantitation) and samples could not be successfully blanked using this fluorometric assay. CadB is the protein responsible for cadaverine transport in *E. coli*. It is not only responsible for cadaverine uptake, but also cadaverine excretion via cadaverine-lysine antiport activity (216). CadB is classified as a member of the Amino acid-Polyamine-Organocation (APC) superfamily of transporters (199). Although direct evidence of cadaverine secretion in mycobacteria could not be provided in this study, BLAST searches and multiple-sequence alignments showed that putative transporters of cadaverine are present in *M. tuberculosis*, *M. bovis* BCG and *M. smegmatis* **(Figure 35)**. The amino acid sequence of Rv1999c of *M. tuberculosis* shares 23% identity and 40% similarity with CadB of *E. coli*. Although the function of Rv1999c has not been characterized, it is hypothesized to be an integral membrane protein involved in the transport of cationic amino acids across the membrane (102). This possible CadB orthologue of *M. tuberculosis* shares 100% and 74% identity with orthologues in *M bovis* BCG (Mb2022c) and *M. smegmatis* respectively. Both orthologues have also been identified as hypothetical amino acid transporters (101, 157). A comprehensive analysis of the APC superfamily by Jack *et al* revealed the presence of 6 such

transporters in *M. tuberculosis* belonging to various sub-families (104). This further supports the hypothesis that *M. tuberculosis* is able secrete (or uptake) endogenous polyamines.

In this study, spermidine-induced inhibition of ciprofloxacin accumulation demonstrated dose-dependency up to 30mM. The trend displayed suggests that increasing concentrations of spermidine beyond 30mM inhibits fluoroquinolone penetration to the point where all porin-facilitated transport is suspended and only unassisted passive diffusion is reflected by residual accumulation. We suggest that the fraction of the fluoroquinolone pool that passively diffuses through the hydrophobic core of the outer membrane, independent of porin proteins, is the reason why increasing the concentration of spermidine is not able to completely block all uptake. Alternatively, this phenomenon could be explained by the hypothesis suggested by Nikaido and Thanassi in their work with porin –deficient mutants of *E. coli.* The inhibition of porin-mediated fluoroquinolone transport may mean that only the uncharged species, as opposed to Mg^{2+} -chelated molecules, are able to transverse the outer membrane. Because the uncharged species are unable to respond to the interior –negative Donnan potential across the membrane, there is no uphill concentration of fluoroquinolones within the cytoplasm (168).

Presented data suggest that porins account for fluoroquinolone cell wall permeation in *M. bovis* BCG to varying degrees, but are on the whole greater determinants of intracellular fluoroquinolone accumulation than efflux pumps in the wild-type strain. The trend seen with ciprofloxacin, ofloxacin and gatifloxacin suggests that greater hydrophilicity results in greater dependence on the porin transport pathway **(Table 17)**. Moxifloxacin is an outlier to this trend. Being the most hydrophobic of the group, is most likely effective at diffusing through the lipid-rich membrane in a porin-independent manner, as has also been demonstrated previously in *M.*

smegmatis. Alternatively, molecular dimensions which determine the fit of the molecules through the porin constriction zone may be a determinant of porin-mediated drug uptake (61).

Our observation of the first 10min of ciprofloxacin uptake in *M. bovis* BCG showed that treatment with spermidine reduced net steady-state intracellular accumulation rather than delaying it. Similar results were obtained in the study of norfloxacin and cefepime uptake by F porins in *Enterobacter cloacae* (45). Despite the inhibition of porin-mediated uptake, the intracellular/extracellular concentration gradient should ultimately drive the equilibration of drug concentration between the two compartments. We suggest a cellular model where uptake and efflux processes work in concert to achieve steady-state conditions. A reduction in net steady-state accumulation without impeding efflux processes suggests that polyamines reduce the rate of fluoroquinolone influx. Efflux pump inhibitors verapamil and reserpine were not able to elicit distinct shifts in steady-state fluoroquinolone accumulation (Chapter 3, **Figure 21**), but we acknowledge that these non-specific inhibitors are unlikely to account for the extensive list of bacterial efflux pumps, with their broad range of structural and substrate specificities.

First-line standard TB drugs ethambutol and rifampicin have much lower and higher molecular masses than ciprofloxacin respectively. Intracellular steady-state accumulation of both drugs by *M. bovis* BCG failed to reduce significantly upon polyamine pre-treatment, indicating that these drugs are not similarly affected by spermidine and that porin-mediated drug uptake is more drug class specific than it is molecular mass-dependent. While linezolid and ciprofloxacin have comparable molecular masses, they have significantly differing hydrophobicity (ClogP of 0.168 and -0.725 respectively). Interestingly, the inhibition of porin transport causes a 33% and 71% reduction in intracellular accumulation of hydrophobic linezolid and hydrophilic ciprofloxacin respectively.

Iyer and Delcour suggested at least 2 polyamine binding sites in OmpF and OmpC, one of which resides within the pore (103). Although we are unable to confirm the position of the polyamine binding site on the mycobacterial porin, we now understand that this binding is reversible because saline washes enable spermidine dissociation and restoration of channel activity. The positive charge of spermidine is an important determinant of its inhibitory mechanism. An increase in pH from 8 to 9 brought about a decrease in the inhibitory effects of spermidine by half. From the pK_a values of spermidine (8.34, 9.61 and 10.88) (194), one can calculate that the ratio of trivalent to divalent species is 10 fold higher at pH8 than 9. Similarly, previous work has demonstrated that a reduction in concentration of the most highly charged species of cadaverine has the direct effect of relieving its porin-inhibitory capacity by decreasing the total number of closed events (71).

The complex effect of polyamines thus far appears limited to cation-specific porins such as OmpF and OmpC. PhoE of *E. coli*, for example, is completely unaffected by spermine and cadaverine (201). This phosphate transporter is induced by phosphate-starvation and displays a general selectivity for anions (23). Fluoroquinolones are generally amphoteric at physiological pH due to the presence of acidic carboxyl group and basic quinolone nitrogen. However, chelation with Mg^{2+} as described earlier (Chapter 2, Discussion) lends fluoroquinolones net positive charges that may enable their transport by cation-specific porins. This possibly explains why polyamines have an effect on the uptake of these amphoteric molecules.

The possibility of weak non-specific interactions between amines groups of polyamines and the carboxyl groups of fluoroquinolones may explain some of our results because it potentially depletes the amount of free drug available for accumulation in the intracellular environment. Thus far, the effect of polyamines has been established for the uptake of fluoroquinolones and β-

lactams, both of which possess a carboxylic acid functional group (45, 70, 203). However, Iyer and Delcour presented results from the probing of membrane vesicles from the outer membrane of *E. coli*, expressing only OmpC and OmpF, by the patch clamp technique. Concentration- and voltage-dependent inhibitory effects of polyamines were observed, proving that the modulation of porin activity by polyamines is independent of the presence of the substrate (103). We acknowledge the possibility that polyamines such as spermidine and cadaverine may alter drug accumulation by affecting other transporter proteins within mycobacteria. Thus far, we found no published evidence of such activity with regards to bacterial efflux pumps. One study has shown that substituted polyamines such as N-benzylated polyazaalkanes and N-benzylated polyaminoalkanes are efflux pump inhibitors. However, the structures of these compounds differ significantly from the short, straight-chained polyamines used in this study.

It has been hypothesized that the development of fluoroquinolone resistance in some bacterial species may be the result of diminished production of porins acting in conjunction with enhanced efflux capabilities (100). Studies on porin knockout mutants of *M. smegmatis* have shown several fold-increase in resistance to sparfloxacin and moxifloxacin when compared to the wild-type strain (61). We have demonstrated that spermidine concentrations of 1 to 2.5mM rescue *M. bovis* BCG from ciprofloxacin bactericidal activity. These concentrations are below the spermidine MIC of 4mM. It should be noted however that partial growth inhibition was observed at 2.5mM while growth remained unaffected at 1mM spermidine. Thus it is possible that partial growth inhibition may have contributed to the reduced killing activity of ciprofloxacin in the presence of 2.5mM spermidine. Nevertheless, the dose-proportional response we observe between 1 and 2.5mM spermidine supports the notion that transport processes play an important role in maintaining fluoroquinolone susceptibility in mycobacteria. Decreased synthesis,

mutation, inhibition by endogenous molecules, and internalization and degradation of porins are therefore all viable mechanisms of fluoroquinolone resistance acquisition in mycobacteria (171).

We attempted to generate spontaneous mutants of *M. bovis* BCG against spermidine in order to help with the identification of the specific target interacting with polyamines. Unfortunately, no spontaneous mutants were isolated despite the use of high bacterial densities and multiple bacterial generations. The lowest concentration of spermidine at which the inhibition of CFU-growth was observable (3.5mM) corresponds with the MIC of the polyamine. The lack of mutant isolation generally hints at the essentiality of the interacting target /s. Because endogenous polyamines are essential to a multitude of biological pathways that regulate cell growth and replication in all cell types, spontaneous mutants would have to carry multiple mutations on a range of targets. Therefore, the probability of isolating a single mutant colony may be extremely low and unhelpful in identifying a porin target.

Figure 35 Multiple amino-acid sequence alignment of CadB orthologues from *E. coli* and various mycobacterial species. Sequence alignment was performed by ClustalW (27). Stars indicate identical amino acids between all 6 sequences, while dots represent similar amino acids.

```
Mycobacterium tuberculosis      -----MRRPLDPRDIPDELRRRLGLLDAVVIGLGSMIGAGIFAALAPAAY
Mycobacterium bovis BCG         -----MRRPLDPRDIPDELRRRLGLLDAVVIGLGSMIGAGIFAALAPAAY
Mycobacterium smegmatis         MTAEATAHEHTGDTADSKLARKITGPLLFLFILGDVLGAGVYALMGVLAG
Escherichia coli                ----------------MSSAKKIGLFACTGVVAGNMMGSGIALLPANLAS
                                                 .  :::      .  *.::*:*:    .  *

Mycobacterium tuberculosis      AAGSGLLLGLAVAAVVAYCNAISSARLAARYPASGGTYVYGR--------
Mycobacterium bovis BCG         AAGSGLLLGLAVAAVVAYCNAISSARLAARYPASGGTYVYGR--------
Mycobacterium smegmatis         KVGGALWAPLLAALMLALLTAGSYAELVTKYPKAGGAAVFAERAFKQPLV
Escherichia coli                IGGIAIWG-WIISIIGAMSLAYVYARLATKNPQQGGPIAYAG-EISPAFG
                                  * .:     : : *   *   *.*.:: *  **. .:.

Mycobacterium tuberculosis      MRLGDFWGYLAGWGFVVGKTASCAAMALTVGFYVWPAQAHAVAVAVVVAL
Mycobacterium bovis BCG         MRLGDFWGYLAGWGFVVGKTASCAAMALTVGFYVWPAQAHAVAVAVVVAL
Mycobacterium smegmatis         SFLVGFSMLAAGVTSAAGLSLAFAGDYLATFIDVPAVPAAIVFLALVGAL
Escherichia coli                FQTGVLYYHANWIGNLAIGITAVSYLSTFFPVLNDPVPAGIACIAIVWVF
                                     :          .   : :       .   .. *  . :*:* .:

Mycobacterium tuberculosis      TAVNYAGIQKSAWLTRSIVAVVLVVLTAVVVAAYGSGAADPARLDIG--V
Mycobacterium bovis BCG         TAVNYAGIQKSAWLTRSIVAVVLVVLTAVVVAAYGSGAADPARLDIG--V
Mycobacterium smegmatis         NARGISESVKSNVVMTVIELSGLLIVIIAGAVMVGGGRGDLGRLGEFPES
Escherichia coli                TFVNMLGGTWVSRLTTIGLVLVLIPVVMTAIVGWHWFDAATYAANWNTAD
                                .  .        :       *: :  .  .     .    .

Mycobacterium tuberculosis      DAHVWGMLQAAGLLFFAFAGYARIATLGEEVRDPARTIPRAIPLALGITL
Mycobacterium bovis BCG         DAHVWGMLQAAGLLFFAFAGYARIATLGEEVRDPARTIPRAIPLALGITL
Mycobacterium smegmatis         TAPAVAILAGAIIAYYSFVGFETSANVAEEIRNPSKVYPAALFGSLITAG
Escherichia coli                TTDGHAIIKSILLCLWAFVGVESAAVSTGMVKNPKRTVPLATMLGTGLAG
                                 :   .:: .  :  ::*.*    *     :::* :. * *   .   :

Mycobacterium tuberculosis      AVYALVAVAVIAVLGPQRLARAAAPLSEAMRVAGVNWLIPVVQIGAAVAA
Mycobacterium bovis BCG         AVYALVAVAVIAVLGPQRLARAAAPLSEAMRVAGVNWLIPVVQIGAAVAA
Mycobacterium smegmatis         VVYVLVGMASAAVLAPDELAASSGPLLEVVSESGLGVPDWVFSAIALIAV
Escherichia coli                IVYIAATQVLSGMYPSSVMAASGAPFAISASTILGNWAAPLVSAFTAFAC
                                 **  .  .  .:  .. :* :..*:         .    :..  : .*

Mycobacterium tuberculosis      LGSLLALILGVSRTTLAMARDRHLPRWLAAVHPRFKVPFRAELVVGAVVA
Mycobacterium bovis BCG         LGSLLALILGVSRTTLAMARDRHLPRWLAAVHPRFKVPFRAELVVGAVVA
Mycobacterium smegmatis         ANGALLTMIMASRLAFGMAEHRLLPSVLSRVLTKRRTPWVAIVATTAVAM
Escherichia coli                LTSLGSWMMLVGQAGVRAANDGNFPKVYGEVDS-NGIPKKGLLLAAVKMT
                                  .    :: ..:  .  *..  :*   . * .    *  . : . .

Mycobacterium tuberculosis      ALAATADIRGAIGFSSFGVLVYYAIANASALTLG-----LDEGRPR----
Mycobacterium bovis BCG         ALAATADIRGAIGFSSFGVLVYYAIANASALTLG-----LDEGRPR----
Mycobacterium smegmatis         VLTAIGELSTLAETVVLLLLFVFTATNIAVLVLRRDTVEHDHFRVW----
Escherichia coli                ALMILITLMNSAGGKASDLFGELTGIAVLLTMLPYFYSCVDLIRFEGVNI
                                .*    :         ::   :       *      *  *

Mycobacterium tuberculosis      --RLIPLVGLIGCVVLAFALP-LSSVAAGAAVLGVGVAAYGVRRIITRRA
Mycobacterium bovis BCG         --RLIPLVGLIGCVVLAFALP-LSSVAAGAAVLGVGVAAYGVRRIITRRA
Mycobacterium smegmatis         --TAVPVLGVASCVLLMTQQT-AKVWMFAGILMAVGVVLYFVARAATNRT
Escherichia coli                RNFVSLICSVLGCVFCFIALMGASSFELAGTFIVSLIILMFYARKMHERQ
                                     : .: .**.       .    .. .:   :     *   .*

Mycobacterium tuberculosis      RQTDSGDTQRSGHPSAT
Mycobacterium bovis BCG         RQTDSGDTQRSGHPSAT
Mycobacterium smegmatis         ADETV------------
Escherichia coli                SHSMDNHTASNAH----
                                .
```

Table 17 The molecular weights, ClogP and Polar Surface Area (PSA) of four fluoroquinolones and their spermidine-induced reductions in intracellular accumulation.

Fluoroquinolone	Mol. Weight	ClogP	PSA	% Decrease
Ciprofloxacin	331.35	-0.725	77.04	69%
Moxifloxacin	437.9	-0.082	86.27	49%
Ofloxacin	361.4	-0.508	77.48	58%
Gatifloxacin	375.4	-0.266	86.27	31%

CHAPTER 5

UNDERSTANDING FLUOROQUINOLONE SUSCEPTIBILITY AND UPTAKE IN NON-REPLICATING *M. TUBERCULOSIS*

Parts of this project have been included in the following manuscript:

Sarathy JP, Dartois V, Dick T, Gengenbacher M. Impaired drug uptake contributes to phenotypic resistance in nutrient-starved non-replicating *Mycobacterium tuberculosis*. *Antimicrobial Agents and Chemotherapy*. 2013; 57(4): 1648-53.

5.1 Overview

About one third of the world's population is suspected to be latently infected with latent TB (242). Latent TB is characterized by long-term asymptomatic infections where the bacteria persists in a state of non-replication and slowed metabolism until host defenses are compromised (138). One crucial concern regarding latent *M. tuberculosis* is its display of decreased drug susceptibility, making it difficult to eradicate (247). This phenotypic drug resistance is reversible and not genetically predetermined. Some suspected mechanisms for the development of phenotypic resistance include cell wall thickening and changes in drug target essentiality (234). The main objective of this part of the study was to examine the possibility that decreased drug susceptibility of NRP *M. tuberculosis* is the result of decreased drug permeation. A shift from the use of *M. bovis* BCG in earlier chapters to *M. tuberculosis* in this and subsequent chapters was necessary in order for us to understand the latency of the disease in human infections. For this purpose, we used the well-established Loebel's nutrient starvation model which mimics the limiting conditions of human granulomas *in vivo* for the generation of non-replicating bacteria (127, 128). We believe that the results from earlier experiments that used BCG can be extrapolated to these ones because BCG is widely accepted as a good surrogate model for *M. tuberculosis* for the reasons already discussed in the Introduction section.

As discussed in the Literature Review section, NRP *M. tuberculosis* is less susceptible to a wide variety of antimicrobial agents. We began this chapter by comparing the susceptibility of actively -replicating and nutrient-starved non-replicating *M. tuberculosis* to a comprehensive panel of anti-tuberculous agents that includes first, second and third-line drugs, clinical development compounds, and existing drugs with other clinical applications. This part of the study extended beyond the fluoroquinolone class because we felt it necessary to demonstrate the gravity of the

matter by showing that the phenomenon affects a range of drug classes with antimycobacterial activity. Drastic losses in cidal activity were demonstrated with majority of the agents tested. We then proceeded to compare the permeability of these 10 drugs in both bacteria-types. With 7 of the 10 drugs, including all fluoroquinolones and rifamycins, significant reductions in intracellular accumulation were associated with the nutrient starvation state. This reduction is the result of a downward shift in the equilibrated state rather than slowed equilibration. These reductions were shown to be independent of enhanced efflux pump activity or changes in cellular dimensions.

Starvation conditions have been known to cause changes in porin protein synthesis in other bacterial species. *M. smegmatis* responds to glycerol starvation by shutting down *mspA* expression, similar to *E. coli's* shut down of OmpF synthesis is response to nutrient depletion (184). Hillman *et al* reported that MspA expression is barely detectable in *M. smegmatis* during the stationary phase of growth (96). It was suggested that other mycobacterial species respond similarly to nutrient starvation. Using our knowledge of the effects of polyamines on the inhibition of intracellular fluoroquinolone accumulation (Chapter 4), we compared the sensitivity of replicating and non- replicating *M. tuberculosis* to spermidine and cadaverine. Our objective was to investigate the hypothesis that a reduction in porin-mediated drug uptake is the main cause of reduced drug permeation in the latter. We found that the treatment of actively-replicating *M. tuberculosis* with spermidine reduced ciprofloxacin accumulation by half while non-replicating nutrient-starved cultures showed marginal sensitivity to polyamines. We suggest that a reduction in this porin-mediated transport contributes to the phenotypic drug resistance to fluoroquinolones demonstrated by *M. tuberculosis* in the non-replicating state.

5.2 Materials and Methods

5.2.1 Culture Conditions

Exponentially-replicating *M. tuberculosis* was cultured in supplemented 7H9 medium as previously described till an OD_{600} of 0.4 – 0.6 was obtained. Nutrient-starved non-replicating *M. tuberculosis* cultures were generated by re-suspending exponentially-growing H37Rv in PBS (0.025% Tween80) and incubating at 37°C with constant rolling for 14 days (24, 82). This method of generating nutrient-starved *M. tuberculosis* was pioneered by Loebel *et al* (127, 128) and in-house validation of the protocol proved that cell viability is maintained during the 2 – week starvation period.

5.2.2 Susceptibility Testing

MBC_{90} (minimum bactericidal concentration 90) was defined as the concentration of drug required to kill 90% of the bacteria. LCC_{90} (Loebel cidal concentration 90) was similarly defined as the concentration of drug required to kill 90% of nutrient-starved non-replicating bacteria. *M. tuberculosis* was incubated with each drug at various concentrations for a 5-day period, and subsequently grown on agar plates for 2-3 weeks. MBC_{90} and LCC_{90} were obtained upon CFU enumeration and plotting of CFU-drug concentration curves.

5.2.3 Drug Penetration Assay and Quantitative Analysis

The standard drug penetration was assay was conducted as described in Chapter 3 for the measurement of steady-state intracellular drug accumulation. When the assay was conducted on

nutrient-starved cultures, pellets were re-suspended in sterile PBS-tween instead of 7H9 medium in order to concentrate the culture. The kinetics of drug uptake was examined by taking duplicate samples over the following time intervals: 0, 1, 2, 3, 5, 10, 15, 20, 25, and 30min. In efflux pump inhibition experiments, verapamil and reserpine were added (75μM and 20μM respectively) 3min after the addition of the anti-tuberculous agent (10μM). In polyamine- inhibition experiments, cultures were pre-incubated with the specified polyamine for a period of 10min at a concentration of 10mM unless otherwise mentioned. Quantitative analysis of drug concentration was achieved by LC/MS as described previously. The LC-gradient methods used for each compound have been listed in Chapter 2.

5.2.4 Calculation of intracellular concentration

The method of calculation of cellular concentrations was adapted from Cai *et al* (38). In instances when drug accumulation between various penetration assays was compared, drug concentrations in cell lysates were multiplied by the solvent-crashed lysate volume and normalized to the number of CFU per 300 μl sample. The result is an expression of the absolute amount of drug (nmol) per bacterial unit. Given the average cell width of 0.25 μm and length ranging from 1.5 - 4 μm for *M. tuberculosis* (56, 91), the estimated average cell volume of 0.5 μm^3 was used for the calculation of intracellular drug concentrations in this study (in $\mu mol/dm^3$). Intracellular concentration/extracellular concentration ratios (IC/EC) were also calculated by normalizing to the drug incubation concentration (10μM).

5.2.5 Measurement of cell size distribution

Samples of exponentially-growing and nutrient-starved *M. tuberculosis* were fixed for 2 hrs in 4% para-formaldehyde, applied onto poly-lysin glass slides and stained using the TB stain kit (Becton Dickinson) prior microscopic analysis. The individual length of 500 bacilli per sample was measured at 1000-fold magnification (phase contrast bright field) using a Leica DMLB microscope system equipped with a Jenoptik ProgRes CT5 digital camera and ProgRes CapturePro 2.7.7 software. Results were expressed as mean and standard deviation of three independent experiments.

5.2.6 Statistical tests

For the determination of statistical significance of differences in individual drug uptake between replicating and non-replicating *M. tuberculosis*, unpaired *t*-tests with Welch's correction (assuming unequal variances) (GraphPad Prism v5.0) were used. Significant, very significant and extremely significant differences were benchmarked at *p*-values of 0.05 (*****), 0.01 (******) and 0.005 (*******) respectively.

5.3 Results

5.3.1 Antibiotic Susceptibility

The bactericidal activities of 10 anti-tuberculous drugs were determined in both exponentially growing and nutrient-starved non-replicating cultures of the pathogen. The results of these tests are presented in Table 1. Except for mefloquine and thioridazine, a drastic drop of drug susceptibility was observed with nutrient-starved *M. tuberculosis*. All fluoroquinolones as well as ethambutol and linezolid showed LCC_{90}s higher than 100 μM. The three rifamycins tested here were highly-active against replicating bacteria but displayed a >100-fold decrease in bactericidal activity against nutrient-starved cultures. These results show that nutrient-starved non-replicating bacteria is highly tolerant to a variety of anti-tuberculous agents (upper section of **Table 18**). Data obtained with moxifloxacin, ofloxacin, rifampicin and ethambutol are in agreement with previous studies on nutrient-starved *M. tuberculosis* (82, 245). Non-standard drugs mefloquine and thioridazine (bottom section of **Table 18**), though much less cidal than standard anti-tuberculous agents against replicating bacteria, displayed almost unchanged activity against nutrient-starved cultures.

Table 18 The bactericidal activity of 10 standard anti-tuberculous drugs on both replicating and non-replicating *M. tuberculosis*.

Drug	MBC_{90} (μM) [a]	LCC_{90} (μM) [b]
Moxifloxacin	0.31-0.63	>100
Ofloxacin	0.31-0.63	>100
Levofloxacin	1.25-2.5	>100
Rifampicin	0.078	>10
Rifabutin	0.039	10
Rifapentene	0.078	10
Ethambutol	2.5-5.0	>100
Mefloquine	25.0	25.0
Thioridazine	40.0	50.0
Linezolid	10.0	>100

[a] MBC_{90} (minimum bactericidal concentration 90) is defined as the drug concentration required to kill 90% of the bacteria.

[b] LCC_{90} (Loebel cidal concentration 90) is defined as the drug concentration required to kill 90% of nutrient-starved non-replicating bacteria.

5.3.2 Accumulation of 10 Standard TB Drugs in non-replicating *M. tuberculosis*

Drug penetration assays with 10 anti-tuberculous drugs were performed on *M. tuberculosis* using a constant incubation concentration of 10 µM. Steady-state intracellular drug accumulation was determined by sampling at the 30min time point in replicating and non-replicating cultures. The amount of drug per CFU for each drug in both culture types is presented in **Figure 36**. Intracellular concentrations, IC/EC ratios, statistical significance and fold-differences in intracellular accumulation were calculated and are presented in **Table 19**.

Fluoroquinolones - The three fluoroquinolones tested accumulated comparably in the intracellular compartment of *M. tuberculosis*. Moxifloxacin, ofloxacin and levofloxacin all produced intracellular concentrations of approximately 125µM and IC/EC ratios of approximately 12 in replicating bacteria. Of the different drug classes tested, the fluoroquinolones produced the greatest decrease in intracellular accumulation as a result of nutrient- starvation ($p < 0.05$). Ofloxacin accumulation decreased by 12 -fold and was most sensitive to the starvation state. Ofloxacin did not accumulate above the incubation concentration in nutrient-starved non-replicating bacteria (IC/EC ratio of 1.0). The effect of varying the incubation concentration of ofloxacin was tested.

Rifamycins - Intracellular accumulation of rifampicin and rifapentine in replicating *M. tuberculosis* were comparable (19.6 µM and 13.2 µM respectively). Rifabutin, however, accumulated much more efficiently, with an intracellular concentration of up to 89 µM in replicating bacteria. The IC/EC ratio of rifabutin (8.9) was the highest among the rifamycins studied. Nutrient-starvation caused significant decreases in intracellular accumulation of all three rifamycins ($p < 0.05$). Fold-decrease in intracellular accumulation upon nutrient starvation

ranged between 1.5 and 2.7. The effect of varying rifampicin incubation concentrations was also tested at 1, 5 and 20 µM.

Other anti-tuberculous agents - The intracellular concentration of linezolid in replicating *M. tuberculosis* reached 68.5 µM. This decreased by half in non-replicating bacteria ($p < 0.05$). Comparatively, the intracellular accumulation of ethambutol, mefloquine and thioridazine did not significantly decrease in the non-replicative state. Intracellular concentrations of ethambutol reached 23 µM and 21 µM in replicating and non-replicating bacteria respectively. Of all the antibiotics tested, mefloquine accumulated most in replicating bacteria. The intracellular concentration of mefloquine in replicating bacteria was almost 400 µM while the IC/EC ratio approached 40. Mefloquine accumulation did not decrease significantly in non-replicating bacteria. IC/EC ratios reached 24 despite the starvation conditions, much higher than for other antibiotics in either state of replication. Only thioridazine failed to accumulate within the intracellular compartment of *M. tuberculosis*. Intracellular concentrations of thioridazine in both replicating and non-replicating bacteria were around 0.7 to 0.8 µM. IC/EC ratios for thioridazine reached only 0.07 regardless of bacterial starvation/growth state, much lower than for all other study drugs.

Collectively, our results reveal that the extent of drug penetration in replicating *M. tuberculosis*, as well as the effect of dormancy on intracellular accumulation, varies between drugs and drug classes.

Figure 36 Intracellular accumulation of 10 anti-tuberculous agents in *M. tuberculosis* in two different growth states (exponentially-growing and nutrient-starved non-replicating) following a 30min incubation period at 10µM. Drug content is expressed as the amount of drug (nmol) per colony-forming unit (CFU). Inset figure displays data for thioridazine. The experiment was conducted with biological triplicates and standard deviations are shown as error bars.

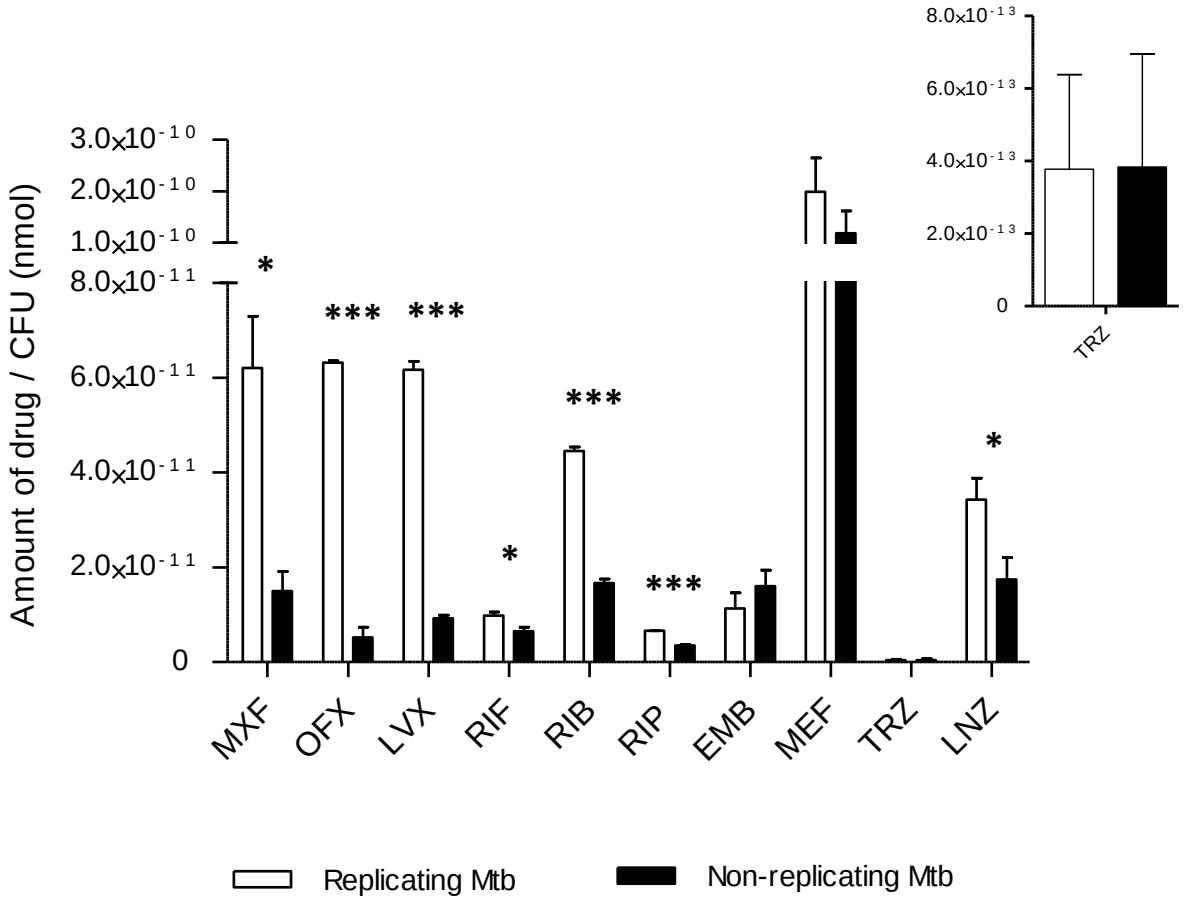

Table 19 The intracellular concentrations of 10 anti-tuberculous agents in replicating and non-replicating *M. tuberculosis*. Accumulation factors are IC/EC ratios; intracellular concentrations were divided by the incubation concentrations of 10µM. p-values obtained from unpaired t-tests indicate significance of difference between intracellular drug concentrations from both growth phases whereas fold-differences represent the ratios between intracellular drug concentrations. Significant p-values (p <0.05) are bolded.

	Intracellular Conc (µmol/dm3)		**Accumulation Factors**		***p*-value**	**Fold-difference**
	Exponentially-replicating MTB	Non-replicating MTB	Exponentially-replicating MTB	Non-replicating MTB		
Moxifloxacin	124.1±21.9	30.0±8.37	12.4	3.0	**0.0199**	4.14
Ofloxacin	126.4±0.72	10.4±4.34	12.6	1.0	**0.0005**	12.2
Levofloxacin	123.4±3.58	18.6±1.36	12.3	1.86	**0.0004**	6.64
Rifampicin	19.6±1.66	13.1±1.68	1.96	1.30	**0.0174**	1.50
Rifabutin	89.2±6.42	33.3±9.59	8.92	3.33	**< 0.0001**	2.68
Rifapentene	13.2±0.12	7.02±0.34	1.32	0.70	**0.0011**	1.89
Ethambutol	22.7±6.64	21.1±6.82	2.27	2.11	0.8154	1.07
Mefloquine	398.8±132.5	238.8±86.4	39.9	23.9	0.1782	1.67
Thioridazine	0.753±0.52	0.765±0.62	0.0753	0.0765	0.9812	0.98
Linezolid	68.5±9.02	35.1±0.91	6.85	3.51	**0.0199**	1.95

5.3.3 Effect of efflux pump inhibitors on drug accumulation in non-replicating bacteria

Several efflux pumps have been shown to actively transport fluoroquinolones out of *M. tuberculosis*. To test the hypothesis that increased efflux could be responsible for the reduced IC/EC ratios observed in the non-replicating state, we performed drug accumulation assays in the presence of two efflux pump inhibitors: verapamil and reserpine. There was no observable change in ofloxacin accumulation upon pre-incubation of bacteria in either growth state in the presence of either efflux inhibitor **(Figure 37)**.

5.3.4 Kinetics of drug accumulation in non-replicating bacteria

Next we set out to determine whether reduced intracellular concentrations at the 30min mark were due to delayed equilibrium or reduced IC/EC at steady-state. Ofloxacin accumulation by replicating and non-replicating bacteria was examined over a 30min time course by removing samples at specific time points. The plots of intracellular ofloxacin accumulation over time in both culture types are presented in **Figure 38**. In replicating bacteria, intracellular ofloxacin accumulation proceeded rapidly within the first 3min of incubation, and continued to gradually increase until end of the experiment. Likewise, steady-state accumulation was reached within the first 3min in non-replicating *M. tuberculosis*, but intracellular concentrations remained consistently lower than in replicating cells over the entire incubation period. The results demonstrate that nutrient starvation brings about a drastic reduction in steady-state ofloxacin accumulation without delaying the equilibrated state.

Figure 37 The effects of reserpine (RES) and verapamil (VER) on intracellular drug accumulation of ofloxacin (OFX) in replicating and non-replicating *M. tuberculosis*. Intracellular drug content is presented as amount of drug per CFU (nmol/CFU). Standard deviations are shown as error bars.

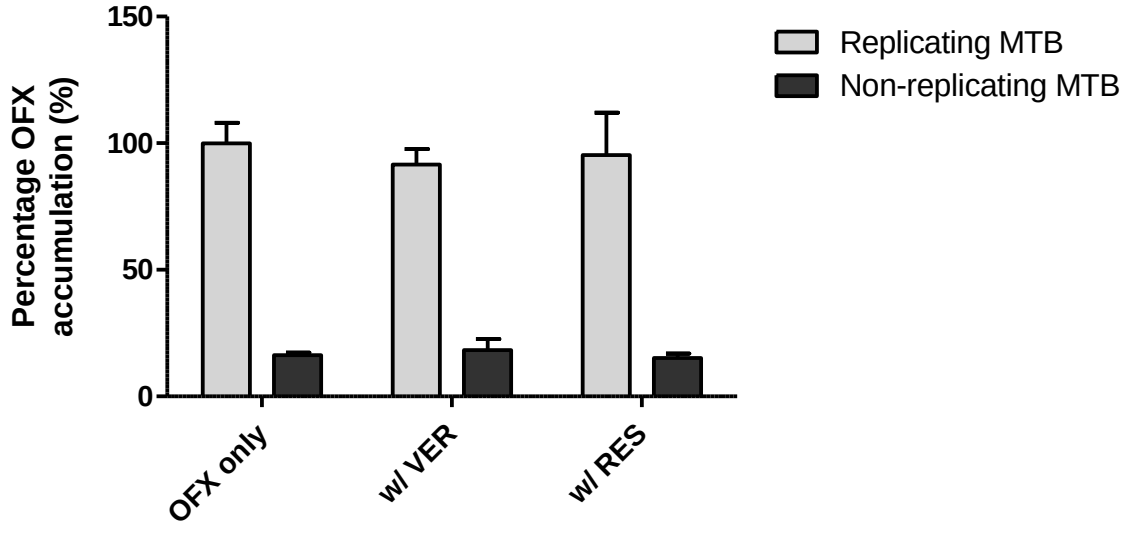

Figure 38 The kinetics of ofloxacin accumulation in replicating and non-replicating *M. tuberculosis* over a 30min incubation period. Drug content is expressed as the amount of drug (nmol) per colony-forming unit (CFU). Standard deviations are shown as error bars.

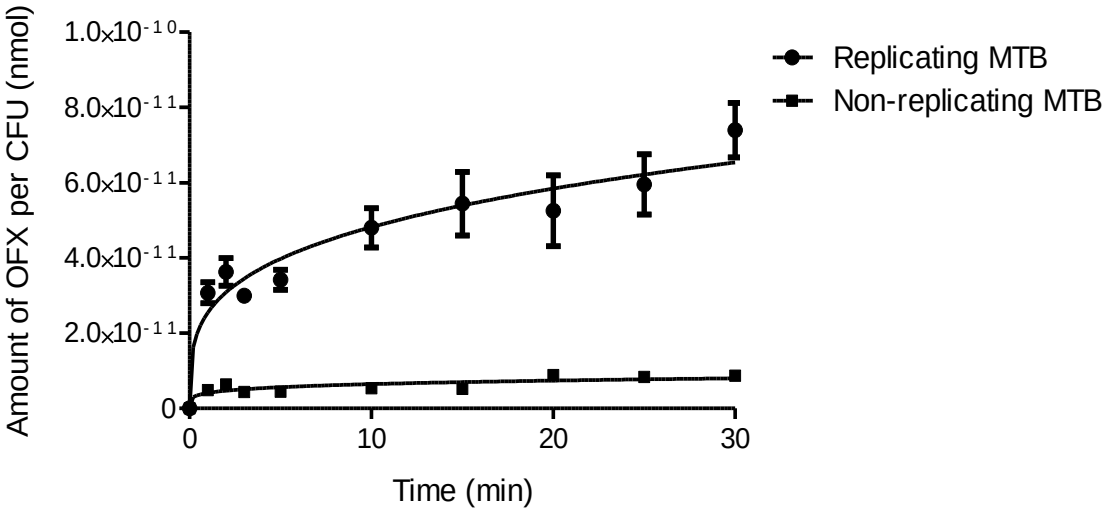

5.3.5 Polyamine treatment of *M. tuberculosis*

We tested the hypothesis that fluoroquinolone accumulation in non-replicating *M. tuberculosis* is decreased due to a reduction in porin-mediated uptake. Spermidine, a known porin inhibitor, has been shown to significantly reduce ciprofloxacin permeation in replicating *M. bovis* BCG (Chapter 4). Its effects on non-replicating cultures of *M. tuberculosis* were examined. Ciprofloxacin penetration assays were performed on replicating and non-replicating cultures and results were expressed as the amount of ciprofloxacin per colony-forming unit. A comparison of uninhibited ciprofloxacin accumulation between the two cultures, as shown in **Figure 39**, confirmed that replicating *M. tuberculosis* when untreated by polyamines is 2.3-fold greater ($p < 0.05$) than non-replicating cultures. Spermidine and cadaverine at 10mM produced a 49% and 41% reduction in ciprofloxacin accumulation in replicating *M. tuberculosis* respectively. In the non-replicating culture, however, spermidine and cadaverine decreased accumulation by just 9% and 13% respectively. Also, the differences in ciprofloxacin accumulation between both culture-types following spermidine or cadaverine treatment are insignificant ($p > 0.05$).

Figure 39 The effects of spermidine on ciprofloxacin (CPX) accumulation in replicating and non-replicating *M. tuberculosis*. Results are expressed as the amount of CPX (nmol) per colony forming unit (CFU); cell lysate concentrations were normalized against bacterial counts for each experiment. The experiment was conducted with biological triplicates and standard deviations are shown as error bars.

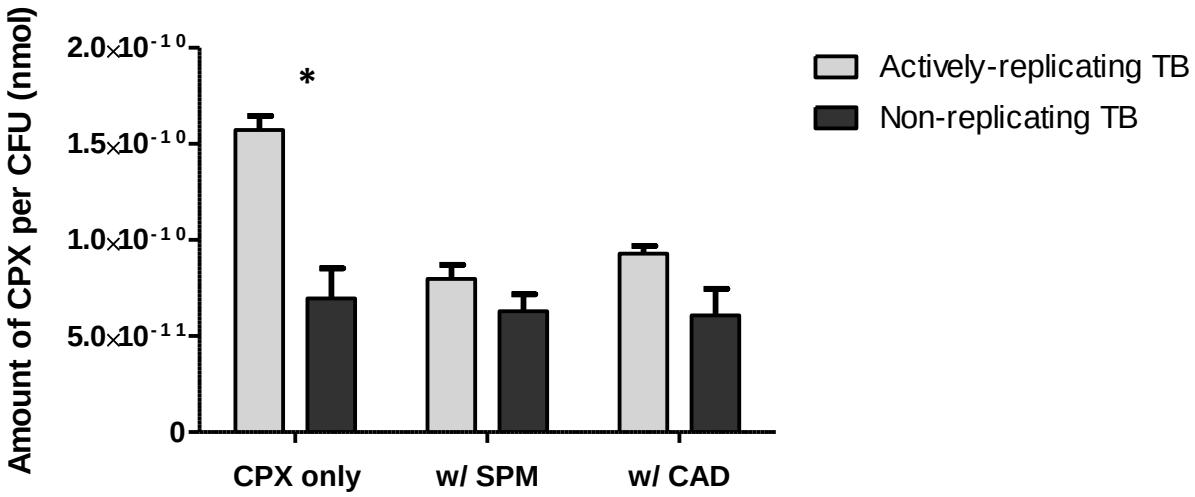

5.3.6 Measurement of cell size distribution

In order to exclude the possibility that differences in drug accumulation between replicating and non-replicating *M. tuberculosis* is due to changes in cell size brought about by nutrient starvation, measurements of cell size distribution were made. Results were expressed as mean and standard deviation of three independent experiments. It was found that cell size distribution is independent of the two growth phases; the average *M. tuberculosis* bacillus length at exponential phase was 1.8±0.4 µm, n=500, as compared to 1.7±0.3 µm, n=500, in the nutrient-starved phase **(Figure 40)**. The difference in average dimensions was not statistically significant ($p > 0.05$).

Figure 40 Comparison of cell length between (A) exponentially-replicating and (B) nutrient-starved non-replicating *M. tuberculosis*. Average length measurements were 1.8±0.4 µm and 1.7±0.3 µm respectively (n=500 for both).

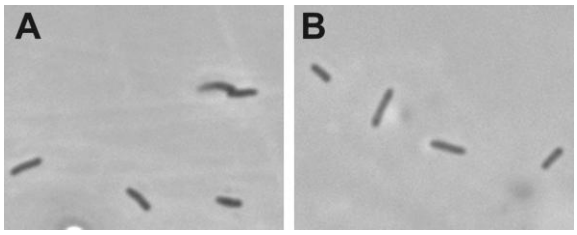

5.4 Discussion

In this part of the study, we have focused on the cell wall and membrane barrier in replicating versus non-replicating *M. tuberculosis*. Unlike microbial drug resistance conferred by genetic mutations, the phenotypic drug tolerance observed in this species during NRP is mediated by the physiological state of dormancy. Accordingly, full drug susceptibility is restored once growth resumes. While the cell envelope of exponentially growing bacteria is notably impermeable to small molecules (105, 159), we speculated that non-replicating bacilli are even more impermeable, and that this contributes to the phenomenon of phenotypic drug tolerance.

To test our hypothesis, we selected a panel of drugs and drug classes active against *M. tuberculosis*, and compared their intracellular accumulation in replicating versus nutrient-starved non-replicating bacilli. Nutrient-starvation has been studied and validated as a model of persistence, causing *M. tuberculosis* to arrest growth, minimize aerobic metabolism and become resistant to existing drugs while maintaining viability, thereby mimicking some of the features of persistent bacteria (24, 84). We understand that a limitation of this study is that only one model of non-replicating persistence was employed. Apart from nutrient-starvation, shifts in pH, specific growth-limiting factors and hypoxic conditions are understood to initiate NRP (239). Nevertheless, Loebel's starvation model was selected since it allows for repeated sampling without disturbing culture conditions and the physiological state of the bacilli.

In replicating bacteria, we observed that fluoroquinolones accumulate within the intracellular compartment many-fold over the external concentration (IC/EC >> 1). This extensive accumulation of fluoroquinolones within *M. tuberculosis* should be explained by a more complex process than simple diffusion. It is known that fluoroquinolones chelate magnesium ions (Mg^{2+}) (173, 229). These cations are abundant on the surface of the outer membrane which

is rich in acidic groups. These Mg^{2+}-chelated compounds then acquire net positive charges that allow them to preferentially diffuse through porin channels which are traditionally cation-specific. Nikaido and Thanassi explained that the interior-negative Donnan potential across the outer membrane should result in the uphill accumulation of chelated fluoroquinolones in the cytoplasm relative to the concentration of the external medium. Conventional fluoroquinolones that chelate Mg^{2+} carry the net positive charge of 2. The intracellular accumulation of such compounds is predicted to reach 8 – 10 times that of the extracellular medium (168). Our observation of high IC/EC ratios is consistent with this hypothesis.

The majority of the drugs tested in this study showed significantly decreased accumulation in nutrient starved *M. tuberculosis* bacilli. Uptake of the fluoroquinolones was most affected by the non-replicating state, consistent with the marked loss of bactericidal activity in starved versus replicating cultures. Intracellular accumulation of the rifamycins was impaired to a lesser extent under starvation conditions, also consistent with the observation that they retain measurable bactericidal activity against persisters, though much reduced compared to that achieved in growing cultures. However, the decrease in rifamycin and fluoroquinolone uptake alone was not able to account for the loss of drug susceptibility exhibited by non-replicating cultures. For instance, ofloxacin accumulation decreased 12-fold while its cidal activity was 300-fold lower in non-replicating bacilli. These results indicate that several factors including altered cellular permeability contribute collectively to the drug tolerance phenotype of persistent *M. tuberculosis*. Fluoroquinolones and rifamycins impede DNA replication and transcription by inhibiting DNA gyrase and RNA polymerase respectively. It is believed that both processes are slowed down in non-replicating *M. tuberculosis*. Hence, the inhibition of these less-essential targets may produce a limited response in latent infections. The same applies for linezolid, which inhibits the process

of translation during protein biosynthesis. Interestingly, IC/EC of the fluoroquinolones and rifamycins in non-replicating bacilli approached 1 for most compounds and was independent of the extracellular concentration used in the assay, suggesting mostly passive uptake.

Intracellular penetration of ethambutol remained unchanged in replicating and non-replicating *M. tuberculosis*, while its cidal activity decreased drastically against the latter. Ethambutol affects cell wall biosynthesis by specifically inhibiting the arabinosyltransferase, a pathway which is dispensable during non-replicating survival. In addition, penetration of ethambutol in the cytosol is likely not required for its activity given the transmembrane location of its target (137, 146). These two factors likely account for the 'disconnect' between cytosol accumulation and activity of ethambutol. Similarly, thioridazine is believed to inhibit the type II NADH dehydrogenase, a key component of the respiratory chain within the cellular membrane of *M. tuberculosis*. In addition, the highly hydrophobic phenothiazines are thought to be largely sequestered in the mycobacterial cell wall (30), in agreement with the very low intracellular concentrations of thioridazine observed in this study.

Mutations in or induction of efflux systems are thought to confer low resistance levels to the fluoroquinolones and rifamycins, consistent with their MIC being affected by efflux pump inhibitors (verapamil and/or reserpine) in selected clinical isolates resistant to these two drug classes (87, 130, 213). Mycobacterial efflux pumps suspected to be associated with fluoroquinolone and rifampicin resistance include members of the Major Facilitator Superfamily and ATP Binding Cassette transporters (88, 130). To test the possibility that enhanced efflux might reduce intracellular drug concentrations in starved cells, we tested the effects of standard efflux inhibitors on intracellular fluoroquinolone accumulation in replicating and nutrient-starved cultures. Neither reserpine nor verapamil had a significant effect on ofloxacin accumulation

Collectively, the results of this study demonstrate that intracellular penetration of different drugs and drug classes is affected to different extents in the non-replicating state. Uptake of various drug classes is likely driven by a combination of multiple active and passive mechanisms, each of which is differentially affected once *M. tuberculosis* ceases to grow and enters a dormant life style. To date however, outer membrane protein candidates that could mediate facilitated or active transport into the TB bacillus have not been unambiguously identified (163). Besides the modulation of active transport systems, cell wall alterations have been suggested to account for the loss of cidal activity of small molecules against non-replicating *M. tuberculosis*. The biosynthesis of cell wall components is controlled by global regulators such as sigma factors, serine threonine kinases and two-component systems. Cell wall components implicated in virulence are induced under conditions that mimic the pathogen's environment during infection (84). The precise remodelling mechanisms and structural changes brought about during dormancy remain to be elucidated in order to understand how they affect small molecule permeation.

While there is evidence of cell wall thickening in *M. tuberculosis* upon the onset of dormancy, it remains unclear how porins orientate themselves across these thickened walls, amongst other still undocumented changes in porin expression and channel activity (58). Porin dimensions presumably remain static despite these external changes. In this case, it is conceivable that porin function is significantly impaired because the thickened cell wall reduces or blocks access by small molecules and impacts 'sensing' of the extracellular microenvironment. The treatment of *M. tuberculosis* with polyamines in this study demonstrated that nutrient-starved bacteria is less sensitive to the inhibitory effects of polyamines on intracellular fluoroquinolone accumulation. This shows that decreased drug susceptibility of non-replicating bacteria is likely the result of

decreased porin-mediated drug uptake. The additional possibility that channel activity of porins of *M. tuberculosis* may be regulated by endogenous molecules in response to unfavorable conditions, as observed with *E.coli* (203), awaits further investigation.

The possible mechanisms for resistance acquisition in persistent *M. tuberculosis* via porin modifications are illustrated in **Figure 41**. Although this phenomenon could not be confirmed in this study with the generation and testing of a specific porin knock-out strains, it corresponds with the published observation that *mspA* expression decreases significantly in *M. smegmatis* even under moderate decreases in glycerol concentrations. It appears that the down-regulation of porin-mediated transport to reduce overall outer membrane permeability may be a crucial protective mechanism of mycobacteria against harsh environmental conditions. On a side note, *M. smegmatis* isolates lacking outer membrane-bound MspA are also resistant to ubiquitin-derived peptides. These peptides are localized to lysosomes of macrophages where they are believed to contribute to mycobacterial clearance during autophagy. MspA provides access to these peptides so that they may access the inner membrane and disrupt membrane integrity, thereby exerting its bactericidal activity (186). This phenomenon also lends credit to our hypothesis that the loss of porin-mediated permeability in *M. tuberculosis* grants it a survival advantage. While reduced outer membrane permeability contributes to phenotypic drug resistance of latent *M. tuberculosis in vivo*, it also enables it to persist within the phagosomes of macrophages despite immune responses.

Figure 41 Four hypothetical mechanisms for drug resistance acquisition in persistent *M. tuberculosis* via porin modifications. Yellow cylinders represent cross-sections of porin channels. This diagram is not drawn to scale.

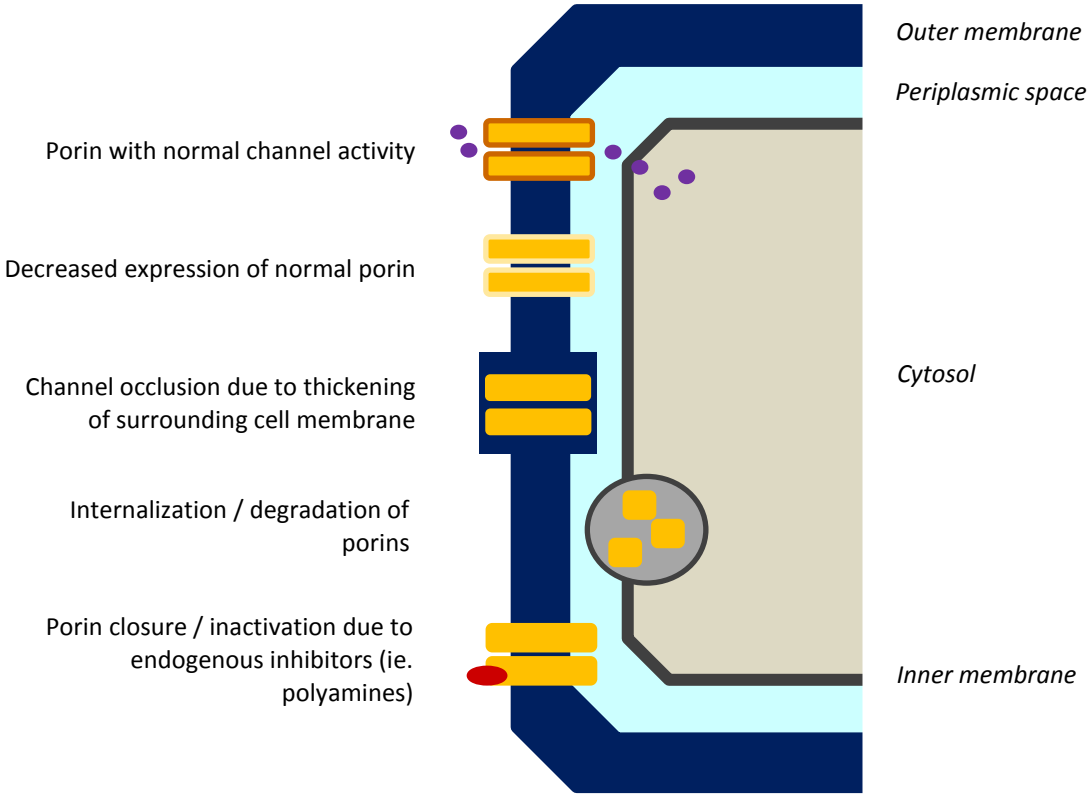

CHAPTER 6

UNDERSTANDING PORIN GENE EXPRESSION IN NON-REPLICATING *M. TUBERCULOSIS*

6.1 Overview

Results from the previous chapters of this thesis have demonstrated that reduced drug permeability of the outer membrane contributes to reduced drug susceptibility in latent *M. tuberculosis*. Preliminary studies using polyamines showed that a reduction in porin-mediated drug transport is one possible cause of this reduced permeability in non-replicating cultures. A review of published work showed that no attempt has yet been made to characterize changes in porin expression levels with respect to the growth-state of *M. tuberculosis*. This challenge is compounded by the limited identification and characterization of porin proteins of this species. OmpATb (Rv0899) was the first suggested porin in *M. tuberculosis* (207). This has since been disputed by structural and functional studies (217, 228). Bioinformatics approaches have been undertaken to predict porin proteins in mycobacteria. One particular study based their approach on the proof of principle that MspA of *M. smegmatis* shares its β-barrel structure, presence of a signal peptide, and absence of hydrophobic α-helices with OMPs of gram-negative bacteria. The combination of secondary structure prediction and the computation of amphiphilicity allowed for the genome-wide prediction of OMPs in *M. tuberculosis*. Two hypothetical proteins, Rv1698 and Rv1973 were identified (218). Mah *et al*'s search for outer membrane pore proteins led to the further refinement of this algorithm, enabling the additional identification of a range of putative OMPs from seven mycobacterial species. Their *M. tuberculosis* homologues are Rv1968, Rv1970, Rv1351, Rv1352, Rv2270, Rv0431 and Rv0227 (133).

A panel of the 10 OMPs from *M. tuberculosis* mentioned above was put together and attempts were made to study their expression levels during non-replication. Total RNA from replicating and non-replicating nutrient-starved bacterial cultures was extracted, purified and reverse-transcribed. Quantitative real-time PCR (qRT-PCR) using SYBR Green as the fluorescent

reporter allowed for the quantitation of porin expression levels in both cell-types. The SYBR Green-based technique was chosen for its cost-effectiveness, ease of performance and availability of instrumentation. OMPs that showed marked reductions in expression levels in the latter were identified. Results from the analyses helped identify Rv1698 as a possible candidate for transporter of fluoroquinolones in *M. tuberculosis*.

6.2 Materials and Methods

6.2.1 Chemicals

Trizol was purchased from Invitrogen (California, U.S.A.) and stored at 4°C. Isoamyl alcohol and isopropanol were purchased from Merck (Darmstadt, Germany), while EDTA and chloroform were obtained from Sigma (Missouri, U.S.A.). Ethanol was obtained from Fisher Scientific (New Hampshire, U.S.A.).

6.2.2 Analysis of Porin Protein Expression

6.2.2.1 Total RNA extraction

Cultures were grown to an OD_{600} of 0.4-0.5. 30ml of culture was harvested by centrifugation at 3,200rpm for 10min at room temperature. Cells were re-suspended in 1ml of Trizol (ice-cold) and bead-beaten at 6,500rpm with approximately 300µl of silica beads (3 x 30s with intermittent cooling on ice) to achieve homogenization. Lysates were then spun down at 12,000rpm for 1min. The supernatant was removed and 300µl of chloroform: isoamyl alcohol (24:1) added. After 15min incubation at room temperature, samples were spun down at 12,000rpm for 15min. The aqueous phase was transferred and 0.9 volumes of isopropanol added to achieve RNA precipitation. After incubating at room temperature for 10min, samples were spun down at 12,000rpm for 10min at 4°C. RNA pellets were washed with 75% ethanol and stored at -20°C. When pellet needed to be re-dissolved, 100µl of RNase-free water was added and samples were incubated at 55°C for 5min. RNA purification was performed with the RNeasy Mini Kit (Qiagen; California, U.S.A.). 3.5µl of mercaptoethanol and 350µl of RLT buffer were added to the RNA

solution and vortexed. 265µl of ethanol was added and the total volume spun down over an RNeasy column at 12,000rpm for 15s. The column was washed with 500ul of ethanol: RPE buffer (4:1) twice with intermittent 12,000rpm spins for 1min each. RNA was then eluted from the columns into fresh collection tubes twice with 20µl of RNase-free water. The purity of extracted RNA was estimated based on the ratio between A_{260} and A_{280} measurements. A ratio between 1.9 and 2.1 is optimal.

DNase digestion of the total RNA extract was performed using the the RNase-Free DNase Set (Qiagen; California, U.S.A.). Briefly, approximately 1µg of RNA was incubated with 2µl of 10x DNase buffer, 0.5Kunitz units of DNase and RNase-free water (to make total volume of 20µl) for 30min at 37°C. Subsequently, 2µl of 25mM EDTA was added and the mixture incubated for 5min at 65°C to achieve DNase inactivation.

6.2.2.2 cDNA preparation

cDNA synthesis from total RNA extracts was performed using the iScript Select cDNA Synthesis Kit and random primers (BioRad; California, U.S.A.).The final reaction mix consisted of 4µl of 5x reaction mix, 2µl of random primers, 1µl of reverse transcriptase and 5µl of DNase-treated RNA. RNase-free water was added to make up the total reaction volume of 20µl. The RNA load per well ranged from 0.5-1.0µg. Reverse transcription was performed at 42°C for 30min on a T3000 Thermocycler (Biometra; Goettingen, Germany) and enzyme inactivation achieved at 85°C for 5min.

6.2.2.3 Quantitative RT-PCR

Quantitative RT-PCR was performed by the iQ5 Real Time Detection System (BioRad; California, U.S.A.) using the SYBR Green Supermix Kit (BioRad). The final reaction mix consisted of 25µl SYBR Green, 2.5µl of each primer (to make 250nM) and 5µl of the cDNA template. RNase-free water was added to make up the final reaction volume of 50µl. DNA sequences as provided by the National Centre for Biotechnology Information (NCBI) for *ompATB (rv0899), rv1698, rv1973, rv0227, rv0431, rv1351, rv1352, rv1968, rv1970* and *rv2270* were used for primer design. The primer sets for each gene studied is listed in **Table 20**. The housekeeping gene *16s rRNA* was used as a positive controls. Negative controls were generated with the exclusion of reverse transcriptase (No Amplification Control) or the cDNA template (No Template Control). Each experiment was conducted at least twice, with triplicate samples each time. The amplification method consisted of 40 cycles of 95°C for 30s, 61°C for 30s and 72°C for 30s. The specificity of the PCR method was confirmed using melting curves. This involved subjecting the RT-PCR products to a temperature gradient of 55°C to 95°C with optical detection of SYBR Green at every 0.5°C increment. Relative fluorescence is then plotted as a derivative. Single peaks on the melting curves indicated single amplification products. Single products were further confirmed by gel electrophoresis. Products were run on 0.8% agarose gels. Relative gene expression data was expressed using the $2^{-\Delta\Delta CT}$ method as detailed by Livak and Schmittgen (126).

Table 20 Sequences of oligonucleotides used in this study

Gene name	Direction	Oligonucleotide sequence (5^1 - 3^1)	Length	Product Length (bp)
rv0899 (ompATb)	Forward	A C C G T T A C T C T G A T C G G T G A C T	22	140
	Reverse	G A G A A A T C A A G T G A T C G C A C A A	22	
rv1698	Forward	G G T C T C A T T G A C C C A G G A G T T	21	105
	Reverse	A G T T T G G T G C T C A A C T G G C T A C	22	
rv1973	Forward	G A C G C C T A C A C A C A G C T G A C	20	148
	Reverse	T G A T G G T C T G G T T T A C G A A C A G	22	
rv0227	Forward	C C G A G A A G A A G A C A T A C C C C T A	22	100
	Reverse	C G G T A T G T G G T T A A A C C G T T G	21	
rv0431	Forward	T C T A C A A C A T C T C A G G C A C A G A	22	107
	Reverse	G A C G T C G G G T A A C G A T A G A T T C	22	
rv1351	Forward	C T G G G T G T T A T T G G C T T G C T C G	22	125
	Reverse	T C A A G T A C C T A T G A C G G T G C T G	22	
rv1352	Forward	C G A A T C C C C T T A T T T T G G T G T	21	106
	Reverse	T T G G T G T C G A C A A T G T T C T C A T	22	
rv1968	Forward	C T A T C C G G T G G G A A A A G T G T C	21	125
	Reverse	A C A A G C C C T T G G T T T T G A T T G	21	
rv1970	Forward	C C C G A A C G A G A C G T T C C A A A A T	22	131
	Reverse	G A G C T G G G T C A G A T G A C A C T C	21	

rv2270	Forward	A C G A A C A T G A A T C C G A C A A A C	21	105
	Reverse	T T G A A G G T T A A T C C A G G T C T C G	22	
16s rRNA	Forward	G G A C A C C T A T T A C G A T C A C C A G	22	139
	Reverse	C A A A A C C T C A T C G G A A T C A C G	21	

6.2.3 Structural predictions and Sequence alignment

Multiple sequence alignment of Rv1698 orthologues from various mycobacterial species was performed by ClustalW (Kyoto University Bioinformatics Centre; Japan) which was made available at www.genome.jp/tools/clustalw/ (27). Predictions of transmembrane domains on the protein sequence of Rv1698 were performed by TMHMM Server v 2.0 (Center for Biological Sequence Analysis, DTU; Denmark) at www.cbs.dtu.dk/services/TMHMM/ (40).

6.3 Results

6.3.1 RT-PCR analysis of porin gene expression in replicating and non-replicating *M. tuberculosis*

We set out to investigate if a decrease in porin-mediated transport is the reason for decreased fluoroquinolone uptake in non-replicating *M. tuberculosis*. The quantitative RT-PCR assays were run to measure the transcript level of 10 OMP genes in actively-replicating and nutrient-starved non-replicating bacteria. Each assay was conducted at least twice with independent bacterial cultures and one representative data set was presented. **Table 21** shows results obtained from the quantification of expression levels of *ompATB (rv0899), rv1698, rv1973, rv0227, rv0431, rv1351, rv1352, rv1968, rv1970* and *rv2270.* The housekeeping gene 16srRNA was used as the internal control gene to normalize the PCRs for the amount of RNA added to the reverse transcription reaction. Transcription levels of actively-replicating *M. tuberculosis* were set as the calibrator for the $2^{-\Delta\Delta Ct}$ method and data is presented as fold change in gene expression relative to this control **(Figure 42)**. An effect on gene expression levels was considered significant when the corresponding fold-change ratios were ≤0.4 or ≥2.5.

The expression levels of all selected 10 OMP genes, inclusive of uncharacterized predicted pore proteins derived from computational methods, were detectable by qRT-PCR. Of the 10 OMP genes tested, only *rv1698*, *rv1973* and *rv0431* displayed significant reductions in expression levels in non-replicating bacteria. Specifically, *rv1698* and *rv0431* expression was reduced by ≥25-fold. *OmpATb* and *rv2270* expression levels were increased by 3.0- and 5.1- fold respectively. Interestingly, the expression of *rv1352* was significantly increased by over 1000-

fold in non-replicating bacteria. This was the largest change in expression level observed from all the OMP genes tested.

Figure 22 (Appendix III) illustrates the melting curve for all 12 genes (in duplicate). For all genes, Tm values from replicating and non-replicating cultures aligned and produced only single peaks. No significant primer-dimer pairs (or other unspecific DNA fragments) were detected. Gel electrophoresis of RT-PCR products confirmed that only single amplification products were obtained **(Appendix III, Figure 23)**.

Table 21 Results from qRT-PCR analysis of 10 genes of both actively-replicating and non-replicating cultures of *M. tuberculosis.* ΔCt is difference in mean Ct between each OMP gene and the control (*16srRNA).* ΔΔCt is the difference in ΔCt between the two culture types for each OMP gene. $2^{-\Delta\Delta Ct}$ is the calculated fold change in normalized OMP gene expression relative to the replicating culture. The experiment was conducted with biological triplicates.

		Gene	Mean Ct	ΔCt	ΔΔCt	$2^{-\Delta\Delta Ct}$
Actively-replicating TB	1	*16s rRNA*	24.16 ± 0.145	0 ± 0.205		
	2	*ompATb*	25.28 ± 0.06	1.12 ± 0.157		
	3	*rv1698*	20.53 ± 0.196	-3.63 ± 0.243		
	4	*rv1973*	28.31 ± 0.14	4.15 ± 0.202		
	5	*rv0227*	20.62 ± 0.23	-3.54 ± 0.272		
	6	*rv0431*	22.87 ± 0.316	-1.29 ± 0.348		
	7	*rv1351*	23.51 ± 0.396	-0.65 ± 0.422		
	8	*rv1352*	21.05 ± 0.055	6.89 ± 0.155		
	9	*rv1968*	27.9 ± 0.134	3.74 ± 0.197		
	10	*rv1970*	26.33 ± 0.11	2.17 ± 0.182		
	11	*rv2270*	28.8 ± 0.238	4.64 ± 0.279		

		Gene	Mean Ct	ΔCt	ΔΔCt	$2^{-\Delta\Delta Ct}$
Non-replicating TB	1	*16s rRNA*	27.98 ± 0.057	0 ± 0.08	0	1.00
	2	*ompATb*	27.51 ± 0.357	-0.47 ± 0.36	-1.59	**3.01**
	3	*rv1698*	29.09 ± 0.413	1.11 ± 0.41	4.74	**0.04**
	4	*rv1973*	30.95 ± 0.232	2.97 ± 0.23	-1.18	2.27
	5	*rv0227*	26.47 ± 0.301	-1.51 ± 0.31	2.03	**0.24**
	6	*rv0431*	32.54 ± 0.394	4.56 ± 0.40	5.21	**0.03**
	7	*rv1351*	28.13 ± 0.297	0.15 ± 0.30	0.8	0.57
	8	*rv1352*	24.63 ± 0.007	-3.35 ± 0.06	-10.24	**1209.34**
	9	*rv1968*	30.5 ± 0.174	2.52 ± 0.18	-1.22	2.33
	10	*rv1970*	30.83 ± 0.367	2.85 ± 0.37	0.68	0.62
	11	*rv2270*	30.26 0.093	2.28 ± 0.11	-2.36	**5.13**

Figure 42 Expression levels of 10 OMP genes of *M. tuberculosis* (in increasing order) following a shift to the non-replicating state. The relative expression of each OMP was calculated using the 16srRNA transcript to normalize for the amount of RNA. Replicating cultures of *M. tuberculosis* served as controls.

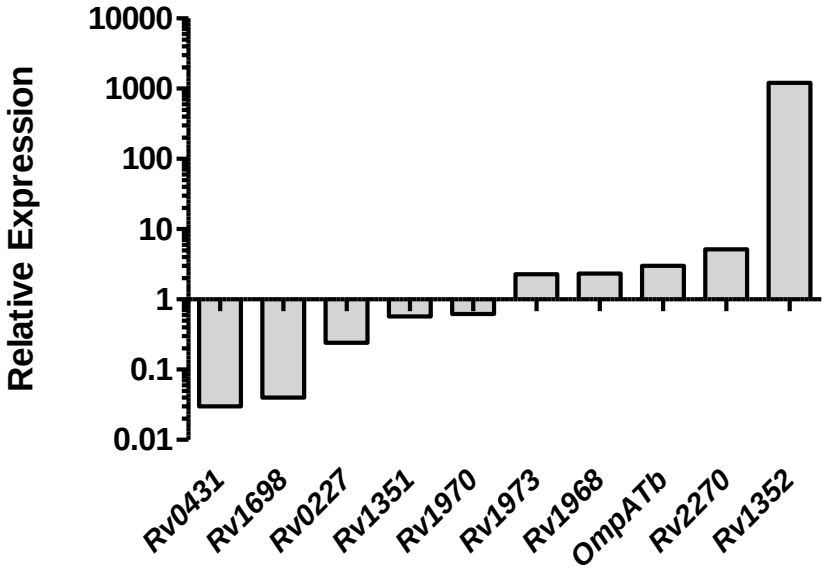

6.4 Discussion

The acquisition of drug resistance due to decreased membrane permeability has been demonstrated in several bacterial species. Multiple antibiotic resistant (MAR) mutants of *E. coli*, for example, have reduced OmpF porins amongst other changes in their outer membrane. Further investigation led scientists to understand that this reduction is primarily mediated by a post-translational mechanism that affects OmpF mRNA stability (50). Several studies also make reference to the starvation state and how changes in porin expression in *E. coli* aid in survival under stressful conditions (62, 170). Darcan *et al* made specific reference to the existence of a 'viable but nonculturable' (VNBC) state of *E. coli* which conceptually compares with the non-replicating state of *M. tuberculosis* covered in this study. These studies, in combination with results from previous chapters of this thesis, led us to the hypothesis that porins of non-replicating *M. tuberculosis* are similarly down -regulated.

Gene expression profiling of 10 putative porin genes in replicating and non-replicating *M. tuberculosis* was conducted to identify the cause of decreased drug permeability of nutrient-starved cells. Both *rv1698* and *rv0431* were identified as being severely under-expressed (>25 fold) during nutrient-starvation. Changes in expression levels of *ompATb*, *rv0227* and *rv2270* were more marginal, although significant. Rv1352, surprisingly, demonstrated >1000-fold increase in expression in nutrient-stared bacteria. Together with Rv1351, these two predicted OMPs are in an operon conserved between *M. tuberculosis* and *M. bovis* BCG. These putative proteins are also specific to these species, with no other identifiable orthologues in the five other non-pathogenic, facultative- and opportunistic-pathogenic mycobacterial species analyzed by Mah *et al* (133). Because the function of this non-essential gene remains uncharacterized (205), and its increased expression suggests that it does not significantly contribute to fluoroquinolone

permeation of non-replicating *M. tuberculosis*, Rv1352 was not further explored in this discussion.

Rv1698 is significantly under-expressed in non-replicating *M. tuberculosis*. Having shown that such bacteria display significant reductions in fluoroquinolone permeability and susceptibility (Chapter 5), we suggest that this OMP is a likely transporter of fluoroquinolones in this species. Rv1698 has recently been profiled as a channel-forming protein in *M. tuberculosis*. Previous studies showed that this protein localizes in the outer membrane and is surface-accessible (218). It also restored sensitivity to ampicillin and chloramphenicol of a *M. smegmatis* mutant with MspA knocked-out. It was suggested that this pore protein may oligomerize in the outer membrane. Rv1698-like proteins are only found in the suborder Corynebacterineae. It is the first channel protein to be identified specifically for mycolic-acid containing outer membranes (214). Multiple amino acid sequence alignment of Rv1698 orthologues from several Corynebacterineae species revealed that this protein is conserved in this suborder **(Figure 44)**. The *M. tuberculosis* and *M. bovis* BCG orthologues are completely identical. The *R. equi* orthologue is 47% identical and 66% similar to that of *M. tuberculosis*, the highest homology demonstrated amongst the non-mycobacterial species compared. The *C. diphtheria* orthologue was least identical with only 33% identity. *R. equi*, *N. brasiliensis* and *C. diphtheria* are weakly infectious, causing mainly opportunistic infections in immune-compromised patients.

TMHMM is a widely used bioinformatics tool that predicts transmembrane helices of integral membrane proteins based on the principles of the hidden Markov model (HMM) (114). Analysis by TMHMM Server v 2.0 (Center for Biological Sequence Analysis, DTU) predicts the existence of just one transmembrane domain (residues 7 – 29) in the amino acid sequence of Rv1698. This is preceded by a short intracellular domain (residues 1 – 6) and succeeded by a

long extracellular domain that spans the rest of the protein (residues 30 – 314) **(Figure 45)**. The presence of just one transmembrane domain is unusual with outer membrane transport proteins. However, in the study of putative transport proteins from 18 bacterial species, Paulsen *et al* noted that *M. tuberculosis* has the largest number of proteins with just one transmembrane segment (TMS) and the lowest percentage proteins with multiple (2 – 3, 4 – 6 or 7 – 9) TMS. The unusual composition and structure of the mycobacterial cell envelope is offered as an explanation for this observation (176). From our analysis of its hypothetical structure alone, it appears unlikely that the Rv1698 monomer forms a functional transmembrane porin protein on its own. However, the possibility that this OMP oligomerizes in *M. bovis* BCG has been reported previously. This was based on the observations of dimeric Rv1698 protein and the multiple conductance states of its channel-complexes in lipid bilayers. Also a significant proportion of this protein displays a pattern of alternating hydrophobic and hydrophilic amino acid residues which is typical of transmembrane β-barrel channels (214). We therefore support the hypothesis that Rv1698 forms a functional porin that is responsible for fluoroquinolone uptake in *M. tuberculosis*, and that its down-regulated expression causes decreased permeability during latency.

Rv0431, the putative OMP that also displayed significant under-expression in non-replicating culture, is another possible candidate for the porin that transports fluoroquinolones in *M. tuberculosis*. This protein contains an ACT domain at its C-terminal that has been associated with the genus *Corynebacteria.* Orthologues of this OMP can be found in all seven of the pathogenic and non-pathogenic mycobacterial species studied by Mah *et al* (133). It is also interesting that the two OMPs which showed the most significant reductions in expression levels are associated with bacteria that have mycolic-acid-rich outer membranes. A potential

transmembrane domain lies between the 19th and 37th amino acid. Other than the identification of Rv0431 as a putative tuberculin-related peptide, this hypothetical protein has not been further functionally characterized (102).

The results from our gene expression analysis would have to be confirmed by other techniques. Microarray analysis could be a useful method to expand on our study of OMP expression in *M. tuberculosis* under different conditions. The performance of western blot analysis using membrane protein extracts would allow us to confirm that Rv1698 is indeed under-expressed in nutrient-starved cells. Unfortunately, the generation of either *rv1698* or *rv0431* knock-outs of *M. tuberculosis* was not successfully completed in this study. Further experimentation with such OMP knock-outs, especially in the nutrient-starved state, would provide us with clearer insight into the mechanism of reduced drug permeability in latent TB.

Figure 43 Multiple amino-acid sequence alignment of Rv1698 orthologues from various species of the Corynebacterineae suborder. Sequence alignment was performed by ClustalW (27). Stars indicate identical amino acids between all 6 sequences, while dots represent similar amino acids.

```
Mycobacterium tuberculosis          -MISLRQHAVSLAAVFLALAMGVVLGSGFFSDTLLSSLRSEKRDLYTQID
Mycobacterium bovis BCG             -MISLRQHAVSLAAVFLALAMGVVLGSGFFSDTLLSSLRSEKRDLYTQID
Mycobacterium leprae                -MISLRQHAFSLAAVFLALAVGVVLGSGFLSDTLLSSLRDEKRDLYTQIS
Rhodococcus equi                    ----MRQHAISIAAIFLALAIGVVLGSGLLSNGMLSGLRDDKADLQSRIE
Norcardia brasiliensis              -MISLRQHAVSIVAIFLALAIGVVLGSQTLAADLLSGLRADKSDLRQQVD
Corynebacterium diphtheriae         MARKSGRTATAIAGLSFGLALGIGAGMYVLAPNVAGGPNQTTSTLERERD
                                          : * ::..: :.**:*:  *   ::  : .. .  .  *  . .

Mycobacterium tuberculosis          RLTDQRDALREKLSAADNFDIQVGSRIVHDALVGKSVVIFRTPDAHDDDI
Mycobacterium bovis BCG             RLTDQRDALREKLSAADNFDIQVGSRIVHDALVGKSVVIFRTPDAHDDDI
Mycobacterium leprae                GLNDQKNMLNEKVSAANNFDNQLLGRIVHDVLGGTSVVVFRTPDAKDDDV
Rhodococcus equi                    DLNTTNNQLNEQLTAADGFDSVVSDRIVRDTLAQRSVVVVTTPDADPGEA
Norcardia brasiliensis              TVSEQNRQLTDQLNAADRFIAGSAGRILGGTLADRSVVVFTTPDADPADI
Corynebacterium diphtheriae         DALESAQIAKAQAKSADSVVSALGRGITTDLLKEKKVLVFRTSDSLDSDA
                                               : .:*: .       *  . *   .*::. *.*:   :

Mycobacterium tuberculosis          AAVSKIVGQAGGAVTATVSLTQEFVEANSAEKLRSVVNSSILPAGSQLST
Mycobacterium bovis BCG             AAVSKIVGQAGGAVTATVSLTQEFVEANSAEKLRSVVNSSILPAGSQLST
Mycobacterium leprae                AAVSKIVVQAGGTVTGTVSLTQEFVDANSTEKLRSVVNSSILPAGAQLST
Rhodococcus equi                    EGINRLISQAGGNVTGRVALTKSFVDSVNGDQLRTTVTN-VIPAGIQLRT
Norcardia brasiliensis              EGVTKSLETSGAAITGRIALTDAFADATEGDRMRTAVTN-VIPAGAQLRT
Corynebacterium diphtheriae         DALSEALKSAGAENAGTIKLGEEFFTQEGADGLKNIIAT-TLPAGAQLST
                                     .:.. :  :*.  :. : * . *      : ::. : .  :*** ** *

Mycobacterium tuberculosis          KLVDQGSQAGDLLGIALLSNADPAAPTVEQAQRDTVLAALRETGFITYQP
Mycobacterium bovis BCG             KLVDQGSQAGDLLGIALLSNADPAAPTVEQAQRDTVLAALRETGFITYQP
Mycobacterium leprae                KLVDQGSQAGDLLGITLLVNANPAVPNVGDAQRSTVLVALRDTGFITYQT
Rhodococcus equi                    GAVDQGSLAGDLLGSVLLLDPQTAQPQTTPEERALALDALRGGGFVDF--
Norcardia brasiliensis              GAVDQGSMAGDLLGLVLLLDPANGQTRGTPQELGLVLETLRGGGFLAY--
Corynebacterium diphtheriae         EKMDSGTHAGDALGSALLLNKDDGSEQANKEDRGIVLGALRESGYIDFDE
                                      :*.*: *** ** .** :   .       :   .* :**  *:: :

Mycobacterium tuberculosis          RDR---IGTANATVVVTGGALSTDAGNQGVSVARFAAALAPRGSGTLLAG
Mycobacterium bovis BCG             RDR---IGTANATVVVTGGALSTDAGNQGVSVARFAAALAPRGSGTLLAG
Mycobacterium leprae                YNRNDHLGAANAALVITGGLLPQDAGNQGVSVARFSAALAPHGSGTLLAG
Rhodococcus equi                    -DGN-VAPAQFAIVLTGSGDPENTSGNRGAVIARFAAAMDGRGAGAVLVG
Norcardia brasiliensis              -GDTPIQPAQLAVVITGNG-AKSAENSQGANIARFAGALRGRGAGVVLAG
Corynebacterium diphtheriae         ASVK----PAHAIVLLSGDSDGSKAAFSIKNQASFATALKSKGSGLLVAG
                                     .      .  * ::  ..             * *: *:  :*:* ::.*

Mycobacterium tuberculosis          RDGSANRPAAVAVTRADADMAAEISTVDDIDAEPGRITVILALHDLINGG
Mycobacterium bovis BCG             RDGSANRPAAVAVTRADADMAAEISTVDDIDAEPGRITVILALHDLINGG
Mycobacterium leprae                RDGSATGVAAVAVARADAGMAATISTVDNVDAEPGRITAILGLHDLLSGG
Rhodococcus equi                    PPAAAEGSGPIAVARADAGVSATLSTVDNVDRESGRITTVLALQEQLGG-
Norcardia brasiliensis              RAGAAENPGPIAVVRTDGALATSVTTVDNLDREIGRVTTVLALTEQLNG-
Corynebacterium diphtheriae         RIHTASDAGLLGTIRTSAQDKQAVSTIDSIDQNWAQIVAILALKEQLDGK
                                       :*   . :.. *:..     ::*:*.:* : .::..:*.* : :.*

Mycobacterium tuberculosis          HVGHYGTGHGAMSVTVSQ---
Mycobacterium bovis BCG             HVGHYGTGHGAMSVTVSQ---
Mycobacterium leprae                HTGQYGVGHGATSITVPQ---
Rhodococcus equi                    GAGRYGTGPGATSVTVGAPAQ
Norcardia brasiliensis              GAGRYGTGDKATSLTLASAPR
Corynebacterium diphtheriae         SGAYGAAGNVDATSPGIKNPE
                                      .  ..*    : .
```

Figure 44 A graphic representation of the predicted transmembrane helices in Rv1698. The probability of regions of the protein sequence lying extracellularly, intracellularly, or within a membrane is expressed on a scale of 0 – 1. Predictions were performed by TMHMM Server v 2.0 (40).

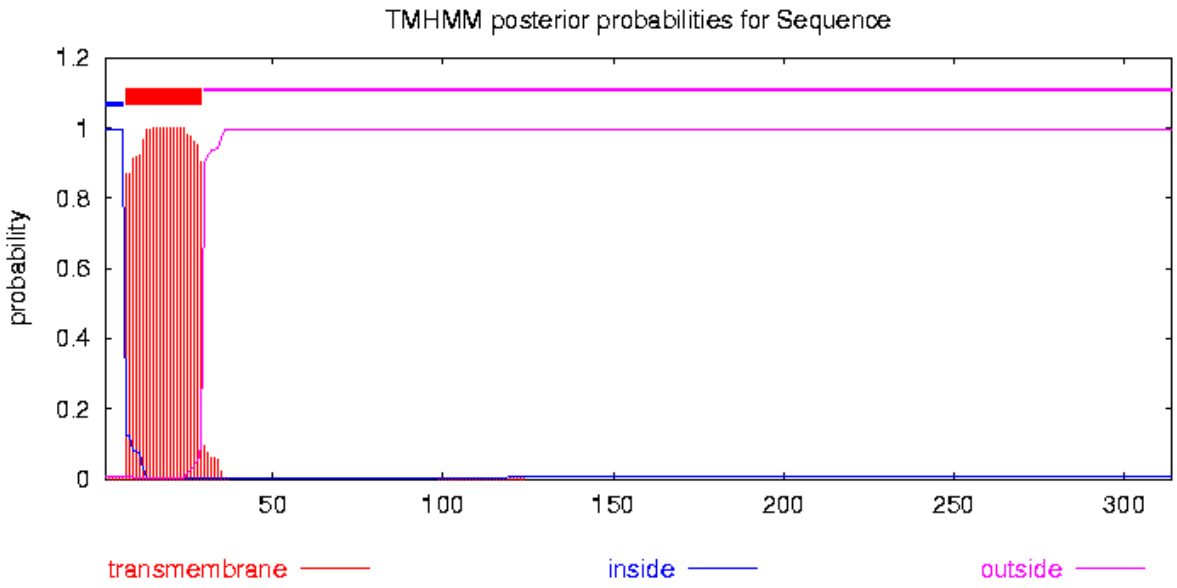

CHAPTER 7

CONCLUSION

7.1 Conclusion

A drug penetrations assay for *M. tuberculosis* involving use of glycine HCl and sonication to achieve cell lysis, and LC/MS analytical methods to quantify drug accumulation, was developed. This assay was evaluated by comparing against one involving the widely-accepted bead-beating procedure, and proved more effective at reflecting total drug penetration. *M. bovis* BCG was used as a surrogate model for the characterization of fluoroquinolone uptake in *M. tuberculosis* because of the genetic and physiological similarities between both species. However, we understand from comparative genomics of the *M. tuberculosis* complex that attenuation of BCG is in part related to the loss of ESX-1, a protein secretion system. This is the result of several independent deletions in the region of deletion-1 (RD1) locus, which remains intact in the virulent strain (35). Studies have shown that, as a result of this deletion, BCG lacks certain secreted antigens such as ESAT-6 and CFP-10. The loss of this function has unknown effects on the structure and permeability of the outer membrane. For future studies, we suggest the use of newly developed attenuated strains of *M. tuberculosis* with their secretory mechanisms intact, such as the Δ*lysA*Δ*panCD* mutant $mc^2$6020 (204).

The specificity and sensitivity of LC/MS analysis allows for this assay to be applicable to the testing of permeability of a wide range of compounds. In the past few decades, we have seen a shift in antimicrobial drug discovery from being largely based on natural product sources to being more target-oriented. Target-based screens encompass the search for inhibitors of specific enzymes in the target organism. However, it is of the opinion of some researchers that single enzymes do not make good antibacterial targets because of the potential for rapid resistance development. Also, such assays ignore the fact that net permeability is a critical determinant of intrinsic drug sensitivity in bacteria, especially in species with formidable outer membranes. Our

new assay bears the potential to be conducted in a medium-throughput manner to aid in anti-mycobacterial drug discovery programs by bridging the gap between *in vitro* target-based inhibition assays to whole cell activity screens.

Most recently, we are seeing increasing emphasis on designing drugs to better permeate the bacterial cell. This represents a new aspect of structure-function relationships. Certain physicochemical properties may confer a molecule the advantage of being able to move efficiently cross the outer membrane and even circumvent efflux processes. Lipinski's Rule of 5 is a set of chemical descriptors that are related to intestinal absorption and cell membrane permeability. This raises the question: Is it possible to design a similar set of descriptors that define the characteristics for accumulation in bacteria and, more specifically, in mycobacteria? Nestorovich *et al* resolved the movement of single drug molecules through the bacterial porins in an effort to characterize drug uptake pathways. Their study concluded that the interactions between charges on the drug molecule and charges on the porin's constriction zone facilitate permeation, and that antibiotic classes have been 'evolving' to become more channel specific (158).

In this study, the drug penetration assay was specifically used to study the transport processes of fluoroquinolones in mycobacteria. Although our findings agree with previous studies on the passive nature of fluoroquinolone uptake in *M. tuberculosis*, we conclude that porin-mediated uptake in addition to un-facilitated diffusion through the mycobacterial outer membrane significantly contributes to intracellular fluoroquinolone accumulation. This conclusion is supported by observations of rapid, unsaturable uptake that is dependent on the hydrophilicity of the fluoroquinolone. We also discussed the novel observation that fluoroquinolone uptake in mycobacteria is pH-dependent. The possibility that efficient intracellular accumulation of

fluoroquinolones is dependent on the acquisition of a net positive charge following chelation with Mg^{2+} ions further supports the hypothesis that such uptake is porin-mediated. Furthermore, we made a case for the testing of finafloxacin, an investigational fluoroquinolone with enhanced activity under acidic pH, for the treatment of TB infections based on our knowledge of vacuole acidification during phagocytosis of *M. tuberculosis*. We believe that finafloxacin may be more efficacious than other fluoroquinolones at eradicating intracellular bacteria.

The assay was critical for proving of the long-held hypothesis that phenotypic drug resistance of *M. tuberculosis* in the dormant state is in part related to reduced drug permeation. The absolute difference in intracellular accumulation of fluoroquinolones and several other anti-tuberculous agents between replicating- and nutrient-starved non-replicating bacteria provides quantitative evidence of this phenomenon. Because this observation of reduced drug permeability appears independent of active efflux mechanisms, we suggest that structural remodeling of the outer membrane (ie. thickening) influences the development of persistent bacilli. Our findings indicate that new lead compounds aiming to shorten tuberculosis chemotherapy must not only target functions relevant in dormancy but also effectively penetrate the persistent bacillus. The inclusion of drug penetration assays in replicating and non-replicating populations may prove critical during lead optimization campaigns.

Most recently, researchers have made headway using MALDI mass spectrometric imaging (MALDI-MSI) to map the distribution of drugs and metabolites in biological tissues. This means that scientists now have a way to directly measure drug levels in tissues and, hence, drug penetration into granuloma lesions. As is the case with the *M. tuberculosis* bacillus, drug penetration into such lesions is both drug-specific and lesion-specific. For example, Prideaux *et al* discovered that moxifloxacin accumulates well in the cellular regions of granulomas (mostly

containing macrophages) while accumulating relatively poorly in the central region of necrotic caseum (185). Such studies offer us a unique insight into drug localization at the site of action and help us interpret ongoing fluoroquinolone efficacy studies. Taken together with our current knowledge of drug accumulation in replicating and latent *M. tuberculosis*, we may be able to develop more effective combined treatment regiments.

We reported the novel discovery that natural polyamines have an inhibitory effect on intracellular fluoroquinolone accumulation in mycobacteria. The concentration and pH-dependent nature of this inhibition is similar to the phenomenon reported with *E. coli*. The significant rescue of *M. bovis* BCG from fluoroquinolone-induced killing suggests that exposure to exogenous (within macrophages or released from infected tissue) polyamines could potentially result in the development of phenotypic drug resistance of *M. tuberculosis*. Most importantly, our investigation of the effects of polyamines on drug uptake in non-replicating bacteria revealed that reduced permeability of persistent bacteria is likely the result of decreased porin-mediated drug uptake. We propose that the modulation of porin channel-activity, either by down-regulation of protein expression, internalization or degradation, could represent a novel mechanism that enables the development of drug tolerant and persistent *M. tuberculosis*.

The inhibition of porins by polyamines has *in vivo* implications as well. Porin-deletion mutants of *M. smegmatis* exhibit enhanced persistence in macrophages, demonstrating that intracellular persistence of mycobacteria is dependent on reduced permeability of the outer membrane (208). Proliferating and infected tissue reportedly have increased levels of polyamines such as spermine (7, 48, 53). Interestingly, Hirsh and Dubos first reported increased local spermine levels at sites of mycobacterial infection over 60 years ago (97). They suggested that spermine possesses tuberculostatic activity *in vivo* that is distinct from conventional immune processes. It was later

shown that human monocytes express a non-selective polyamine transporter, and that increased monocyte uptake of spermidine upon stimulation plays a role in the modulation of inflammatory responses. In light of our recent observation that polyamines can reduce the overall drug permeation of *M. tuberculosis*, it appears that endogenous polyamines in eukaryotic macrophages may contribute towards the development of dormancy and phenotypic drug resistance of the intracellular tubercle bacillus.

Direct evidence of porin-mediated fluoroquinolone uptake in mycobacteria could not be provided in this study without the generation of a porin knock-out mutant. However, knowledge that polyamine-induced decrease in drug permeation of *E. coli* is the direct result of complex inhibition of OmpF and OmpC provides a strong argument for a similar mechanism of action on as-of-yet unidentified porins in *M. tuberculosis*. Our analysis of expression levels of OMPs revealed that Rv1698 is a likely candidate for the transport protein responsible for fluoroquinolone uptake. Its significant down-regulated expression during non-replication would therefore explain the drastic loss in fluoroquinolone susceptibility observed. It would be interesting to pursue the generation of an Rv1698 knock-out of *M. tuberculosis* and to study the polyamine-sensitivity of this mutant.

Ultimately, we must consider the clinical relevance of antibiotic-resistance acquired due to reduced drug permeability. The incidence of resistance in bacterial strains due to known porin modifications are reportedly low compared to other mechanisms of resistance. The moderate increases in MICs of such strains are likely easily overcome by sufficient increases in drug exposure. However, *M. tuberculosis* is often sequestered in *in vivo* environments with limited drug accessibility. First-line agents such as isoniazid, rifampicin and pyrazinamide have already been shown to partition unfavorably into pulmonary lesions as compared to blood plasma (110).

Compounding problems of improper treatment regiments and poor patient compliance during chemotherapy with the described phenomenon of decreased drug permeability at the lesion and bacterial levels may contribute to the overall selection of drug resistant *M. tuberculosis*.

This brings us to the question of whether mycobacterial porins are possible targets for antimicrobial agents. Small molecules that upregulate porin expression or induce porins to remain permanently in the open configuration could bring about the increased accumulation of drugs in the intracellular compartment and hence increase drug susceptibility. Alternatively, inhibitory molecules could induce channel closures and inhibit membrane permeability to essential solutes. These mechanisms of bactericidal activity are purely hypothetical and remain to be tested.

We are also the first to confirm the production of endogenous cadaverine in mycobacteria. As explained earlier, other bacterial species have been known to decrease their outer membrane permeability during adverse conditions by increasing cadaverine secretion. The high estimated intracellular content of cadaverine in *M. bovis* BCG could provide a new rationalization of its impermeability to drugs. Although we were not able to prove that intracellular cadaverine is excreted, the reported presence of amino acid / polyamine transporters in the outer membrane of *M. tuberculosis* maintains the possibility for this excretion. The hypothesis that *M. tuberculosis* alters its outer membrane permeability by self-modulating its porin channel-activity with endogenous polyamines opens up an exciting field for study.

References

1. **Adams, K. N., K. Takaki, L. E. Connolly, H. Wiedenhoft, K. Winglee, O. Humbert, P. H. Edelstein, C. L. Cosma, and L. Ramakrishnan.** 2011. Drug Tolerance in Replicating Mycobacteria Mediated by a Macrophage-Induced Efflux Mechanism. Cell **145:**39-53.
2. **Agrawal, D., Z. F. Udwadia, C. Rodriguez, and A. Mehta.** 2009. Increasing incidence of fluoroquinolone-resistant Mycobacterium tuberculosis in Mumbai, India. Int J Tuberc Lung Dis **13:**79-83.
3. **Ahmad, S., and E. Mokaddas.** 2012. Role of fluoroquinolones in the treatment of tuberculosis. Rev in Health Care **3**.
4. **Ainsa, J. A., M. C. Blokpoel, I. Otal, D. B. Young, K. A. De Smet, and C. Martin.** 1998. Molecular cloning and characterization of Tap, a putative multidrug efflux pump present in Mycobacterium fortuitum and Mycobacterium tuberculosis. J Bacteriol **180:**5836-5843.
5. **Altaf, M., C. H. Miller, D. S. Bellows, and R. O'Toole.** 2010. Evaluation of the Mycobacterium smegmatis and BCG models for the discovery of Mycobacterium tuberculosis inhibitors. Tuberculosis (Edinb) **90:**333-337.
6. **Annesley, T. M.** 2003. Ion suppression in mass spectrometry. Clin Chem **49:**1041-1044.
7. **Babbar, N., and E. W. Gerner.** 2011. Targetting polyamines and inflammation for cancer prevention, p. 49-64. *In* H. J. Senn and F. Otto (ed.), Clinical Cancer Prevention. Springer, Berlin.
8. **Balganesh, M., S. Kuruppath, N. Marcel, S. Sharma, A. Nair, and U. Sharma.** 2010. Rv1218c, an ABC transporter of Mycobacterium tuberculosis with implications in drug discovery. Antimicrob Agents Chemother **54:**5167-5172.
9. **Ball, P., L. Mandell, Y. Niki, and G. Tillotson.** 1999. Comparative tolerability of the newer fluoroquinolone antibacterials. Drug safety : an international journal of medical toxicology and drug experience **21:**407-421.
10. **Bansal, S., and A. DeStefano.** 2007. Key elements of bioanalytical method validation for small molecules. AAPS J **9:**E109-114.
11. **Barbosa, J., D. Barron, E. Jimenez-Lozano, and V. Sanz-Nebot.** 2001. Comparison between capillary electrophoresis, liquid chromatography, potentiometric and spectrophotometric techniques for evaluation of pKa values of zwitterionic drugs in acetonitrile–water mixtures. Anal Chim Acta **437:**309-321.
12. **Bardou, F., C. Raynaud, C. Ramos, M. A. Laneelle, and G. Laneelle.** 1998. Mechanism of isoniazid uptake in Mycobacterium tuberculosis. Microbiology **144 (Pt 9):**2539-2544.
13. **Barry, C. E.** 2001. Mycobacterium smegmatis: an absurd model for tuberculosis? Response from Barry, III. Trends Microbiol, News and Comments **9:**473-474.
14. **Barry, C. E., 3rd.** 2001. Interpreting cell wall 'virulence factors' of Mycobacterium tuberculosis. Trends Microbiol **9:**237-241.
15. **Barry, C. E., D. C. Crick, and M. R. McNeil.** 2007. Targeting the formation of the cell wall core of M. tuberculosis. Infect Disord Drug Targets **7:**182-202.
16. **Basle, A., and A. H. Delcour.** 2004. Regulation of Bacterial Porin Function, p. 79-98. *In* R. Benz (ed.), Bacterial and Eukaryotic Porins: Structure, Function and Mechanism. Wiley-VCH, Germany.
17. **Bedard, J., S. Wong, and L. E. Bryan.** 1987. Accumulation of enoxacin by Escherichia coli and Bacillus subtilis. Antimicrob Agents Chemother **31:**1348-1354.
18. **Beggs, W. H., and N. E. Auran.** 1972. Uptake and binding of 14C-ethambutol by tubercle bacilli and the relation of binding to growth inhibition. Antimicrob Agents Chemother **2:**390-394.
19. **Belisle, J. T., and M. G. Sonnenberg.** 1998. Isolation of genomic DNA from mycobacteria. Methods Mol Biol **101:**31-44.

20. **Benz, R., and R. E. Hancock.** 1981. Properties of the large ion-permeable pores formed from protein F of Pseudomonas aeruginosa in lipid bilayer membranes. Biochim Biophys Acta **646:**298-308.
21. **Benz, R., J. Ishii, and T. Nakae.** 1980. Determination of ion permeability through the channels made of porins from the outer membrane of Salmonella typhimurium in lipid bilayer membranes. J Membr Biol **56:**19-29.
22. **Benz, R., and F. Orlik.** 2005. Functional Reconstitution of Specific Porins, p. 183-212. *In* R. Benz (ed.), Bacterial and Eukaryotic Porins: Structure, Function, Mechanism. Wiley-VCH Verlag GmbH & Co. KGaA, Weinheim, FRG.
23. **Benz, R., A. Schmid, and R. E. Hancock.** 1985. Ion selectivity of gram-negative bacterial porins. J Bacteriol **162:**722-727.
24. **Betts, J. C., P. T. Lukey, L. C. Robb, R. A. McAdam, and K. Duncan.** 2002. Evaluation of a nutrient starvation model of Mycobacterium tuberculosis persistence by gene and protein expression profiling. Mol Microbiol **43:**717-731.
25. **Bhamidi, S., M. S. Scherman, V. Jones, D. C. Crick, J. T. Belisle, P. J. Brennan, and M. R. McNeil.** 2011. Detailed structural and quantitative analysis reveals the spatial organization of the cell walls of in vivo grown Mycobacterium leprae and in vitro grown Mycobacterium tuberculosis. J Biol Chem **286:**23168-23177.
26. **Bianco, M. V., F. C. Blanco, B. Imperiale, M. A. Forrellad, R. V. Rocha, L. I. Klepp, A. A. Cataldi, N. Morcillo, and F. Bigi.** 2011. Role of P27 -P55 operon from Mycobacterium tuberculosis in the resistance to toxic compounds. BMC Infect Dis **11:**195.
27. **Bioinformatics Center**, posting date. Multiple Sequence Alignment by CLUSTALW. Institute for Chemical Research, Kyoto University.Kyoto, Japan [Online.] http://www.genome.jp/tools/clustalw/
28. **Boon, C., and T. Dick.** 2012. How Mycobacterium tuberculosis goes to sleep: the dormancy survival regulator DosR a decade later. Future Microbiol **7:**513-518.
29. **Boon, C., and T. Dick.** 2002. Mycobacterium bovis BCG response regulator essential for hypoxic dormancy. J Bacteriol **184:**6760-6767.
30. **Boshoff, H. I., T. G. Myers, B. R. Copp, M. R. McNeil, M. A. Wilson, and C. E. Barry, 3rd.** 2004. The transcriptional responses of Mycobacterium tuberculosis to inhibitors of metabolism: novel insights into drug mechanisms of action. J Biol Chem **279:**40174-40184.
31. **Braibant, M., P. Gilot, and J. Content.** 2000. The ATP binding cassette (ABC) transport systems of Mycobacterium tuberculosis. FEMS Microbiol Rev **24:**449-467.
32. **Brennan, P. J.** 2003. Structure, function, and biogenesis of the cell wall of Mycobacterium tuberculosis. Tuberculosis (Edinb) **83:**91-97.
33. **Brennan, P. J., and H. Nikaido.** 1995. The envelope of mycobacteria. Annu Rev Biochem **64:**29-63.
34. **Brosch, R., S. V. Gordon, M. Marmiesse, P. Brodin, C. Buchrieser, K. Eiglmeier, T. Garnier, C. Gutierrez, G. Hewinson, K. Kremer, L. M. Parsons, A. S. Pym, S. Samper, D. van Soolingen, and S. T. Cole.** 2002. A new evolutionary scenario for the Mycobacterium tuberculosis complex. P Natl Acad Sci USA **99:**3684-3689.
35. **Brosch, R., S. V. Gordon, T. Garnier, K. Eiglmeier, W. Friqui W, P. Valenti, S. Dos Santos, S. Duthoy, C. Lacroix, C. Garcia-Pelayo, J. K. Inwald, P. Golby, J. N. Garcia, R. G. Hewinson, M. A. Behr, M. A. Quail, C. Churcher, B. G. Barrell, J. Parkhill, S. T. Cole.** 2007. Genome plasticity of BCG and impact on vaccine efficacy. P Natl Acad Sci USA **104:**5596-601.
36. **Brown, A. C., and T. Parish.** 2008. Dxr is essential in Mycobacterium tuberculosis and fosmidomycin resistance is due to a lack of uptake. BMC Microbiol **8**.

37. **Bryan, L. E., and J. Bedard.** 1991. Impermeability to quinolones in gram-positive and gram-negative bacteria. Eur J Clin Microbiol Infect Dis **10:**232-239.
38. **Cai, H., K. Rose, L. H. Liang, S. Dunham, and C. Stover.** 2009. Development of a liquid chromatography/mass spectrometry-based drug accumulation assay in Pseudomonas aeruginosa. Anal Biochem **385:**321-325.
39. **Caminero, J. A.** 2006. Treatment of multidrug-resistant tuberculosis: evidence and controversies. Int J Tuberc Lung Dis **10:**829-837.
40. **Center for Biological Sequence Analysis** 2009, posting date. TMHMM Server. Prediction of transmembrane helices in proteins. Technical University of Denmark v2.0.Denmark [Online.] http://www.cbs.dtu.dk/services/TMHMM/
41. **Chan, E. D., V. Laurel, M. J. Strand, J. F. Chan, M. L. Huynh, M. Goble, and M. D. Iseman.** 2004. Treatment and outcome analysis of 205 patients with multidrug-resistant tuberculosis. Am J Respir Crit Care Med **169:**1103-1109.
42. **Chao, M. C., and E. J. Rubin.** 2010. Letting sleeping dos lie: does dormancy play a role in tuberculosis? Annu Rev Microbiol **64:**293-311.
43. **Chapman, J. S., and N. H. Georgopapadakou.** 1989. Fluorometric assay for fleroxacin uptake by bacterial cells. Antimicrob Agents Chemother **33:**27-29.
44. **Chapman, J. S., and N. H. Georgopapadakou.** 1988. Routes of quinolone permeation in Escherichia coli. Antimicrob Agents Chemother **32:**438-442.
45. **Chevalier, J., M. Mallea, and J. M. Pages.** 2000. Comparative aspects of the diffusion of norfloxacin, cefepime and spermine through the F porin channel of Enterobacter cloacae. Biochem J **348 Pt 1:**223-227.
46. **Choudhuri, B. S., S. Bhakta, R. Barik, J. Basu, M. Kundu, and P. Chakrabarti.** 2002. Overexpression and functional characterization of an ABC (ATP-binding cassette) transporter encoded by the genes drrA and drrB of Mycobacterium tuberculosis. Biochem J **367:**279-285.
47. **Cimino, M., L. Alamo, and L. Salazar.** 2006. Permeabilization of the mycobacterial envelope for protein cytolocalization studies by immunofluorescence microscopy. BMC Microbiol **6:**35.
48. **Clarke, J. R., and A. S. Tyms.** 1991. Polyamine biosynthesis in cells infected with different clinical isolates of human cytomegalovirus. J Med Virol **34:**212-216.
49. **Coates, A., Y. Hu, R. Bax, and C. Page.** 2002. The future challenges facing the development of new antimicrobial drugs. Nature reviews. Nat Rev Drug Discov **1:**895-910.
50. **Cohen, S. P., L. M. McMurry, and S. B. Levy.** 1988. marA locus causes decreased expression of OmpF porin in multiple-antibiotic-resistant (Mar) mutants of Escherichia coli. J Bacteriol **170:**5416-5422.
51. **Colangeli, R., D. Helb, S. Sridharan, J. Sun, M. Varma-Basil, M. H. Hazbon, R. Harbacheuski, N. J. Megjugorac, W. R. Jacobs, Jr., A. Holzenburg, J. C. Sacchettini, and D. Alland.** 2005. The Mycobacterium tuberculosis iniA gene is essential for activity of an efflux pump that confers drug tolerance to both isoniazid and ethambutol. Mol Microbiol **55:**1829-1840.
52. **Cole, S. T., R. Brosch, J. Parkhill, T. Garnier, C. Churcher, D. Harris, S. V. Gordon, K. Eiglmeier, S. Gas, C. E. Barry, 3rd, F. Tekaia, K. Badcock, D. Basham, D. Brown, T. Chillingworth, R. Connor, R. Davies, K. Devlin, T. Feltwell, S. Gentles, N. Hamlin, S. Holroyd, T. Hornsby, K. Jagels, A. Krogh, J. McLean, S. Moule, L. Murphy, K. Oliver, J. Osborne, M. A. Quail, M. A. Rajandream, J. Rogers, S. Rutter, K. Seeger, J. Skelton, R. Squares, S. Squares, J. E. Sulston, K. Taylor, S. Whitehead, and B. G. Barrell.** 1998. Deciphering the biology of Mycobacterium tuberculosis from the complete genome sequence. Nature **393:**537-544.
53. **Colombatto, S., M. De Agostini, D. Corsi, and A. Sinicco.** 1989. Polyamines in lymphocytes from patients infected by human immunodeficiency virus. Biol Chem Hoppe-Seyler **370:**745-748.

54. **Conde, M. B., A. Efron, C. Loredo, G. R. De Souza, N. P. Graca, M. C. Cezar, M. Ram, M. A. Chaudhary, W. R. Bishai, A. L. Kritski, and R. E. Chaisson.** 2009. Moxifloxacin versus ethambutol in the initial treatment of tuberculosis: a double-blind, randomised, controlled phase II trial. Lancet **373:**1183-1189.
55. **Connell, N. D., and H. Nikaido.** 1994. Membrane permeability and transport in Mycobacterium tuberculosis., p. 333-352. *In* B. R. Bloom (ed.), Tuberculosis: Pathogenesis, Protection, and Control. ASM Press, Washington, DC.
56. **Cook, G. M., M. Berney, S. Gebhard, M. Heinemann, R. A. Cox, O. Danilchanka, and M. Niederweis.** 2009. Physiology of mycobacteria. Adv Microb Physiol **55:**81-182, 318-189.
57. **Corti, S., J. Chevalier, and A. Cremieux.** 1995. Intracellular accumulation of norfloxacin in Mycobacterium smegmatis. Antimicrob Agents Chemother **39:**2466-2471.
58. **Cunningham, A. F., and C. L. Spreadbury.** 1998. Mycobacterial stationary phase induced by low oxygen tension: cell wall thickening and localization of the 16-kilodalton alpha-crystallin homolog. J Bacteriol **180:**801-808.
59. **Daffe, M., and P. Draper.** 1998. The envelope layers of mycobacteria with reference to their pathogenicity. Adv Microb Physiol **39:**131-203.
60. **Daffe, M., and G. Etienne.** 1999. The capsule of Mycobacterium tuberculosis and its implications for pathogenicity. Tuber Lung Dis **79:**153-169.
61. **Danilchanka, O., M. Pavlenok, and M. Niederweis.** 2008. Role of porins for uptake of antibiotics by Mycobacterium smegmatis. Antimicrob Agents Cemother **52:**3127-3134.
62. **Darcan, C., R. Ozkanca, O. Idil, and K. P. Flint.** 2009. Viable but non-culturable state (VBNC) of Escherichia coli related to EnvZ under the effect of pH, starvation and osmotic stress in sea water. Pol J microbiol **58:**307-317.
63. **Dartois, V., and C. E. Barry.** 2010. Clinical pharmacology and lesion penetrating properties of second- and third-line antituberculous agents used in the management of multidrug-resistant (MDR) and extensively-drug resistant (XDR) tuberculosis. Curr Clin Pharmacol **5:**96-114.
64. **Davidson, A. L., and J. Chen.** 2004. ATP-binding cassette transporters in bacteria. Annu Rev Biochem **73:**241-268.
65. **Davin-Regli, A., J. M. Bolla, C. E. James, J. P. Lavigne, J. Chevalier, E. Garnotel, A. Molitor, and J. M. Pages.** 2008. Membrane permeability and regulation of drug "influx and efflux" in enterobacterial pathogens. Curr Drug Targets **9:**750-759.
66. **De la Cruz, M. A., and E. Calva.** 2010. The complexities of porin genetic regulation. J Mol Microbiol Biotechnol **18:**24-36.
67. **De Rossi, E., J. A. Ainsa, and G. Riccardi.** 2006. Role of mycobacterial efflux transporters in drug resistance: an unresolved question. FEMS Microbiol Rev **30:**36-52.
68. **De Rossi, E., M. Branzoni, R. Cantoni, A. Milano, G. Riccardi, and O. Ciferri.** 1998. mmr, a Mycobacterium tuberculosis gene conferring resistance to small cationic dyes and inhibitors. J Bacteriol **180:**6068-6071.
69. **de Steenwinkel, J. E., G. J. de Knegt, M. T. ten Kate, A. van Belkum, H. A. Verbrugh, K. Kremer, D. van Soolingen, and I. A. Bakker-Woudenberg.** 2010. Time-kill kinetics of anti-tuberculosis drugs, and emergence of resistance, in relation to metabolic activity of Mycobacterium tuberculosis. J Antimicrob Chemother **65:**2582-2589.
70. **Dela Vega, A. L., and A. H. Delcour.** 1996. Polyamines decrease Escherichia coli outer membrane permeability. J Bacteriol **178:**3715-3721.
71. **delaVega, A. L., and A. H. Delcour.** 1995. Cadaverine induces closing of E. coli porins. EMBO J **14:**6058-6065.
72. **Delcour, A. H.** 1997. Function and modulation of bacterial porins: insights from electrophysiology. FEMS Microbiol Lett **151:**115-123.

73. **Dhillon, J., and D. A. Mitchison.** 1989. Activity and penetration of antituberculosis drugs in mouse peritoneal macrophages infected with Mycobacterium microti OV254. Antimicrob Agents Chemother **33:**1255-1259.
74. **Dick, T.** 2012. Presented at the Grand Challenge TB meeting, Cape Town.
75. **Doran, J. L., Y. Pang, K. E. Mdluli, A. J. Moran, T. C. Victor, R. W. Stokes, E. Mahenthiralingam, B. N. Kreiswirth, J. L. Butt, G. S. Baron, J. D. Treit, V. J. Kerr, P. D. Van Helden, M. C. Roberts, and F. E. Nano.** 1997. Mycobacterium tuberculosis efpA encodes an efflux protein of the QacA transporter family. Clin Diagn Lab Immunol **4:**23-32.
76. **Drage, M. G., H. C. Tsai, N. D. Pecora, T. Y. Cheng, A. R. Arida, S. Shukla, R. E. Rojas, C. Seshadri, D. B. Moody, W. H. Boom, J. C. Sacchettini, and C. V. Harding.** 2010. Mycobacterium tuberculosis lipoprotein LprG (Rv1411c) binds triacylated glycolipid agonists of Toll-like receptor 2. Nat struct Mol Biol **17:**1088-1095.
77. **Dutta, N. K., S. Mehra, and D. Kaushal.** 2010. A Mycobacterium tuberculosis sigma factor network responds to cell-envelope damage by the promising anti-mycobacterial thioridazine. PLoS ONE **5:**e10069.
78. **Emrich, N. C., A. Heisig, W. Stubbings, H. Labischinski, and P. Heisig.** 2010. Antibacterial activity of finafloxacin under different pH conditions against isogenic strains of Escherichia coli expressing combinations of defined mechanisms of fluoroquinolone resistance. J Antimicrob Chemother **65:**2530-2533.
79. **Engelhardt, H., C. Heinz, and M. Niederweis.** 2002. A tetrameric porin limits the cell wall permeability of Mycobacterium smegmatis. J Biol Chem **277:**37567-37572.
80. **Franklin, T. J., and G. A. Snow.** 2005. Attack and defense: drug transport across cell walls and membranes, p. 121-134. *In* Franklin TJ and S. GA (ed.), Biochemistry and Molecular Biology of Antimicrobial Drug Action. Springer, New York.
81. **Gengenbacher, M., and S. H. Kaufmann.** 2012. Mycobacterium tuberculosis: success through dormancy. FEMS Microbiol Rev **36:**514-532.
82. **Gengenbacher, M., S. P. Rao, K. Pethe, and T. Dick.** 2010. Nutrient-starved, non-replicating Mycobacterium tuberculosis requires respiration, ATP synthase and isocitrate lyase for maintenance of ATP homeostasis and viability. Microbiology **156:**81-87.
83. **Ginsburg, A. S., J. H. Grosset, and W. R. Bishai.** 2003. Fluoroquinolones, tuberculosis, and resistance. Lancet Infect Dis **3:**432-442.
84. **Goude, R., and T. Parish.** 2008. The genetics of cell wall biosynthesis in Mycobacterium tuberculosis. Future Microbiol **3:**299-313.
85. **Grzegorzewicz, A. E., H. Pham, V. A. Gundi, M. S. Scherman, E. J. North, T. Hess, V. Jones, V. Gruppo, S. E. Born, J. Kordulakova, S. S. Chavadi, C. Morisseau, A. J. Lenaerts, R. E. Lee, M. R. McNeil, and M. Jackson.** 2012. Inhibition of mycolic acid transport across the Mycobacterium tuberculosis plasma membrane. Nat Chem Biol **8:**334-341.
86. **Guillemin, I., W. Sougakoff, E. Cambau, V. Revel-Viravau, N. Moreau, and V. Jarlier.** 1999. Purification and inhibition by quinolones of DNA gyrases from Mycobacterium avium, Mycobacterium smegmatis and Mycobacterium fortuitum bv. peregrinum. Microbiology **145 (Pt 9):**2527-2532.
87. **Gupta, A. K., D. S. Chauhan, K. Srivastava, R. Das, S. Batra, M. Mittal, P. Goswami, N. Singhal, V. D. Sharma, K. Venkatesan, S. E. Hasnain, and V. M. Katoch.** 2006. Estimation of efflux mediated multi-drug resistance and its correlation with expression levels of two major efflux pumps in mycobacteria. J Commun Dis **38:**246-254.
88. **Gupta, A. K., V. M. Katoch, D. S. Chauhan, R. Sharma, M. Singh, K. Venkatesan, and V. D. Sharma.** 2010. Microarray analysis of efflux pump genes in multidrug-resistant Mycobacterium

tuberculosis during stress induced by common anti-tuberculous drugs. Microb Drug Resist **16:**21-28.

89. **Gutmann, L., R. Williamson, and E. Collatz.** 1984. The possible role of porins in bacterial antibiotic resistance. Ann Intern Med **101:**554-557.
90. **Hancock, R. E., G. M. Decad, and H. Nikaido.** 1979. Identification of the protein producing transmembrane diffusion pores in the outer membrane of Pseudomonas aeruginosa PA01. Biochim Biophys Acta **554:**323-331.
91. **Harries, A. D., D. Maher, and S. Graham.** 2004. Diagnosis of pulmonary tuberculosis in adults, TB / HIV: A Clinical Manual, 2nd ed. Stop TB Initiative (World Health Organization), Geneva.
92. **Hayashi, N., Y. Nakata, and A. Yazaki.** 2004. New findings on the structure-phototoxicity relationship and photostability of fluoroquinolones with various substituents at position 1. Antimicrob Agents Chemother **48:**799-803.
93. **Heinz, C., and M. Niederweis.** 2000. Selective extraction and purification of a mycobacterial outer membrane protein. Anal Biochem **285:**113-120.
94. **Herbert, D., C. N. Paramasivan, P. Venkatesan, G. Kubendiran, R. Prabhakar, and D. A. Mitchison.** 1996. Bactericidal action of ofloxacin, sulbactam-ampicillin, rifampin, and isoniazid on logarithmic- and stationary-phase cultures of Mycobacterium tuberculosis. Antimicrob Agents Chemother **40:**2296-2299.
95. **Higgins, C. F.** 2007. Multiple molecular mechanisms for multidrug resistance transporters. Nature **446:**749-757.
96. **Hillmann, D., I. Eschenbacher, A. Thiel, and M. Niederweis.** 2007. Expression of the major porin gene mspA is regulated in Mycobacterium smegmatis. J Bacteriol **189:**958-967.
97. **Hirsch, J. G., and R. J. Dubos.** 1952. The effect of spermine on tubercle bacilli. J Exp Med **95:**191-208.
98. **Hoffmann, C., A. Leis, M. Niederweis, J. M. Plitzko, and H. Engelhardt.** 2008. Disclosure of the mycobacterial outer membrane: cryo-electron tomography and vitreous sections reveal the lipid bilayer structure. Proc Natl Acad Sci U S A **105:**3963-3967.
99. **Hollenstein, K., R. J. Dawson, and K. P. Locher.** 2007. Structure and mechanism of ABC transporter proteins. Curr Opin Struct Biol **17:**412-418.
100. **Hooper, D. C.** 2003. Mechanisms of quinolone resistance, p. 41-68. *In* D. C. Hooper and E. Rubinstein (ed.), Quinolone Antimicrobial Agents. ASM Press, Washington.
101. **Institut Pasteur** 2003, posting date. Bovilist. v3.1.Paris, France [Online.] http://genolist.pasteur.fr/BoviList/
102. **Institut Pasteur** 2008, posting date. Tuberculist. v3.1.Paris, France [Online.] http://genolist.pasteur.fr/TubercuList/
103. **Iyer, R., and A. H. Delcour.** 1997. Complex inhibition of OmpF and OmpC bacterial porins by polyamines. J Biol Chem **272:**18595-18601.
104. **Jack, D. L., I. T. Paulsen, and M. H. Saier.** 2000. The amino acid/polyamine/organocation (APC) superfamily of transporters specific for amino acids, polyamines and organocations. Microbiology **146 (Pt 8):**1797-1814.
105. **Jarlier, V., and H. Nikaido.** 1994. Mycobacterial cell wall: structure and role in natural resistance to antibiotics. FEMS Microbiol Lett **123:**11-18.
106. **Jarlier, V., and H. Nikaido.** 1990. Permeability barrier to hydrophilic solutes in Mycobacterium chelonei. J Bacteriol **172:**1418-1423.
107. **Jiang, X., W. Zhang, Y. Zhang, F. Gao, C. Lu, X. Zhang, and H. Wang.** 2008. Assessment of efflux pump gene expression in a clinical isolate Mycobacterium tuberculosis by real-time reverse transcription PCR. Microb Drug Resist **14:**7-11.

108. **Kehrenberg, C., A. Cloeckaert, G. Klein, and S. Schwarz.** 2009. Decreased fluoroquinolone susceptibility in mutants of Salmonella serovars other than Typhimurium: detection of novel mutations involved in modulated expression of ramA and soxS. J Antimicrob Chemother **64:**1175-1180.
109. **Kishii, R., and M. Takei.** 2009. Relationship between the expression of ompF and quinolone resistance in Escherichia coli. J Infect Chemother **15:**361-366.
110. **Kjellsson, M. C., L. E. Via, A. Goh, D. Weiner, K. M. Low, S. Kern, G. Pillai, C. E. Barry, 3rd, and V. Dartois.** 2012. Pharmacokinetic evaluation of the penetration of antituberculosis agents in rabbit pulmonary lesions. Antimicrob Agents Chemother **56:**446-457.
111. **Kjellsson, M. C., L. E. Via, A. Goh, D. Weiner, K. M. Low, S. Kern, G. Pillai, C. E. B. III, and V. Dartois.** 2011. Penetration of anti-tuberculosis agents in rabbit pulmonary lesions: a pharmacokinetic evaluation. Antimicrob Agents Chemother **56:**446-457.
112. **Kobayashi, Y., I. Takahashi, and T. Nakae.** 1982. Diffusion of Beta-Lactam Antibiotics through Liposome Membranes Containing Purified Porins. Antimicrob Agents Chemother **22:**775-780.
113. **Koul, A., E. Arnoult, N. Lounis, J. Guillemont, and K. Andries.** 2011. The challenge of new drug discovery for tuberculosis. Nature **469:**483-490.
114. **Krogh, A., B. Larsson, G. von Heijne, and E. L. Sonnhammer.** 2001. Predicting transmembrane protein topology with a hidden Markov model: application to complete genomes. J Mol Biol **305:**567-580.
115. **La Rosa, V., G. Poce, J. O. Canseco, S. Buroni, M. R. Pasca, M. Biava, R. M. Raju, G. C. Porretta, S. Alfonso, C. Battilocchio, B. Javid, F. Sorrentino, T. R. Ioerger, J. C. Sacchettini, F. Manetti, M. Botta, A. De Logu, E. J. Rubin, and E. De Rossi.** 2012. MmpL3 is the cellular target of the antitubercular pyrrole derivative BM212. Antimicrob Agents Chemother **56:**324-331.
116. **Lanigan, M. D., J. A. Vaughan, B. J. Shiell, G. J. Beddome, and W. P. Michalski.** 2004. Mycobacterial proteome extraction: comparison of disruption methods. Proteomics **4:**1094-1100.
117. **Lemaire, S., F. Van Bambeke, and P. M. Tulkens.** 2011. Activity of finafloxacin, a novel fluoroquinolone with increased activity at acid pH, towards extracellular and intracellular Staphylococcus aureus, Listeria monocytogenes and Legionella pneumophila. Int J Antimicrob Ag **38:**52-59.
118. **Li, X. Z., D. M. Livermore, and H. Nikaido.** 1994. Role of Efflux Pump(S) in Intrinsic Resistance of Pseudomonas-Aeruginosa - Resistance to Tetracycline, Chloramphenicol, and Norfloxacin. Antimicrob Agents Chemother **38:**1732-1741.
119. **Li, X. Z., and H. Nikaido.** 2004. Efflux-mediated drug resistance in bacteria. Drugs **64:**159-204.
120. **Li, X. Z., and H. Nikaido.** 2009. Efflux-mediated drug resistance in bacteria: an update. Drugs **69:**1555-1623.
121. **Lim, A., M. Eleuterio, B. Hutter, B. Murugasu-Oei, and T. Dick.** 1999. Oxygen depletion-induced dormancy in Mycobacterium bovis BCG. J Bacteriol **181:**2252-2256.
122. **Linton, K. J., and C. F. Higgins.** 1998. The Escherichia coli ATP-binding cassette (ABC) proteins. Mol Microbiol **28:**5-13.
123. **Lipinski, C. A.** 2000. Drug-like properties and the causes of poor solubility and poor permeability. J Pharmacol Toxicol Methods **44:**235-249.
124. **Liu, J., C. E. Barry, 3rd, G. S. Besra, and H. Nikaido.** 1996. Mycolic acid structure determines the fluidity of the mycobacterial cell wall. J Biol Chem **271:**29545-29551.
125. **Liu, J., H. E. Takiff, and H. Nikaido.** 1996. Active efflux of fluoroquinolones in Mycobacterium smegmatis mediated by LfrA, a multidrug efflux pump. J Bacteriol **178:**3791-3795.
126. **Livak, K. J., and T. D. Schmittgen.** 2001. Analysis of relative gene expression data using real-time quantitative PCR and the 2(T)(-Delta Delta C) method. Methods **25:**402-408.

127. **Loebel, R. O., E. Shorr, and H. B. Richardson.** 1933. The influence of adverse conditions upon the respiratory metabolism and growth of human tubercle bacilli. J Bacteriol **26:**167-200.
128. **Loebel, R. O., E. Shorr, and H. B. Richardson.** 1933. The influence of foodstuffs upon the respiratory metabolism and growth of human bacilli. J Bacteriol **26:**139-166.
129. **Lomovskaya, O., and K. A. Bostian.** 2006. Practical applications and feasibility of efflux pump inhibitors in the clinic--a vision for applied use. Biochem Pharmacol **71:**910-918.
130. **Louw, G. E., R. M. Warren, N. C. Gey van Pittius, R. Leon, A. Jimenez, R. Hernandez-Pando, C. R. McEvoy, M. Grobbelaar, M. Murray, P. D. van Helden, and T. C. Victor.** 2011. Rifampicin reduces susceptibility to ofloxacin in rifampicin-resistant Mycobacterium tuberculosis through efflux. Am J Respir Crit Care Med **184:**269-276.
131. **Louw, G. E., R. M. Warren, N. C. Gey van Pittius, C. R. McEvoy, P. D. Van Helden, and T. C. Victor.** 2009. A balancing act: efflux/influx in mycobacterial drug resistance. Antimicrob Agents Chemother **53:**3181-3189.
132. **Machado, D., I. Couto, J. Perdigao, L. Rodrigues, I. Portugal, P. Baptista, B. Veigas, L. Amaral, and M. Viveiros.** 2012. Contribution of efflux to the emergence of isoniazid and multidrug resistance in Mycobacterium tuberculosis. PloS ONE **7:**e34538.
133. **Mah, N., C. Perez-Iratxeta, and M. A. Andrade-Navarro.** 2010. Outer membrane pore protein prediction in mycobacteria using genomic comparison. Microbiol-Sgm **156:**2506-2515.
134. **Mahairas, G. G., P. J. Sabo, M. J. Hickey, D. C. Singh, and C. K. Stover.** 1996. Molecular analysis of genetic differences between Mycobacterium bovis BCG and virulent M-bovis. J Bacteriol **178:**1274-1282.
135. **Mahfoud, M., S. Sukumaran, P. Hulsmann, K. Grieger, and M. Niederweis.** 2006. Topology of the porin MspA in the outer membrane of Mycobacterium smegmatis. J Biol Chem **281:**5908-5915.
136. **Mailaender, C., N. Reiling, H. Engelhardt, S. Bossmann, S. Ehlers, and M. Niederweis.** 2004. The MspA porin promotes growth and increases antibiotic susceptibility of both Mycobacterium bovis BCG and Mycobacterium tuberculosis. Microbiol-Sgm **150:**853-864.
137. **Malen, H., S. Pathak, T. Softeland, G. A. de Souza, and H. G. Wiker.** 2010. Definition of novel cell envelope associated proteins in Triton X-114 extracts of Mycobacterium tuberculosis H37Rv. BMC Microbiol **10:**132.
138. **Manabe, Y. C., and W. R. Bishai.** 2000. Latent Mycobacterium tuberculosis-persistence, patience, and winning by waiting. Nat Med **6:**1327-1329.
139. **Marassi, F. M.** 2011. Mycobacterium tuberculosis Rv0899 defines a family of membrane proteins widespread in nitrogen-fixing bacteria. Proteins **79:**2946-2955.
140. **Maseda, H., Y. Hashida, A. Shirai, T. Omasa, and T. Nakae.** 2011. Mutation in the sdeS gene promotes expression of the sdeAB efflux pump genes and multidrug resistance in Serratia marcescens. Antimicrob Agents Chemother **55:**2922-2926.
141. **Matuszewski, B. K., M. L. Constanzer, and C. M. Chavez-Eng.** 1998. Matrix effect in quantitative LC/MS/MS analyses of biological fluids: a method for determination of finasteride in human plasma at picogram per milliliter concentrations. Anal Chem**70:**882-889.
142. **Mazurkiewicz, P., A. J. Driessen, and W. N. Konings.** 2005. What do proton motive force driven multidrug resistance transporters have in common? Curr Issues Mol Biol **7:**7-21.
143. **McCaffrey, C., A. Bertasso, J. Pace, and N. H. Georgopapadakou.** 1992. Quinolone accumulation in Escherichia coli, Pseudomonas aeruginosa, and Staphylococcus aureus. Antimicrob Agents Chemother **36:**1601-1605.
144. **McPhee, J. B., S. Tamber, M. D. Brazas, S. Lewenza, and R. E. W. Hancock.** 2009. Antibiotic Resistance Due to Reduced Uptake. *In* D. L. Mayers (ed.), Antimicrobial Drug Resistance. Humana Press, New York.

145. **Meena, L. S., and Rajni.** 2010. Survival mechanisms of pathogenic Mycobacterium tuberculosis H37Rv. FEBS J **277:**2416-2427.
146. **Mikusova, K., R. A. Slayden, G. S. Besra, and P. J. Brennan.** 1995. Biogenesis of the mycobacterial cell wall and the site of action of ethambutol. Antimicrob Agents Chemother **39:**2484-2489.
147. **Mishra, A. K., N. N. Driessen, B. J. Appelmelk, and G. S. Besra.** 2011. Lipoarabinomannan and related glycoconjugates: structure, biogenesis and role in Mycobacterium tuberculosis physiology and host-pathogen interaction. FEMS Microbiol Rev **35:**1126-1157.
148. **Mitchison, D. A.** 1985. The action of antituberculosis drugs in short-course chemotherapy. Tubercle **66:**219-225.
149. **Molle, V., N. Saint, S. Campagna, L. Kremer, E. Lea, P. Draper, and G. Molle.** 2006. pH-dependent pore-forming activity of OmpATb from Mycobacterium tuberculosis and characterization of the channel by peptidic dissection. Mol Microbiol **61:**826-837.
150. **Mor, N., B. Simon, N. Mezo, and L. Heifets.** 1995. Comparison of activities of rifapentine and rifampin against Mycobacterium tuberculosis residing in human macrophages. Antimicrobial Agents Chemother **39:**2073-2077.
151. **Morgan, D. M. L.** 1999. Polyamine Biosynthesis , Catabolism and Homeostasis: An Overview, p. 3-26. *In* S. Bardocz and A. White (ed.), Polyamines in Health and Nutrition. Kluwer Academic Publishers, U.S.A.
152. **Mortimer, P. G., and L. J. Piddock.** 1993. The accumulation of five antibacterial agents in porin-deficient mutants of Escherichia coli. J Antimicrob Chemother **32:**195-213.
153. **Muehlbacher, J.** 2005. InSilico Profile, v3.2 ed. Novartis, Basel.
154. **Muttucumaru, D. G., G. Roberts, J. Hinds, R. A. Stabler, and T. Parish.** 2004. Gene expression profile of Mycobacterium tuberculosis in a non-replicating state. Tuberculosis (Edinb) **84:**239-246.
155. **Naenna, P., P. Noisumdaeng, P. Pongpech, and C. Tribuddharat.** 2010. Detection of outer membrane porin protein, an imipenem influx channel, in Pseudomonas aeruginosa clinical isolates. Southeast Asian J Trop Med Public Health **41:**614-624.
156. **Nakae, T.** 1976. Identification of the outer membrane protein of E. coli that produces transmembrane channels in reconstituted vesicle membranes. Biochem Biophys Res Commun **71:**877-884.
157. **National Center for Biotechnology Information (NCBI) U.S. National Library of Medicine** 2008, posting date. Gene.Maryland, U.S.A. [Online.]http://www.ncbi.nlm.nih.gov/gene
158. **Nestorovich E. M., C. Danelon, M. Winterhalter, S. M. Bezrukov.** 2002. Deigned to penetrate: time-resolved interaction of single antibiotic molecules with bacterial pores. Proc Natl Acad Sci USA **99:** 9789-94.
159. **Nguyen, L., and C. J. Thompson.** 2006. Foundations of antibiotic resistance in bacterial physiology: the mycobacterial paradigm. Trends Microbiol **14:**304-312.
160. **Niederweis, M.** 2008. Mycobacterial porins, p. 153-166. *In* M. Daffe and J. M. Reyrat (ed.), The Mycobacterial Cell Envelope. ASM Press, Washington DC.
161. **Niederweis, M.** 2003. Mycobacterial porins--new channel proteins in unique outer membranes. Mol Microbiol **49:**1167-1177.
162. **Niederweis, M.** 2008. Nutrient acquisition by mycobacteria. Microbiology **154:**679-692.
163. **Niederweis, M., O. Danilchanka, J. Huff, C. Hoffmann, and H. Engelhardt.** 2010. Mycobacterial outer membranes: in search of proteins. Trends Microbiol **18:**109-116.
164. **Niederweis, M., S. Ehrt, C. Heinz, U. Klocker, S. Karosi, K. M. Swiderek, L. W. Riley, and R. Benz.** 1999. Cloning of the mspA gene encoding a porin from Mycobacterium smegmatis. Mol Microbiol **33:**933-945.

165. **Nikaido, H.** 1994. Diffusion of inhibitors across the cell wall, p. 547-558. *In* J. M. Ghuysen and R. Hakenbeck (ed.), Bacterial Cell Wall. Elsevier Amsterdam, Netherlands.
166. **Nikaido, H.** 2003. Molecular basis of bacterial outer membrane permeability revisited. Microbiol Mol Biol Rev **67:**593-656.
167. **Nikaido, H., and E. Y. Rosenberg.** 1981. Effect on solute size on diffusion rates through the transmembrane pores of the outer membrane of Escherichia coli. J Gen Physiol **77:**121-135.
168. **Nikaido, H., and D. G. Thanassi.** 1993. Penetration of lipophilic agents with multiple protonation sites into bacterial cells: tetracyclines and fluoroquinolones as examples. Antimicrob Agents Chemother **37:**1393-1399.
169. **Nikaido, H., and M. Vaara.** 1985. Molecular basis of bacterial outer membrane permeability. Microbiol Rev **49:**1-32.
170. **Ozkanca, R., and K. P. Flint.** 2002. The effect of starvation stress on the porin protein expression of Escherichia coli in lake water. Lett Appl Microbiol **35:**533-537.
171. **Pages, J. M., C. E. James, and M. Winterhalter.** 2008. The porin and the permeating antibiotic: a selective diffusion barrier in Gram-negative bacteria. Nature reviews. Microbiology **6:**893-903.
172. **Park, H. D., K. M. Guinn, M. I. Harrell, R. Liao, M. I. Voskuil, M. Tompa, G. K. Schoolnik, and D. R. Sherman.** 2003. Rv3133c/dosR is a transcription factor that mediates the hypoxic response of Mycobacterium tuberculosis. Mol Microbiol **48:**833-843.
173. **Park, H. R., K. Y. Chung, H. C. Lee, J. K. Lee, and K. M. Bark.** 2000. Ionization and divalent cation complexation of quinolone antibiotics in aqueous solution. B Kor Chem Soc **21:**849-854.
174. **Pasca, M. R., P. Guglierame, F. Arcesi, M. Bellinzoni, E. De Rossi, and G. Riccardi.** 2004. Rv2686c-Rv2687c-Rv2688c, an ABC fluoroquinolone efflux pump in Mycobacterium tuberculosis. Antimicrob Agents Chemother **48:**3175-3178.
175. **Pasca, M. R., P. Guglierame, E. De Rossi, F. Zara, and G. Riccardi.** 2005. mmpL7 gene of Mycobacterium tuberculosis is responsible for isoniazid efflux in Mycobacterium smegmatis. Antimicrob Agents Chemother **49:**4775-4777.
176. **Paulsen, I. T., L. Nguyen, M. K. Sliwinski, R. Rabus, and M. H. Saier, Jr.** 2000. Microbial genome analyses: comparative transport capabilities in eighteen prokaryotes. J Mol Biol **301:**75-100.
177. **Payne, D. J., M. N. Gwynn, D. J. Holmes, and D. L. Pompliano.** 2007. Drugs for bad bugs: confronting the challenges of antibacterial discovery. Nat Rev Drug Discov **6:**29-40.
178. **Pegg, A. E., and A. J. Michael.** 2010. Spermine synthase. Cell Mol Life Sci **67:**113-121.
179. **Phan, A. P., T. T. Ngo, and H. M. Lenhoff.** 1982. Spectrophotometric assay for lysine decarboxylase. Anal Biochem **120:**193-197.
180. **Piddington, D. L., A. Kashkouli, and N. A. Buchmeier.** 2000. Growth of Mycobacterium tuberculosis in a defined medium is very restricted by acid pH and Mg2+ levels. Infect Immun **68:**4518-4522.
181. **Piddock, L. J., and Y. F. Jin.** 1999. Antimicrobial activity and accumulation of moxifloxacin in quinolone-susceptible bacteria. J Antimicrob Chemother **43 Suppl B:**39-42.
182. **Piddock, L. J., and V. Ricci.** 2001. Accumulation of five fluoroquinolones by Mycobacterium tuberculosis H37Rv. J Antimicrob Chemother **48:**787-791.
183. **Piddock, L. J., K. J. Williams, and V. Ricci.** 2000. Accumulation of rifampicin by Mycobacterium aurum, Mycobacterium smegmatis and Mycobacterium tuberculosis. J Antimicrob Chemother **45:**159-165.
184. **Pratt, L. A., W. H. Hsing, K. E. Gibson, and T. J. Silhavy.** 1996. From acids to osmZ: Multiple factors influence synthesis of the OmpF and OmpC porins in Escherichia coli. Mol Microbiol **20:**911-917.

185. **Prideaux B., V. Dartois, D. Staab, D. M. Weiner, A. Goh, L. E. Via, C. E. Barry 3rd, M. Stoeckli.** 2011. High-sensitivity MALDI-MRM-MS imaging of moxifloxacin distribution in tuberculosis-infected rabbit lungs and granulomatous lesions. Anal Chem **83:** 2112-8.
186. **Purdy, G. E., M. Niederweis, and D. G. Russell.** 2009. Decreased outer membrane permeability protects mycobacteria from killing by ubiquitin-derived peptides. Mol Microbiol **73:**844-857.
187. **Ramaswamy, S. V., R. Reich, S. J. Dou, L. Jasperse, X. Pan, A. Wanger, T. Quitugua, and E. A. Graviss.** 2003. Single nucleotide polymorphisms in genes associated with isoniazid resistance in Mycobacterium tuberculosis. Antimicrob Agents Chemother **47:**1241-1250.
188. **Ramon-Garcia, S., C. Martin, J. A. Ainsa, and E. De Rossi.** 2006. Characterization of tetracycline resistance mediated by the efflux pump Tap from Mycobacterium fortuitum. J Antimicrob Chemother **57:**252-259.
189. **Ramon-Garcia, S., C. Martin, C. J. Thompson, and J. A. Ainsa.** 2009. Role of the Mycobacterium tuberculosis P55 efflux pump in intrinsic drug resistance, oxidative stress responses, and growth. Antimicrob Agents Chemother **53:**3675-3682.
190. **Ramon-Garcia, S., V. Mick, E. Dainese, C. Martin, C. J. Thompson, E. De Rossi, R. Manganelli, and J. A. Ainsa.** 2012. Functional and genetic characterization of the tap efflux pump in Mycobacterium bovis BCG. Antimicrob Agents Chemother **56:**2074-2083.
191. **Raynaud, C., M. A. Laneelle, R. H. Senaratne, P. Draper, G. Laneelle, and M. Daffe.** 1999. Mechanisms of pyrazinamide resistance in mycobacteria: importance of lack of uptake in addition to lack of pyrazinamidase activity. Microbiology **145 (Pt 6):**1359-1367.
192. **Reyrat, J. M., and D. Kahn.** 2001. Mycobacterium smegmatis: an absurd model for tuberculosis? Trends Microbiol **9:**472-474.
193. **Rezwan, M., M. A. Laneelle, P. Sander, and M. Daffe.** 2007. Breaking down the wall: fractionation of mycobacteria. J Microbiol Methods **68:**32-39.
194. **Rock, D. M., and R. L. MacDonald.** 1992. Spermine and related polyamines produce a voltage-dependent reduction of N-methyl-D-aspartate receptor single-channel conductance. Mol Pharmacol **42:**157-164.
195. **Rodrigues, L., D. Machado, I. Couto, L. Amaral, and M. Viveiros.** 2011. Contribution of efflux activity to isoniazid resistance in the Mycobacterium tuberculosis complex. Infect Genet Evol.
196. **Rohde, K., R. M. Yates, G. E. Purdy, and D. G. Russell.** 2007. Mycobacterium tuberculosis and the environment within the phagosome. Immunol Rev **219:**37-54.
197. **Russell, A. D.** 1969. The Mechanism of Action of Some Antibacterial Agents. *In* E. G.P. and G. B. West (ed.), Progress in Medicinal Chemistry, vol. 6. Elsevier, New York, U.S.A.
198. **Sacchettini, J. C., E. J. Rubin, and J. S. Freundlich.** 2008. Drugs versus bugs: in pursuit of the persistent predator Mycobacterium tuberculosis. Nat Rev Microbiol **6:**41-52.
199. **Saier Lab Bioinformatics Group** 2005, posting date. Transporter Classification Database (TCDB).California, U.S.A. [Online.]http://www.tcdb.org/
200. **Saint, N., K. L. Lou, C. Widmer, M. Luckey, T. Schirmer, and J. P. Rosenbusch.** 1996. Structural and functional characterization of OmpF porin mutants selected for larger pore size. II. Functional characterization. J Biol Chem **271:**20676-20680.
201. **Samartzidou, H., and A. H. Delcour.** 1999. Distinct sensitivities of OmpF and PhoE porins to charged modulators. FEBS Lett **444:**65-70.
202. **Samartzidou, H., and A. H. Delcour.** 1999. Excretion of endogenous cadaverine leads to a decrease in porin-mediated outer membrane permeability. J Bacteriol **181:**791-798.
203. **Samartzidou, H., M. Mehrazin, Z. H. Xu, M. J. Benedik, and A. H. Delcour.** 2003. Cadaverine inhibition of porin plays a role in cell survival at acidic pH. J Bacteriol **185:**13-19.
204. **Sambandamurthy, V. K., S. C. Derrick, K. V. Jalapathy, B. Chen, R.G. Russell, S. L. Morris, W. R. Jacobs Jr.** 2005. Long-term protection against tuberculosis following vaccination with a severely

attenuate double lysine and pantothenate auxotroph of Mycobacterium tuberculosis. Infect Immun **73:** 1196-203.

205. **Sassetti, C. M., D. H. Boyd, and E. J. Rubin.** 2003. Genes required for mycobacterial growth defined by high density mutagenesis. Mol Microbiol **48:**77-84.
206. **Seiler, P., T. Ulrichs, S. Bandermann, L. Pradl, S. Jorg, V. Krenn, L. Morawietz, S. H. Kaufmann, and P. Aichele.** 2003. Cell-wall alterations as an attribute of Mycobacterium tuberculosis in latent infection. J Infect Dis **188:**1326-1331.
207. **Senaratne, R. H., H. Mobasheri, K. G. Papavinasasundaram, P. Jenner, E. J. Lea, and P. Draper.** 1998. Expression of a gene for a porin-like protein of the OmpA family from Mycobacterium tuberculosis H37Rv. J Bacteriol **180:**3541-3547.
208. **Sharbati-Tehrani, S., J. Stephan, G. Holland, B. Appel, M. Niederweis, and A. Lewin.** 2005. Porins limit the intracellular persistence of Mycobacterium smegmatis. Microbiology **151:**2403-2410.
209. **Sharbati, S., K. Schramm, S. Rempel, H. Wang, R. Andrich, V. Tykiel, R. Kunisch, and A. Lewin.** 2009. Characterisation of porin genes from Mycobacterium fortuitum and their impact on growth. BMC Microbiol **9:**31.
210. **Sharma, P. C., A. Jain, and S. Jain.** 2009. Fluoroquinolone antibacterials: a review on chemistry, microbiology and therapeutic prospects. Acta Pol Pharm **66:**587-604.
211. **Sharma, S., M. Kumar, A. Nargotra, S. Koul, and I. A. Khan.** 2010. Piperine as an inhibitor of Rv1258c, a putative multidrug efflux pump of Mycobacterium tuberculosis. J Antimicrob Chemother **65:**1694-1701.
212. **Silva, P. E., F. Bigi, M. P. Santangelo, M. I. Romano, C. Martin, A. Cataldi, and J. A. Ainsa.** 2001. Characterization of P55, a multidrug efflux pump in Mycobacterium bovis and Mycobacterium tuberculosis. Antimicrob Agents Chemother **45:**800-804.
213. **Singh, M., G. P. Jadaun, Ramdas, K. Srivastava, V. Chauhan, R. Mishra, K. Gupta, S. Nair, D. S. Chauhan, V. D. Sharma, K. Venkatesan, and V. M. Katoch.** 2011. Effect of efflux pump inhibitors on drug susceptibility of ofloxacin resistant Mycobacterium tuberculosis isolates. Indian J Med Res **133:**535-540.
214. **Siroy, A., C. Mailaender, D. Harder, S. Koerber, F. Wolschendorf, O. Danilchanka, Y. Wang, C. Heinz, and M. Niederweis.** 2008. Rv1698 of Mycobacterium tuberculosis represents a new class of channel-forming outer membrane proteins. J Biol Chem **283:**17827-17837.
215. **Skinner, P. S., S. K. Furney, D. A. Kleinert, and I. M. Orme.** 1995. Comparison of activities of fluoroquinolones in murine macrophages infected with Mycobacterium tuberculosis. Antimicrob Agents Chemother **39:**750-753.
216. **Soksawatmaekhin, W., A. Kuraishi, K. Sakata, K. Kashiwagi, and K. Igarashi.** 2004. Excretion and uptake of cadaverine by CadB and its physiological functions in Escherichia coli. Mol Microbiol **51:**1401-1412.
217. **Song, H., J. Huff, K. Janik, K. Walter, C. Keller, S. Ehlers, S. H. Bossmann, and M. Niederweis.** 2011. Expression of the ompATb operon accelerates ammonia secretion and adaptation of Mycobacterium tuberculosis to acidic environments. Mol Microbiol **80:**900-918.
218. **Song, H., R. Sandie, Y. Wang, M. A. Andrade-Navarro, and M. Niederweis.** 2008. Identification of outer membrane proteins of Mycobacterium tuberculosis. Tuberculosis (Edinb) **88:**526-544.
219. **Stahl, C., S. Kubetzko, I. Kaps, S. Seeber, H. Engelhardt, and M. Niederweis.** 2001. MspA provides the main hydrophilic pathway through the cell wall of Mycobacterium smegmatis. Mol Microbiol **40:**451-464.
220. **Stephan, J., C. Mailaender, G. Etienne, M. Daffe, and M. Niederweis.** 2004. Multidrug resistance of a porin deletion mutant of Mycobacterium smegmatis. Antimicrob Agents Chemother **48:**4163-4170.

221. **Tabor, C. W., and H. Tabor.** 1966. Transport Systems for 1,4-Diaminobutane Spermidine and Spermine in Escherichia Coli. J Biol Chem **241:**3714-&.
222. **Tahlan, K., R. Wilson, D. B. Kastrinsky, K. Arora, V. Nair, E. Fischer, S. W. Barnes, J. R. Walker, D. Alland, C. E. Barry, 3rd, and H. I. Boshoff.** 2012. SQ109 Targets MmpL3, a Membrane Transporter of Trehalose Monomycolate Involved in Mycolic Acid Donation to the Cell Wall Core of Mycobacterium tuberculosis. Antimicrob Agents Chemother **56:**1797-1809.
223. **Takiff, H., and E. Guerrero.** 2011. Current Prospects for the Fluoroquinolones as First-Line Tuberculosis Therapy. Antimicrob Agents Chemother **55:**5421-5429.
224. **Takiff, H. E., L. Salazar, C. Guerrero, W. Philipp, W. M. Huang, B. Kreiswirth, S. T. Cole, W. R. Jacobs, and A. Telenti.** 1994. Cloning and Nucleotide-Sequence of Mycobacterium-Tuberculosis Gyra and Gyrb Genes and Detection of Quinolone Resistance Mutations. Antimicrob Agents Chemother **38:**773-780.
225. **Tavio, M. D., J. Vila, J. Ruiz, J. Ruiz, A. M. Martin-Sanchez, and M. T. J. de Anta.** 1999. Mechanisms involved in the development of resistance to fluoroquinolones in Escherichia coli isolates. J Antimicrob Chemoth **44:**735-742.
226. **Telenti, A., P. Imboden, F. Marchesi, D. Lowrie, S. Cole, M. J. Colston, L. Matter, K. Schopfer, and T. Bodmer.** 1993. Detection of rifampicin-resistance mutations in Mycobacterium tuberculosis. Lancet **341:**647-650.
227. **Teoh-Chan, C. H., A. Cowlishaw, A. Eley, G. Slater, and D. Greenwood.** 1985. Laboratory evaluation of enoxacin: comparison with norfloxacin and nalidixic acid. J Antimicrob Chemother **15:**45-52.
228. **Teriete, P., Y. Yao, A. Kolodzik, J. Yu, H. Song, M. Niederweis, and F. M. Marassi.** 2010. Mycobacterium tuberculosis Rv0899 adopts a mixed alpha/beta-structure and does not form a transmembrane beta-barrel. Biochemistry **49:**2768-2777.
229. **Timmers, K., and R. Sternglanz.** 1978. Ionization and divalent cation dissociation constants of nalidixic and oxolinic acids. Bioinorg Chem **9:**145-155.
230. **Trias, J., V. Jarlier, and R. Benz.** 1992. Porins in the Cell-Wall of Mycobacteria. Science **258:**1479-1481.
231. **Trufelli, H., P. Palma, G. Famiglini, and A. Cappiello.** 2011. An overview of matrix effects in liquid chromatography-mass spectrometry. Mass Spectrom Rev **30:**491-509.
232. **Tyagi, J. S., and D. Sharma.** 2002. Mycobacterium smegmatis and tuberculosis. Trends Microbiol **10:**68-69.
233. **Vasbinder, E., G. Van der Weken, Y. Vander Heyden, W. R. Baeyens, A. Debunne, J. P. Remon, and A. M. Garcia-Campana.** 2004. Quantitative determination of p-aminosalicylic acid and its degradation product m-aminophenol in pellets by ion-pair high-performance liquid chromatography applying the monolithic Chromolith Speedrod RP-18e column. Biomed Chromatogr **18:**55-63.
234. **Velayati, A. A., P. Farnia, M. R. Masjedi, G. K. Zhavnerko, M. A. Merza, J. Ghanavi, P. Tabarsi, N. N. Poleschuyk, and G. Ignatyev.** 2011. Sequential adaptation in latent tuberculosis bacilli: observation by atomic force microscopy (AFM). Int J Clin Exp Med **4:**193-199.
235. **Viverios, M., M. Martins, L. Rodrigues, D. Machado, I. Couto, J. Ainsa, and L. Amaral.** 2012. Inhibitors of mycobacterial efflux pumps as potential boosters for anti-tubercular drugs. Expert Rev Anti Infect Ther **10:**983-998.
236. **Walburger, A., A. Koul, G. Ferrari, L. Nguyen, C. Prescianotto-Baschong, K. Huygen, B. Klebl, C. Thompson, G. Bacher, and J. Pieters.** 2004. Protein kinase G from pathogenic mycobacteria promotes survival within macrophages. Science **304:**1800-1804.

237. **Warner, D. M., W. M. Shafer, and A. E. Jerse.** 2008. Clinically relevant mutations that cause derepression of the Neisseria gonorrhoeae MtrC-MtrD-MtrE Efflux pump system confer different levels of antimicrobial resistance and in vivo fitness. Mol Microbiol **70:**462-478.
238. **Wayne, L. G., and L. G. Hayes.** 1996. An in vitro model for sequential study of shiftdown of Mycobacterium tuberculosis through two stages of nonreplicating persistence. Infect Immun **64:**2062-2069.
239. **Wayne, L. G., and C. D. Sohaskey.** 2001. Nonreplicating persistence of mycobacterium tuberculosis. Annu Rev Microbiol **55:**139-163.
240. **WHO** 2010, posting date. 2010/2011 Tuberculosis Global Facts. http://www.who.int/tb/publications/2010/factsheet_tb_2010.pdf
241. **WHO.** 2011. TUBERCULOSIS MDR-TB & XDR-TB 2011 PROGRESS REPORT.
242. **WHO Media Centre** 2012, posting date. Tuberculosis. World Health Organization.Geneva, Switzerland [Online.] http://www.who.int/mediacentre/factsheets/fs104/en/
243. **Williams, K. J., G. A. Chung, and L. J. Piddock.** 1998. Accumulation of norfloxacin by Mycobacterium aurum and Mycobacterium smegmatis. Antimicrob Agents Chemother **42:**795-800.
244. **Wilson, M., J. DeRisi, H. H. Kristensen, P. Imboden, S. Rane, P. O. Brown, and G. K. Schoolnik.** 1999. Exploring drug-induced alterations in gene expression in Mycobacterium tuberculosis by microarray hybridization. Proc Natl Acad Sci U S A **96:**12833-12838.
245. **Xie, Z., N. Siddiqi, and E. J. Rubin.** 2005. Differential antibiotic susceptibilities of starved Mycobacterium tuberculosis isolates. Antimicrob Agents Chemother **49:**4778-4780.
246. **Yang, Y., D. Auguin, S. Delbecq, E. Dumas, G. Molle, V. Molle, C. Roumestand, and N. Saint.** 2011. Structure of the Mycobacterium tuberculosis OmpATb protein: a model of an oligomeric channel in the mycobacterial cell wall. Proteins **79:**645-661.
247. **Zhang, Y.** 2004. Persistent and dormant tubercle bacilli and latent tuberculosis. Front Biosci **9:**1136-1156.
248. **Zhang, Y., M. M. Wade, A. Scorpio, H. Zhang, and Z. Sun.** 2003. Mode of action of pyrazinamide: disruption of Mycobacterium tuberculosis membrane transport and energetics by pyrazinoic acid. J Antimicrob Chemother **52:**790-795.
249. **Zhang, Y., and W. W. Yew.** 2009. Mechanisms of drug resistance in Mycobacterium tuberculosis. Int J Tuberc Lung Dis **13:**1320-1330.
250. **Zhang, Z. Q., and M. Ishaque.** 1997. Evaluation of methods for isolation of DNA from slowly and rapidly growing mycobacteria. Int J Lepr Other Mycobact Dis **65:**469-476.
251. **Zhou, J. F., Y. H. Dong, X. L. Zhao, S. W. Lee, A. Amin, S. Ramaswamy, A. Domagala, J. M. Musser, and K. Drlica.** 2000. Selection of antibiotic-resistant bacterial mutants: Allelic diversity among fluoroquinolone-resistant mutations. J Infect Dis **182:**517-525.
252. **Zimic, M., P. Fuentes, R. H. Gilman, A. H. Gutierrez, D. Kirwan, and P. Sheen.** 2012. Pyrazinoic acid efflux rate in Mycobacterium tuberculosis is a better proxy of pyrazinamide resistance. Tuberculosis (Edinb) **92:**84-91.
253. **Zuber, B., M. Chami, C. Houssin, J. Dubochet, G. Griffiths, and M. Daffe.** 2008. Direct visualization of the outer membrane of mycobacteria and corynebacteria in their native state. J Bacteriol **190:**5672-5680.

Appendix I

UNIT	VERSION	DATE:	PAGES
PH	2.0	12th April 2011	5

PROTOCOL BIOSAFETY 3

PREPARED BY:
Version 1.0- Jansy Passiflora Sarathy (02.06.10)
Version 2.0- Jansy Passiflora Sarathy

REVIEWED BY(name + signature+date): Sabai Phyu
(IBC member)

APPROVED BY (name + signature + date): Luis Camacho
(IBC member)

PROTOCOL TITLE: Drug Penetration Assay for *Mycobacterium tuberculosis*

Protocol #: 66

Materials

1. Roller bottle (Corning, 490cm^2, cat. no.: 430195)
2. Spectrophotometer (Spectramax M2, Molecular Devices or Novaspec Plus, GE Health Care)
3. Pipette aid
4. Gilsan pipetteman
5. Plastic cuvettes plus caps
6. Centrifuge Centrifuge bucket with 50ml tube holder(Heraeus)
7. Microcentrifuge plus rotor
8. 50ml Falcon tubes
9. 15ml Falcon tubes
10. 7H9-ADS liquid media
11. 7H11- OADC agar plates
12. Filter pipette tips
13. Antibiotic stock solution (10mM)
14. 2ml Sarstedt tubes (screw cap)
15. Phosphate Saline Buffer with 0.05% Tween 80 (PBS-T)
16. 0.1M Glycine HCl (pH3)
17. Lock-lock box
18. Water-bath sonicator (HF-frequency-35Hz, type-T460/H: Gen-Probe, Germany)
19. Millipore MILLEX-GV filter unit (0.22uM, PVDF, 13mm) (Cat No. SLGV013SL)
20. BD 1ml Tuberculin Syringe (Cat No. 302100)
21. Zip lock bag

PROCEDURES

Day 1

1. All procedures are carried out inside the BSC unless otherwise stated.
2. Grow MTB culture in 7H9-ADS to an OD_{600} of 0.5 according to BSL3 Protocol #11.
3. Set up BSC.
4. Bring a steel canister containing log-growing MTB culture bottle into BSC. Transfer 45ml of culture to each 50ml falcon tube and close cap tightly.
5. Wipe down tubes with 1% Aniosyme and place in sealed centrifuge bucket. Wipe down centrifuge bucket with 1% Aniosyme. Take centrifuge bucket out of BSC; centrifuge at 3200rpm at RT for 10min.
6. Bring sealed bucket back into BSC. Discard supernatant into liquid waste pot containing 1% Aniosyme. Resuspend pellet in appropriate amount of fresh 7H9-ADS to bring culture to desired optical density. Spread concentrated culture equally among 15ml Falcon tubes.
7. Add antibiotic stock solution to MTB culture in 15ml Falcon tubes to make final desired drug concentration (eg. 10uM). Leave MTB to incubate with drug for desired length of time (eg. 30min, 60min) within BSC.
8. From 15ml Falcon tube, transfer aliquot (eg. 300µl) of drug-incubated MTB culture to 3 x 2ml screw-cap tubes. Squeeze 1% Aniosyme onto tubes, wipe away excess, and transfer the tubes into the microcentrifuge rotor. Wipe down sealed rotor with 1% Aniosyme and bring out of BSC. Spin samples down at 13,000rpm at 4 degrees for 3min.
9. Return rotor to BSC. Remove supernatant using pipette tips and discard in liquid waste pot. Wash pellet in screw-cap tube by resuspending in equal volume of PBS-T. Replace tubes to rotor and repeat the process of pelleting as mentioned in Step #8.
10. Return rotor to BSC. Remove supernatant as mentioned in Step #9 and resuspend pellet in screw-cap tube with equal volume of 0.1M Glycine HCl (pH3) using filter pipette tips.
11. Squeeze 1% Aniosyme onto screw-cap tubes, place tubes in rack, place rack in lock-lock box and wipe down box with 1% Aniosyme. Transfer the lock-lock box to 37°C incubator (with shaking). During shaking, a lead ring must be placed on the box.

Day 2

12. Set up a “clean” BSC.
13. After shaking overnight, bring lock-lock box back into the BSC. Take out tubes and **properly seal screw-cap tops with parafilm**.
14. Bring water-bath sonicator into the BSC and set it up over a newabsorbent pad. Place tubes in a floating device and start sonication (as in Protocol #23) within the BSC. **Do not allow tubes to touch bottom or sides of sonicator**. Apply sonication for 5 min. **Wear ear-mufflers during sonication**. Ask other users to leave the room during sonication.
15. Remove tubes from floating device and place tubes in microcentrifuge rotor. Wipe down sealed rotor with 1% Aniosyme, bring out of BSC and centrifuge for 3.5min at RT at 13,000rpm.

Wipe down water-bath sonicator with 1% Aniosyme and remove from the BSC. Pour out water from the sonicator into the water containing bucket.

16. Bring the rotor back into BSC and remove tubes. From tubes, carefully withdraw the supernatant through 1ml syringes and pass through Millipore 0.22uM filter units. Filtrates are collected in fresh screw-cap tubes (as in Protocol #29)
17. Repeat filtration process as in Step #16 with new filter units and fresh screw-cap tubes.

Transfer of sterile supernatant to BSL2 (as in Protocol #29)

1. Take small roller bottle and add 1% Aniosyme to disinfect inner side of bottle.
2. Squeeze 1% Aniosyme onto screw-cap tubes and transfer into sterilized small roller bottle.
3. Seal bottle and wipe outer surface with 1% Aniosyme. Remove bottle from BSC.
4. Carry bottle out of BSL3 lab in a zip lock bag and transfer to BSL2 lab.
5. In BSL2 lab, samples from BSL3 are handled within BSCs only.

RISK ASSESSMENT

Pathogen(s):

(See Pathogen Risk Assessment for general risks associated with this pathogen)

Most high risk conditions & procedures:	**Possible incident:**	**Possible consequences:**
Incubation/growth of MTB in a 1 L roller bottle.	Leakage of the roller bottle containing infectious MTB.	Exposure of MTB to lab workers when lab workers do not ware PPE properly
Discarding MTB contamainted liquid waste into a 1% Aniosyme contianing pot	Users discard larger volume of MTB contaminated liquid waste into a pot. Insufficient chemical sterilsation of infectiouse liquids could happen. Coincidnetly such liquid waste pot may not be autoclaved out properly.	Exposure of MTB to associates and environment
Using a centrifuge/micro-centrifuge to spin down MTB	Imbalance could cause rotor damage. Tubes get destroyed when	Contamination of centrifuge because of

cells	placed incorrectly.	damage to tubes. Contamination to room if user opens lid without knowing a leak has occured inside centrifuge.
Sonication of samples in water bath	Screw-cap tubes are not screwed on tightly within BSC before transfer out to water bath sonicator. Screw-caps come losen during the sonication process.	Leakage of MTB-contaminated cell lysate from tubes or the release of aerosols generated during the process results in contamination of room and infection of user if PPE is worn inappropriately.
Filtrating supernatant contaminated with MTB bacilli	Filter unit becomes lose/detaches from syringe while pushing the plunger. If filter unit is defective, samples are not propoerly filtered.	Due to aerosol generation, instruments and surface areas within the BSC, gloves and sleeves of user may get contaminated. Contaminated filtrate used in BSL2 lab can infect BSL2 users with MTB since they do not need to wear a suitable PPE required for protection against the MTB pathogen.

Instructions and measures to reduce risk:

Our experience showed that 1 L roller bottles sometimes leak due to cracks caused by
- Manufacturing problems
- Transport damage
- Inappropriate handling by end users

To minimize the risk, lab staff is advised to
- Visibly check roller bottles for any cracks
- Pre-roll the bottles intended to use in BSL3 for 24 h containing a non-infectious liquid
- Handle roller bottles carefully

To further reduce the risk of leakage, the roller bottles used in BSL3 for culturing MTB were incubated inside a stainless steel canister carrying absorbing paper towels (ref. BSL3 protocol #11) in order to

contain infectious liquids inside the canister. The lid of the canister is tapped down properly, and when more than one canister is being transferred between the BSC and incubator, the basket should be used to avoid dropping the canister.

Chemical sterilization of MTB containing liquids prior to autoclaving is an integral contribution to biosafety. Lab staff is advised to sterilize any infectious liquid by mixing with 1% Aniosyme in at least a 1:1 ratio. Autoclaving represents a second layer of biosafety: this step is carefully carried out/monitored according to validated procedures as well as documented and witnessed by the respective end users (ref. WI: BSL3 WI-001 Autoclaves.pdf). The risk that both sterilization steps fail is in minimal.

Always ensure centrifuge buckets/rotors are sealed before centrifugation. This ensures that any potential culture spill is contained within buckets/rotors which are only subsequently opened within BSCs. Make sure buckets/rotors are balanced to prevent damage to centrifuge.

Before sonication, screw-caps are screwed on tightly and top of tubes are always wrapped with parafilm to prevent the loosening of the screw-caps and the release of any aerosols from within the tube. The parafilm is subsequently only unwrapped within the BSC.

During filtration, do not push the plunger forcefully to prevent filter unit from detaching from syringe. Apply gentle and steady force when pushing plunger. Do not fill syringe completely. Allow at least ¼ volume of air within syringe to reduce the risk of overflowing (See Protocol #29 Risk Assessment).

Repeat filtration step with new filter unit to ensure complete sterilization of samples that are brought out of BSL3.

Users should adhere to BSL3 SOP5.2.4 while dealing with any spill occurs inside the BSC and outside the BSC.

Users should adhere to all general work rules mentioned in the Biosafety policy 5.2 while working with MTB.

Appendix II

Figure 1 (A) A snapshot of a chromatogram from the LC/MS analysis of ciprofloxacin (CPX) using the analytical method described in Table 6. Mass transition 332.3 / 288.4, eluting at 4.6min, was chosen for quantitation of sample CPX concentration. (B) A snapshot of a calibration curve derived from CPX standard preparations ranging from 5 to 500mM.

A

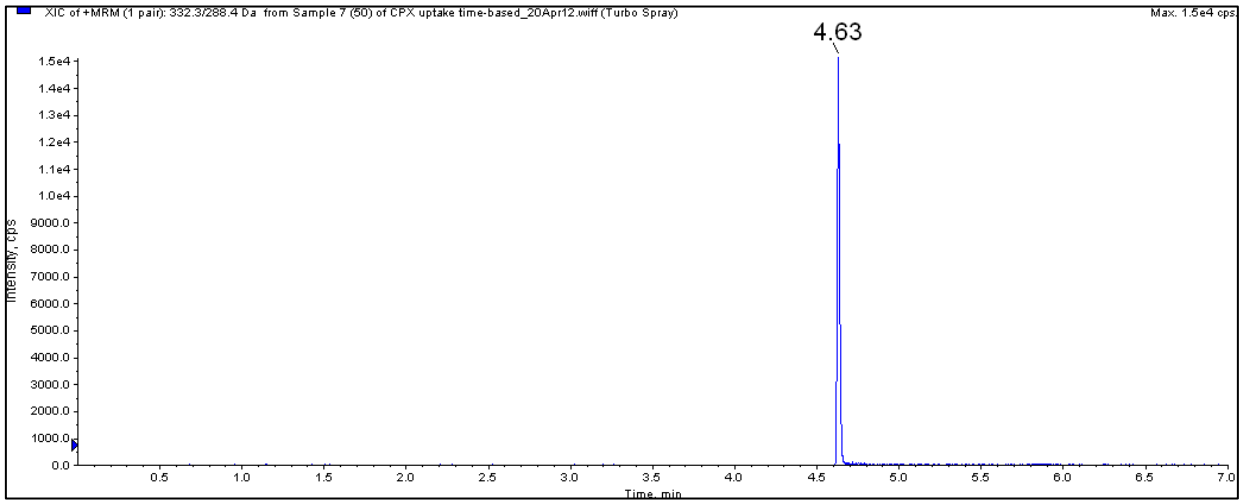

B

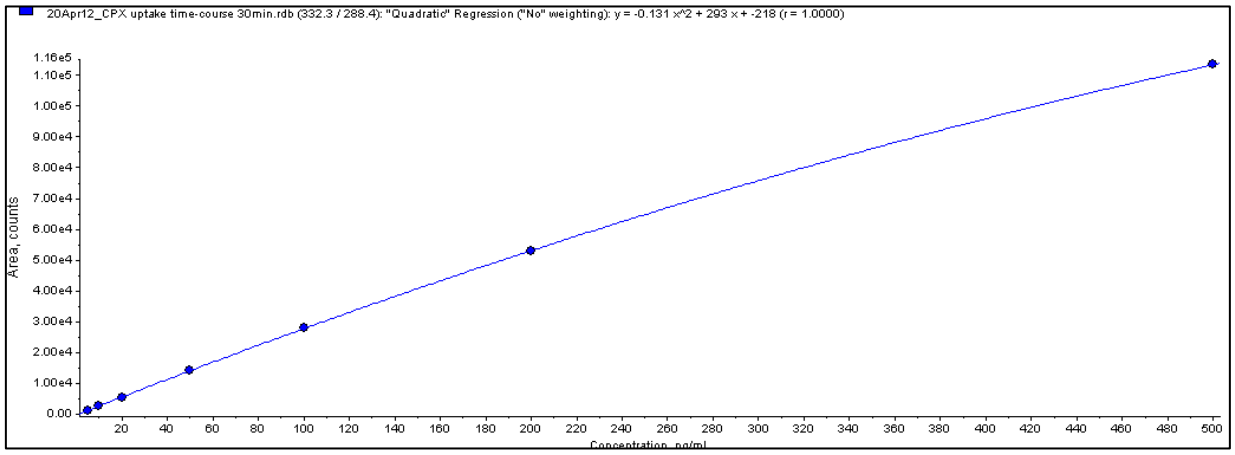

Table 1 Several compound-dependent parameters that were optimized for MRM (multiple reaction monitoring) analysis of CPX.

Parameter	Magnitude (units)
Q1 mass	332.3 Da
Declustering potential (DP)	60
Entrance potential (EP)	6
Q3 mass	288.4
Collision energy (CE)	26
Collision cell exit potential (CXP)	9

Figure 2 (A) A snapshot of a chromatogram from the LC/MS analysis of moxifloxacin (MXF) using the analytical method described in Table 6. Mass transition 402.4 / 384.3, eluting at 4.9min, was chosen for quantitation of sample MXF concentration. (B) A snapshot of a calibration curve derived from MXF standard preparations ranging from 5 to 500mM.

A

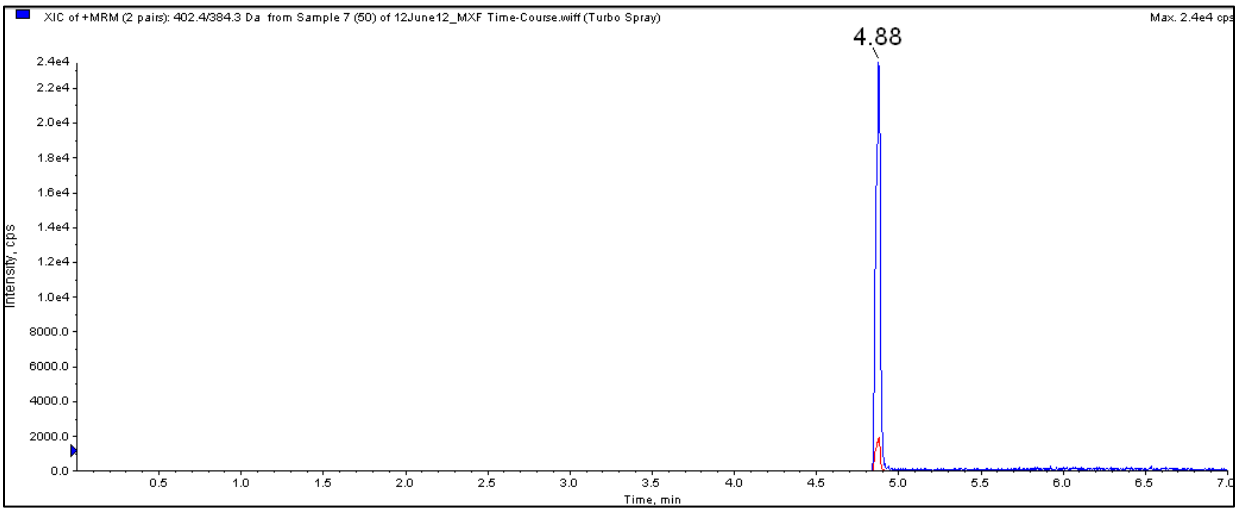

B

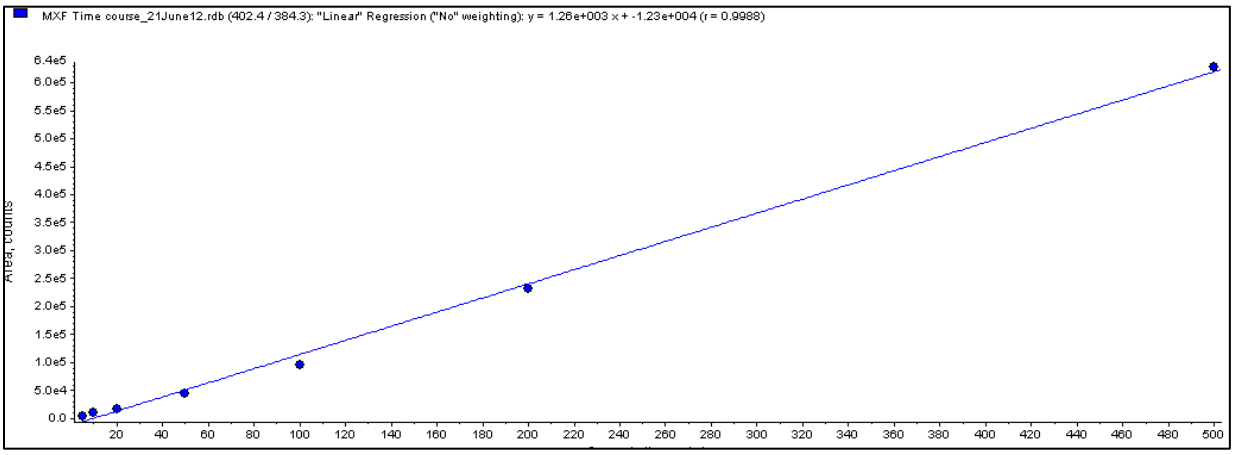

Table 2 Several compound-dependent parameters that were optimized for MRM (multiple reaction monitoring) analysis of MXF.

Parameter	Magnitude (units)	
Q1 mass	402.4	
Declustering potential (DP)	85	
Entrance potential (EP)	10	
Q3 masses	384.3	364.5
Collision energies (CE)	32	36
Collision cell exit potentials (CXP)	13.5	15

Figure 3 (A) A snapshot of a chromatogram from the LC/MS analysis of ofloxacin (OFX) using the analytical method described in Table 6. Mass transition 361.9 / 318.4, eluting at 4.6min, was chosen for quantitation of sample OFX concentration. (B) A snapshot of a calibration curve derived from OFX standard preparations ranging from 5 to 500mM.

A

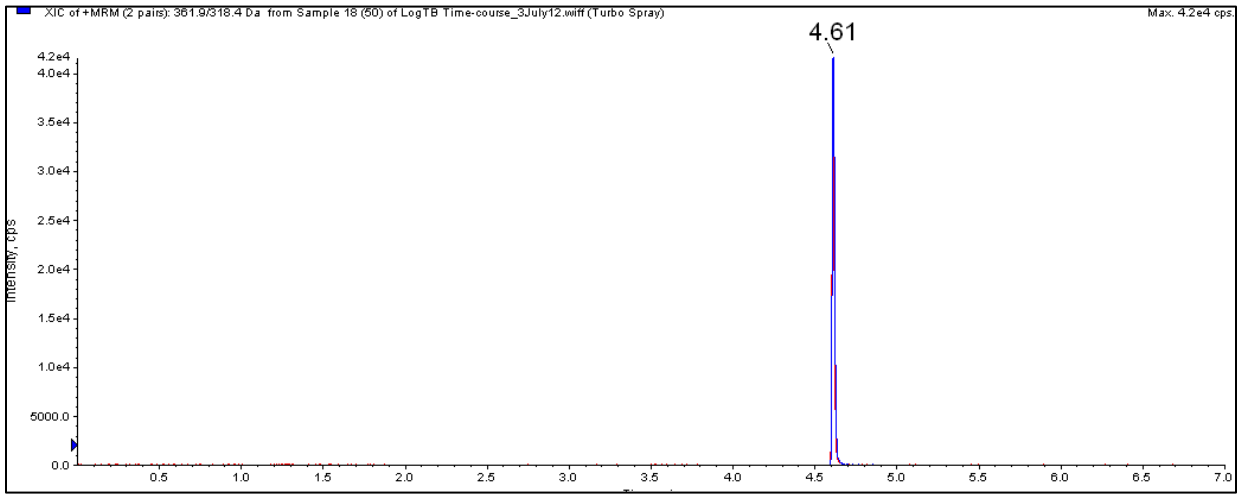

B

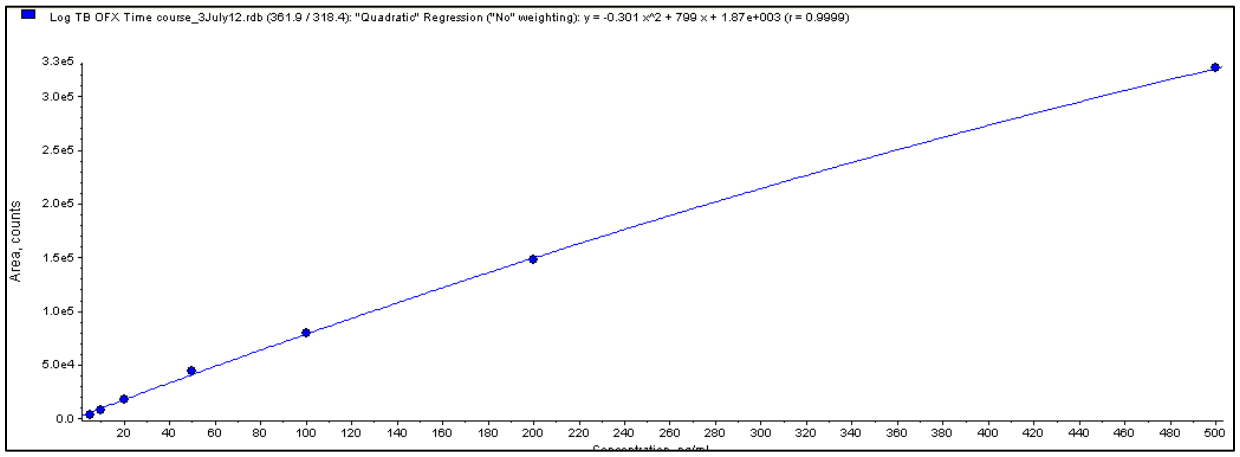

Table 3 Several compound-dependent parameters that were optimized for MRM (multiple reaction monitoring) analysis of OFX.

Parameter	Magnitude (units)	
Q1 mass	361.9	
Declustering potential (DP)	90	
Entrance potential (EP)	6.5	
Q3 masses	318.4	344.1
Collision energies (CE)	27	30
Collision cell exit potentials (CXP)	25	25

Figure 4 (A) A snapshot of a chromatogram from the LC/MS analysis of levofloxacin (LFX) using the analytical method described in Table 6. Mass transition 361.9 / 318.4, eluting at 4.6min, was chosen for quantitation of sample LVX concentration. (B) A snapshot of a calibration curve derived from LVX standard preparations ranging from 5 to 500mM.

A

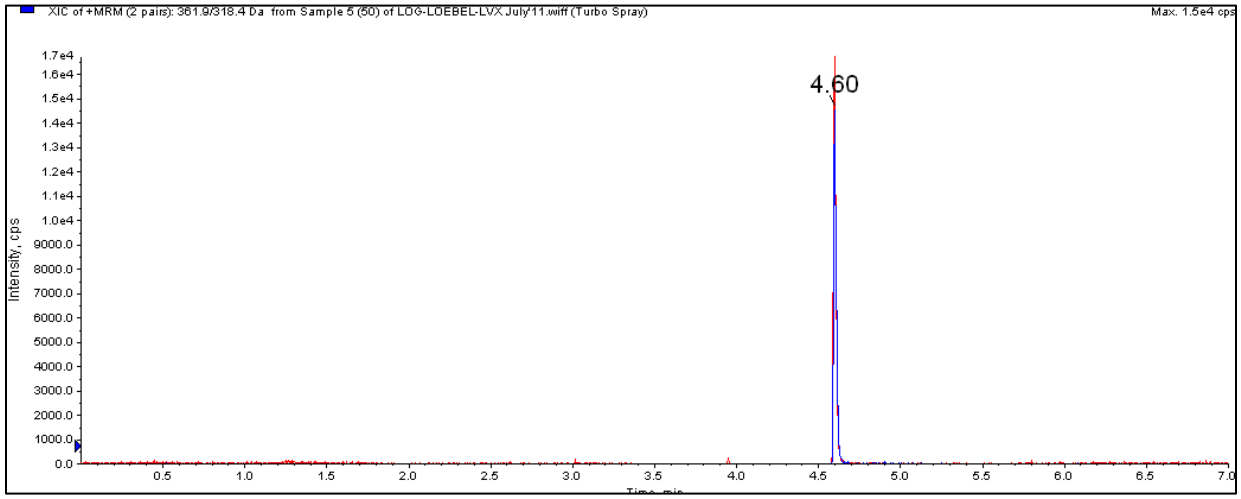

B

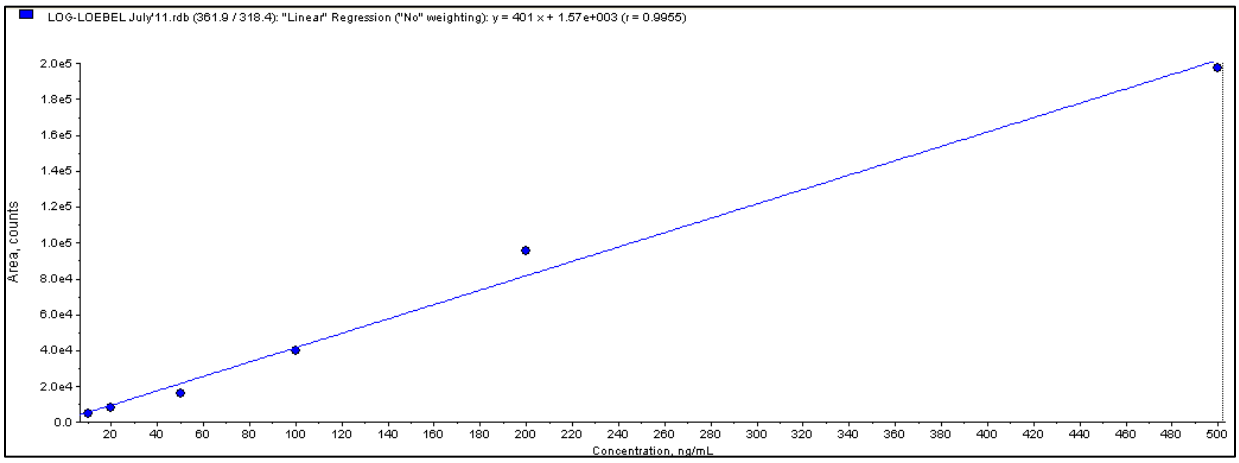

Table 4 Several compound-dependent parameters that were optimized for MRM (multiple reaction monitoring) analysis of LVX.

Parameter	Magnitude (units)	
Q1 mass	361.9	
Declustering potential (DP)	90	
Entrance potential (EP)	6.5	
Q3 masses	318.4	344.1
Collision energies (CE)	27	30
Collision cell exit potentials (CXP)	25	25

Figure 5 (A) A snapshot of a chromatogram from the LC/MS analysis of gatifloxacin (GFX) using the analytical method described in Table 6. Mass transition 376.0 / 289.7, eluting at 4.6min, was chosen for quantitation of sample GFX concentration. (B) A snapshot of a calibration curve derived from GFX standard preparations ranging from 5 to 500mM.

A

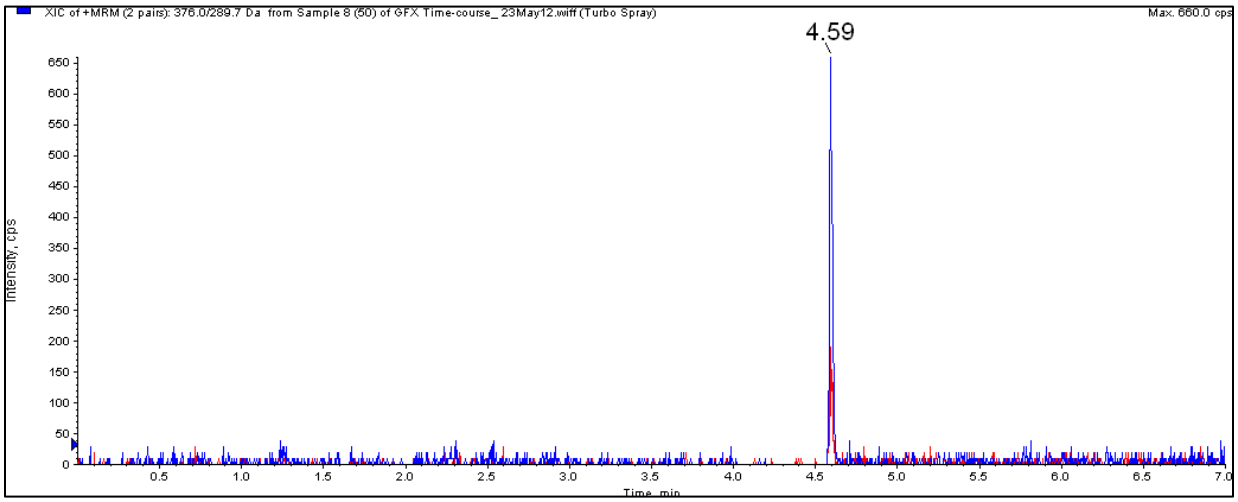

B

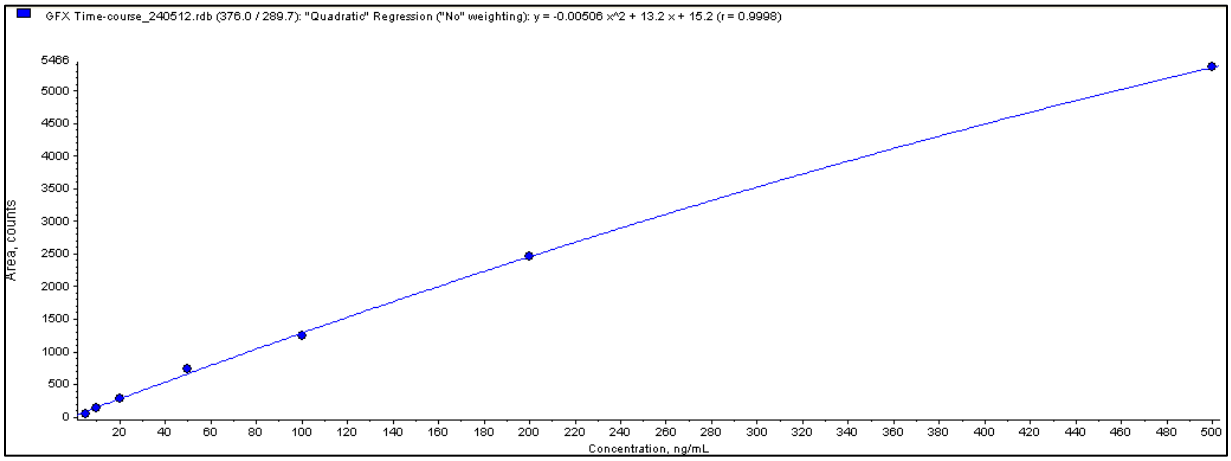

Table 5 Several compound-dependent parameters that were optimized for MRM (multiple reaction monitoring) analysis of GFX.

Parameter	Magnitude (units)	
Q1 mass	376.0	
Declustering potential (DP)	25	
Entrance potential (EP)	10	
Q3 masses	289.7	332.9
Collision energies (CE)	33	26
Collision cell exit potentials (CXP)	24	28

Figure 6 (A) A snapshot of a chromatogram from the LC/MS analysis of clinafloxacin (CNX) using the analytical method described in Table 6. Mass transition 365.9 / 322.1, eluting at 4.6min, was chosen for quantitation of sample CNX concentration. (B) A snapshot of a calibration curve derived from CNX standard preparations ranging from 5 to 500mM.

A

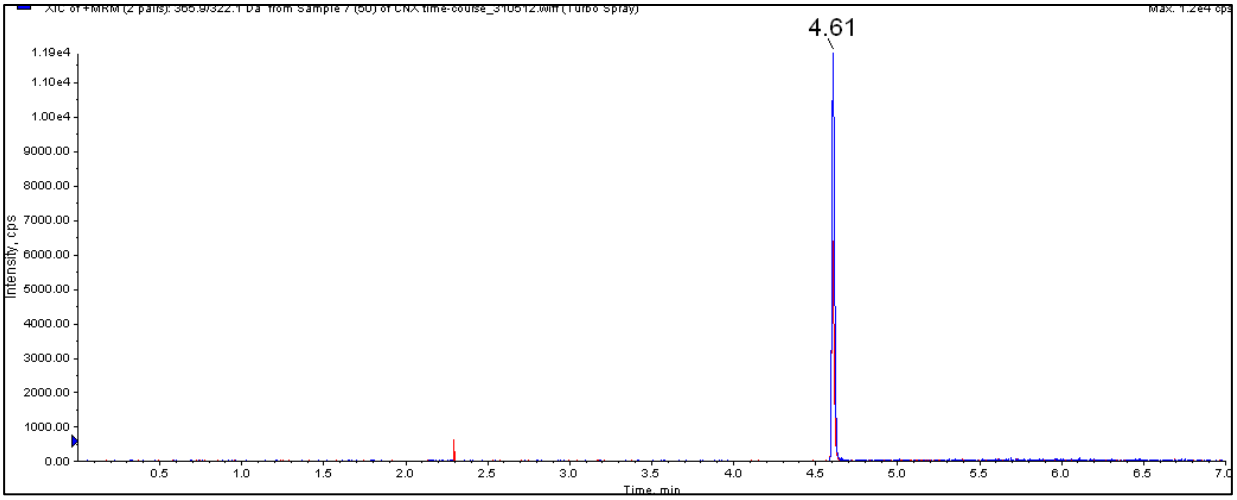

B

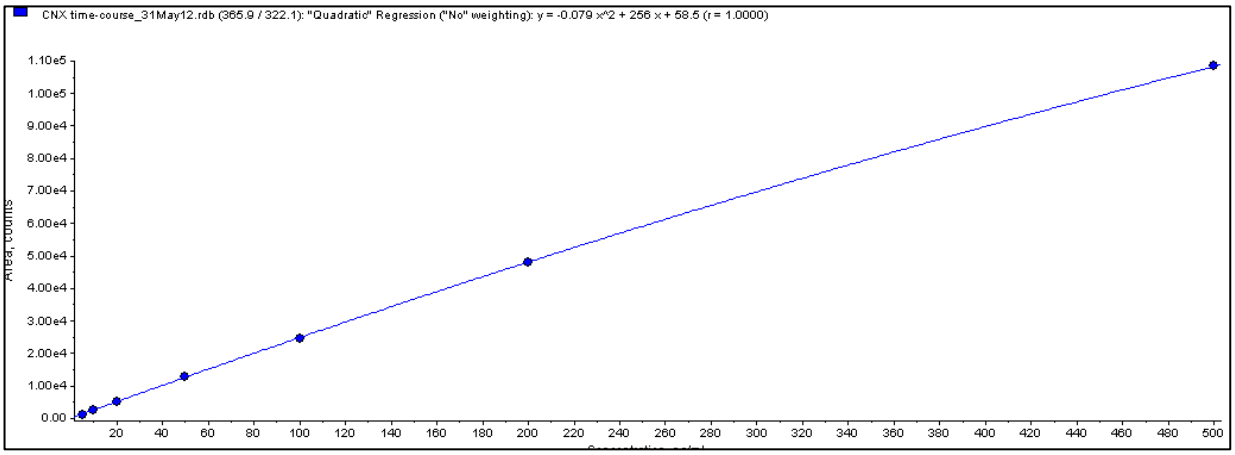

Table 6 Several compound-dependent parameters that were optimized for MRM (multiple reaction monitoring) analysis of CNX.

Parameter	Magnitude (units)	
Q1 mass	365.9	
Declustering potential (DP)	80	
Entrance potential (EP)	5	
Q3 masses	322.1	279.2
Collision energies (CE)	25	34
Collision cell exit potentials (CXP)	8	6.5

Figure 7 (A) A snapshot of a chromatogram from the LC/MS analysis of sparfloxacin (SPX) using the analytical method described in Table 6. Mass transition 392.7 / 349.3, eluting at 4.9min, was chosen for quantitation of sample SPX concentration. (B) A snapshot of a calibration curve derived from SPX standard preparations ranging from 5 to 500mM.

A

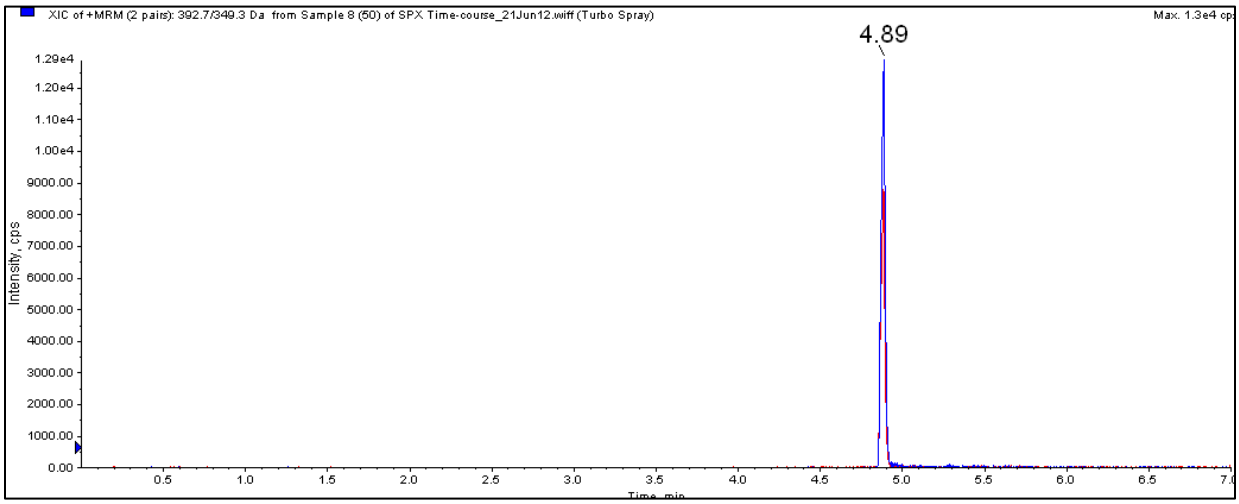

B

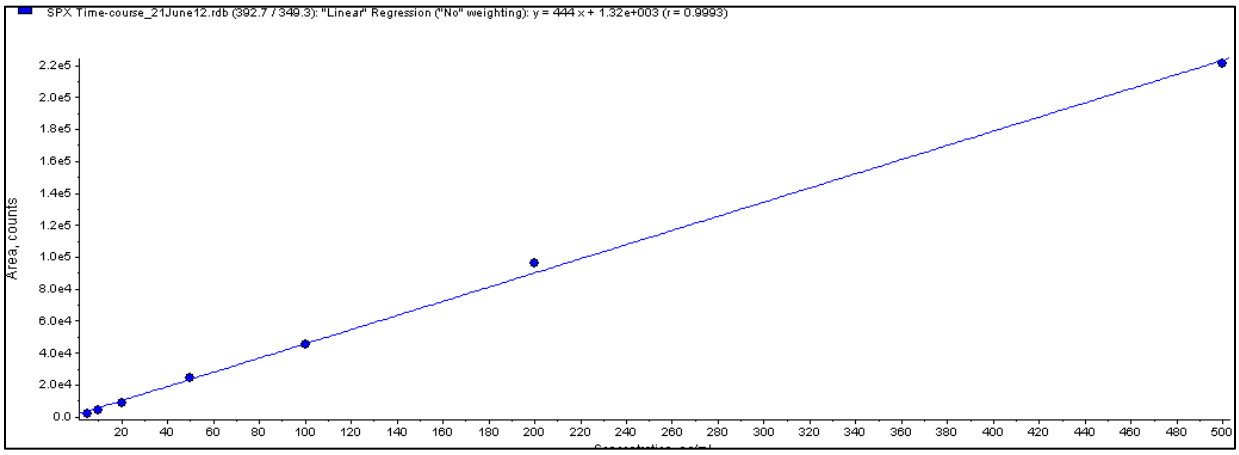

Table 7 Several compound-dependent parameters that were optimized for MRM (multiple reaction monitoring) analysis of SPX.

Parameter	Magnitude (units)	
Q1 mass	392.7	
Declustering potential (DP)	80	
Entrance potential (EP)	6	
Q3 masses	349.3	292.1
Collision energies (CE)	28	34
Collision cell exit potentials (CXP)	10	15

Figure 8 (A) A snapshot of a chromatogram from the LC/MS analysis of rifampicin (RIF) using the analytical method described in Table 7. Mass transition 823.6 / 791.9, eluting at 5.3min, was chosen for quantitation of sample RIF concentration. (B) A snapshot of a calibration curve derived from RIF standard preparations ranging from 5 to 500mM.

A

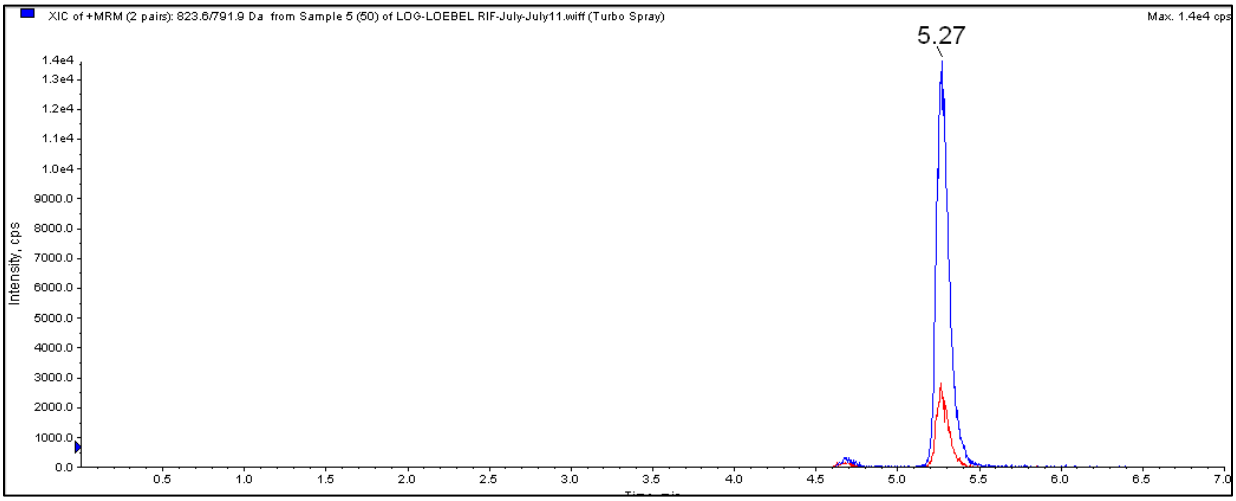

B

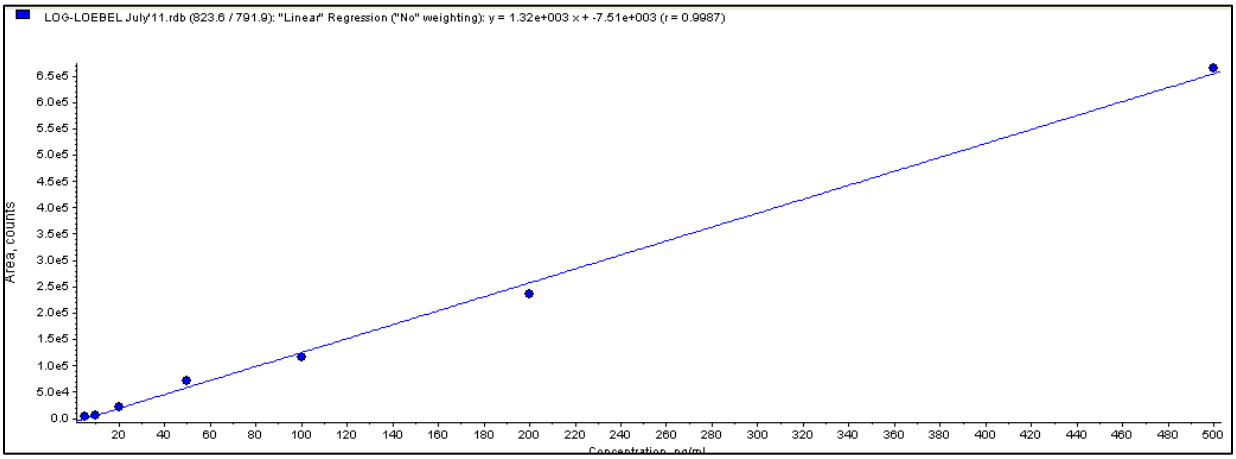

Table 8 Several compound-dependent parameters that were optimized for MRM (multiple reaction monitoring) analysis of RIF.

Parameter	Magnitude (units)	
Q1 mass	823.6	
Declustering potential (DP)	100	
Entrance potential (EP)	6.5	
Q3 masses	791.9	399.6
Collision energies (CE)	24	35
Collision cell exit potentials (CXP)	25	10

Figure 9 (A) A snapshot of a chromatogram from the LC/MS analysis of rifabutin (RIB) using the analytical method described in Table 7. Mass transition 847.2 / 815.8, eluting at 4.7min, was chosen for quantitation of sample RIB concentration. (B) A snapshot of a calibration curve derived from RIB standard preparations ranging from 5 to 500mM.

A

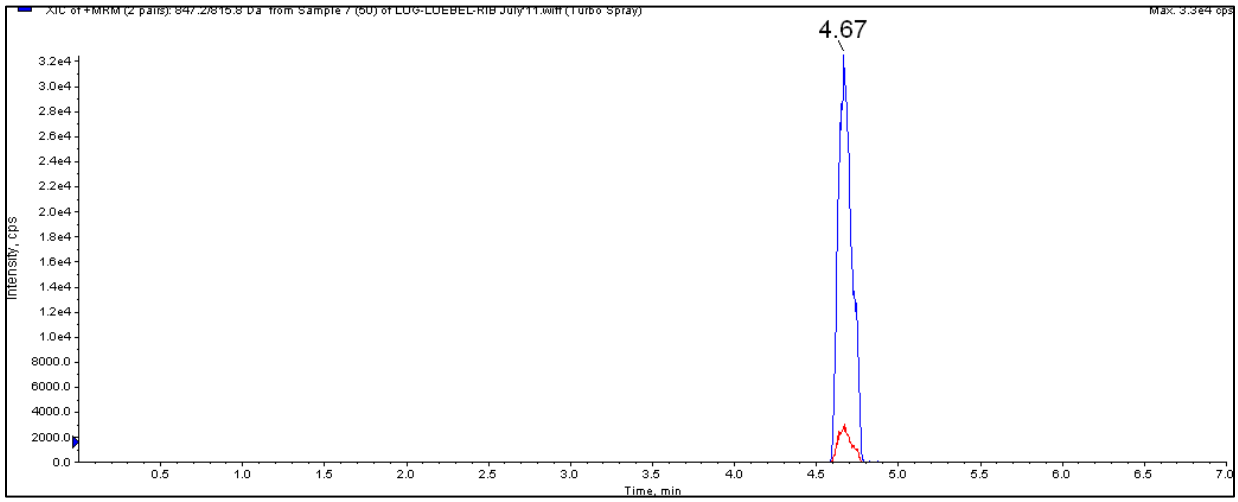

B

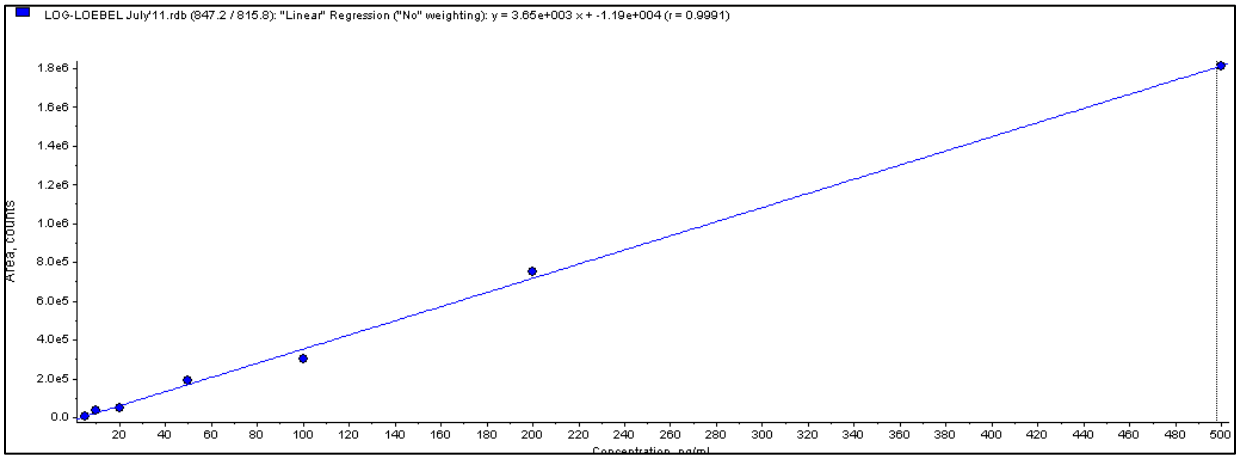

Table 9 Several compound-dependent parameters that were optimized for MRM (multiple reaction monitoring) analysis of RIB.

Parameter	Magnitude (units)	
Q1 mass	847.2	
Declustering potential (DP)	100	
Entrance potential (EP)	6.0	
Q3 masses	815.8	755.9
Collision energies (CE)	36	41
Collision cell exit potentials (CXP)	22	24

Figure 10 (A) A snapshot of a chromatogram from the LC/MS analysis of rifapentine (RIP) using the analytical method described in Table 8. Mass transition 877.6 / 845.7 eluting at 4.7min was chosen for quantitation of sample RIP concentration. (B) A snapshot of a calibration curve derived from RIP standard preparations ranging from 5 to 500mM.

A

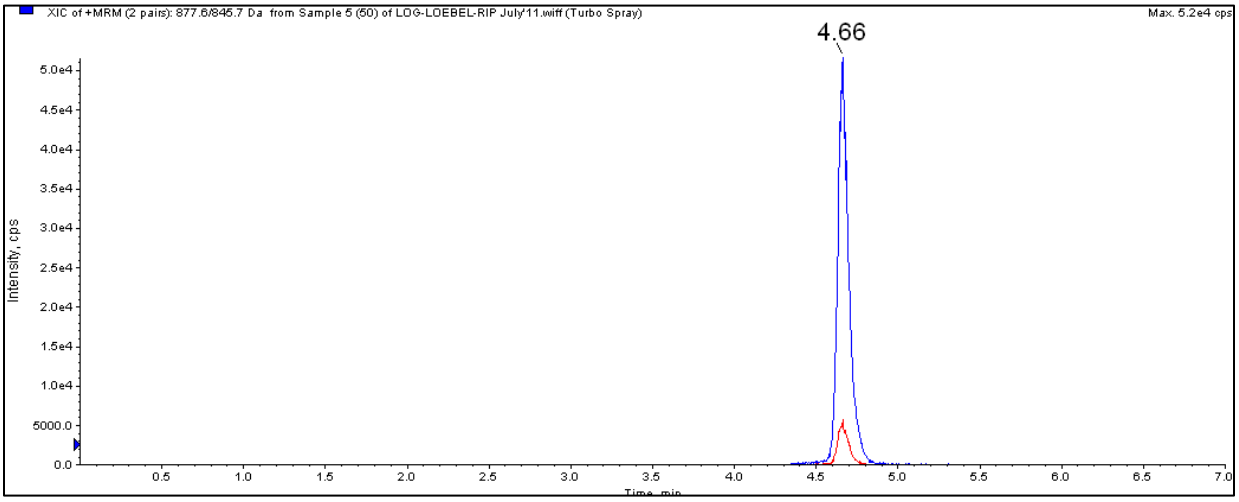

B

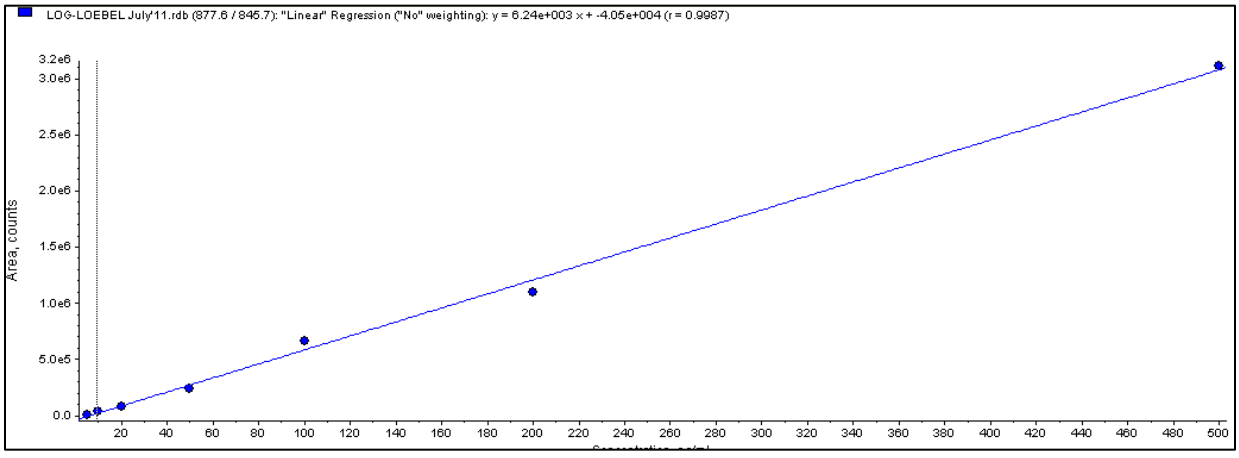

Table 10 Several compound-dependent parameters that were optimized for MRM (multiple reaction monitoring) analysis of RIP.

Parameter	Magnitude (units)	
Q1 mass	877.6	
Declustering potential (DP)	100	
Entrance potential (EP)	9	
Q3 masses	845.7	453.4
Collision energies (CE)	28	41
Collision cell exit potentials (CXP)	25	13

Figure 11 (A) A snapshot of a chromatogram from the LC/MS analysis of ethambutol (EMB) using the analytical method described in Table 9. Mass transition 205.1 / 116.0, eluting at 1.3min, was chosen for quantitation of sample EMB concentration. (B) A snapshot of a calibration curve derived from EMB standard preparations ranging from 2 to 200mM.

A

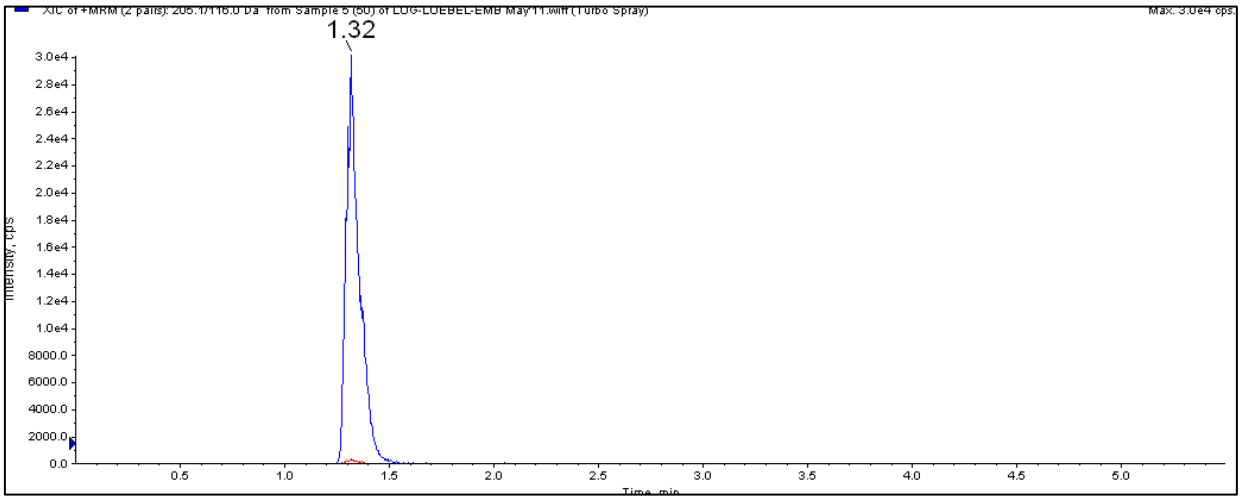

B

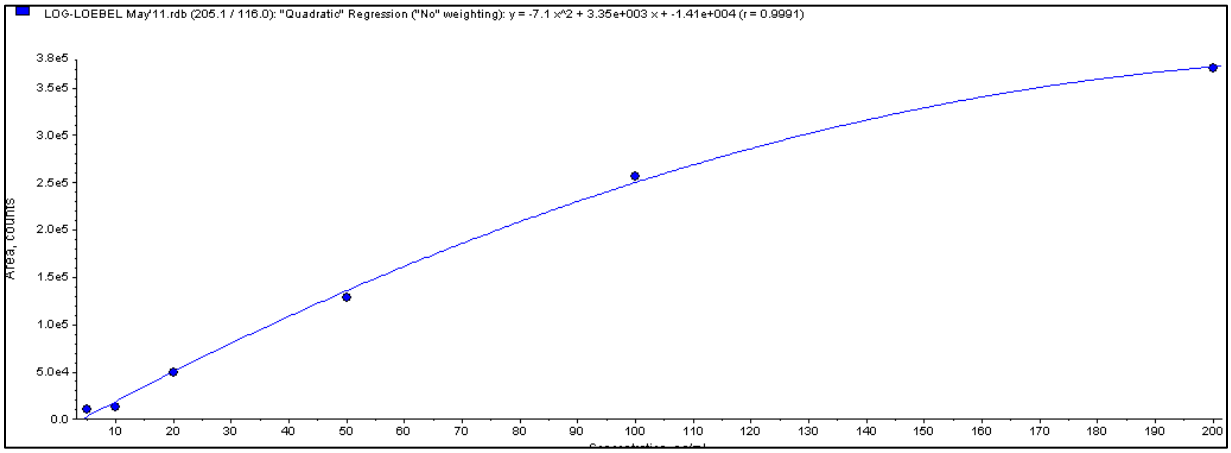

Table 11 Several compound-dependent parameters that were optimized for MRM (multiple reaction monitoring) analysis of EMB.

Parameter	Magnitude (units)	
Q1 mass	205.1	
Declustering potential (DP)	60	
Entrance potential (EP)	5.5	
Q3 masses	116	98
Collision energies (CE)	21	28
Collision cell exit potentials (CXP)	20	16

Figure 12 (A) A is a snapshot of a chromatogram from the LC/MS analysis of mefloquine (MEF) using the analytical method described in Table 7. Mass transition 379.0 / 361.1, eluting at 4.7min, was chosen for quantitation of sample MEF concentration. (B) A snapshot of a calibration curve derived from MEF standard preparations ranging from 5 to 500mM.

A

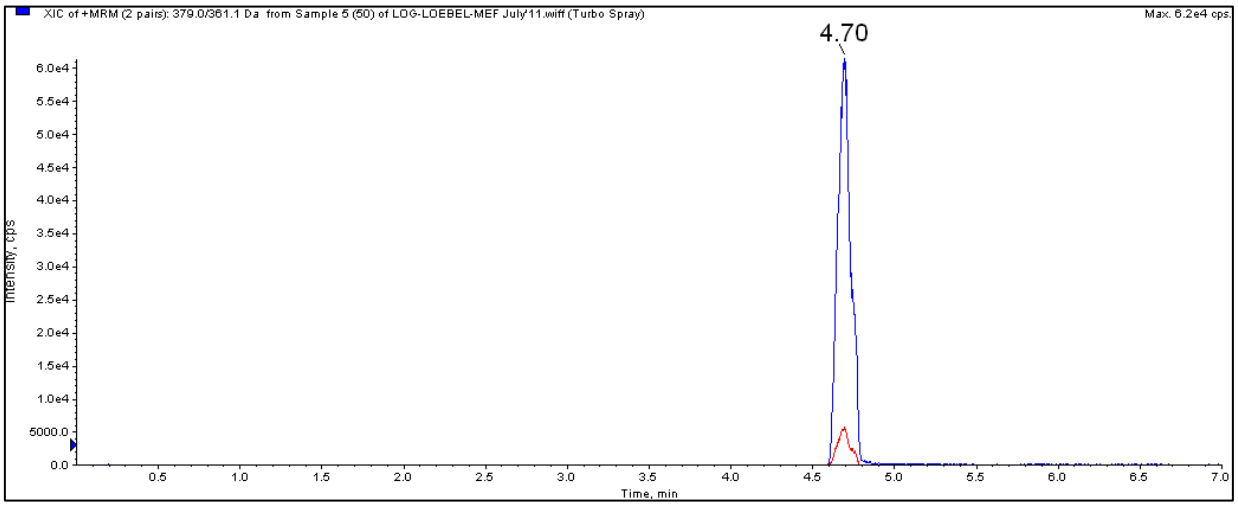

B

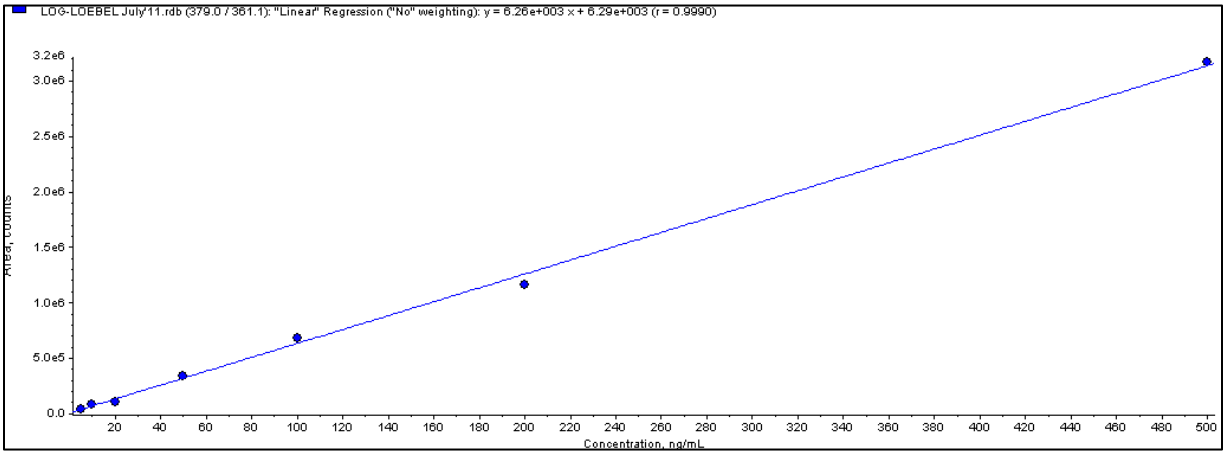

Table 12 Several compound-dependent parameters that were optimized for MRM (multiple reaction monitoring) analysis of MEF.

Parameter	Magnitude (units)	
Q1 mass	379.0	
Declustering potential (DP)	75	
Entrance potential (EP)	9	
Q3 masses	361.1	321.1
Collision energies (CE)	30	45
Collision cell exit potentials (CXP)	10	27

Figure 13 (A) A snapshot of a chromatogram from the LC/MS analysis of linezolid (LNZ) using the analytical method described in Table 7. Mass transition 338.2 / 296.2, eluting at 5.2min, was chosen for quantitation of sample LNZ concentration. (B) A snapshot of a calibration curve derived from LNZ standard preparations ranging from 5 to 500mM.

A

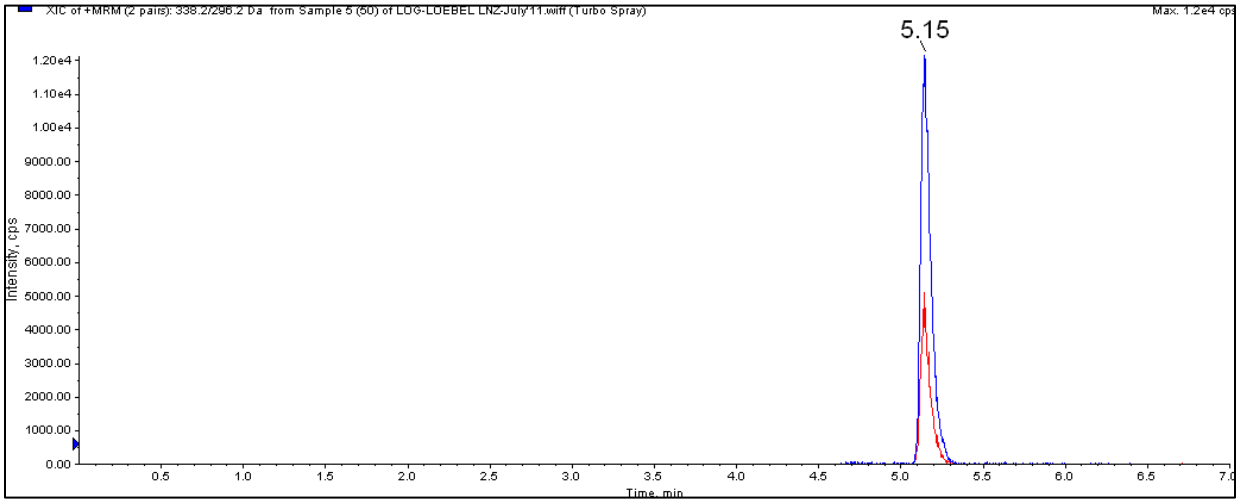

B

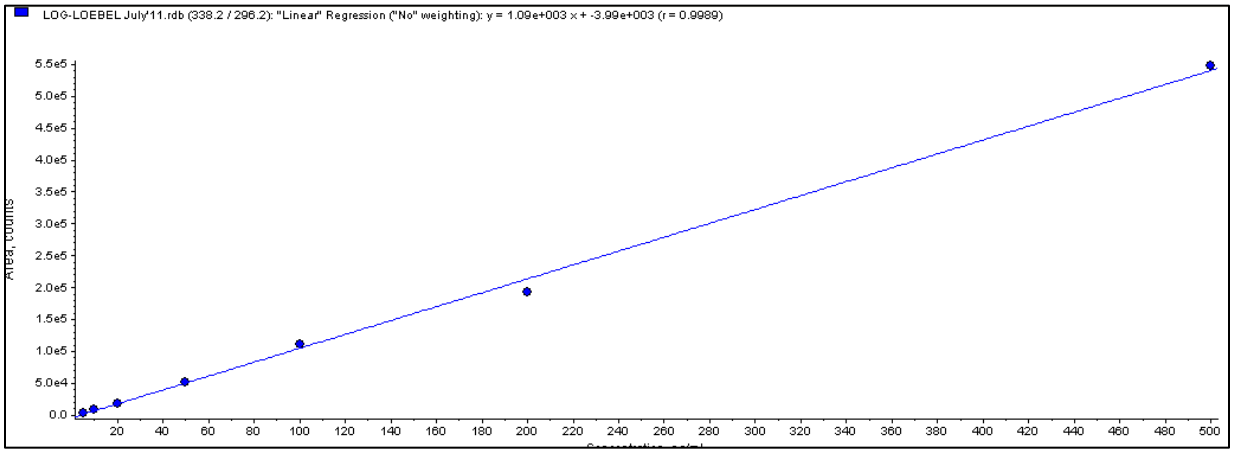

Table 13 Several compound-dependent parameters that were optimized for MRM (multiple reaction monitoring) analysis of LNZ.

Parameter	Magnitude (units)	
Q1 mass	338.2	
Declustering potential (DP)	100	
Entrance potential (EP)	5	
Q3 masses	296.2	235.2
Collision energies (CE)	27	31
Collision cell exit potentials (CXP)	16	19

Figure 14 (A) A snapshot of a chromatogram from the LC/MS analysis of thioridazine (TRZ) using the analytical method described in Table 7. Mass transition 371.3 / 126.1, eluting at 5.2min, was chosen for quantitation of sample TRZ concentration. (B) A snapshot of a calibration curve derived from TRZ standard preparations ranging from 1 to 200mM.

A

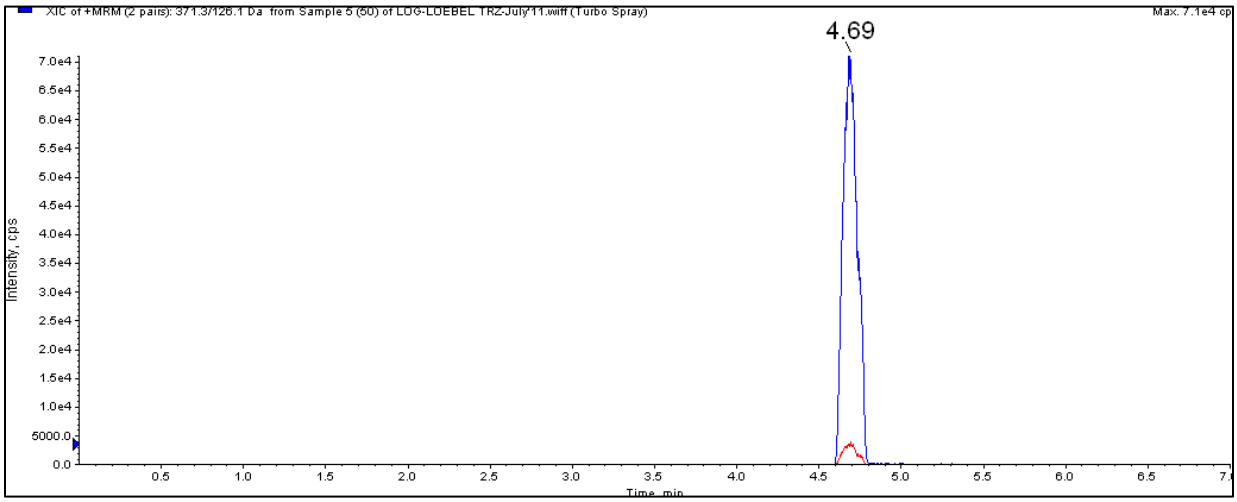

B

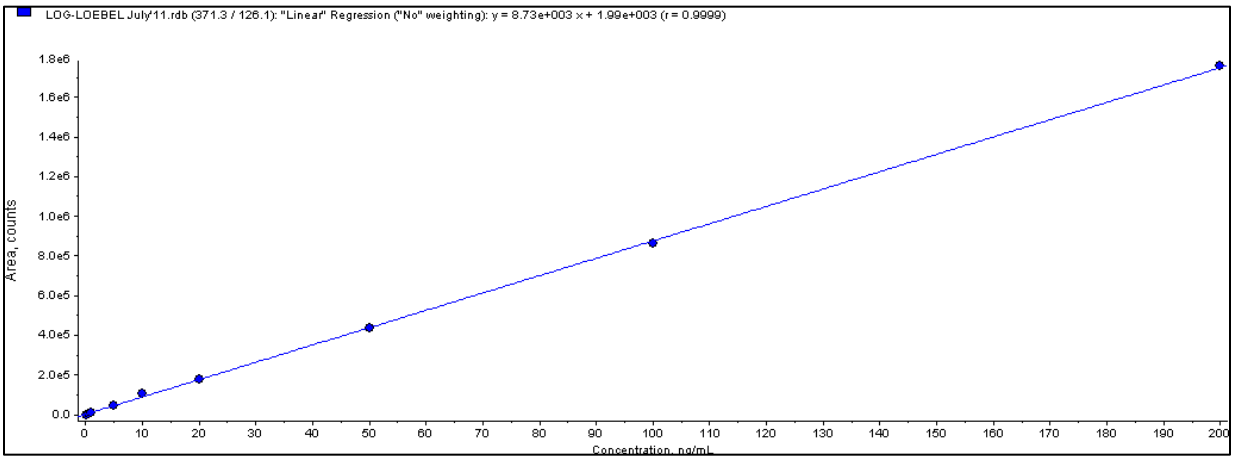

Table 14 Several compound-dependent parameters that were optimized for MRM (multiple reaction monitoring) analysis of TRZ.

Parameter	Magnitude (units)	
Q1 mass	371.3	
Declustering potential (DP)	80	
Entrance potential (EP)	4.5	
Q3 masses	126.1	257.9
Collision energies (CE)	35	37
Collision cell exit potentials (CXP)	35	37

Figure 15 (A) A snapshot of a chromatogram from the LC/MS analysis of TMC207 (TMC) using the analytical method described in Table 10. Mass transition 555.2 / 328.1, eluting at 5.2min, was chosen for quantitation of sample TMC concentration. (B) A snapshot of a calibration curve derived from TMC standard preparations ranging from 5 to 500mM.

A

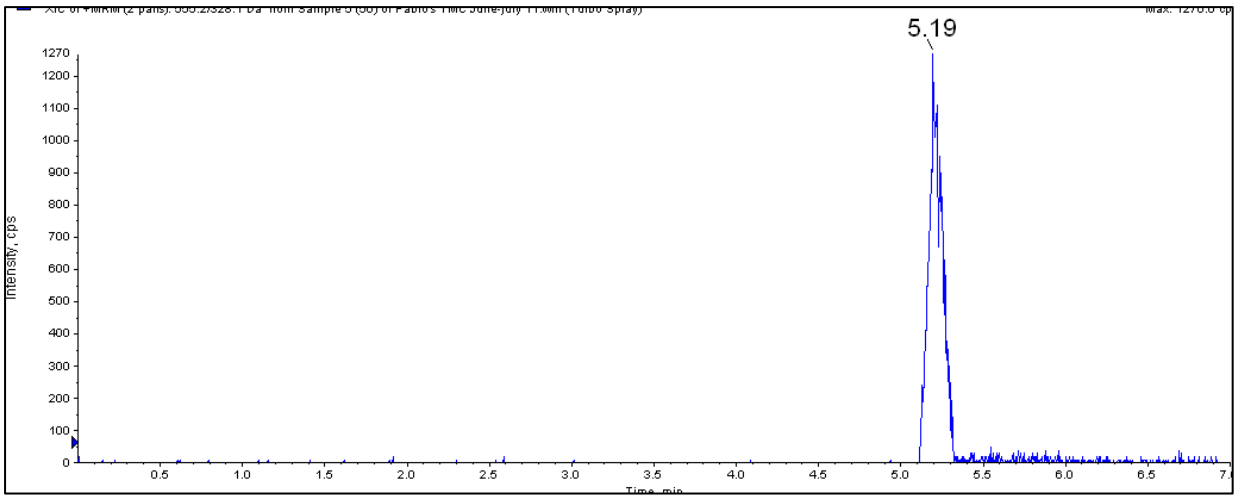

B

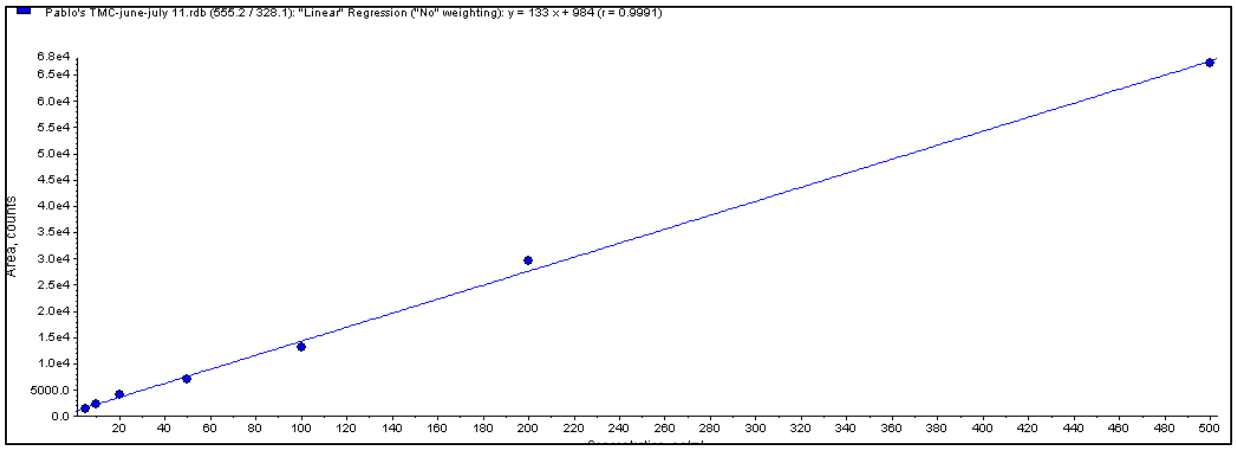

Table 15 Several compound-dependent parameters that were optimized for MRM (multiple reaction monitoring) analysis of TMC.

Parameter	Magnitude (units)
Q1 mass	555.2
Declustering potential (DP)	80
Entrance potential (EP)	5
Q3 masses	328.1
Collision energies (CE)	33
Collision cell exit potentials (CXP)	26

Figure 16 (A) A snapshot of a chromatogram from the LC/MS analysis of *para*-aminosalicylic acid (PAS) using the analytical method described in Table 11. Mass transition 152.0 / 107.8, eluting at 6.1min, was chosen for quantitation of sample PAS concentration. (B) A snapshot of a calibration curve derived from PAS standard preparations ranging from 5 to 500mM.

A

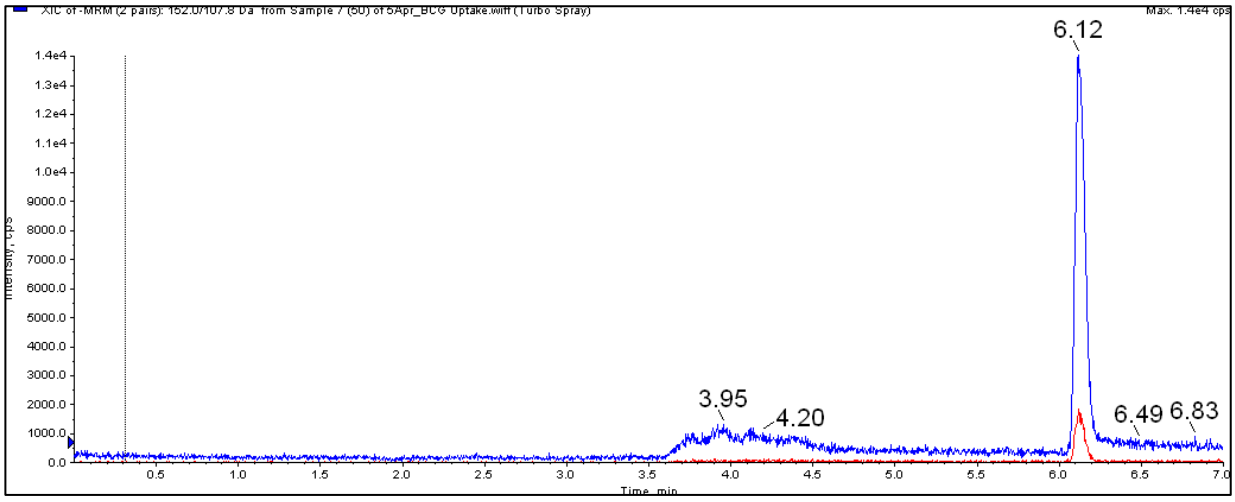

B

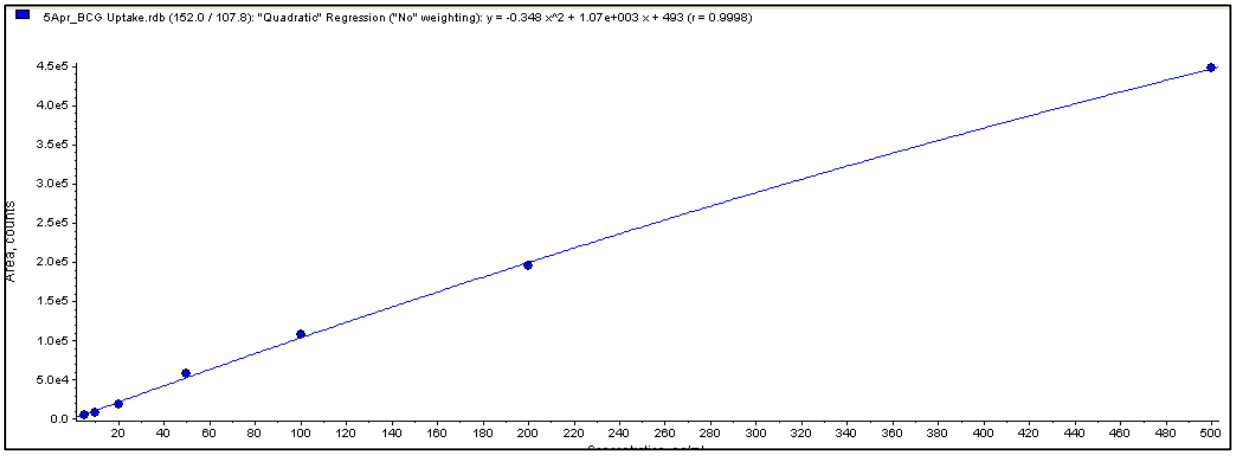

Table 16 Several compound-dependent parameters that were optimized for MRM (multiple reaction monitoring) analysis of PAS.

Parameter	Magnitude (units)	
Q1 mass	152.0	
Declustering potential (DP)	-50	
Entrance potential (EP)	-5	
Q3 masses	107.8	65.7
Collision energies (CE)	-20	-35
Collision cell exit potentials (CXP)	-18	-10

Appendix III

Figure 17 (A) The relative levels of rifabutin (RIB) recovery from different cell lysis procedures. Data is expressed as the concentration of RIB (nmol/dm^3) is cell lysate. (B) Comparison of signal strengths of RIB from standard solutions (100nM) prepared in different matrices. Data is presented as absolute signal peak areas from LC/MS chromatograms. Standard deviations are shown as error bars.

A

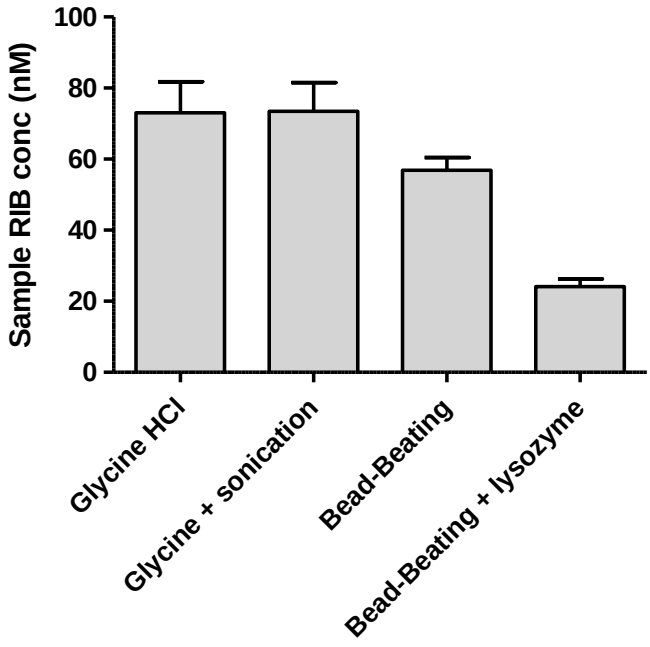

B

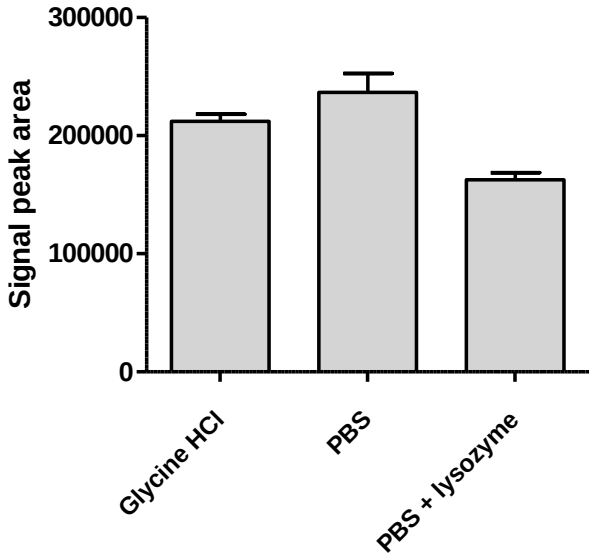

Figure 18 (A) The relative levels of mefloquine (MEF) recovery from different cell lysis procedures. Data is expressed as the concentration of MEF (nmol/dm^3) is cell lysate. (B) Comparison of signal strengths of MEF from standard solutions (100nM) prepared in different matrices. Data is presented as absolute signal peak areas from LC/MS chromatograms. Standard deviations are shown as error bars.

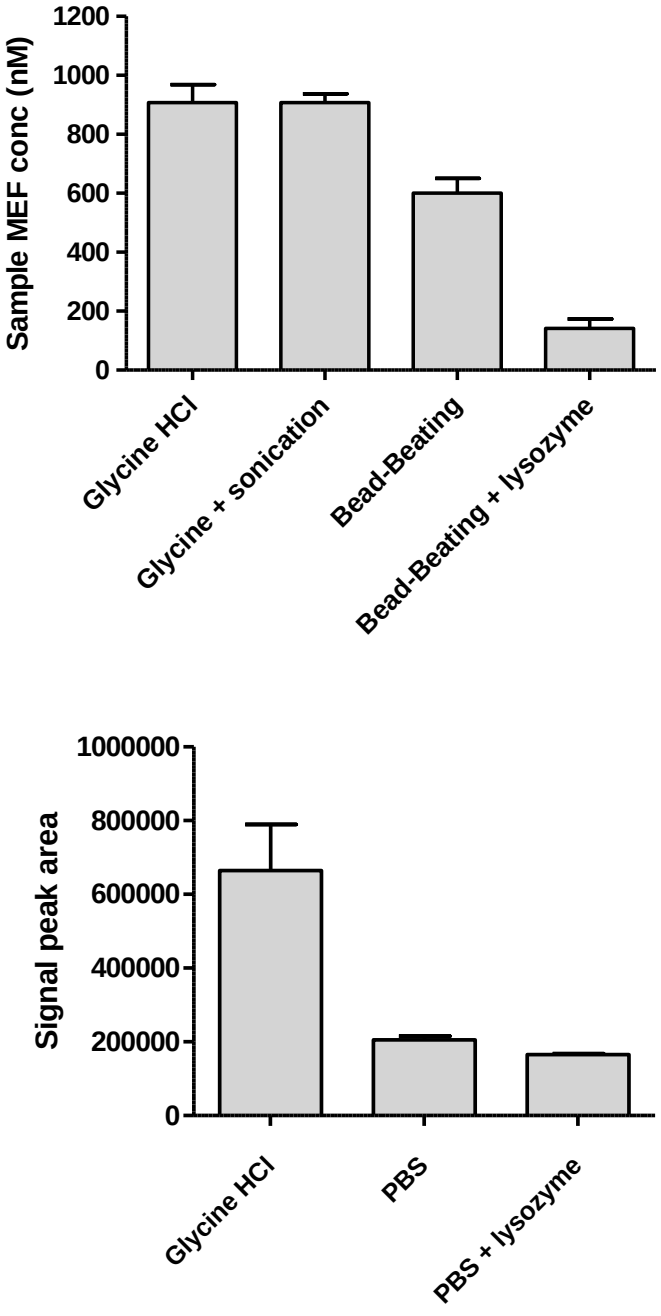

Table 17 Intra- and inter- day variabilities of (A) rifabutin and (B) mefloquine analysis. 5nM, 50nM and 500nM standard solutions of both drugs were analyzed for their drug contents using respective LC/MS methods and the variations in analysis were calculated. RE, relative error; CV, coefficient of variation.

A

Rifabutin	Standard conc. (nM)	Mean measured conc. (nM)	RE range (%)	CV (%)
Intra-day variability (n = 6)	5	5.59	11 – 12	0.64
	50	56.5	3.0 – 8.8	2.1
	500	499.5	-3.2 – 3.4	2.5
Inter-day variability (n = 18)	5	5.62	6.8 – 20	3.4
	50	57.0	3.0 – 14	6.6
	500	499.4	-4.6 – 3.4	2.1

B

Mefloquine	Standard conc. (nM)	Mean measured conc. (nM)	RE range (%)	CV (%)
Intra-day variability (n = 6)	5	5.64	7.6 – 16	2.9
	50	49.4	-3.4 – 2.6	2.7
	500	500	-2.2 – 2.0	1.8
Inter-day variability (n = 18)	5	5.8	-13 – 16	15.8
	50	49.2	-10 – 3.2	3.4
	500	500.1	-2.2 – 2.0	1.3

Figure 19 Accumulation of 8 anti-tuberculous drugs (non-fluoroquinolones) in *M. bovis* BCG following a 30 min incubation period at 10μM. Drug content is expressed as the amount of drug (nmol) per CFU. The applications / statuses of each drug are stated below the bar chart. Standard deviations are shown as error bars.

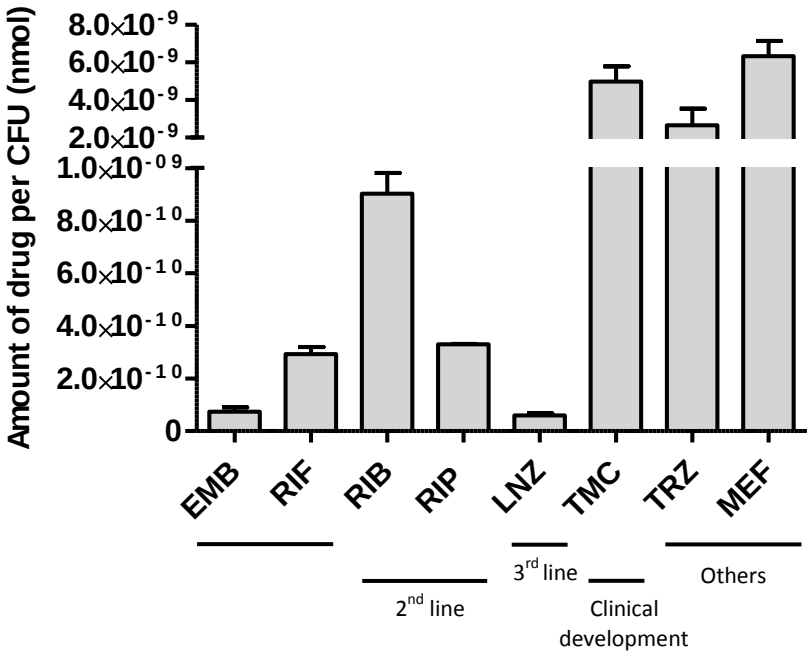

Figure 20 (A – F) MIC curves of six fluoroquinolones tested in this study. Growth of *M. bovis* BCG was evaluated as optical density readings at 600nm. Drug concentrations are plotted on log scales.

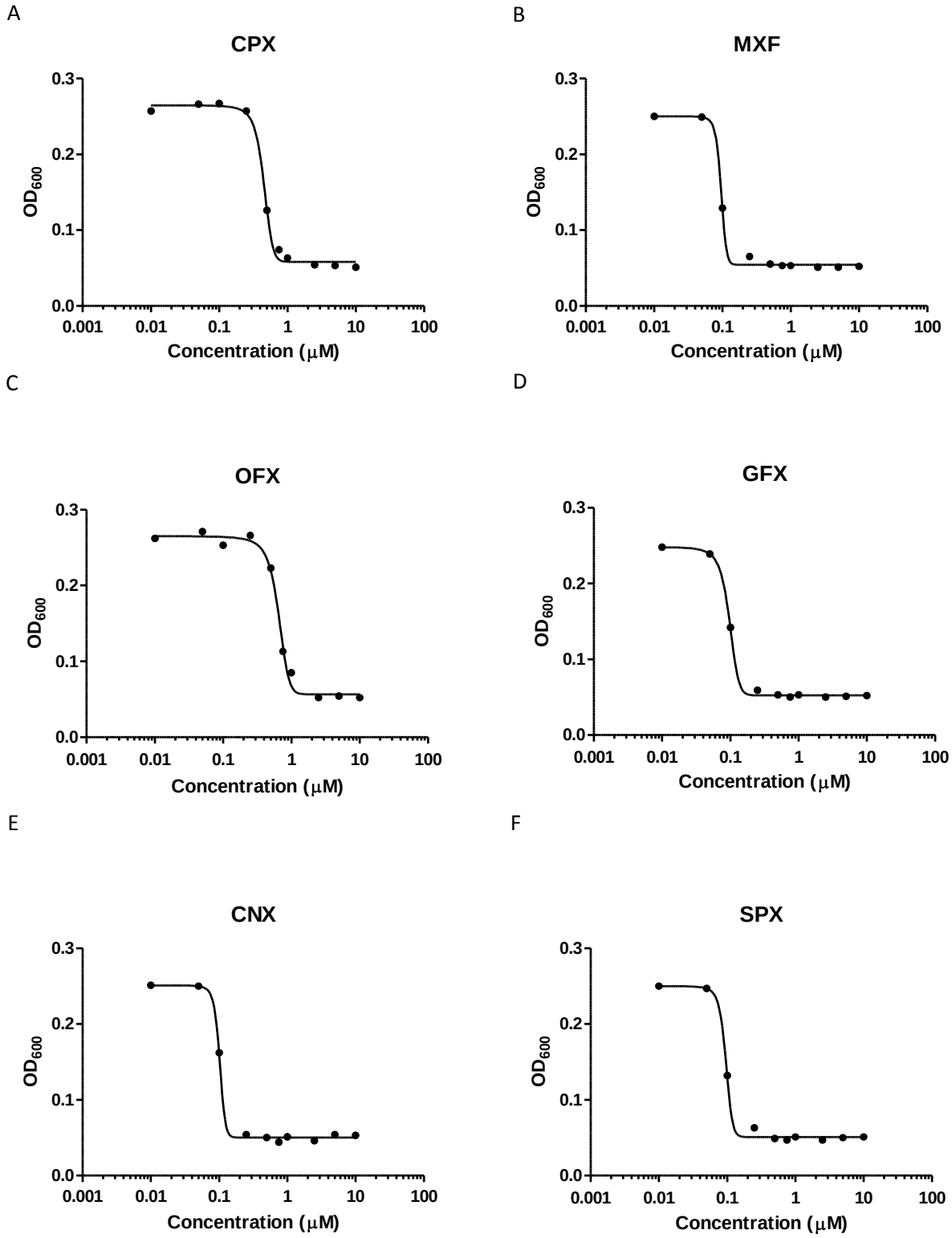

Figure 21 A calibration curve derived from a spectrophotometric assay for cadaverine. Absorbance measurements at 340nm were made for standard dilutions of cadaverine after adduct formation with TNBS and extraction of the chromophore, while using appropriate blanks. The assay is linear over the absorbance range of 0.1 – 1.0.

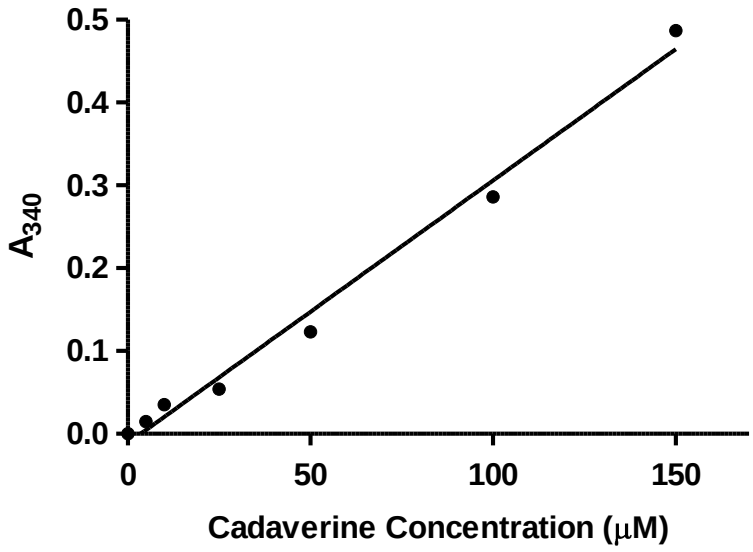

Figure 22 A snapshot of the melting curves chart for the 12 *M. tuberculosis* genes analysed by RT-PCR. Relative fluorescence unit (RFU) measurements during the step-wise increase from 55°C to 95°C are plotted as the derivative.

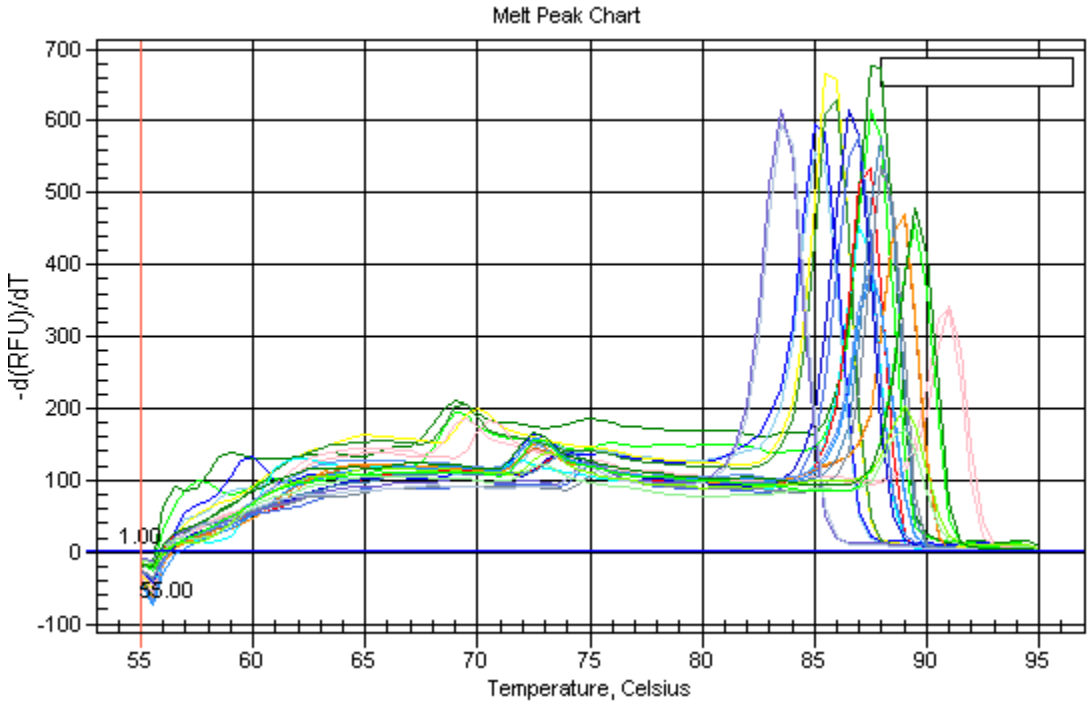

Figure 23 Image of an agarose gel confirming single RT-PCR products. **Table 18** below lists the PCR products loaded into each well by gene and sample type.

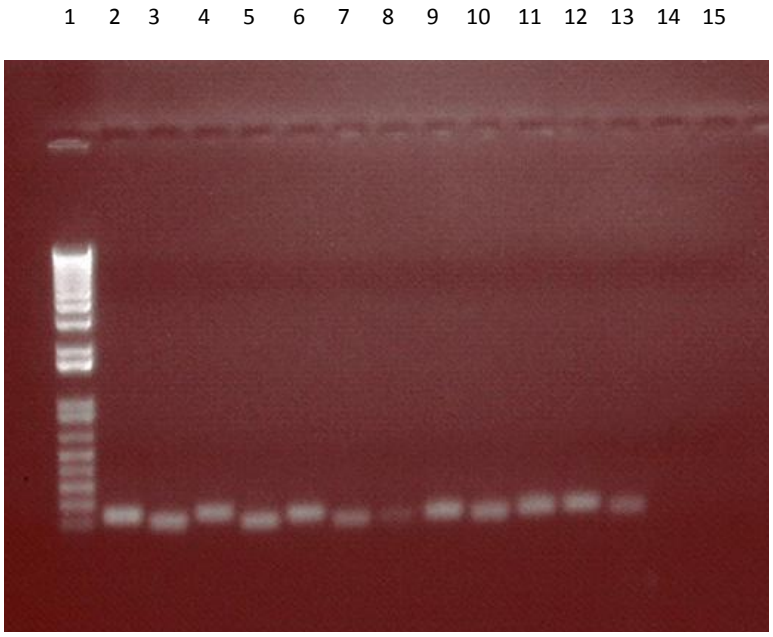

Lane	Gene	Sample Type
1	-	DNA ladder
2	*ompATb*	unknown
3	*rv1698*	unknown
4	*rv1973*	unknown
5	*rpoB*	unknown
6	*16s rRNA*	unknown
7	*rv0227*	unknown
8	*rv0431*	unknown
9	*rv1351*	unknown
10	*rv1352*	unknown
11	*rv1968*	unknown
12	*rv1970*	unknown
13	*rv2270*	unknown
14	*16s rRNA*	No Amplification
15	*16s rRNA*	No Transcription